IN-VESSEL COMPOSTING MODEL WITH MULTIPLE SUBSTRATE AND MICROORGANISM TYPES

by

PHILIP BERNARD WOODFORD

B.T., University of Dayton, 1971
M.S., Rutgers University, 1973
M.S., Kansas State University, 1979

AN ABSTRACT OF A DISSERTATION

submitted in partial fulfillment of the requirements for the degree

DOCTOR OF PHILOSOPHY

Department of Biological and Agricultural Engineering
College of Engineering

KANSAS STATE UNIVERSITY
Manhattan, Kansas

2009

Abstract

This research provides a deterministic model of in-vessel composting, based on Monod's growth kinetics, to mirror biological-mixture decomposition. Existing models predict temperature curves assuming a single temperature-range organism, using a soluble (simple sugar) substrate, with bacteria as the microorganism, and they ignore the different temperature range environments that impact the growth rates of mesophilic and thermophilic microorganisms. The new computer-simulated model, written in MATLAB® by The MathWorks, has six unique features. First, three major carbon chain substrate groups are utilized: soluble, hemicellulose/cellulose, and lignin. An additional substrate group is used for inert substrates. Second, three major microorganism groups are utilized: bacteria for soluble substrate, actinomycetes for cellulose substrate, and fungi for lignin substrate. Third, two temperature-range microorganisms are included: mesophilic and thermophilic. Fourth, the model accounts for the death of microorganisms as the temperature transitions between the temperature ranges. Most of the dead cellular mass is returned to soluble substrate for reutilization and a portion is considered resistant to biological decomposition and is added into the lignin substrate. Fifth, stoichiometric equations account for substrate and microorganism compositions, oxygen and nitrogen requirements, and carbon dioxide and water production. Sixth, the relationship between biological activity and water is better defined. Experimental research was conducted to validate the model. Laboratory analysis distinguished the substrate types. The results indicate the model did differentiate between different levels of substrate types, and the mesophilic and thermophilic microorganism types. Also, the model did differentiate between the bacteria, actinomycetes and fungi. The influence was small, however, because of the different maximum growth rates of the three types of microorganisms. Returning dead microbes to the substrate pools as a result of temperature transitions affected the model results positively. Additional research is needed to account for the influence of volume reduction, develop a better microbial growth curve, include particle size influence, add temporal temperature fluctuations to

the external boundary conditions, incorporate pH and nitrogen availability, and develop a three-dimensional model.

KEY WORDS. Aerobic composting, mathematical composting model, substrate types, microorganism types, microorganism temperature range, mesophilic, thermophilic, microbial death utilization, moisture composting relationship.

IN-VESSEL COMPOSTING MODEL WITH MULTIPLE SUBSTRATE AND MICROORGANISM TYPES

by

PHILIP BERNARD WOODFORD

B.T., University of Dayton, 1971
M.S., Rutgers University, 1973
M.S., Kansas State University, 1979

A DISSERTATION

submitted in partial fulfillment of the requirements for the degree

DOCTOR OF PHILOSOPHY

Department of Biological and Agricultural Engineering
College of Engineering

KANSAS STATE UNIVERSITY
Manhattan, Kansas

2009

Approved by:

Major Professor
Dr. James K. Koelliker

Copyright

Abstract

This research provides a deterministic model of in-vessel composting, based on Monod's growth kinetics, to mirror biological-mixture decomposition. Existing models predict temperature curves assuming a single temperature-range organism, using a soluble (simple sugar) substrate, with bacteria as the microorganism, and they ignore the different temperature range environments that impact the growth rates of mesophilic and thermophilic microorganisms. The new computer-simulated model, written in MATLAB® by The MathWorks, has six unique features. First, three major carbon chain substrate groups are utilized: soluble, hemicellulose/cellulose, and lignin. An additional substrate group is used for inert substrates. Second, three major microorganism groups are utilized: bacteria for soluble substrate, actinomycetes for cellulose substrate, and fungi for lignin substrate. Third, two temperature-range microorganisms are included: mesophilic and thermophilic. Fourth, the model accounts for the death of microorganisms as the temperature transitions between the temperature ranges. Most of the dead cellular mass is returned to soluble substrate for reutilization and a portion is considered resistant to biological decomposition and is added into the lignin substrate. Fifth, stoichiometric equations account for substrate and microorganism compositions, oxygen and nitrogen requirements, and carbon dioxide and water production. Sixth, the relationship between biological activity and water is better defined. Experimental research was conducted to validate the model. Laboratory analysis distinguished the substrate types. The results indicate the model did differentiate between different levels of substrate types, and the mesophilic and thermophilic microorganism types. Also, the model did differentiate between the bacteria, actinomycetes and fungi. The microbial influence was small because of the different maximum growth rates of the three types of microorganisms. Returning dead microbes to the substrate pools as a result of temperature transitions affected the model results positively. Additional research is needed to account for the influence of volume reduction, develop a better microbial growth curve, include particle size influence, add temporal temperature fluctuations to

the external boundary conditions, incorporate pH and nitrogen availability, and develop a three-dimensional model.

KEY WORDS. Aerobic composting, mathematical composting model, substrate types, microorganism types, microorganism temperature range, mesophilic, thermophilic, microbial death utilization, moisture composting relationship.

Table of Contents

List of Figures

List of Tables

CHAPTER 1 - INTRODUCTION

Composting is a waste management technique that utilizes the natural decomposition ecosystem. Control is imposed on the process to achieve the desired results; various factors interact with each other physically, chemically, and biologically. "A slight change in a single factor may cause a drastic change in the overall process…because of its complicated nature, the composting process is one of the most intractable processes from an engineering viewpoint" (Seki, 2000).

The biological decomposition as it occurs nature was well defined by Singer and Munns (1999).

> Soil organisms collectively decompose organic matter, returning its elements to the mineral state utilized by plants. Decomposition has three phases: Animals chew up raw material and mix it with the soil; special fungi and bacteria release enzymes that break large molecules into small molecules; and the general microbial population assimilates and metabolizes these soluble breakdown products. Metabolism, which energizes heterotrophic microbes, proceeds via respiration if oxygen is available or fermentation if oxygen is deficient. … During decomposition, solid organic by-products accumulate as humus, which itself decomposes slowly. The rates of breakdown of both fresh and humified organic matter depend on the composition and physical state of the organic material and on temperature, water supply, nutrient supply, and oxygen supply (p. 189).

Golueke (1977) concisely defined composting as "the biological decomposition of organic wastes under controlled conditions to a state where storage, handling, and land application can be achieved without affecting the environment." Haug (1993) stated, "There is no universally accepted definition of composting." He described it as:

> the biological decomposition and stabilization of organic substrates, under conditions that allow development of thermophilic temperatures as a result of biologically produced heat, to produce a final product that is stable, free of pathogens and plant seeds, and can be beneficially applied to land (p. 1).

The U.S. Environmental Protection Agency (1994) defined composting as "the biodegradation, usually aerobic and thermophilic, that involves an organic substrate in

the solid state; evolves by passing through a thermophilic stage with a temporary release of phytotoxins; results in the production of carbon-dioxide, water, minerals, and stabilized organic matter" (p. 139). Epstein (1997) stated composting was "the biological decomposition of organic matter under controlled, aerobic conditions into a humus-like stable product. The term *controlled* indicates that the process is managed or optimized to achieve the objectives desired" (p. 1).

According to Miller (1996), composting occurred within an ecologically-complex physical matrix. This, in fact, is demonstrated in the terms of the above definitions: biological, decomposition, aerobic, organic substrates (solid state), thermophilic, heat, stable, free of pathogens/weed seeds, carbon-dioxide, water, minerals. Both natural decomposition and composting are forms of waste stabilization. The difference is that composting is a process that is *controlled* to obtain certain objectives. There are several major objectives of composting (Epstein, 1977; Haug, 1993):

- decompose putrescible organic matter into a stable state, producing a material that may be used for soil improvement or other beneficial uses;
- disinfect pathogenically-infected organic wastes so that they may be beneficially used in a safe manner; destroy plant diseases, weed seeds, insects, and insect eggs;
- bioremediate or biodegrade hazardous wastes;
- reduce odors;
- be an economically favorable alternative compared to other disposal methods; and
- be more environmentally acceptable than other conventional solid waste management methods.

Composting occurs within a heterogeneous system that has multiple components in multiple phases (Seki, 2002). To design a composting waste disposal system, the system designer must understand key characteristics of the organic matter to be decomposed, including nitrogen availability, required moisture level, aeration requirements, and temperatures obtained. Initially, laboratory bench experiments/pilot plants were conducted to ascertain outcomes. Today, to reduce the cost of physical experiments, numerical experiments that use mathematical models have been developed.

Seki (2002) detailed the value of conducting numerical experiments using mathematical models to grasp the characteristics of the process quickly with lower costs than physical experiments, provided the principal mechanisms of the full process are understood.

Seki (2002) differentiated two types of compost models: deterministic and stochastic models. Deterministic models add differences. Every set of variables is determined by the unique parameters of the model and by the sets of previous states of these variables. Deterministic models perform the same way for a given set of conditions. Stochastic models determine quantities of reactants and products in chemical reactions. Randomness is present, and variable states are not described by unique values but, rather, by probability distributions. Available models have several inherent limitations:

- Substrate is considered either easily decomposable (soluble) or inert.
- All microorganisms are considered to have the same characteristics even though they are discussed as being different. For example, the active temperature range is considered one large range, although the habitat is discussed in terms of mesophilic and thermophilic ranges.
- Microbial death is considered by removing that portion of the microorganisms from the analysis. In limited cases their biomass is made available to the living microorganisms for decomposition.
- Moisture content calculation does reflect the full spectrum of influence to microorganisms where too little moisture causes desiccation, and too much restricts oxygen diffusion.

According to Seki (2002), "there is no satisfying model affording … both locally detailed and holistic information, although many deterministic models have been reported (Finger et al., 1976; Fujita, 1980; Seki & Komori, 1984; Bach et al., 1987; Nakasaki et al., 1987; Hamelers, 1993; Keener et al., 1993; Haug, 1993; Kaiser, 1996; Stombaugh & Nokes, 1996; VanderGheynst et al., 1997; Das & Keener, 1997)."

Mason (2006) reviewed eighteen composting models. He noted:

> A deterministic approach has been adapted for all published models … However, stochastic elements have been incorporated into two of these models … Modelers have typically looked at the composting system on a macro-scale, in which the focus of

> analytical attention has been on the reactor as a whole; however, several authors have approached the problem by starting from a microbiological point of view (Kaiser, 1996; Stombaugh & Nokes, 1996; Seki, 2000). Adapting a different perspective, Hamelers (1993) used the composting particle as the basis for analysis.

The complexity of the composting process and the existence of uncertainties in many modeling parameters and their interrelationships pose a research challenge (Qin et al., 2007). Qin et al. stated:

> Most of the previous studies achieved successes in modeling specific portions of the composting processes from either a biological or physiochemical point of view. In fact, the composting process generally has significant temporal variations because of the dynamic features of many process components and their interactions. Design of a cost-effective composting system should, thus, be based on modeling efforts from a more comprehensive point of view.

The goal of this research in this dissertation is a move toward a more comprehensive mathematical, computer-simulation model. This research presents a comprehensive mathematical composting model that predicts outcome based on the different substrates available or those that are chosen. Repeated runs can be made. Each run can concentrate on a particular issue by varying amounts and types of substrates, moisture, aeration rate, and reactor size and its heat loss to predict the decomposition of the waste(s) before any pilot work is initiated. It is based on the methodology utilized by Stombaugh and Nokes (1996), employing the Monod equation for biomass production, and it uses stoichiometric equations to develop yield coefficients for substrate consumption, nitrogen consumption, oxygen consumption, water production, and carbon-dioxide production.

The objectives of this research are to advance mathematical compost modeling by:

- dividing the substrate into four parts: soluble substrate, cellulose/hemicellulose substrate, lignin/lignocellulose substrate, and inert

(ash/inorganic) substrate; (This component establishes a common level that all materials to be composted can be broken into, the common basic building blocks that microorganisms utilize for energy. All organic materials can be analyzed and partitioned into the four substrate parts.)

- dividing the basic microbiological approach into three parts: bacteria, actinomycetes, and fungi, to reflect the different major decomposers substrate preferences, and the time required to decompose the different substrates; (This component establishes that modeling needs to focus on the microorganism predominately responsible for a substrate's biodegradation.)
- separating the microbiological organism processes into mesophilic and thermophilic temperature ranges; (This component solves the problem of assigning all microorganisms to just one temperature range. This model considers the dynamics between mesophilic and thermophilic microorganisms.)
- developing the three stoichiometric equations, where each equation reflects a specific microbial type and their major substrate type; (This component allows a more accurate accounting of the requirements for composting to occur and product yields. Each equation considers the substrate type, the amount of oxygen required bases on substrate type and microorganism type, the growth of the specific microorganism type, carbon dioxide and water produced.)
- accounting for dead microorganisms, which a majority is added into the soluble substrate to be reutilized, and the remainder is entered into the resistant-to-biodegrade category; and (This component allows a more accurate capture of the effects microbial death has on the substrate availability.)
- developing a more exact moisture equation that indicates the effect on microbiological activity. (This component is another initial step to account for the effects of percent moisture content has on the microbial population. This component is focused on the effect on bacterial microorganism; from

desiccation due to low moisture to the lack of oxygen diffusion at high moisture.)

This research used industry values for the carbon to nitrogen (C/N) ratio (Rynk et al., 1992) in determining how much, if any, additional nitrogen was required. Gray et al. (1971) recommended a particle size of 1.3 cm to 7.6 cm (0.5 in to 3 in) be used. The lower end of the scale is suitable for forced aeration while the upper end is suitable for windrow and other passively aerated systems. The size of the particle used in this research fell into the above size range, therefore particle size was not evaluated.

The experimental portion of this research focused on providing experimental data to evaluate the model's prediction capability. Three mixtures were prepared utilizing four different ingredients. The mixtures represent the range of compostable materials: readily-biodegradable, slower-to-biodegrade, and resistant-to-biodegradation.

This dissertation is organized into nine chapters and an Appendix. Chapter 1 is the introduction, presenting background information, and research objectives. Chapter 2 reviews literature pertaining to deterministic composting models. Chapter 3 describes the biological details and parameter development for the mathematical in-vessel composting model. Each detail and parameter is presented along with a structure that represents the research model. Each detail and parameter delineates the limit or constraint, or defines the operating range within/on the composting process, by assigning a numerical constant that is a measure of a property for a particular substance. Chapter 3 is divided into six sections: substrate, microbial components, moisture, stoichiometric equation, nitrogen coefficient, and parameter summary.

Chapter 4 presents the materials and methods used in conducting the experimental portion of this work. The chapter delineates the experimental design, setup, and procedures to compare the mathematical model results to the experimental data. Chapter 4 is divided into four sections: matrix design; experimental design; experimental equipment setup; experimental procedure; and statistical analysis methodology.

Chapter 5 presents and discusses the results of the experimental work. It is divided into three sections: substrate analysis for mixtures, analysis of the composted mixtures and recorded temperature profiles during composting. Chapter 6 discusses the mathematical simulation model. The model is based on differential equations to describe

microbial growth, substrate consumption, oxygen concentration, moisture content and temperature. The microbial process utilizes Monod's growth kinetics to describe microbial growth and microbial maintenance as functions of specific growth rate or maintenance coefficient, substrate and oxygen concentrations. The equations are solved using finite differences. The time step utilized in this model is one minute.

Chapter 7 presents and discusses the results of the mathematical simulation model. The results compare the differences between the three microorganism types, the difference between the two temperature scenarios, the one temperature profile verses the mesophilic and thermophilic profile, and the three substrate types. The model results are compared to the experimental results.

Chapter 8 presents the conclusion and recommendations for future work. Chapter 9 presents references. The Appendix is divided into: A- list of symbols, B-additional photographs of the experimentation, C-laboratory analyses results, D-experimentation data results, E- model coding in MATLAB®, and F-experimental temperature profile data (cleaned). Appendix F is only a part of the electronic version.

CHAPTER 2 - LITERATURE REVIEW

The composting process is divided into two sequential phases: active and curing. The active phase is defined as a function of microbiological activity as measured by oxygen uptake, carbon-dioxide production, or heat released (Wu et al., 2000). The primary concern in industrial composting is the active phase, during which decomposition of easily biodegradable substances occurs (Seki, 2000). The curing phase is when compost maturity occurs; the decomposition of phytotoxic organic substances produced during the active composting stage (Wu et al., 2000). The curing phase, passive in nature, produces humus (Seki, 2000).

The emphasis in modeling is on the active phase. The time required for the active phase is dependent upon the carbon source. "The time required for the loss of half the added carbon in the form of CO_2 from most residues varied from 3 days for glucose to 500 days for pine needles" (Haider et al., 1975, p. 197). The model's run time must be

capable of being adjusted to meet active phase requirements. In addition, models are often limited to specific physical specifications of the composter.

The composting process obeys physico-chemical principles where two phenomena occur (Seki, 2002). The first phenomenon is the stoichiometric and chemical kinetics of microbial reaction. The stoichiometric relationship is concerned with substrate mass utilization and microbial biomass production, the oxygen and nitrogen requirements, and the production of carbon dioxide and water. The second phenomenon is the transport event. It is concerned with the volume decrease of the compost mass, heat conduction and liquid water transfer.

Various deterministic models have been presented. Smith and Eilers (1980) developed a two-dimensional finite difference model of a forced aerated windrow composting system; it included spatial and temporal solutions of airflow, substrate degradation, and heat, moisture, and oxygen balances. They assumed the flow patterns and quantities of airflow were independent of time. It was necessary to solve the flow equations spatially as the geometry of the windrow was not uniform and the boundary conditions varied spatially. However, the assumption of constant permeability throughout the bed, and temporally-constant airflow pattern, caused the model to be insufficient for studying the rapidly changing spatial and temporal variations in properties during high-rate composting. The field validation of the model proved that dry matter, volatile matter, and moisture content were accurately predicted, but temperature predictions were not close in two of the four field trials. The data presented from their simulations and validations did not compare to the spatial predictions.

Nakasaki et al. (1987) attempted to develop a lumped-parameter model consisting of only one layer. The experimental reactor was an autothermal packed-bed, 300 mm in diameter and 400 mm in depth, covered with a Styrofoam insulator. The temperature was measured at the bottom, center, and top of the reactor, and the model assumed the substrate and air temperatures to be identical throughout the reactor. The experiment, which simulated temperature based on carbon-dioxide-evolution rate as a function of the volatile-matter-degradation rate, was halted when the temperature decreased to 45 °C because temperature control by aeration became impossible. Although results for temperature, dry matter loss, and moisture were reasonably accurate when compared to

average values from a validation run, and "the simulated data coincided well with the data of the two bench-scale experiments, the results did not follow well for the large system" (Ekinci et al., 2005).

Keener et al. (1993) developed an analytical model describing macroscopic phenomena that occurred during composting that showed interdependence between the biological and physical factors. Keener et al. predicated, "the variables of interest are the compost (dry matter and water), air (oxygen and moisture), and enthalpies (compost and air)". They assumed the disappearance of the biomass followed a first-order equation, and equations were analyzed using a layered system. They introduced the concepts of equilibrium-mass and compost-mass ratio, providing for the fraction of the material that is not composted at a given time. The authors presented a database of properties of various compostable substrates. Procedures also were presented that outlined optimization of parameters (e.g., depth of compost bed) and included comparisons and calculations for special cases, producing analytical expressions that showed the relationship between compost properties and maturity.

Hamelers (1993) developed a particle-level mathematical model based on biofilm theory, using an insoluble polymeric substrate, a soluble monomeric substrate, microbial biomass, oxygen, and water concentrations as the state variables. According to Hamelers, "A particle is understood to consist of an outer aerobic layer and an anaerobic core. In the anaerobic core polymeric substrate is converted into soluble substrate. This soluble substrate diffuses into the aerobic layer where it is oxidized by the aerobic population." The model, called a composting-particle-kinetics model, was to predict the oxygen uptake rate. Reaction rates that described conversion of substrate and biomass growth were modeled using first-order kinetics and a Monod-type equation. The decay of aerobic biomass was modeled as a first-order equation where the living biomass transitioned to polymeric substrate. Through hydrolysis, the polymeric substance converted to soluble substrate. Hamelers corrected for the difference in the molecular composition of polymeric substances and biomass by keeping the energy content of the two constant. For the differential equation, the conversion rates of the different compounds were calculated based their stoichiometric factors

To validate his model, Hamelers (1993) utilized an experimental vessel constructed of stainless-steel walls and bottom. The cap was high-density polyethylene plastic. The experimental composter was 0.14 m in diameter and 0.3 m in height. A 6-cm grate installed 6 cm from the bottom supported the compost. Air entered the reactor at the bottom through a small, punctured pipe. The data indicated a 250-hour run time was required to complete the oxygen-uptake-simulation runs. Hamelers made a significant contribution by including the biological component which examined the kinetics of composting at the particle level, calculating gradients of oxygen, biomass, and soluble and polymeric substrate in the boundary layer surrounding individual particles (Stombaugh & Nokes, 1996). A limitation to this model is that the "temperature is treated as an exogenous variable since no relevant temperature gradient develops in a waste particle. The particle temperature is assumed to be constant" (Hamelers, 1993). Because the temperature gradient within the composting material is not considered, the effects on the microorganisms cannot be evaluated.

Haug (1993) developed a model to simulate a continuous-feed, complete-mix composter. The model was based on first-order kinetics that detailed heat, moisture, substrate and gas balances. Haug stated the model should include the entire composting process, the active stage and the curing phase, and that up to ten different substrate types could be included. Each substrate was divided into slow- and fast-biodegradability fractions, non-biodegradable fraction, and ash; and, a biodegradability coefficient was utilized to identify between fast and slow degradability. All materials were mixed and, therefore, considered as homogenous substrate. Each stage was treated as an individual unit, solving the process conditions within it. The model required the sum of heat and materials for the individual stages to equal that of the entire system. Also, a portion of the mixed substrate was recycled back into the initial stage. "Haug's multi-stage model could be used to calculate spatial profile within a bed, but this implementation was not done explicitly" (Ekinci et al., 2005).

Lynch and Cherry (1995) developed equations to describe airflow in passively-aerated windrows. Their model was based on free-convection flow, and it described an anticipated air-velocity profile along the length of the windrow. However, the model did

not describe other phenomena, such as degradation, temperature increases, oxygen consumption, carbon-dioxide evolution, and moisture loss.

Kaiser (1996) presented a mathematical model that included mass transfer, heat transfer and conversion of organic matter into carbon dioxide and humic substances. The model is similar to the Nakasaki et al. (1987) model. Kaiser described a consumption of four substrates by a four-component microflora, and the model considered sugars, starches, hemicellulose, cellulose, and lignin. The microorganisms considered were bacteria, actinomycetes, brown-rot fungi, and white-rot fungi. Kaiser stated a major assumption of this model was that bacteria utilized only the easily-degradable substrate, the actinomycetes utilized both the easily-degradable substrates and hemicellulose, the brown-rot fungi utilized the first two substrates and cellulose, and the white-rot fungi utilized all substrates. The model equated the loss of organisms (microbial death rate) to the increase of humic substances. "It (*Humus*) is primarily derived from the higher plants, which grow upon the soil, and forms during the microbial decomposition of the original plant constituents and of new substances synthesized by the soil microorganisms (Haider et al., 1975). "Humus consists of compounds belonging to recognizable classes of organic compounds, such as polysaccharides, polypeptides, and altered lignins" (Clapp & Hayes, 1999), and of microbial melanins (Gramss et al., 1998), specifically some fungal cell walls (Haider et al., 1975). Hence, humic substances are just one component of microbial death.

Stombaugh and Nokes (1996) developed a lumped-parameter, simulation-model matrix, which was divided into layers that had uniform properties. The model utilized differential equations to describe microbial growth, substrate consumption, oxygen concentration, moisture content and temperature that were derived as a function of the aeration rate and vessel size. Based on microbial biological processes utilizing Monod's first-order-growth kinetics, the model described both the microbial growth and microbial maintenance as functions of specific-growth rate (or maintenance coefficient), substrate, and oxygen concentrations. Coefficients were added for moisture content and temperature. The only substrate type considered was the readily-degradable fraction of the dry matter; the remaining substrate was labeled non volatile. Microbial mass was defined to include mesophilic and thermophilic bacteria, actinomycetes, and fungi. To

validate their model, a laboratory composter was constructed from cylindrical PVC tubing with an inside diameter of 0.305 m and a maximum compost depth of 0.91 m. Commercially-available end caps were utilized. A 0.10-m air space was provided between the compost and each end cap. A mixture of cracked corn and pelletized corncobs was composted for 250 hours.

Stombaugh and Nokes (1996) concluded the model provided an excellent way to explain and demonstrate the complex interactions that occur during the composting process. They noted, "The model appeared to provide realistic predictions of temperature fluctuations, oxygen-uptake rate, moisture exchanges, and substrate degradation for a readily-composted input mixture." They also stated that as growth and death rates and yield coefficients are refined, "The formation of biomass from substrate and the return of biomass could be included in the stoichiometric equations and in the differential equations for biomass … and substrate". In addition, Stombaugh and Nokes indicated that, if the model was adapted to research purposes, refinements could be made for the effects of the C/N ratio, moisture content, particle size, and substrate solubility on biomass growth. This model was restricted to two types of substrate, the soluble and the inert. The hemicellulose, cellulose and lignin may contribute slightly to the soluble component, but because of their resistance to be degraded, they were considered to be inert. The model considered all microorganisms to be one group of decomposers. There was no discrimination between the differences in the two-temperature-range organisms which exist during composting.

Das and Keener (1997) stated, "Several attempts at modeling of compost systems have been made using both analytical modeling approaches (Nakasaki et al., 1987; Keener et al., 1993; Hamelers, 1993; Haug, 1993; Lynch & Cherry, 1995) and numerical modeling approaches (Smith & Eilers, 1980; Stombaugh & Nokes, 1994)." Das and Keener asserted that these attempts to model composting systems "have assumed uniform properties within the compost bed" and, therefore, these models were unable to quantify the formation and effects of non-homogenous profiles and spatial variations.

Das and Keener (1997) developed a numerical-simulation model to solve governing equations of airflow in a two-dimensional domain resembling a cross-section of a compost vessel. To validate their model, they utilized a concrete-walled bin

composting vessel, 6.0-m wide, with a perforated steel floor that was filled with 0.3 m of gravel covered with 0.15 m of shredded bark; the compost was filled to a depth 3.0 m. The data indicated a simulation run time of 168 hours, and the state variables were degradation of dry matter, temperature, moisture content, and oxygen concentration. The validation model was to determine the effective management strategies on aeration energy requirements and homogeneity within the vessel. They reported the measured peak temperatures which were similar to the results predicted by their model. However, the predicted moisture values were close to the measured values only in the middle layer but not in the top or bottom layers. They stated their assumption that the air was saturated with moisture at all locations within the bed was limiting and it needed improvement. They also reported a need to refine the parts of the model that related to microbial activity and to temperature effects when the temperature of the bed was reduced to a low value. Their simulation time was very short, less than one week. Peak temperatures were reached in less than 24 hours, and then dropped gradually. Das and Keener did report they increased the aeration requirements to keep the composting beds cool.

VanderGheynst et al. (1997) developed an energy-transport model to "capture the temporal and spatial changes in temperature observed within a high-solids-degradation process employing forced aeration. Model components included energy lost through air flow, heat generated from microbial activity, and energy accumulated in the matrix". They developed an empirical equation that represented heat generation, based on pilot-scaled experimental data. The pilot-scale experiment was carried out using a 770-L insulated bioreactor, constructed of 2.7-m smooth-lined, corrugated, high-density polyethylene pipe with an inner diameter of 0.6 m. A simulation-run time of 100 hours was given. VanderGheynst et al. (1997) reported, "The spatial-dependent solution of the characteristic equation was found to follow the experimental profiles well during the early stages of the process. Deviations were observed as temperature and time increased. These deviations were concluded to be a result of the empirical heat generation of the model."

Seki (2000) developed a stochastic model for batch-type composting where the "variables vary stochastically with each increment of concentration." A master equation,

based on a balance equation of a probability distribution of the state, was developed and then converted into a continuous-type master equation. Seki indicated the stated variables were microbial concentrations, substrate concentrations, and temperature. Seki further stated that, through the use of numerical solutions of the Fokker-Plank equation, the model would predict the expected values and standard deviations of the variables at the end of the first, or active, stage of composting only if the value of concentration was known in advance. He utilized a laboratory, pilot-scale, silo-type composter with a diameter of 200 mm and a compost depth of 600 mm, insulated with 50-mm thick polystyrene foam, to validate the model. The simulation run time was 200 hours. Seki also reported the deterministic model could determine the spatial averages of the state variables, but could not determine the secondary values, such as variances of the state variables. To obtain this information, a stochastic model was developed by extending the deterministic model. The stochastic-model results for temperature were similar to the experimental results. This model considered only soluble and inert substrates, all microorganisms as if they are one group of decomposers, and no discrimination between the differences in the two-temperature-range organisms which exist during composting. The simulation length of 200 hours is short when considering the active phase of the composting process.

Hamelers (2001) presented a mechanistic model to describe the relationship between dry-matter content and the maximum oxygen-uptake rate, indicating that both the density and the structure of the waste influenced the optimum-moisture level. The model presented the adverse effects of size reduction on the maximum-oxygen rate. Hamelers reflected on the use of this model as a management tool. First, he believed it was an appropriate tool in feedstock preparation, matching the characteristics to the facility's unique configuration and process characteristics to improve biodegradation. Second, he proposed it as a tool to control the final moisture content by adjusting moisture-control points over the course of the process.

Seki (2002) presented a deterministic model to simulate a batch-type, unturned composting process. He stated his model included "the effects of volume decrease, heat conduction, and liquid-water transfer… to predict the empirical results of changes in moisture content, substrate concentration, and temperature". The model was limited to

the active-composting phase. He considered five principle variables: microbial concentration, substrate concentration, moisture content, gaseous-oxygen concentration, and temperature. Seki utilized the stoichiometric relationship and chemical kinetics of the microbial reaction as the bases of his model. According to Seki, "there has been thus far no satisfactory model on composting that affords us locally-detailed and holistic information because the composting process is a multi-component, multi-phased, and heterogeneous system." He reviewed the four groups of transport phenomena (molecular, microscopic, macroscopic and megascopic [Bear & Bachmat, 1991]) and concluded the molecular and microscopic models were difficult to apply because compost is extremely heterogeneous and it is difficult to anticipate the randomness of physical properties of the compost matrix.

Macroscopic models have been confined to batch composting processes without turning (Finger et al., 1976; Seki & Komori, 1984; Stombaugh & Nokes, 1996; Das & Keener, 1997; VanderGheynst et al., 1997). These models were verified to roughly simulate spatial and temporal changes in the variables (Seki, 2002). Seki noted the temporal volume decrease during composting was not taken into account. Volume reduction was necessary to more accurately predict temperature and moisture profiles. Megascopic models treated the variables averaged over the entire compost mass to simulate mixing. Seki, clearly influential in the study of composting models, developed his megascopic view by integrating the basic equations for principal variables over the entire volume of the compost mass, determining the effects of volume decrease of the compost mass, heat conduction, and liquid-water transfer. To test the model, Seki utilized a laboratory, pilot-scale, silo-type composter with a diameter of 2.4 m and a compost depth of 2.4 m, with a simulation run time of 600 hours. He concluded "the simulated results by the megascopic model were about 8 °C higher in the maximum attainable temperature, 25% smaller in the final substrate concentration, and about 20% larger in the final moisture content compared with the spatial average values of the macroscopic model." Seki stated "the megascopic model may not well simulate a reaction delay due to non-uniformity of the compost mass, it can be used for rough estimates of change in state variables in batch-type composting processes."

Ekinci et al. (2005) developed a two-dimensional, finite-difference numerical model based on a two-component, first-order-kinetic model, and heat- and mass-balance equations. The model is based on the equations described by Keener et al. (1993) and the two-dimensional, finite-difference model developed by Das and Keener (1997). Validation of the model was based on four different aeration strategies: one-directional airflow, one-directional airflow with air recirculation, reversed-direction airflow, and reversed-direction airflow with recirculation. The airflow was pulsed because Elwell et al. (2001) demonstrated better efficiency and less odor emission with pulsed aeration than with continuous aeration. The reactor had a diameter of 0.57 m and a height of 0.685 m, and the simulations ran for 168 hours. The temperature-profile and moisture-content simulations correlated with the experimental data for the three, innermost layers but not the upper- and lower-boundary layers. The decomposition gradients were highly variable in the experimental studies but not highly correlated with the simulation results.

In summary, there are several major issues with the existing models. All models presented, except for Kaiser (1996), were restricted to two types of substrate: the soluble and the inert. The remaining two substrate types (cellulose/hemicellulose and lignin) need to be considered. All models, except for Kaiser (1996), considered all microorganisms as if they were one group of decomposers. The three microbial groups associated with decomposition need to be considered. No model makes a distinction between the differences in the two-temperature ranges in which the decomposition microorganisms exist. Two models considered the death of the microorganism; one considered the reintroduction of the dead-microbial material into the equation as substrate (Hamelers, 1993), the other as humus (Kaiser, 1996). Both the death of microorganisms and the accumulation need to be considered separately. The death of microorganisms needs to be considered in two ways: as a general, specific-death rate of the population; and at the point of transition between the two-population-temperature ranges. The accumulation also needs to be considered in two ways: as soluble substrate for that portion of the microorganism that is readily-biodegradable, and as a resistant-to-biodegradation portion for the remaining cell parts. Moisture content of is a component that plays an important role in decomposition. Currently, only a portion of the moisture range is calculated. The full-moisture-content range must be considered from desiccation

of the bacterial microorganism due low moisture content to the lack of oxygen diffusion at high moisture content. The Model run times varied from 100 hours (4.2 days) (VanderGheynst et al., 1997) to 600 hours (25 days) (Seki, 2002). The simulation duration run must be of sufficient length to cover the active phase of the composting process.

CHAPTER 3 - MODEL DEVELOPMENT

This chapter describes the biological details and parameter development of the in-vessel, composting model. Each detail and parameter is presented along with a structure that represents the research model. Each detail and parameter delineates the limit or constraint, or defines the operating tolerance within/on the composting process, by assigning a numerical constant that is a measure of a property for a particular substance. This chapter is divided into five sections: substrate, microbial components, moisture, stoichiometric equation, and parameter summary.

The process of organic matter degradation by soil organisms in a natural ecosystem setting was well defined by Singer and Munn (1999):

> Decomposition has three phases: Animals chew up raw material and mix it with the soil; special fungi and bacteria release enzymes that break large molecules into small molecules; and the general microbial population assimilates and metabolizes these soluble breakdown products. Metabolism, which energizes heterotrophic microbes, proceeds via respiration if oxygen is available or fermentation if oxygen is deficient. … During decomposition, solid organic by-products accumulate as humus, which itself decomposes slowly. The rates of breakdown of both fresh and humified organic matter depend on the composition and physical state of the organic material and on temperature, water supply, nutrient supply, and oxygen supply. (p. 189-190)

Composting attempts to duplicate natural decomposition degradative processes but in a controlled situation. To effectively and efficiently accomplish this, the major factors affecting the decomposition process must be taken into account. Models are developed for a specific set of given composting conditions, and to provide an indication of what to anticipate by attempting to account for the major factors affecting the decomposition process. The general parameter model must be capable of simulating, on a reasonable basis, the outcome for a range of conditions. In composting, for example, some mixtures might be high in soluble substrate or high in cellulose and hemicelluloses

or high in lignin; the carbon to nitrogen (C/N) ratio may be low; insufficient moisture available; etc. Whatever the limiting factor, a general, parameter model must be able to reasonably predict the outcome.

This research presents a numerical finite-difference, composting model. The approach is a lumped-parameter matrix that is divided into layers that have uniform properties for the initial boundary condition. The properties are substrate type (soluble, cellulose/hemicelluloses, lignin, and inert), moisture content, ambient temperature, oxygen and carbon dioxide. The approach is based on the method of Stombaugh and Nokes (1996). For biomass growth, the Monod's growth-kinetics is used as a function of degradable-substrate concentration, oxygen concentration, and moisture content. The stoichiometric equation is calculated on a molar level and utilized as the basis of determining substrate consumption, oxygen consumption, nitrogen consumption, and water and carbon-dioxide production. The variables are evaluated using a series of equations that describe the composting process one level at a time in a mult-layered system.. Previously-determined values are then passed to the subsequent layer and/or time step as initial input variables. The variables are temperature, moisture, substrate concentrations (soluble, cellulose/hemicelluloses, lignin, and inert), microbial concentrations (bacteria, actinomycetes, and fungi), oxygen and carbon-dioxide concentrations.

Substrate

Substrate characterization is one of the major pieces to this research model. As stated above, substrate is identified as one of four types: soluble, cellulose/hemicelluloses, lignin, and inert. The researcher must understand the major characteristics of the wastes being composted to identify what substrate types are present and to understand what to expect. It is important to ascertain the analytical method that identifies each substrate characteristic.

Chemical Characterization

Substrate biodegradability is defined by the chemical structures of the major organic macromolecules. There are four major organic macromolecules: carbohydrates, lipids, proteins, and nucleic acids (Mader, 1998). The basic unit of structure for a

particular group of organic macromolecules is known as its monomer: the glucose molecule for carbohydrates; the fatty acids for lipids; the amino acids for proteins; and the nucleotides for nucleic acids. This model considers these four major organic macromolecules and divides their components into one of the four major types of substrate: 1) readily-biodegradable or soluble; 2) slower-to-biodegrade substrate; 3) resistant-to-biodegradation; and 4) all inert material remaining (ash/inorganic). Current composting models divide substrate between the soluble or readily-degradable material and non-volatile solids. This substrate characterization is one of the pillars on which the deterministic, mathematical model developed in this research is based.

Carbohydrates

The first organic macromolecule is the carbohydrate. Carbohydrates, or saccharides, are compounds with the stoichiometric formula $\left[CH_2O\right]_n$ or are derivatives of such compounds (Voet & Voet, 2004). Saccharides were thought of as hydrated carbon, thus, the term carbohydrates. There are two types: the monosaccharides composed of simple, monomeric molecules; and polysaccharides, composed of monosaccharide monomers linked together forming polymers. These chained polymers are short to long, branched as well as linear (Voet & Voet, 2004).

Monosaccharides, the first carbohydrate group, are simple sugars, consisting of three to seven carbon atoms linked with hydrogen and oxygen. Each different monosaccharide is a different sugar monomer. Some examples of common sugars are: glucose $\left[C_6H_{12}O_6\right]$ found in blood of animals; fructose, also $\left[C_6H_{12}O_6\right]$, but the mirror image of glucose, found in fruits; and ribose, a five-carbon sugar (pentose). The simple saccharide is the basic structure as the result of decomposition. They are water soluble (Morrison & Boyd, 1970) and are taken directly into the microbial cell and metabolized. Soil microbes can metabolize simple sugars completely in one to two days (Sylvia et al., 1998).

The second carbohydrate group is the polysaccharides. There are two major groups of polysaccharides: the storage polysaccharides, starch and glycogen, and structural polysaccharides, such as cellulose and chitin (Mathews & van Holde, 1996). All these molecules have glucose $\left[C_6H_{12}O_6\right]_n$ as the base unit structure but can be

constructed from a number of different kinds of monosaccharide monomer units (Mathews & van Holde, 1996), and are bonded together to form chains (Morrison & Boyd, 1970). There is a group of polysaccharides known as oligosaccharide, which contain only a few monomers, such as disaccharides. Oligosaccharides molecules are considered "intermediate products in the degradation of much longer polysaccharides" (Mathews & van Holde, 1996). They are water soluble and can be taken into the cell, but they then must be broken in monomer units to be metabolized (Adl, 2003; Voet & Voet, 2004).

There are two main storage polysaccharides: starch and glycogen. Starch is the principle food reserve for plants (Voet & Voet, 2004). It is a linear and branched polymer of glucose consisting of aggregates of polymers (Adl, 2003). These chains are for rapid mobilization of glucose when needed (Mathews & van Holde, 1996). Extracellular enzymes are required to split the polymers into a mixture of oligosaccharides, which can then be hydrolyzed into their component monomers (Voet & Voet, 2004). Starch is rapidly decomposed by soil microbes (Alexander, 1977).

The other main storage polysaccharide is glycogen, the storage polysaccharide for animals (Voet & Voet, 2004). Its structure is similar, but is a shorter chain and more highly branched (Mathews & van Holde, 1996). These chains are also utilized for rapid mobilization of glucose when required (Voet & Voet, 2004). "Glycogen … is probably digested through the same enzymes" as starch (Adl, 2003).

The second major grouping of polysaccharides is structural. Cellulose, the most abundant single polymer (Mathews & van Holde, 1996), provides the structural rigidity to plant cell walls (Sylvia et al., 1998). It is a large water-insoluble polymer whose structure is composed of up to 15,000 glucose units bound together in a long, linear chain by $\beta(1 \rightarrow 4)$ linkages (Mathews & van Holde, 1996; Voet & Voet, 2004). These long, unbranched polymers of glucose are known as fibrils. Because of the $\beta(1 \rightarrow 4)$ linkage, each glucose residual is flipped 180 degrees with respect to the residual on both sides of it, allowing long chains to form (Mathews & van Holde, 1996). The parallel cellulose chains or "fibrils are held together by in a three-dimensional matrix by inter- and intramolecular hydrogen bonds," (Adl, 2003) which generate a planar structure. The planer structure sheets are then stacked vertically (Voet & Voet, 2004). In addition, the

microfibrils of cellulose are embedded in a matrix of hemicellulose (Mathews & van Holde, 1996). "This highly cohesive, hydrogen-bonded structure gives cellulose fibers exceptional strength and makes them water insoluble despite their hydrophilicity" (Voet & Voet, 2004). The basic stoichiometric formula for cellulose is $[C_{12}H_{24}O_{13}]_n$.

Microorganisms release enzyme complexes, cellulases, into the water film to degrade cellulose by eliminating the crystalline-like structure. "Degradation of cellulose is a slow process because its tightly-packed and hydrogen-bonded, glutan chains are not easily accessible to cellulase and do not separate readily even after many of the glycosidic bonds have been hydrolyzed" (Voet & Voet, 2004). The cellulose long-polymer chain is split into linear chains of two to three glucose units once the crystalline-like structure is degraded (Sylvia et al., 1998). These short chains, cellobiose and cellotriose, are brought into the cell, hydrolyzed into single glucose units, and then metabolized for energy and biomass production (Sylvia et al., 1998).

Another structural polysaccharide is chitin. Chitin is a structural molecule, found in the exoskeleton of crabs and related animals, such as lobsters and insects, and a major cell wall component of most fungi and some algae (Voet & Voet, 2004). "Chitin and cellulose have similar structures" (Voet & Voet, 2004). Chitin, insoluble in water, is degraded enzymatically (Alexander, 1977). In soil, the decomposition rate of chitin is comparable to cellulose (Alexander, 1977).

Hemicelluloses are the class of polysaccharides present in cell walls in higher plants, but they have no structural relationship with cellulose (Alexander, 1977). Within the plant cell wall, the cellulose is embedded in the hemicellulose (Mathews & van Holde, 1996). Hemicelluloses are generally-branched polymers, usually containing more than one type of sugar monomer and uronic acids (Alexander, 1977; Mader, 1998; Sylvia et al., 1998). This is opposed to the linear arrangement of glucose found in cellulose. Hemicelluloses usually contain from 50 to 200 sugar units (Sylvia et al., 1998). The polymer ranges from 30 to 300 units long and is partially soluble in water (Adl, 2003). Hemicellulose can also cross-link with lignin, creating a complex web of bonds that provide structural strength. The basic stoichiometric formula for hemicellulose is $[C_{12}H_{20}O_{15}]_n$.

Decomposition of hemicelluloses follows the same steps as cellulose but with an initial rapid rate that exceeds the rate for cellulose. The subsequent rate, however, then appears to slow (Alexander, 1977). Hemicelluloses must be hydrolyzed into simple carbohydrate molecules before they can be assimilated into the cell (Alexander, 1977). Three types of enzymes may be involved in cleaving the different bonds within the hemicellulose molecule (Alexander, 1977).

The last carbohydrate is lignin. Lignin is a "plastic like phenolic polymer" (Voet & Voet, 2004), containing three elements, carbon, hydrogen and oxygen, the same as the other carbohydrates. However, this carbohydrate structure is an aromatic rather than the straight-structure characteristic of cellulose and hemicellulose (Alexander, 1977). "The basic building block is the phenylpropene unit consisting of a hydroxylated $6\text{-}C$ aromatic benzene ring (phenol) and a $3\text{-}C$ linear side chain" (Alexander, 1977). Typically, lignin is composed of 500 to 600 phenylpropene units with randomly-condensed units of substantial cross-linkages. The linkages are a variety of different chemical bonds which can involve either $C\text{-}C\text{-}C$ or $C\text{-}C$ linkages. These linkages may occur between benzene rings, side chains, or rings to side chains (Alexander, 1977; Sylvia et al., 1998).

There are three common phenylalcohols in lignin: the coumaryl alcohol, with no $\text{-}OCH_3$ groups; coniferyl alcohol, with one $\text{-}OCH_3$ group; and sinapyl alcohol, with two $\text{-}COH_3$ groups (Sylvia et al., 1998). It is not possible to present a specific structure because of the chemical variations (Sylvia et al., 1998). The basic stoichiometric formulas for the three common lignins are: $[C_9H_{10}O_2]_n$ for coumaryl; $[C_{10}H_{12}O_3]_n$ for coniferyl; and $[C_{11}H_{14}O_4]_n$ for sinapyl (Zumdahl, 1993).

Lignin is the most recalcitrant of the plant cell-wall molecules. Higher proportion of lignin present results in lower bioavailability of the substrate. Decomposition can occur in the presence or absence of oxygen (Alexander, 1977). Under anaerobic conditions, decomposition is limited and lignin accumulates (Sylvia et al., 1998). The effect of lignin on the bioavailability of other cell-wall components is thought to be largely a physical restriction, with lignin molecules reducing the surface area available to enzymatic penetration and activity (Alexander, 1977). According to Adl (2003), "the

reason for slow decomposition…is the scarcity of primary saprotrophs that are able to digest it." Some organisms, particularly fungi, have developed the necessary enzymes to break lignin apart. The initial reactions are mediated by extracellular lignin and anganese peroxidases, primarily produced by white-rot fungi, mostly *Basidiomycetes* (Adl, 2003). Actinomycetes can also decompose lignin, but typically they degrade less than 20% of the total lignin present.

A detailed biochemical characterization as related to degradation is limited because of lignin's complexity (Sylvia et al., 1998). Sylvia et al. (1998) describe the decomposition as follows: decomposition of lignin generally begins outside the cell with the oxidation and removal of the exposed side chains; next is depolymerization, in which individual phenolic units with side chains are removed. The microbial cell can absorb the chains; once inside the cell, side chains are removed. If hydroxyl groups exist on adjacent carbons on the phenolic ring, the ring can be cleaved; and finally, the resulting molecules are then metabolized for energy and biomass production.

Lipids

The second major organic macromolecule is the lipid. Lipids are small molecules, not polymers. They have a polar, hydrophilic head and a nonpolar, hydrophobic, hydrocarbon tail (Mathews & van Holde, 1996). The polar, hydrophilic head is a carboxyl group and is water soluble. The nonpolar, hydrophobic tail tends to clump in a noncovalent association, and is insoluble in water. Mathews and van Holde (1996) state that when in contact with water lipids form a structure that "depends on the specific molecular structure of the hydrophilic and hydrophobic parts of the lipid molecule."

There are five general types of lipids. The simplest lipid is the fatty acid. The fatty-acid molecule is the basic lipid structure and is composed of one long hydrocarbon chain, 16 to 18 carbon atoms, with a carboxyl group at one end (Mader, 1998). Most are rarely free by themselves but are combined. An example is waxes. Waxes are long-chain, fatty-acid bonds with a long-chain alcohol. The molecule is weakly hydrophilic because the polar head is attached to two hydrocarbon chains. Thus, they are waterproof and resistant to decomposition.

The second group, the triacylglycerols, is referred to as triglycerides or neutral fats. It is composed of a glycerol with three hydroxyl groups (Mathews & van Holde, 1996). These are the fats (of animal origin, solid at room temperature) and oils (plant origin, liquid at room temperature). They are water insoluble.

The last three lipid groups constitute biological membranes. The first is glycerophosolipids (Voet & Voet, 2004), commonly known as phospholipids (Mathews & van Holde, 1996). They have a very polar head and, in most cases, two hydrogen tails (Mathews & van Holde, 1996). Phospholipids are constructed like a neutral fat, except in the place of a fatty acid is a phosphate group or a group that contains both a phosphate and nitrogen. This phosphate group is polar and thus water soluble (Mathews & van Holde, 1996). According to Stevenson and Cole (1999), phospholipids are insoluble in water. The second group is steroids. Steroids are a major component of animal plasma membranes, of which the most abundant is cholesterol (Voet & Voet, 2004), also classified as a sterol (Voet & Voet, 2004). The last group is sphingolipids. The head group contains saccharides. The membrane lipids are readily digested (Adl, 2003).

Proteins

The third major organic macromolecule is the protein. The monomer is the α-amino carboxylic acid (Morrison & Boyd, 1970). All amino acids contain two important functional groups: a carboxyl (acid) group ($-COOH$) and an amino group ($-NH_2$) (Mader, 1998). Because both of these functional groups are ionic, all amino acids are hydrophilic (Mader, 1998). The linkage between amino acids is known as amides ($-NHCO-$) and is referred to as a peptide bond (Morrison & Boyd, 1970).

Polymers containing only a few amino groups are known as peptides (Mathews & van Holde, 1996). If the chain of amino acids is long and linear, it is called a polypeptide (Voet & Voet, 2004). Proteins are extremely complex molecules consisting of one or more polypeptide chains (Mathews & van Holde, 1996; Voet & Voet, 2004) with structural and metabolic functions (Mader, 1998). Hair, nails, and collagen fibers are structural proteins (Mader, 1998). Cellular proteins, or enzymes, insulin, hemoglobin are metabolic proteins (Mader, 1998). Polypeptides may range in length from approximately

40 to approximately 33,000 amino acid units, although only a few have more than 1500 units (Voet & Voet, 2004).

Some proteins rapidly degrade while others are quite stable (Adl, 2003; Voet & Voet, 2004). Polymers of amino acids decompose readily in soil (Sylvia et al., 1998). Proteins are broken down by splitting the chain at the peptide bonds, releasing more soluble and less hydrophobic peptides or soluble amino acid monomers. Deamination reactions release ammonia ion (NH_3^+) from the amino acids or amino sugars (Adl, 2003). Proteins are the only major macromolecule that contains sulfur, an essential macronutrient.

Nucleic Acids

The fourth major organic macromolecule is the nucleic acid. The nucleotide is the nucleic acid's monomeric unit (Voet & Voet, 2004), containing a molecular complex of three types of unit molecules: phosphate (phosphoric acid), a pentose sugar (5 carbons), and a nitrogen-containing base (Mathews & van Holde, 1996). Nucleic acid chains can be hundreds of million units long (Mathews & van Holde, 1996), containing most of the phosphorous found in cells (Singer & Munns, 1999). Nucleotides have metabolic functions in the cell (Mader, 1998). Examples of nucleic acids are ribonucleic acid (RNA), deoxyribonucleic acid (DNA), and adenosine triphosphate (ATP) (Mader, 1998).

Nucleic acids are degraded to its monomer by nucleases (Stevenson & Cole, 1999). "Pure nucleic acids added to soil are rapidly dephosphorylated (Alexander, 1977)." An example is RNA, which is naturally unstable outside the cytoplasm and readily decomposes (Adl, 2003). This mineralization is affected by the pH: as acidity increases, the rate of mineralization decreases (Alexander, 1977).

Summary of macromolecules

A summary of the relative rate of microbial decomposition of the major organic macromolecules, and the elements that constitute these macromolecules is presented in Table 3.1. All the macromolecules contain carbon, hydrogen and oxygen. However, to have biodegradation, the proper C/N/P/S ratio is required. Only the phospholipids and nucleic acids contain phosphorous, and only proteins contain sulfur. These

macromolecules must be present for decomposition. In composting practices only the C:N ratio is calculated (Rynk et al., 1992). An assumption is made that the necessary ratio of phosphorous and sulfur are present. As to biodegradability, with the proper nutrient ratios, all organic compounds can be placed in one of three groups: most of the major organic macromolecules are readily-biodegradable; the cellulose, chitin, and hemicellulose are slower-to-biodegrade; and the lignin is resistant-to-biodegradation.

Analytical Chemistry Methods

All type of materials can be utilized for composting. Some will compost easily; some will be moderate; to others will be very resistant. Since all organic materials fall into one or more of the four major organic macromolecules; their components can be divided into one of the four major types of substrate: 1) readily-degradable or soluble; 2) slower-to-biodegrade substrate; 3) resistant-to-biodegradation; and 4) all inert material remaining (ash/inorganic). This is one of the bases for this research model. Analytical procedures are required to determine the quantity of each substrate type.

An analytical approach used for forage analysis can be readily adapted to determine the quantity of each substrate present in each ingredient type that comprises a composting mixture. This analysis is accomplished in several procedures. The initial procedure is to digest the sample with neutral detergent. The residue is the hemicelluloses, cellulose, lignin fibers, and inert materials such as minerals. The quantity lost is the soluble portion of the sample. Next, the residual from the first procedure is digested with acid detergent. This residual is the celluloses, lignins and inert materials. The quantity lost is the hemicellulose. The third digestion uses a different acid detergent. The residue contains the lignins and inert materials. The quantity lost in this acid detergent digestion is the celluloses. The fourth procedure is to burn the residual. The lost material is the lignins. The residue ash/inorganic is the inert materials. Figure 3.1, adapted from North Dakota State University Extension Office, outlines the schematic utilized in laboratory analysis. To complete the identification, two other analytical procedures are required, one for nitrogen and the other to determine moisture content. These results are sufficient to determine the amount of each substrate, nitrogen, and moisture content for the model. The procedures utilized are published by ANKOM

Technologies, Macedon, New York, and by *Official Methods of Analysis of AOAC International*, by AOAC International, Gaithersburg, Maryland.

Microbial Component

The microbial component in this model deals with the microorganisms that degrade the substrates. Current models are concerned with bacterial microorganisms because they are the primary decomposers of soluble substrate. In Stombaugh and Nokes's (1996) model, the microbial concentration was treated as if it were all bacterial. However, they stated the microbial concentration represents the total microbial biomass, including mesophilic and thermophilic bacteria, actinomycetes, and fungi. Although all microorganism types are involved in the decomposition of a specific substrates type, each type of substrate has a predominate microorganism that degrades the particular substrate: bacteria for the soluble or readily-biodegradable substances, actinomycetes for the cellulose/hemicellulose or slower-to-biodegrade substances, and fungi for the lignin or resistant-to-biodegradation substances.

This research model divides the microbial population into the three major microorganism types, each with a factor to adjust the growth rate according to the degradability of the substrate type (soluble, that is, readily-biodegradable; the hemicellulose/cellulose, that is, slower-to-biodegrade; and, lignin, that is, resistant-to-biodegradability). The bacteria consume the soluble substrate, producing heat, which results in the rapid increase in compost temperature. The actinomycetes utilize the hemicelluloses and cellulose substrate. Because the decomposition is slower, the microorganism growth is slower, and the resulting contributing of heat is small, there is only a slight increase in temperature. The brown- and white-rot fungi utilize the resistant-to-biodegradability lignin in a very slow process that produces insufficient heat to maintain an elevated temperature of the substrate mass; thus the compost returns to ambient temperature.

Table 3.1 Relative rate of microbial decomposition of the major macromolecules

Organic Compounds	Elements Available	Degradability of Substrate					Biodegradability Category
		Stentiford (1993)	Alexander (1977)	Epstein (1977)	Sylvia et al. (1998)	Adl (2003)	
CARBOHYDRATES	C, H, O						
Sugars		readily biodegradable	readily	very susceptible	readily biodegradable		Readily-biodegradable
Starches		readily biodegradable	readily	very susceptible	readily biodegradable		Readily-biodegradable
Glycogen		readily biodegradable	readily	very susceptible	readily biodegradable		Readily-biodegradable
Cellulose		slower to biodegrade	Readily, slower than hemicelluloses	usually susceptible			Slower-to-biodegrade
Chitin		slower to biodegrade	similar to cellulose	usually susceptible			Slower-to-biodegrade
Hemicellulose		slower to biodegrade	readily, but is slow because its presence with other polysaccharides	usually susceptible			Slower-to-biodegrade
Lignin			resistant	resistant	slow compared to cellulose and hemicellulose	very resistant	Resistant-to-biodegradation
LIPIDS	C, H, O						
Fatty Acids		readily biodegradable		very susceptible	readily biodegradable	readily degradable	Readily-biodegradable
Triglycerols				very susceptible		readily degradable	Readily-biodegradable
Glycerophosolipids (Phospholipids)	also P			very susceptible		readily degradable	Readily-biodegradable
Steroids				very susceptible		readily degradable	Readily-biodegradable
Sphingolipids				very susceptible		readily degradable	Readily-biodegradable
PROTEINS	C, H, O, N, S	readily biodegradable		usually susceptible	readily biodegradable	some readily degradable, some stable	Readily-biodegradable
NUCLEIC ACIDS	C, H, O, N, P	readily biodegradable		very susceptible	readily biodegradable	readily degradable	

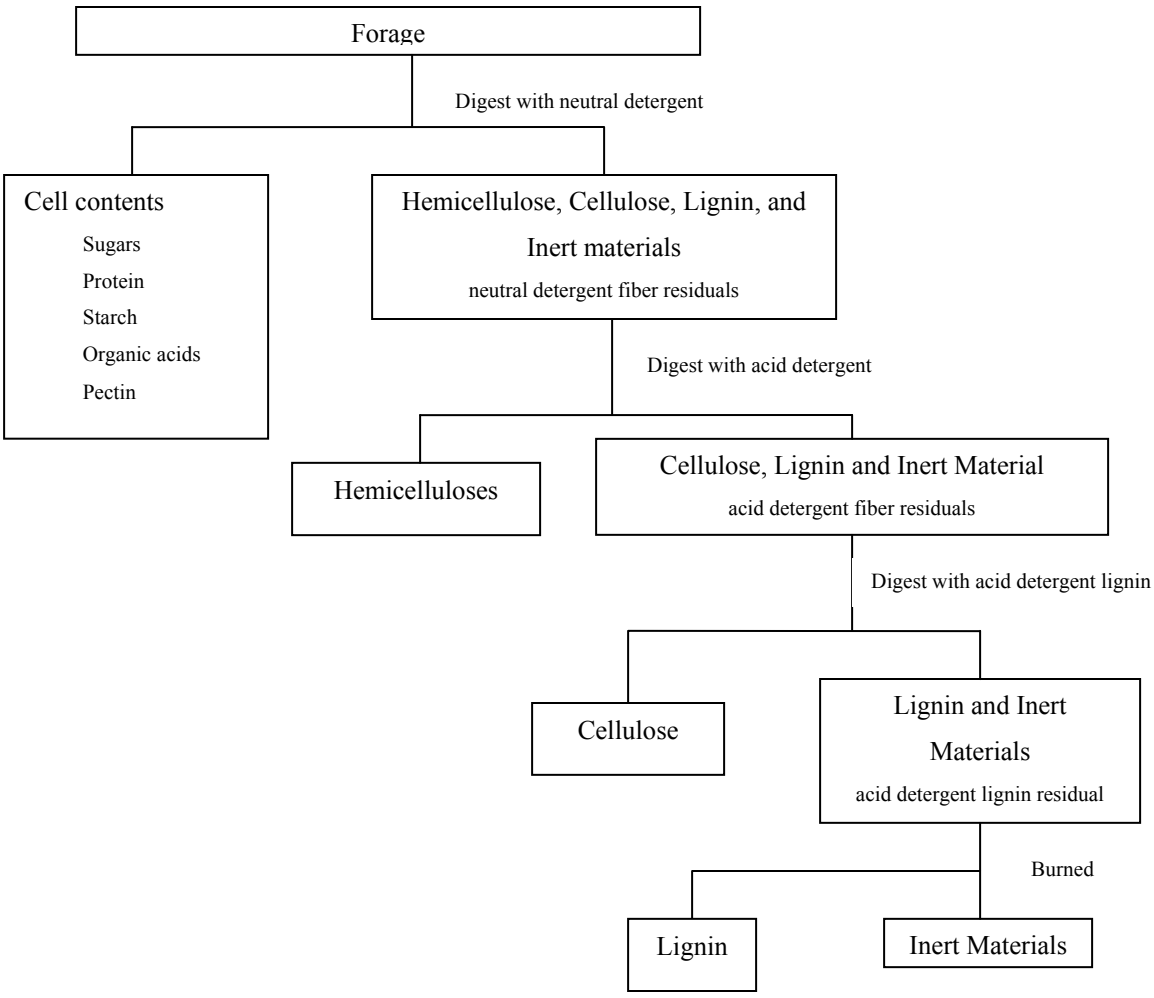

Figure 3.1 Schematic of products utilizing detergent system of forage analysis (North Dakota State University Extension Office, 2004)

Fundamentals of microbial growth

Composting occurs within an ecosystem that initially favors extreme r-strategists, which are those that exhibit rapid growth when readily-available resources are abundant. As these readily-available resources are utilized, the habitat becomes more suitable for K-strategists, those that exhibit slow growth on recalcitrant nutrients (Miller, 1996). Regardless, if the microorganism is an r- or a K-strategist, microbial populations follow a similar growth curve. A microbial population proceeds through growth phases (Figure 3.2) that may be plotted as microbial biomass concentration verses time, if, within a

closed environment, there is a fixed quantity of nutrients available and sufficient not to restrict growth (Berry, 1988; Cundiff & Mankin, 2003; Palmisano & Barlaz, 1996).

The initial phase of this plot is the lag phase. It is in this phase that the organism becomes adjusted to its environment. The lag phase may be short or long depending on the condition of the microorganism and the environment (Cundiff & Mankin, 2003). For example, a finite amount of time is required for fungi spores to germinate and grow (Berry, 1988) or if the compostable material is cold, temperature is not favorable for microbial growth. The organism enters into the acceleration phase after adjusting to the environment. The biomass concentration starts to change at a rate that is increasing but unpredictable (Berry, 1988). Microbial concentration continues to increase but the rate becomes constant. This is the growth phase; in which sufficient substrate is available and environmental conditions do not restrict growth. It is the most significant phase in terms of biomass production (Berry, 1988). The cell's composition is relatively uniform and typical of vegetative growth (Berry, 1988). According to Berry, this phase "is amenable to mathematical analysis which permits prediction of growth characteristics." This prediction is the maximum-specific-growth-rate parameter currently used in models.

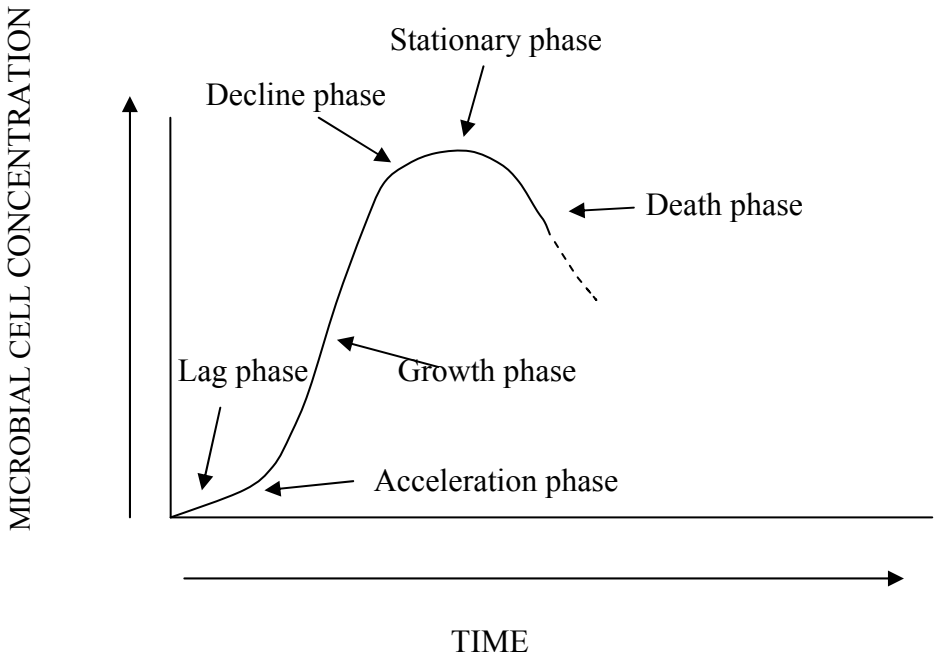

Figure 3.2 Microbial population growth curve

The fourth phase is the deceleration (Berry, 1988) or decline (Cundiff & Mankin, 2003) phase. It represents the occurrence of some nutrient limitation or environmental condition that restricts the organism's growth (Cundiff & Mankin, 2003). The type of nutrient limitation dictates the subsequent response of the cells to the remainder of nutrients available (Berry, 1988). For fungi, carbon limitations can depress the metabolism, releasing a wide range of enzymes; oxygen limitations might cause autolysis; and nitrogen limitations might result in carbohydrate storage compounds (Berry, 1988). In the fifth, or stationary, phase, the slope of the population versus time curve becomes zero as the rate of growth continues to decrease. Microbial growth appears to be constant only as a result of a particular nutrient limitation (Berry, 1988). The stationary phase may represent an equal growth and death rate (Cundiff & Mankin, 2003); it continues until conditions change to allow the increase of either the growth rate or the death rate.

The microbial population declines if insufficient nutrients or energy source are available, if toxic products accumulate, or if environmental conditions remain unsuitable to support the microbial population. This decline is the death phase. The decline is caused by two effects: first, the endogenous metabolism of stored carbohydrates within the cellular material, and second, the death of cells and active decay of material due to autolysis (Berry, 1988). New cell growth does occur in the death phase, as well as in the stationary phase, because the autolysed cells provide the limiting nutrients. It is difficult to predict the decline phenomena mathematically (Berry, 1988).

Microorganisms are also classified according to the temperature of the habitats they tolerate and in which they grow. The three organism classes, psychrophiles or cryophiles, mesophiles, and thermophiles, correspond to the three broad habitat ranges. Generally, the psychrophilic microorganisms grow optimally at temperatures below 15 ºC, the mesophilic grow optimally at 15 ºC to 35 ºC, and the thermophilic thrive in temperatures in excess of 40 ºC to 50 ºC (Sylvia et al., 1998). In composting, the microbial habitats of concern are the mesophiles and thermophiles.

The composting process can be divided into four phases (Figure 3.3) based on temperature: a mesophilic phase (Phase I); a thermophilic phase (Phase II); a cooling phase (Phase III); and a maturation phase (Phase IV) (Gray et al., 1971; Epstein, 1997;

Finstein & Morris, 1975). In Phase I, the compost mass is at ambient temperature and may be slightly acidic. Degradation of easily-mineralized substrate occurs, producing carbon dioxide and water. Rapidly-growing aerobic bacteria are the primary microorganism population. As the indigenous organisms multiply, the temperature, a product of metabolic activity, rises rapidly. Production of simple organic acids during this phase can cause a slight drop in pH. According to Miller (1996), the mesophilic microorganisms die at about 45 °C.

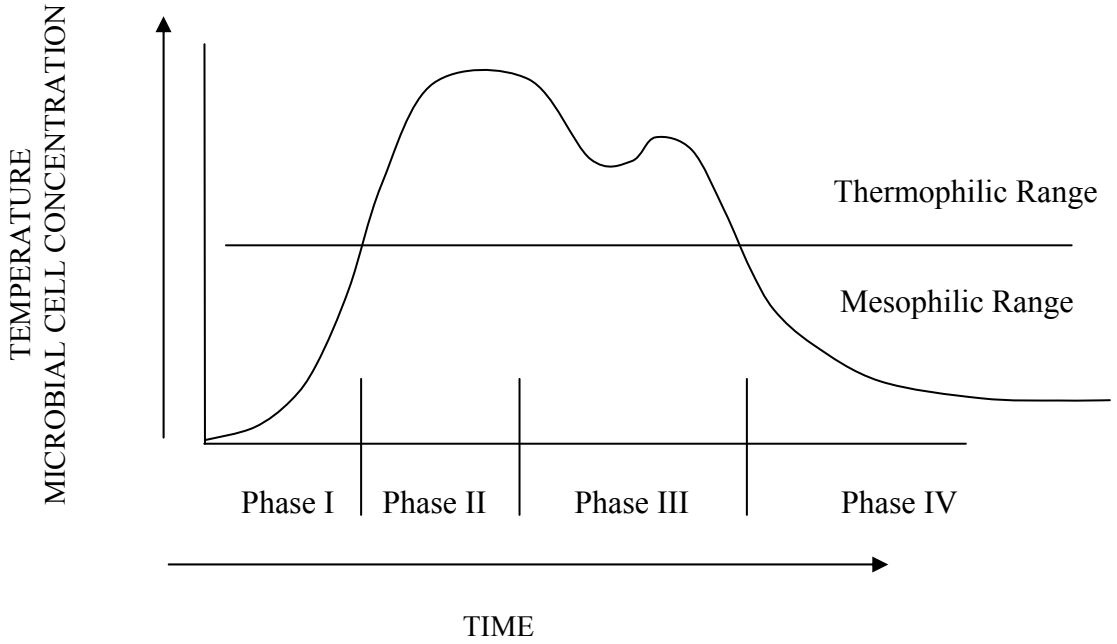

Figure 3.3 Composting phases: mesophilic phase (Phase I), thermophilic phase (Phase II), cooling phase (Phase III) and maturation phase (Phase IV).

In Phase II, the temperature exceeds 40 ºC. The mesophilic population declines and the thermophilic population begin to grow. Depending on the amount of readily-degradable substrate, the temperature continues to rise rapidly. Composting temperatures reach 60 ºC to 70 ºC in two or three days if there is sufficient readily-degradable substrate (Sylvia et al., 1998). This temperature range is important because pathogenic organisms can be destroyed if these temperatures are maintained for a minimum of three consecutive days (Palmisano & Barlaz, 1996). Microbial activity and diversity decreases above 55 ºC to 60 ºC (McKinley & Vestal, 1985a, b; Strom, 1985a, b), substantially limiting the rate of organic matter decomposition. The pH increases, and ammonia may

be liberated following protein deamination. Temperatures above 50 °C allow thermophilic bacteria to be active. Neither fungi nor actinomycetes can withstand these temperatures (Miller, 1996). Miller did not specify if these microorganisms either died or became inactive. As soluble (readily-degradable) substrates decline, heat loss exceeds metabolic heat generation, and the temperature begins to fall. Actinomycetes and fungi populations become more dominate, secreting extracellular enzymes that break down polymers such as cellulose and other complex carbohydrates.

Phase III is the cooling phase. As metabolic activity decreases, the temperature continues to decrease to ambient (Miller, 1996). "Thermophilic bacteria have used up the most-readily-available substrates, and bacterial metabolic activity can no longer liberate heat fast enough to maintain high temperatures" (Miller, 1996). The thermophiles expire or go dormant when the lower limit for thermophilic microorganisms is approached. As temperatures fall below 40 ºC, the mesophilic organisms recommence activity. Early in this stage, actinomycetes populations increase as temperature begins to decline (Miller, 1996), and the more complex substrates are attacked by extracellular enzymes (Miller, 1996). As the temperature drops below 35 °C and the percent concentration of the remaining substrates are ever more resistant to decomposition, the fungal populations become more dominate (Miller, 1996). The pH drops slightly during this time. Nitrifying bacteria, which were inhibited at the higher temperatures, begin to convert ammonia to nitrite (Palmisano & Barlaz, 1996).

Phase IV is compost maturation. Mature compost normally heats to less than 30 ºC (Sylvia et al., 1998). This phase is critical to its agronomic use. Immature compost can introduce phytotoxic materials, such as ammonia or volatile fatty acids, into soils (Iglesias-Jimenez & Perez-Garcia, 1992). The phytotoxic materials are reduced in this phase. Figure 3.3 shows the four composting phases in relationship of temperature as a function of time (Palmisano and Barlaz, 1996). The shape of the curve will vary based on the factors affecting decomposition.

The center piece of composting is microbial decomposition. Combining Figure 3.2, which depicts the different phases of the microbial population growth curve, with Figure 3.3, the composting phases, a view of the changes in the microbial populations as affected by nutrient limitations and the influence of habitat ranges is

developed (Figure 3.4). The curves are a general representation for any of the three major types of microorganisms: bacteria, actinomycetes, or fungi. All three major soil microorganism groups are present when the composting process begins (Sylvia et al., 1998), and each microbial population change is based on their particular environmental requirements as composting proceeds through the four composting phases. Hence, one set of curves can be drawn for each type of microorganism. This is the basis of dividing the composting model into the three microbial populations, the bacterial, the actinomycetes, and the fungi; and into two habitat ranges, the mesophilic and thermophilic.

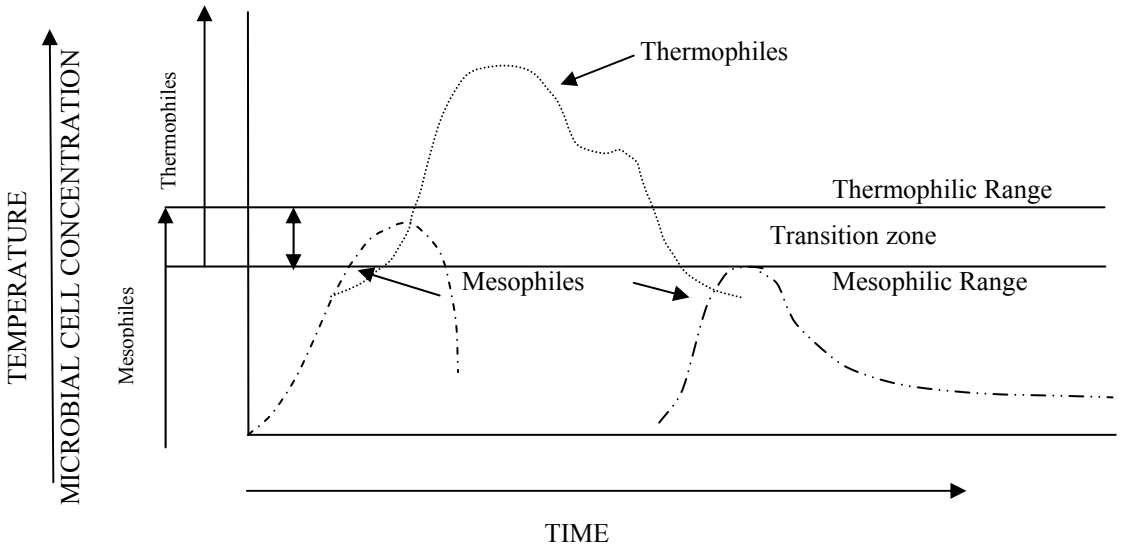

Figure 3.4 Estimated microbial growth curves as a function of temperature for both mesophilic and thermophilic microorganisms

Microbial Populations

Soils contain five major groups of microorganisms: bacteria, actinomycetes, fungi, algae, and protozoa (Alexander, 1977). The bacteria, actinomycetes, and fungi are normally present during composting (Sylvia et al., 1998).

Bacteria

Bacteria are recognized as the most important group of microorganisms in the first and most active stage of the composting process (Miller, 1996). "Bacteria tend to

dominate the earliest stages of composting because they can multiply rapidly on simple and readily-available substrate and many can withstand high temperatures and low oxygen tensions" (Miller, 1996). They are a diverse group of single-celled microorganisms that inhabit soils of every ecosystem. Environmental influences affect density and composition. Primary environmental variables influencing soil bacteria include moisture, aeration, temperature, organic matter, acidity, and inorganic nutrient supply. These microorganisms are "r" strategists, capable of rapid growth and vigorous decomposition when utilizing readily-absorbable compounds. These simple compounds are water-soluble nutrients, which can be absorbed through the organism's cell wall structure. However, if the organic nutrients available to bacteria are large, complex polymers contained in plant and animal residuals, the organism must excrete extracellular enzymes to break the polymer structure into smaller molecules that can be absorbed. This reduces the speed by which decomposition occurs.

Moisture is a critical component for aerobic bacteria because they derive oxygen from that which is dissolved in the water. The amount of dissolved oxygen in the water is limited by the small diffusion coefficient of oxygen in water. The cell obtains the oxygen by diffusing it through the cytoplasmic membrane (Lengeler et al., 1999, p. 261). The amount of oxygen diffused in water is dependent on temperature (Lengeler et al, 1999, p. 261, 726) and the thickness of the water film (Sexstone et al., 1985). In composting, the maximum bacterial density is found in regions of fairly high moisture content. The optimum level for activities of aerobic bacteria is often at 50 to 75 % of soil's moisture-holding capacity, with 60% being the optimum (Paul & Clark, 1996). Within an environment of excessive moisture, microbial proliferation is suppressed because excess moisture limits gaseous exchange and lowers the available-oxygen supply, creating an anaerobic environment.

Actinomycetes

Actinomycetes are a special group of soil bacteria that play an important role in decomposition. They resemble fungi, forming filaments, often branched and sometimes tightly interwoven (Paul & Clark, 1996), but their filaments are strictly morphological (Sylvia et al., 1998). Their slower growth characteristics make the actinomycetes ecologically intermediate between bacteria and fungi (Miller, 1996). They are important

agents in the degradation of high-molecular-weight organic materials, such as cellulose, chitin, proteins, etc., and contribute to the formation of stable humus (Paul & Clark, 1996). Research indicates that actinomycetes, along with fungi, may play an important role in the degradation of lignin (Sylvia et al., 1998). Actinomycetes are often described as slow-growing organisms. Culture plates require one to two weeks of incubation to allow colony differentiation (Sylvia et al., 1998). Actinomycetes do not compete well with the faster-growing bacteria and fungi for readily-available-carbon substrates; however, they are thought to be important in mineralizing carbon and nitrogen formed during the early stages of decomposition (Sylvia et al., 1998).

Actinomycetes tend to respond to environmental influences similar to bacteria (Sylvia et al., 1998). The primary influences include organic matter, pH, moisture and temperature (Alexander, 1977). "They tend to prefer moist, highly-aerobic conditions and a neutral or slightly alkaline pH" (Miller, 1996). They tend to be in the 25 ºC to 60 ºC range and are important in high-temperature transformation of organic substances (Sylvia et al., 1998). Actinomycetes tend to become more abundant in soils subjected to prolonged drying (Sylvia et al., 1998). This shift toward numerical dominance is generally attributed to their being less sensitive to semi-dry conditions (Alexander, 1977; Sylvia et al., 1998).

Thermoactinomycetes, which have an optimal growth range of 35 ºC to 58 ºC, are common and important in compost decomposition (Paul & Clark, 1996). About 90% of all actinomycetes isolations from soil are *Streomyce*. This large and diverse group is widely distributed in soil, litter and composts. Nearly all are saprobic thermotolerants that grow in the range of 45 ºC to 55 ºC and are important decomposers in compost and manure piles (Paul & Clark, 1996). The nutritional mechanism by which these organisms obtain their food is exclusively from the degradation of non-living-organic material. They are capable of degrading many resistant substances, among them lignin, chitin, pectin, keratin, complex aromatics, and humic acids (Sylvia et al., 1998). This can put them at a disadvantage when the density of available substrates is high. Thus, actinomycetes tend to be common in the later stages of composting and can exhibit extensive growth during this period (Bagstam, 1978, 1979; Joshua et al., 1994).

Fungi

Fungi are very similar to organoheterotropic bacteria. Both use most of the same substrates, and competition between them is common. Fungi obtain nutrients by secreting extracellular hydrolytic enzymes to dissolve the long-chain, polymer substances. They often have a lower nitrogen requirement than bacteria. Fungi are less affected by low-moisture environments; they can grow on dry substrate nourished by moisture absorbed from damp environments, and they can extract moisture from materials that have high-osmotic pressures.

Fungi, which are chemorganotrophic (Paul & Clark, 1996), are the dominant agents in organic-matter decomposition. Typically, fungi form slender filaments or hyphae, which can be branched or unbranched, septate or nonseptate, and they commonly are multinucleate. The subgroup basidiomycetes is an important agent in wood rot (Paul & Clark, 1996). Basidiomycetes attack wooden structures that have a moisture content greater than 20% and less than 80%. Wood rots are categorized either as white rots or as brown rots. White rot fungi destroy both lignin and cellulose, leaving a fibrous, white residue, and brown rots destroy cellulose but not lignin, leaving a powdery, brown residue.

Fungi are present in both the mesophilic and thermophilic habitat ranges (Miller, 1996). Work by Straatsma et al. (1994) revealed a vigorous growth of diverse thermophilic fungi at moderately-high temperatures. According to Fermor et al. (1979), temperatures over 55 ºC usually discourage fungal growth during the more active states of waste composting. Most fungi cannot grow at 50ºC and only a few can grow even poorly at 62 ºC (Brock, 1978). Kane and Mullins (1973) found that fungi were excluded from high-temperature stages of composting. Fungi are commonly recovered from composting materials later in processing when temperatures are more moderate and remaining substrates are predominately cellulose and lignin (Chang & Hudson, 1967; Fergus & Sinden, 1969; De Bertoldi et al., 1982). Fungi can break down many complex polymers, including lignin and organic chemicals not produced in nature (Miller, 1996).

Microbial Composition

Microbial composition is required to develop the stoichiometric relationship between the substrate utilized and growth of a microbial population. This relationship

provides data on the nitrogen and oxygen requirements for growth, and the production of carbon dioxide and water. The basic structural formula for bacteria presented by Cundiff and Mankin (2003) is $CH_{1.7}O_{0.49}N_{0.24}$. Lengeler et al. (1999) presents the structural formula for bacteria as $CH_{1.75}O_{0.38}N_{0.25}$. Both present a C/N ratio of 4:1, however the oxygen component differs. This will affect the amount of oxygen required to be supplied for new cell growth. The currently used structural formula, $CH_{1.7}O_{0.49}N_{0.24}$, is chosen.

Actinomycetes are presented as having a similar structural formula as bacteria. They are classified with the bacteria because they are prokaryotic, an organism lacking a unit membrane-bound nucleus and other organelles even though they appear to resemble fungi (Sylvia, et al., 1998). Their resemblance is strictly morphological (Sylvia, et al., 1998). Thus, the same structural formula, $CH_{1.7}O_{0.49}N_{0.24}$, presented for bacteria is utilized for actinomycetes.

Fungi have a different structural formula. According to Lilly (1965), the composition of fungi is as follows: for hydrogen, an average value for fungus cells lies between 6% and 8%; for carbon, there is a range of 40.0% to 44.3%; for nitrogen, the content ranges from 1.34% to 9.72%; and for oxygen, the range lies between 25% to 35%. Based on this information from Lilly, using an average percentage based on dry weight, an average formula for fungi is calculated to be $CH_{1.97}O_{0.53}N_{0.11}$. Berry (1988) gave a stoichiometric equation for the amount of oxygen required in the oxidation process that shows the microbial molecular formula for fungi as $CH_{1.6}O_{0.53}N_{0.15}$. Berry indicated that if fungi have a C/N ratio of 8/1, fungi would have a molecular formula of $CH_{1.6}O_{0.53}N_{0.125}$; if it were a C/N ratio of 4/1, the molecular formula would be $CH_{1.6}O_{0.53}N_{0.15}$. Berry also presented a molecular formula for yeast as $CH_{1.5}O_{0.5}N_{0.125}$. Hence, an average value would be $CH_{1.65}O_{0.52}N_{0.13}$. This is the value used in this research.

Microbial Community Succession

The substrate composition and its availability and the microbial characteristics influence the microbial community dynamics through time. "The compost microbiota determines the rate of composting and the quality of the product" (McKinley & Vestal,

1985). The microbial community follows a predictable microbial-succession pattern (Herrmann & Shann, 1997). The initial decomposers are dominated by mesophilic- and thermophilic-zymogenous organisms. The mesophilic range consists of fungal and bacterial components. During the subsequent thermophilic phase, the actinomycetes appear and the fungal populations decline. The final community is comprised, primarily, of mesophilic-autochthonous organisms. These are microorganisms specifically adapted to grow under low nutrient supply. They are also known as oligotrophs. In the curing phase, the actinomycetes remain and the fungi reappear along with cellulose-decomposing bacteria.

Nutrition is a major factor in the determination of the relative advantage of some microbial populations over others. Assimilation of carbon and nitrogen has a role in growth and nutritional uptake. Generally, microbes that tend to grow quickly will assimilate lower proportions of substrate carbon through metabolic inefficiency, while slower growers are more efficient at carbon assimilation (Miller, 1996). Bacteria and actinomycetes prefer C/N ratios on the order of 10:1 to 20:1, while fungi prefer ratios on the order as high as 150:1 or 200:1, and even higher for some fungi (Griffin, 1985). Bacteria tend to grow well on proteins and other simple nitrogen-containing compounds. Excess nitrogen is primarily released as ammonia at pH 8 and higher or as ammonium ion at pH 7 and lower. Ammonia release is significant because it solubilizes complex carbon sources, making them available for uptake by microbes (Myers & Thien, 1988). However, higher ammonia concentrations (up to about 1,000 mg L^{-1}) are well tolerated by bacteria but are inhibitory to many fungi (Miller et al., 1991). Much of the ammonia released by bacteria from proteins can react with complex carbohydrates (Nommik, 1965, 1970), becoming the preferred nitrogen source for many fungi (Fermor et al., 1985). Also, nitrogen sequestered in bacterial cells provides a stable but available form for nitrogen nutrition when the bacterial cells die and are actively decayed by autolysis (spontaneous lysis) (Berry, 1988).

Based on the above, it is extremely difficult to predict a particular microbial community growth outcome. There are an infinite number of combinations. There are, however, general trends. Walke (1975) studied fluctuations in microbial populations during windrow composting of biosolids and bark. He found that in the initial stages of

decomposition where soluble compounds such as sugars, alcohols, acids, and proteins were available, bacteria dominated. Turning the windrow on the 36th and 68th days also increased bacterial populations. This was the result of re-oxygenating the windrow. Fungi and actinomycetes populations decreased.

De Bertoldi et al. (1980) studied populations of bacteria, fungi, and actinomycetes during windrow and forced-air composting of biosolids with an organic fraction of municipal solid waste. He found bacteria populations increased during the first 14 days, then decreased. A similar pattern, but at a lower magnitude, was observed for the ammonia, proteolytic, pectinolytic, cellulolyic and, nitrogen-fixing bacteria populations, which all increased during the first 7 days, then decreased.

Safwat (1980) studied changes in the microbial populations during composting of cottonseed wastes. He found mesophilic bacteria were higher than populations of thermophilic bacteria throughout the composting period. Composting temperatures exceeded 68ºC. Temperatures exceeded 52ºC from Day 7 through Day 120. Cellulose-decomposing bacteria increased with increasing temperature for the first 60 days, then decreased to undetected levels by the Day 150.

Chino et al. (1983) determined microbial populations during composting of biosolids and rice hulls. He found the highest counts of aerobic bacteria, fungi, ammonifiers, and denitrifiers occurred in the middle stage (35 days). The actinomycetes increased for the first 35 days then decreased. Walke (1975) and De Bertoldi et al. (1980) found similar patterns for thermophilic actinomycetes.

Fungi, especially basidiomycetes, are generally recognized as the major microbial group responsible for lignin degradation. Actinomycetes and bacteria are involved in lignin degradation, but to a much lesser degree (Sylvia et al., 1998). In lignocellulosic wastes, microbial activity during the most active stage of composting is based on the metabolic utilization of cellulose and noncellulosic polysaccharides (Macauley et al., 1993; Nakasaki et al., 1994). Lignin appears to be structurally altered by significant oxidation during the thermophilic stages of mushroom composting, but it is not decomposed (Iiyama et al., 1994). Based on evidence from grease traps wastes, lipids can be utilized rapidly by bacteria, including actinomycetes under thermophilic conditions (Joshua et al., 1994). The decomposition of sugars, polysaccharides, proteins,

and lipids are within the general metabolic capability of species of Bacillus and Clostridium (Brock & Madigan, 1988). Rates of protein decomposition are high early in composting, based on the release of large amounts of ammonia (Miller et al., 1990, 1991).

McKinley and Vestal (1985) stated "a decrease in microbial activity occurred as temperature increased." They reported that,

> within certain temperature ranges (e.g. 60 ºC to 65 °C), a relatively small change in temperature can cause a change of 1 or more orders of magnitude in microbial activity. The maximum microbial activity was generally … from the 35 ºC to 50 °C.

McKinley and Vestal (1985) also reported that,

> temperature has been shown to affect rates of microbial decomposition…However, most of the data are difficult to interpret due to variations in composting materials and practices as well as differences or inadequacies in methods of quantifying microbial biomass and activity.

McKinley and Vestal (1985) indicated bacteria tend to dominate over fungi throughout the composting temperature ascent when adequate moisture is present. As the temperature increases, the numbers of viable fungi declined rapidly as the temperature approaches 60 °C, and they nearly disappear at 65 °C. They also found consistently much lower rates of microbial substrate incorporation in samples taken from the high-temperature areas (> 55 °C to 60 °C) of the compost piles.

As described above, microbial populations change during the composting process. According to Sylvia et al. (1998), the mesophilic bacterial organisms initiate the decomposition process by utilizing the readily-available substrates and increase rapidly in numbers. Few thermophilic microorganisms are present during the mesophilic stage (Phase I). During this phase, heat is generated and retained, and, when sufficient heat is generated and retained, the thermophilic stage (Phase II) is obtained. At this point, the thermophilic organisms begin to decompose more of the readily-available substrate; the thermophilic bacterial numbers increase and the mesophilic numbers decrease. As the

inability of microbial activity to generate sufficient heat, the composting process moves into the stabilization/curing stages (or cooling [Phase III] and maturation [Phase IV]). The mesophilic bacteria numbers remain approximately the same, however the thermophilic bacteria numbers decline.

Fungi follow a similar pattern. While actinomycetes are not especially active in the mesophilic phase, they increase in the thermophilic phase and decrease in the last two phases. This progression in microbial populations is presented in Table 3.2, in which the numbers change based on the type of substrate(s) present. If insufficient readily-available substrates are present, the heat generated would be insufficient to obtain the thermophilic temperature range.

In summary, based on the information presented above, the basic premise is that each major group of microorganisms is associated with a particular substrate. Additionally, to assess what habitat range is present at a particular stage in the composting process, it is necessary to understand the relationship between each microorganism type and temperature.

Table 3.2 Microbial population changes during composting (adapted from Sylvia et al., 1998, pg 487)

Organism	Mesophilic Stage (Phase I)	Thermophilic Stage (Phase II)	Stabilization (*Cooling Phase III*) and Curing (*Maturation Phase IV*) Stages	No. of Species Present
	Colony Forming Units (CFU) g^{-1} dry mass			
Bacteria				
Mesophilic	10^8	10^6	10^6	6
Thermophilic	10^4	10^9	10^7	1
Actinomycetes				
Thermophilic	10^4	10^8	10^5	14
Fungi				
Mesophilic	10^6	10^3	10^5	18
Thermophilic	10^3	10^7	10^6	16

Temperature Habitat Ranges

All biological activities liberate heat as a metabolic waste activity; however the heat dissipates quickly into the environment. During composting, heat liberated

microbially accumulates in the composting material and causes the temperature to increase. The temperature within a composting ecosystem is influenced predominantly by its own heat output: the heat output affects the temperature, and the temperature affects the heat output (Finstein, 1980).

Epstein (1997) published a summary of the habitat ranges for the mesophiles and thermophiles. Table 3.3 summarizes this and other references. The references in Epstein (1997) are:

- Waksman et al. (1939) reported thermophilic fungi, bacteria, and actinomycetes were all active in compost at 50 ºC; fungi were rare, and bacteria and actinomycetes were predominant at 65 ºC; and, spore-forming bacteria were predominant at 75 ºC.
- Waksman and Cordon (1939) indicated that little growth of thermophilic actinomycetes occurred at 28 ºC, optimum growth was at 50 ºC, and no growth occurred at 65 ºC.
- Cooney and Emerson (1964) found the upper limit for fungi to be 60 ºC. Fungi recolonized as the temperature dropped.
- Chang and Hudson (1967) found that both mesophilic and thermophilic fungi decreased in population as the temperature of compost reached 70 ºC. As temperature decreased below 65 ºC, thermophilic fungi resumed growth with populations peaking at approximately 45 ºC.
- Hankin et al. (1976) reported microbial changes during the decomposition of leaves: bacteria increased during the first 10 days and the temperatures ranged between 17 ºC to 36 ºC; many of the mesophilic bacteria were killed at temperatures of 40 ºC to 58 ºC; fungi numbers declined during the thermophilic stage; and, actinomycetes increased in large numbers during the thermophilic stage, but declined as the pile cooled.
- Strom (1985b) concluded that maximum microbial diversity was obtained at 60 ºC. In the laboratory, diversity dropped sharply at incubation temperatures between 60 ºC and 65 ºC. There was no indication that microbial diversity was related to decomposition.

Epstein (1997) presented other studies with wheat straw. He stated mesophilic bacteria increased during the first two days then decreased when the temperature rose to 70 ºC. The bacterial population increased as the temperature decreased to 55 ºC; populations of both thermophilic bacteria and thermophilic fungi grew as temperature increased. The thermophilic fungi growth was limited at temperatures above 70 ºC. The thermophilic bacteria and actinomycetes continued to grow above 77 ºC. The thermophilic fungi began to recolonize as the temperature dropped. The mesophilic fungi began to recolonize at temperatures of 20 ºC to 45 ºC.

Other researchers have reported similar findings. Finstein (1980) reported the impact that temperature has on mesophilic and thermophilic microorganisms. He reported the mesophilic population is stimulated and the thermophilic population is dormant at temperatures between ambient to 38 °C. Between 38 °C and 45 °C, the mesophilic population became inhibited while thermophilic population growth was initiated. Temperatures between 45 °C and 55 °C were catastrophic for the mesophilic population but stimulating for the thermophiles. The thermophilic growth was quite inhibited when the temperature was between 60 °C and 70 °C, and became catastrophic for the thermopiles as temperatures became greater than 70 °C. When temperatures fell to between 55 °C and 60 °C, the thermophiles became slightly inhibited.

According to Miller (1996), "dynamics of population change in various types of self-heating ecosystems show some general trends. Mesophilic bacterial populations tend to peak first, followed by thermophilic bacteria, thermophilic actinomycetes, and thermophilic fungi." Miller (1996) reported mesophilic populations were inhibited by temperatures exceeding the low 40's ºC. Thermotolerant mesophilic bacteria populations, however, can tolerate temperatures up to 50 ºC (Lengeler et al., 1999). Conditions become favorable for growth of thermophiles in the mid 40s ºC. At temperatures in the range of 55 ºC to 65 ºC thermophilic bacteria counts can peak. Optimal decomposition rates are typically in the range of 55 ºC to 59 ºC. Temperatures above 60 ºC start to inhibit microbial activity as the optimum temperature for various thermophiles is exceeded. Fungi normally are absent above 60 ºC when counts of thermophilic bacteria decrease. Actinomycetes are absent above 70 ºC. The maximum temperature achievable through composting is approximately 82 ºC, at which point

biological activity and metabolic heat evolution ceases. In large composting masses, temperatures do not exceed about 80ºC, which is also the temperature at which biological activity effectively stops. As temperatures fall below 65 ºC, actinomycetes counts increase by about an order of magnitude less than the counts of other bacteria. Fungal populations increase later as overall composting activity declines and the temperature drops below 50 ºC.

Table 3.3 summarizes the data presented above. Comparing Table 3.3 with Table 3.2, which shows microbial population changes during composting, indicates both mesophilic and thermophilic bacteria are present in the thermophilic stage (Phase II) and in the cooling phase (Phase III). In addition, there is an obvious absence of mesophilic actinomycetes throughout the entire process. The thermophilic actinomycetes decrease in numbers but are still present during the cooling and maturation stages (Phases III and IV).

Synthesis of all this information yields the following conclusion. A preliminary set of specific temperature ranges for bacteria, actinomycetes, and fungi, in both the mesophilic and thermophilic microorganisms, can be established for the model. Table 3.4 presents the initial temperature range parameters selected for the research model.

Table 3.3 Summary temperature values (habitat ranges) for mesophilic and thermophilic microorganisms

	Lower Limit °C	Mid Range Uninhibited °C	Upper Limits °C
Mesophilic (temperatures for all microorganisms acting as a unit)	<20	38-45 Low 40s 40-58 40-50	45-55
Bacteria	15 17	–	70
Actinomycetes	–	–	–
Fungi	25	45	–
Thermophilic	38 Mid 40s	60 45-60 55-60	>70 82
Bacteria	Mid 40s	50-65 55-60	65 >70 77
Actinomycetes	–	50-65	65 >70 77
Fungi	–	50-60	>60 65 70

Maximum-specific-growth rate

In examining the microbial-growth curve, the growth-phase portion of is the most significant phase in terms of biomass production and "is amenable to mathematical analysis which permits prediction of growth characteristics" (Berry, 1988). In this case, this prediction of growth characteristics, known as the maximum-specific-growth rate parameter ($\mu_{\max}$), is the slope of the population-versus-time line during which the organisms grow exponentially (Zwietering et al., 1990). It is this maximum specific growth rate that is utilized in models. A significant limitation of this parameter is the subjectivity used to determine both the range of the growth curve that is approximately linear and the slope of the linear section (Zwietering et al., 1990).

Table 3.4 Model temperature habitat range selected for the initial research model

	Lower Limit °C	Upper Limit °C
Mesophilic		
Bacteria	15	70
Actinomycetes	Not present	Not present
Fungi	25	45
Thermophilic		
Bacteria	40	77
Actinomycetes	40	70
Fungi	40	65

Zwietering et al. (1990) indicated a better method was to describe the entire set of the microbial growth curve from the lag phase to the stationary phase, estimating the lag phase, maximum-growth rate, and the upper-boundary asymptote. Zwietering et al. (1991) reviewed different models of bacterial growth as a function temperature. They selected a modified model developed by Ratkowsky et al. (1982).

$$\mu_{\max} = \left[b_3 \left(T_C - T_{C\max} \right) \right]^2 * \left\{ 1 - \exp\left[c_3 \left(T_C - T_{C\max} \right) \right] \right\} \qquad (3.1)$$

where:

b_3 = is a Ratkowsky parameter ($^oC^{-1}$ $h^{-0.5}$)

c_3 = is a Ratkowsky parameter ($^oC^{-1}$)

T_C = the temperature (^oC)

$T_{C\max}$ = the maximum temperature at which growth is observed (ºC)

Hamelers (1993) chose to utilize the slope of the line where the organisms grow exponentially as his maximum-specific-growth rate, applying the value of 0.000075 s^{-1} or 0.27 h^{-1}. Stombaugh and Nokes (1996) also chose the linear form, specifying the maximum-specific-growth rate as 0.200 h^{-1}.

Kaiser (1996) considered the microorganisms as four separate groups, basing the maximum specific growth rate parameter on feedback from simulation results. Kaiser (1996) determined that $\mu_{\max}$ for bacteria equaled 0.2 h^{-1}, for actinomycetes 0.1 h^{-1}, for brown-rot fungi 0.05 h^{-1}, and white-rot fungi 0.03 h^{-1}.

According to Seki (2000) the maximum-specific-growth rate ($\mu_{\max}$) and specific-death rate (λ) were the most important parameters in the compost model process. The maximum-specific-growth rate equation utilized by Seki (2000 and 2002) was

$$\mu_{\max,(k,ip)} = \frac{a_1 e^{-b_1/T_{C(k-1,ip)}}}{1+\left(\frac{a_1}{a}\right)e^{-(b_1+b_2)/T_{C(k-1,ip)}}} \qquad (3.2)$$

where:

a_1 = 1.4544 x 10^8

a_2 = 2.0556 x 10^{-35}

b_1 = 6.27 x 10^3

b_2 = 2.601 x 10^4

(k,ip) = indexing notation. Is the cell's reference number identifying the cell's location. The k is the time step and ip is the different levels of the substrate being analyzed mathematically.

T_C = compost temperature, ºC

Seki's (2000, 2002) equation was a function of temperature, developed after work by Aiba et al. (1973) and Fuijita (1993). According to Seki (2000), the constants a_1, a_2, b_1, and b_2 "were determined so the average value of $\mu_{\max}$ in the region of T=20 °C and T=70 °C would be 0.018 h^{-1} … and its maximum would appear at 60 °C." However,

Seki (2000) went on to say, "the parameter μ_{max} and λ are very sensitive to a slight change in condition of the mixed materials such as particle-size distribution even if the material contents are the same. Therefore, their values were modified by multiplying them with correction factors to simulate the composting process." The corrected μ_{max} values Seki (2000) used in his work for different runs were 2.0, 2.7, and 2.6. Hence, his equation as presented is not useful.

Berry (1988) reported most values for the maximum-specific-growth rate for fungi are found to be in the range from 0.1 h^{-1} to 0.2 h^{-1}. Berry (1998) stated, "The rate of fungal growth is influenced by several cellular factors: the rate of hyphal extension, the hyphal radius and the frequency of branching." Griffin (1985) indicated the maximal-growth rates for fungi tend to be about an order of magnitude slower than those of bacteria. Then, if using Kaiser's (1996) number of 0.2 h^{-1}, Stombaugh and Nokes (1996) number of 2.0 h^{-1}, and Seki (2000) maximum number of 2.7 h^{-1}, the maximum-specific-growth rate for fungi would range from 0.02 h^{-1} to 0.27 h^{-1}.

There are two limitations to these rates. One is the rate is applied to the entire biomass concentration and all microorganisms are considered as one group. Second, the rate applied is linear and set at the maximum slope. The maximum-growth rate does not vary as it needs to, as shown in the microbial population growth curve (Fig 3.2). Attempts to vary it have not been successful. Thus, only a linear rate can be considered.

Initially, the maximum-growth rate selected for the research model was 2.0 h^{-1} for bacteria, Stombaugh and Nokes (1996), and 0.1 h^{-1} for actinomycetes, Kaiser (1996). Kaiser's work was also selected for fungi. His two values were averaged to obtain the value of 0.04 h^{-1}. Table 3.6 lists the maximum-specific-growth rates and the rates utilized in the initial research model.

Table 3.5 Maximum-specific-growth rates

Microorganism	Berry 1988	Griffin 1985	Hamelers 1993	Kaiser 1996	Stombaugh and Nokes 1996	Seki 2000, 2002	**Model**
	μ_{max} (h^{-1})						
All microorganism	–	–	0.27	–	2.0	2.0 – 2.7	–
Bacteria	–	–	–	0.2	–	–	**0.02**
Actinomycetes	–	–	–	0.1	–	–	**0.1**
Fungi	0.1 – 0.2	0.02 – 0.27	–	–	–	–	**0.04**
Brown-rot	–	–	–	0.05	–	–	–
White-rot	–	–	–	0.03	–	–	–

Death Rate

Seki (2000) indicated the microbial-death-rate parameter is very sensitive. Hamelers (1993) determined the mass of the dead microbes based on a fraction of the microbial concentration, and used a value of 0.0072 h^{-1}. Hamelers (1993) introduced the dead-microbial fraction back into the substrate as a polymeric substrate, available for hydrolysis. Hamelers considered the polymeric substance to be insoluble, thus exoenzymic reaction must take place outside the cell. To accomplish this, Hamelers utilized a first-order equation.

$$R_1 = K_h * S_P \tag{3.3}$$

where:

R_1 = hydrolysis-reaction rate (mol m^{-3} h^{-1})

K_h = hydrolysis-rate constant (0.00324 h^{-1})

S_P = polymeric substance (mol m^{-3})

Stombaugh and Nokes (1996) also determined the mass of the dead microbes based on a fraction of the microbial concentration. They utilized a value of 0.0250 h^{-1}.

$$\left(\frac{dX}{dt}\right) = \mu * X - \lambda * X \tag{3.4}$$

where:

$\frac{dX}{dt}$ = rate of change of total-microbial-biomass concentration

($kg_{x\ (biomass)}$ m^{-3} h^{-1})

μ = specific-growth rate (h^{-1})

X = total microbial-biomass concentration ($kg_x\ m^{-3}$)

λ = specific-death rate (h^{-1})

This equation considers the fact the death rate directly influences the microbial concentration. However, a reintroduction of dead microorganisms as new substrate was not considered.

Kaiser (1996) handled microbial death as an expired fraction, using a value of 0.001 h^{-1}. This value was subtracted within the microbial-growth equation as follows:

$$\mu_i = \mu_{\max_i} * f_i^{temp}\left(\frac{S_i}{K_{s,i} + S_i}\right) - \lambda \qquad (3.5)$$

where:

μ_i = microbial-growth rate of organism i (h^{-1})

where i equals 1 (bacteria), 2 (actinomycetes), 3 (brown-rot fungi, 4 (white- rot fungi)

$\mu_{\max_i}$ = maximum-growth rate of organism type i (h^{-1})

f_i^{temp} = coefficient of temperature-dependent growth of organism i

S_i = total concentration of growth-defining substrates for organisms i kg kg^{-1} composting material

$K_{s,i}$ = saturation constant of organism i (kg kg^{-1} composting material)

λ = microbial-death rate (h^{-1})

This equation is similar to Stombaugh and Nokes (1996) because they utilized a similar equation to generate the microbial-growth rate. Again, no substrate was considered in the model.

Seki (2002) considered specific-microbial death (λ) to be dependent on temperature only, expressing it using the following Arrhenius-type equation:

$$\lambda = a_d \exp\left\{-b_d\left(T + 273\right)\right\} \qquad (3.6)$$

where:

a_d = constant (h^{-1})

b_d = constant (K)

T = K

Seki (2002) also indicated that, since substrate consumption occurs with microbial growth, dead microbes should be incorporated into substrate. He presented the rate of substrate change as:

$$R_S = \left(-\frac{1}{Y}\mu + \lambda \right) X \tag{3.7}$$

where:

R_s = rate of substrate change (kg kg^{-1} $h^{-1)}$

Y = mass of microbes produced by oxidation per unit mass of substrate (growth yield of microbes) (kg kg^{-1})

μ = specific-microbial-growth rate (h^{-1})

λ = specific-microbial-death rate (h^{-1})

total-microbial-biomass concentration (kg m^{-3})

This equation indicates the rate of substrate use is decreased; the remaining microorganisms become new substrate.

There are other aspects concerning microbial death that need to be considered besides the fraction of the microbial concentration that die per unit time. This is the death of mesophilic organisms as the temperature gradient passes from the mesophilic range into the thermophilic range; the death of all thermophilic microorganisms as the temperature gradient passes from the thermophilic range into the mesophilic range; the death of all microorganisms when the temperature falls below the mesophilic range or exceeds the thermophilic range; and the death of all microorganisms as a result of insufficient substrate. There must be an accounting for this total mass of expired microorganisms. As decomposition progresses, humic substances are produced. Analysis indicates these "compounds belong to recognizable classes of organic compounds, such as polysaccharides, polypeptides, and altered lignins" (Clapp & Hayes, 1999) and "dead microorganism cell walls" (Chefetz et al., 1998). Since these humic substances are resistant to biodegradation, a fraction of the expired microbes must be added to the lignin. The remaining mass of expired microorganisms is reintroduced as soluble substrate for utilization. This is extremely important if the availability of nitrogen is limiting. The nitrogen contained in the expired microbial mass now becomes

available. This is critical if the growth rate is controlled by the amount of nitrogen available, allowing the decomposition action to proceed.

The research model developed herein accounts for all the above aspects. First, there are two death rates established. One is for the fraction of the microbial concentration that dies per unit time. This is 0.025 h^{-1}. The other accounts for the death of the microorganisms as the temperature gradient pass from the mesophilic range into the thermophilic range and vice versa. Since not all die immediately, this value is set at 0.4 h^{-1}. Second, all sources of dead microorganisms are summed with 95% being added to the soluble substrate and 5% added in the lignin substrate as resistant-to-biodegrade material.

Moisture

Moisture is essential for composting because the actual decomposition occurs in an aqueous environment that surrounds the substrate particle. Simple water-soluble molecules diffuse through the film of moisture from the substrate particle's surface to the microorganisms, which in turn absorb these molecules directly into the cell. The complex, high-molecular-weight molecules cannot be directly absorbed by the microorganisms. To accomplish this, the microorganisms produce and release hydrolytic, extra-cellular enzymes into the water film to depolymerize these complex molecules into absorbable-sized molecules (Sylvia et al., 1998). Once the molecules are reduced, the microorganisms are capable of absorbing them.

Sufficient moisture is required for optimum efficiency of microbial stabilization of compost material (Jeris & Regan, 1993). According to Finstein et al. (1987),

> Water affects and is affected by numerous aspects of composting…water is both required for and produced by microbial activity; an increase in water content decreases porosity and gas diffusivity (decreases O_2 penetration into micropores); *and* water is removed via vaporization (evaporative cooling), as driven by microbial heat generation.

Excess or insufficient moisture conditions have a negative impact on aerobic microbial activity. As the moisture film increases in depth around the particle, oxygen diffusion decreases to a point that anaerobic conditions develop. If the particle is too large, anaerobic microsites will develop. Sextone et al. (1985) demonstrated the

existence of anaerobic microsites within saturated soil aggregates for particles having 12-mm to 18-mm diameter. In both of these situations, anaerobic microbial decomposition occurs when alternative electron acceptors such as nitrates and sulfates are utilized. The result in the production of odors that are undesirable, and incomplete decomposition occurs. At the other end of the moisture spectrum, the moisture film decreases around the particle, and there is insufficient moisture available for the microbe to obtain the necessary nutrients for survival (Sylvia et al., 1998).

Golueke (1972) indicated low moisture content, below 40%, seriously limits microbial activity because a majority of microorganisms found in compost typically grow in or below a liquid film on the surface of a compost particle. Finstein and Morris (1975) reported fungi can grow at relative humidities (RH) below 100%; bacteria grow best at RH of 100%. According to Alexander (1977), fungi can withstand semi-arid conditions. Berry (1988) indicated microbiological activity on a substrate progressively decreases at lower water contents, finally ceasing at or near 12% moisture content. Paul and Clark (1996) indicate 60% water-filled pore space is the optimum for bacteria. Grant and Rochette (1994) reported, based on literature, microbial activity is the greatest when the soil water content is about 0.6 of the total pore volume (from Linn & Doran, 1984). And, microbial activity declines when the soil water content is greater or lesser than the 0.6 total pore volume. They reported these declines are the result of several interrelated mechanisms. Microbial activity at low, soil-water content have been attributed to reduced diffusion of soluble substrates and to reduced microbial mobility and consequent access to substrate. This reduced activity has also been attributed to a direct effect on microbial growth due to lower matrix potentials. The declines at higher, soil-water content are attributed to oxygen deprivation caused by reduced oxygen diffusion.

Sylvia et al. (1998) indicates the optimum moisture content for bacterial growth in soil is between 40% to 60% water-filled-pore space. Percent water-filled-pore space (WFPS) is calculated as:

$$\%WFPS = \frac{soil.water.content * bulk.density * 100}{1 - (bulk.density / 2.65)} \tag{3.8}$$

where

$soil.water.content$ = mass of water per mass of dry soil (*substrate*)

($g_{water}\ g_{dry\ substrate}^{-1}$)

bulk.density = oven-dry weight of soil (*substrate*)/soil (*substrate*) volume. ($g\ cm^{-3}$)

% total porosity = 1 – (bulk density/ particle density of 2.65 $g\ cm^{-3}$)

%WFPS = Soil water content (mass of water/mass of substrate).

Stombaugh and Nokes (1996) used a moisture coefficient, (k_{H_2O}, no units), to account for the effect moisture has on microbial growth. They indicated no microbial growth was possible below compost moisture content of 20% (wet basis), limited growth was possible between 20% to 40%, and there was no limitation to growth above 40% (Cundiff & Mankin, 2003). Stombaugh and Nokes' k_{H2O} factor, which does not account for conditions of too much water, is:

$$k_{H2O} = 0.0 \qquad \text{when } m_1 < m \le m_2 \qquad (3.9)$$

$$k_{H2O} = (m/m_2) - 1.0 \qquad \text{when } m_2 < m \le m_3 \qquad (3.10)$$

$$k_{H2O} = 1.0 \qquad \text{when } m_3 \le m \qquad (3.11)$$

where:

k_{H2O} = moisture coefficient (no units)

m = compost-moisture content $kg_{water}\ kg_{(water+substrate)}^{-1}$ (wet basis) (w.b.)

m_1 = compost moisture equals 0.0 $kg\ kg^{-1}$ w.b.

m_2 = compost moisture equals 0.2 $kg\ kg^{-1}$ w.b.

m_3 = compost moisture equals 0.4 $kg\ kg^{-1}$ w.b.

A more exact moisture-content equation for the decomposition process can be developed from a figure found in Paul and Clark (1996), based on Linn and Doran (1984). Figure 3.4 presents the "relative rates of denitrification and other microbial processes as functions of percentage water-filled pore space" (Paul & Clark, 1996). According to Paul and Clark, soil water content regulates oxygen availability and, hence, nitrification. Nitrification is the microbial production of nitrate from the oxidation of reduced nitrogen compounds. Nitrate assimilation requires nitrate be reduced to ammonium before the nitrogen can be incorporated into cell constituents (Sylvia et al., 1998). There must be an absence of oxygen (Paul & Clark, 1996) for denitrification to

occur. The nitrification decreases as denitrification increases. According to Alexander (1977), if the oxygen supply is inadequate for microorganisms, there will be little ammonium oxidation with the reaction ceasing in the total absence of oxygen. Water status of the microbial habitat is a controlling factor, influencing nitrate production (Alexander, 1977). Waterlogged substrate limits the diffusion of oxygen and nitrification is suppressed. In arid conditions, the proliferation of bacteria is limited by insufficient water. Thus, in Figure 3.3, the line "ammonification and respiration" is appropriate for developing a moisture curve.

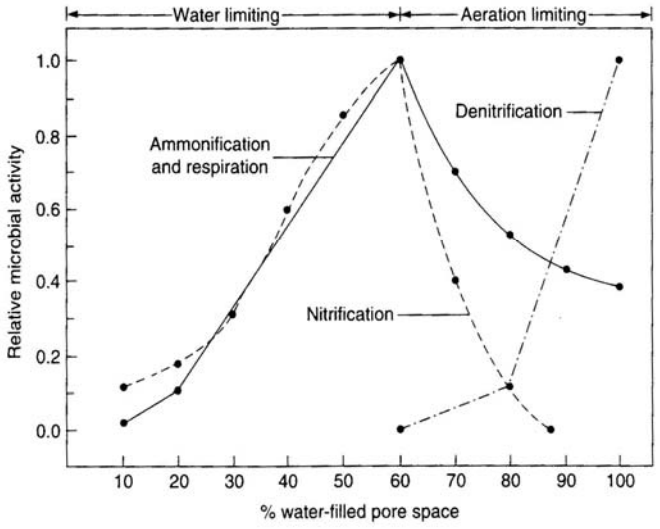

Figure 3.5 Relative moisture based on microbial activity. (Based on figure in Paul & Clark, 1996: Relative rates of denitrification and other microbial processes are functions of percentage water-filled pore space.)

Based on these literature relationships, five equations were developed from the ammonification and respiration graph utilizing Sigma Plot® (Systat Software, Inc, 2006) to define a continuous moisture factor that covers the moisture content from 0% to 100%. The resulting k_{H2O} factor is:

$$k_{H2O} = 0.00 \quad \text{when } 0.00 \geq W_{mc} < 0.10 \tag{3.12}$$

$$k_{H2O} = -0.0759 + 0.9011 * W_{mc} \quad \text{when } 0.10 \geq W_{mc} < 0.20 \tag{3.13}$$

$$k_{H2O} = -0.3482 + 2.2597 * W_{mc} \quad \text{when } 0.20 \geq W_{mc} < 0.60 \tag{3.14}$$

$$k_{H2O} = 1.00 \, \text{k\_H}_2\text{O} = 1.00 \quad \text{when } W_{mc} = 0.60 \tag{3.15}$$

$$k_{H2O} = 7.5844 - 20.5315 * W_{mc} + 19.8468 \left(W_{mc}\right)^2 - 6.5147 * \left(W_{mc}\right)^3$$

$$\text{when } 0.60 \geq W_{mc} \leq 1.0 \qquad (3.16)$$

where: W_{mc} = compost moisture content kg kg^{-1} w.b.

Figure 3.6 is a plot of Equations 3.12 through 3.16.

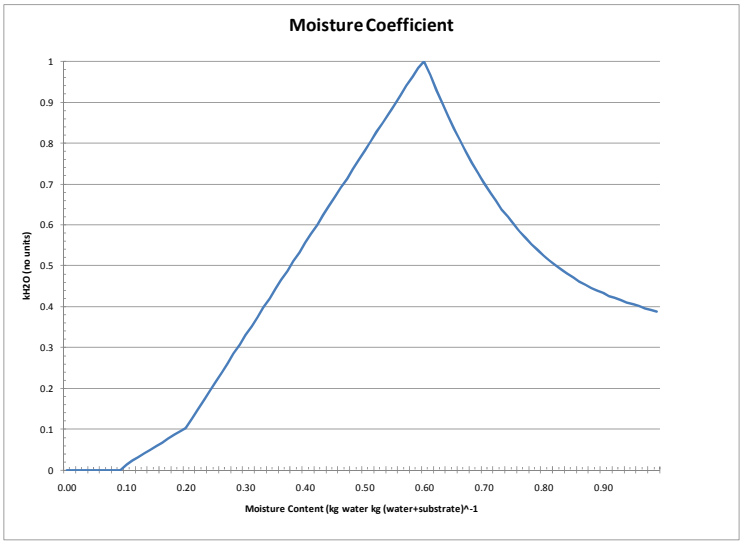

Figure 3.6 Moisture coefficient factor k_{H2O}.

Stoichiometric Equation

The stoichiometric relationship quantifies the mass balance between the fundamental variables of composting: the substrate and microbial concentrations, oxygen concentration, and moisture content (Seki, 2002). It provides a macroscopic view of the microbial-cell-growth relationship between the major reactants and their products (Cundiff & Mankin, 2003). The literature presents several different general forms of this reaction. For instance, some authors list nitrogen as a component of the substrate and ammonia as a product (Seki, 2002; Stombaugh & Nokes, 1996), and Cundiff and Mankin (2003) list nitrogen in the substrate and as a source.

This general stoichiometric equation based on Cundiff and Mankin, (2003) is written as:

$$C_aH_bO_cN_d + \alpha O_2 + \beta H_eO_fN_g \rightarrow \gamma C_hH_iO_jN_k + \delta CO_2 + \varepsilon H_2O \qquad (3.17)$$

where:

$C_aH_bO_cN_d$ = substrate (carbon) source

O_2 = oxygen source

$H_eO_fN_g$ = nitrogen source

$C_hH_iO_jN_k$ = biomass produced

CO_2 = carbon dioxide produced

H_2O = water produced

a, b, c, d, e, f, g, h, i, j, k = element subscripts for the particular substance

$\alpha, \beta, \gamma, \delta, \varepsilon$ = stoichiometric coefficients, number of moles required or produced per substance.

To simplify the equation, no nitrogen is provided by the carbon substrate. Since the form of nitrogen utilized by microorganisms is ammonium, ammonium is designated as the nitrogen source. Making these changes, the general stoichiometric equation can be developed, one for each microbe type, reflecting its associated substrate. This general stoichiometric equation is:

$$C_aH_bO_c + \alpha O_2 + \beta NH_4 \rightarrow \gamma C_hH_iO_jN_k + \delta CO_2 + \varepsilon H_2O \qquad (3.18)$$

Now, two components of the stoichiometric equation remain to be determined–substrate and microorganism. The detailed discussion of the chemical structures of the major organic macromolecules (carbohydrates, lipids, proteins, and nucleic acids) and of their biodegradability defines which particular substrate is assumed to be utilized by which particular microbial organism. The stoichiometric substrate formula $[C_aH_bO_c]_n$ is common to all four macromolecules.

Table 3.1 indicates three substrate types: the readily-biodegradable, slower-to-biodegrade, and resistant-to-biodegrade. First, the soluble or readily-biodegradable major compounds are the sugars, starches, and glycogen carbohydrates; the fatty acids, triglycerols, glycerophosolipids (phospholipids), steroids, and, sphingolipids lipids; the proteins; and the nucleic acids. The basic or simple saccharide structure $\left[C_6H_{12}O_6\right]$ is used to represent this soluble substrate group (Table 3.6; Soluble).

The second substrate type is slower-to-biodegrade. Table 3.1 shows that cellulose, chitin, and hemicellulose carbohydrate are placed into this group. Because chitin is similar to cellulose (Alexander, 1977), it was considered as cellulose. Hemicelluloses are in the class of polysaccharides present in cell walls in higher plants but have no structural relationship with cellulose (Alexander, 1977). To develop the molecular formula for the slower-to-degrade substrate, the cellulose and hemicellulose

molecular formulas were averaged (Table 3.6; Cellulose/hemicellulose Calculated Value).

The third substrate type is composed of the most resistant-to-biodegrade compounds, lignin. Lignin's structure is based on the phenyl propanoid unit (Paul & Clark, 1996). There are three monolignol monomers: the sinapyl alcohol, coniferyl alcohol, and coumaryl alcohol. To obtain a molecular formula and weight, the three monomers were averaged (Table 3.6; Lignin Calculated Value).

The initial research model considers four substrate types: soluble, cellulose/hemicellulose, lignin, and the inert (minerals/ash). Based on the above, only three stoichiometric equations can be developed because there is no carbon source for the inert (ash/inorganic) substrate group. However, the inert substrate must be tracked because it is part of the total substrate concentration and its specific heat affects the energy balance.

Table 3.6 Substrate molecular formulas and molecular weights and the values utilized in stoichiometric equations.

Substrate Basic Unit	Molecular Formula	Molecular Weight ($g\ mol^{-1}$)	References
Readily-biodegradable			
Soluble *	$C_6H_{12}O_6$	180.156	Silva et al.,1998 p. 230
Slower-to-biodegrade			
Cellulose	$[C_{12}H_{18}O_{10}]_n$	322.266	Voet & Voet, 2004 p. 365
Hemicellulose	$[C_{11.4}H_{16.79}O_{10}]_n$	313.840	Alexander, 1977 p. 165
Cellulose/hemicellulose: Calculated Value (averaged)*	$[C_{11.7}H_{17.14}O_{10}]_n$	316.796	–
Resistant-to-biodegradation			
Sinapyl alcohol lignin	$[C_{11}H_{14}O_4]_n$	210.229	Glasser, 2000, p. 218
Coniferyl alcohol lignin	$[C_{10}H_{12}O_3]_n$	180.203	Glasser, 2000, p. 218
Coumaryl alcohol lignin	$[C_9H_{10}O_2]_n$	150.177	Glasser, 2000, p. 218
Lignin: Calculated Value (average)*	$[C_{10}H_{12}O_3]_n$	180.203	–

* Values utilized in the stoichiometric equations.

The microbiological portion completes the stoichiometric equation. As discussed, the three main classes of microorganisms associated with decomposition are bacteria, actinomycetes, and fungi. In general, bacteria are associated with the decomposition of the soluble material; actinomycetes with the celluloses and hemicelluloses; and fungi with lignin. Building on this premise, the basic unit structure for microorganisms is established with their respective substrate. Table 3.7 presents the microbial molecular formulas utilized in the stoichiometric equation for the initial model.

Table 3.7 Stoichiometric microbial formulas and molecular weights

Microorganism Basic Unit	Molecular Formula	Molecular Weight ($g\ mol^{-1}$)
Bacteria	$CH_{1.77}O_{0.49}N_{0.24}$	104.1598
Actinomycetes	$CH_{1.77}O_{0.49}N_{0.24}$	104.1598
Fungi	$CH_{1.65}O_{0.53}N_{0.13}$	165.0629

Three stoichiometric equations can be written and balanced, one for each substrate/microorganism combination. The equations with molecular weights are:

Soluble Substrate and Bacteria (3.17)

$$C_6H_{12}O_6 + 2.01O_2 + NH_4^+ = 4.167CH_{1.77}O_{0.49}N_{0.24} + 1.833CO_2 + 4.312H_2O$$

	Substrate	Oxygen	Ammonium	Microbial Mass	Carbon-dioxide	Water
Molecular Weight:	180.1560	64.3160	18.0390	104.1598	80.6685	76.6807

Cellulose/hemicellulose Substrate and Actinomycetes (3.18)

$$C_{11.7}H_{17.14}O_{10} + 7.1O_2 + NH_4^+ = 4.167CH_{1.77}O_{0.49}N_{0.24} + 7.6CO_2 + 6.87H_2O$$

	Substrate	Oxygen	Ammonium	Microbial Mass	Carbon-dioxide	Water
Molecular Weight:	316.470	226.1858	18.0390	104.1523	33.4680	123.7631

Lignin Substrate and Fungi (3.19)

$$C_{10}H_{12}O_3 + 4.716O_2 + NH_4^+ = 6.849CH_{1.6}O_{0.527}N_{0.146} + 3.151CO_2 + 2.521H_2O$$

	Substrate	Oxygen	Ammonium	Microbial Mass	Carbon-dioxide	Water
Molecular Weight:	180.2030	150.9026	18.0390	165.0629	138.672	45.4158

The theoretical maximum yield coefficients for biomass formation, oxygen and nitrogen consumption, and for carbon-dioxide and water production, can be calculated for

each substrate/microorganism combination on a molar basis. The yield coefficients are presented in Table 3.8.

Table 3.8 Yield coefficients

Coefficient	Soluble/Bacterial	Cellulose/ Actinomycetes	Lignin/Fungal
Respiratory Quotient	$RQ_{CO_2/S_{ss}} = 0.9119$	$RQ_{CO_2/S_{sc}} = 1.0704$	$RQ_{CO_2/S_{sl}} = 0.6682$
Biomass yield	$Y_{X_b/S_{ss}} = 0.5782$	$Y_{X_a/S_{sc}} = 0.3281$	$Y_{X_f/S_{sl}} = 0.9160$
Oxygen consumed	$Y_{O_2/S_{ss}} = 0.3570$	$Y_{O_2/S_{sc}} = 0.7156$	$Y_{O_2/S_{sl}} = 0.8374$
Carbon dioxide produced	$Y_{CO_2/S_{ss}} = 0.3570$	$Y_{CO_2/S_{sc}} = 1.0535$	$Y_{CO_2/S_{sl}} = 0.7695$
Water produced	$Y_{W/S_{ss}} = 0.4312$	$Y_{W/S_{sc}} = 0.3898$	$Y_{W/S_{sl}} = 0.2520$

where:

$RQ_{CO_2/S_{ss}}$	=	Respiratory quotient ratio of carbon dioxide produced to the amount of oxygen consumed during a reaction involving soluble substrate	(No units)
$RQ_{CO_2/S_{sc}}$	=	Respiratory quotient ratio of carbon dioxide produced to the amount of oxygen consumed during a reaction involving cellulose substrate	(No units)
$RQ_{CO_2/S_{sl}}$	=	Respiratory quotient ratio of carbon dioxide produced to the amount of oxygen consumed during a reaction involving lignin substrate	(No units)
$Y_{X_b/S_{ss}}$	=	Amount of bacterial biomass produced per unit mass of soluble substrate utilized	$kg_{xb}\,kg_{ss}^{-1}$
$Y_{X_a/S_{sc}}$	=	Amount of actinomycetes biomass produced per unit mass of cellulose substrate utilized	$kg_{xa}\,kg_{sc}^{-1}$
$Y_{X_f/S_{sl}}$	=	Amount of fungi biomass produced per unit mass of lignin substrate utilized	$kg_{xf}\,kg_{sl}^{-1}$
$Y_{O_2/S_{ss}}$	=	Oxygen-consumption coefficient per mass of soluble substrate utilized	$kg_{O2}\,kg_{ss}^{-1}$
$Y_{O_2/S_{sc}}$	=	Oxygen-consumption coefficient per mass of cellulose substrate utilized	$kg_{O2}\,kg_{sc}^{-1}$
$Y_{O_2/S_{sl}}$	=	Oxygen-consumption coefficient per mass of lignin substrate utilized	$kg_{O2}\,kg_{sl}^{-1}$

$Y_{CO_2/S_{ss}}$	=	Amount of carbon dioxide produced per unit mass of soluble substrate utilized	$kg_{CO2}\, kg_{ss}^{-1}$
$Y_{CO_2/S_{sc}}$	=	Amount of carbon dioxide produced per unit mass of cellulose substrate utilized	$kg_{CO2}\, kg_{sc}^{-1}$
$Y_{CO_2/S_{sl}}$	=	Amount of carbon dioxide produced per unit mass of lignin substrate utilized	$kg_{CO2}\, kg_{sl}^{-1}$
$Y_{W/S_{ss}}$	=	Yield Coefficient: Amount of water generated per unit mass of soluble substrate utilized	$kg_{w}\, kg_{ss}^{-1}$
$Y_{W/S_{sc}}$	=	Yield Coefficient: Amount of water generated per unit mass of cellulose substrate utilized	$kg_{w}\, kg_{sc}^{-1}$
$Y_{W/S_{sl}}$	=	Amount of water generated per unit mass of lignin substrate utilized	$kg_{w}\, kg_{sl}^{-1}$

Temperature coefficient

Stombaugh and Nokes (1996) utilized a temperature coefficient, k_{temp}, to predict microbial growth rates as a function of temperature. "Since the microbial population has several distinct components which respond to temperature differently, the values for k_{temp} represent the summation of the individual populations" (Stombaugh & Nokes, 1996). The research model does not consider this coefficient because the basic design includes three different microbial populations and two temperature-habitat ranges.

Parameter coefficient summary

Table 3.9 lists the initial value of coefficients used for calculations throughout the initial research model as discussed through this chapter. Many of the coefficients utilized by Stombaugh and Nokes (1996) are utilized as the initial values in the research model. This table shows where departures from Stombaugh and Nokes were taken.

Table 3.9 Parameters and coefficients

Definition	Parameter Symbol	Units	Initial Model Value	Reference
				Stombaugh and Nokes (1996)
Expiration factor for all mesophilic organisms outside of their temperature range	k_{dm}	(no units)	0.40	
Expiration factor for all thermophilic organisms outside of their temperature range	k_{dt}	(no units)	0.40	
Fraction of mesophilic microbial population which expire each hour	k_{dm}	$kg_x\ kg_x^{-1}\ h^{-1}$	0.025	0.0250 One value for both mesophilic and thermophilic microorganisms
Fraction of thermophilic microbial population which expire each hour	k_{dt}	$kg_x\ kg_x^{-1}\ h^{-1}$	0.025	
'Half –Velocity' coefficient for substrate	K_S	$kg_s\ m^{-3}$	62.0	62.0
'Half –Velocity' coefficient for oxygen	K_{O_2}	$kg_{O2}\ m^{-3}$	0.07	0.70
Heat of combustion of soluble substrate	$\Delta h_{C_{ss}}{}^{T}$	$kJ\ kg_{ss}^{-1}$	19100	19100
Heat of combustion of cellulose/hemicellulose substrate	$\Delta h_{C_{sc}}{}^{T}$	$kJ\ kg_{sc}^{-1}$	19100	
Heat of combustion of lignin substrate	$\Delta h_{C_{sl}}{}^{T}$	$kJ\ kg_{sl}^{-1}$	19100	
Maximum specific growth rate for mesophiles	μ_{maxm}	h^{-1}	0.20	0.20
Maximum specific growth rate for thermophiles	μ_{maxt}	h^{-1}	0.20	0.20
Maximum maintenance coefficient for mesophiles	η_{maxm}	h^{-1}	0.48	0.48
Maximum maintenance coefficient for thermophiles	η_{maxt}	h^{-1}	0.48	0.48
Microbial seed population mesophilic actinomycetes	$C_{X_{ma}}$	$kg_{x\ ma}\ m^{-3}$	0.008	

Microbial seed population mesophilic bacteria	$C_{X_{mb}}$	$kg_{x\ mb}\ m^{-3}$	0.008	0.008
Microbial seed population mesophilic fungi	$C_{X_{mf}}$	$kg_{x\ mf}\ m^{-3}$	0.008	
Microbial seed population thermophilic actinomycetes	$C_{X_{ta}}$	$kg_{x\ ta}\ m^{-3}$	0.008	
Microbial seed population thermophilic bacteria	$C_{X_{tb}}$	$kg_{x\ tb}\ m^{-3}$	0.008	
Microbial seed population thermophilic fungi	$C_{X_{tf}}$	$kg_{x\ tf}\ m^{-3}$	0.008	
Moisture coefficient	k_{H2O}	kg kg^{-1}	If $0.00 \geq W_{mc} < 0.10$ $k_{H2O} = 0.00$ if $0.10 \geq W_{mc} < 0.20$ $k_{H2O} = -0.0759 + 0.9011 * W_{mc}$ if $0.20 \geq W_{mc} < 0.60$ $k_{H2O} = -0.3482 + 2.2597 * W_{mc}$ if $W_{mc} = 0.60$ $k_{H2O} = 1.00$ k_H_2O = 1.00 if $0.60 \geq W_{mc} \leq 1.0$ $k_{H2O} = 7.5844 - 20.5315 * W_{mc} \ldots$ $+19.8468(W_{mc})^2 - 6.5147 * (W_{mc})^3$ where: W_{mc} = compost moisture content kg kg^{-1} w.b.	If $m_1 < m \leq m_2$ $k_{H2O} = 0.0$ If $m_2 < m \leq m_3$ $k_{H2O} = (m/m_2) - 1.0\ m_3 \geq m$ $k_{H2O} = 1.0$ where: m = compost moisture content (w.b.) m_1 = 0.0 (kg kg^{-1} w.b.) m_2 = 0.2 (kg kg^{-1} w.b.) m_3 = 0.4 (kg kg^{-1} w.b.)
Specific heat of soluble substrate	$c_{S_{ss}}$	kJ kg_{sc}^{-1} K^{-1}	1.480	1.480
Specific heat of cellulose/hemicellulose substrate	$c_{S_{sc}}$	kJ kg_{sc}^{-1} K^{-1}	1.480	1.480

Specific heat of lignin substrate	$c_{S_{sl}}$	kJ kg_{sc}^{-1} K^{-1}	1.480	1.480
Specific heat of inert substrate (non-volatile)	$c_{S_{si}}$	kJ kg_{sc}^{-1} K^{-1}	0.840	0.840
Specific heat of water	c_W	kJ kg_w^{-1} K^{-1}	4.18	4.18
Temperature coefficient	k_{temp}	°C	(Not used)	if $T_1 < T \leq T_2$ $k_{temp} = T/(T_2-T_1)$ if $T_2 < T \leq T_3$ $k_{temp} = 1.0$ if $T_3 > T$ $k_{temp} = 3.75 - [T/T_2 - 10]$ 3.75-[T/(T_2-10)] Where: T = compost moisture content (w.b.) $T_1 = 0$ (kg kg^{-1} w.b.) $T_3 > T$ T_2= 30 (kg kg^{-1} w.b.) $T_3 > T$ T_3= 55 (kg kg^{-1} w.b.)
Yield coefficient-biomass: bacterial biomass concentration produced per unit mass of soluble substrate utilized	$Y_{X_b/S_{ss}}$	kg_{xb} kg_{ss}^{-1}	0.5782	0.3500
Yield coefficient-biomass: actinomycetes biomass concentration produced per unit mass of cellulose/hemicellulose substrate utilized	$Y_{X_a/S_{sc}}$	kg_{xa} kg_{sc}^{-1}	0.3281	
Yield coefficient-biomass: fungal biomass concentration produced per unit mass of lignin substrate utilized	$Y_{X_f/S_{sf}}$	kg_{xf} kg_{sl}^{-1}	0.9160	
Yield coefficient: carbon dioxide produced per mass of soluble substrate utilized	$Y_{CO_2/S_{ss}}$	kg_{CO2} kg_{ss}^{-1}	0.3570	1.720

Yield coefficient: carbon dioxide produced per mass of cellulose/hemicellulose substrate utilized	$Y_{CO_2/S_{sc}}$	$kg_{CO2}\,kg_{sc}^{-1}$	1.0535	
Yield coefficient: carbon dioxide produced per mass of lignin substrate utilized	$Y_{CO_2/S_{sl}}$	$kg_{CO2}\,kg_{sl}^{-1}$	0.7695	
Yield coefficient: oxygen consumed per mass of soluble substrate utilized	$Y_{O_2/S_{ss}}$	$kg_{O2}\,kg_{ss}^{-1}$	0.3570	1.370
Yield coefficient: oxygen consumed per mass of cellulose/hemicellulose substrate utilized	$Y_{O_2/S_{sc}}$	$kg_{O2}\,kg_{sc}^{-1}$	0.7156	
Yield coefficient: oxygen consumed per mass of lignin substrate utilized	$Y_{O_2/S_{sl}}$	$kg_{O2}\,kg_{sl}^{-1}$	0.8374	
Yield coefficient: water produced per mass of soluble substrate utilized	$Y_{W/S_{ss}}$	$kg_{W}\,kg_{ss}^{-1}$	0.4312	0.631
Yield coefficient: water produced per mass of cellulose/hemicellulose substrate utilized	$Y_{W/S_{sc}}$	$kg_{W}\,kg_{sc}^{-1}$	0.3898	
Yield coefficient: water produced per mass of lignin substrate utilized	$Y_{W/S_{sl}}$	$kg_{W}\,kg_{sl}^{-1}$	0.2520	

CHAPTER 4 - MATERIALS AND METHODS

This chapter delineates the experimental design, setup, and procedures to compare the mathematical model results to the experimental data. This chapter is divided into four sections: experimental design; experimental equipment setup; experimental procedure; and statistical analysis methodology. All experiments were conducted at Kansas State University, Manhattan, Kansas.

Matrix Design

A matrix design is required to establish the link between the experimental design and the mathematical model. The compost matrix is divided into layers. Each layer is treated as and solved as a separate unit. These layer units form the y-axis of the matrix. Time is the x-axis of the matrix. Initially, all fixed parameters are set to their assigned values. Next, the initial y-axis boundary values are set for all computational parameters at time equals zero on the x-axis. All values within this unit matrix are solved before the analysis proceeds to the next unit. The model schematic of the matrix is presented as Figure 4.1.

The next step is to develop the nodal scheme (Figure 4.2) based on the matrix design. A nodal scheme is required to solve the differential equations. The experimental design must be aligned to the nodal scheme to allow collection of experimental data that can be compared to the mathematical model data. This procedure indexes the individual cell. The node represents the center of the cell, where the entire cell is assumed to have uniform characteristics. The cell reference number (k, p) identifies the cell location. Again (k) equals time and (p) equals the different layers within the compost unit. The first step is to establish the external boundary or atmospheric conditions at $(k = 1, p = 1)$. At $(k = 1)$ time is equal to zero. Throughout all calculations, the set of nodes $(k(t), p = 1)$ will equal atmospheric conditions. The next step is to establish the initial compost characteristics $(k = 1, p = 2\ to\ n)$. In this case (n) equals 9. At this point all

characteristics within the compost reactor are uniform. At $(k=2)$ the series of calculations are performed. This is the first time step. The atmospheric conditions are reset at $(k=2, p=1)$. Next the microbial process begins. This is layer $(k=2, p=2)$. First, the required values are recalled from either $(k=1, p=2)$, the node one step earlier, or $(k=2, p=1)$, the node in the same step but one layer below. Next, the calculations are performed. Then the new values are saved. This time step continues until $(k=2, p=9)$ is accomplished. At this point the calculations begin over again starting at $(k=3, p=1)$ thru $(k=3, p=9)$. This continues until $(k=(t), p=9)$ is calculated and the program terminates.

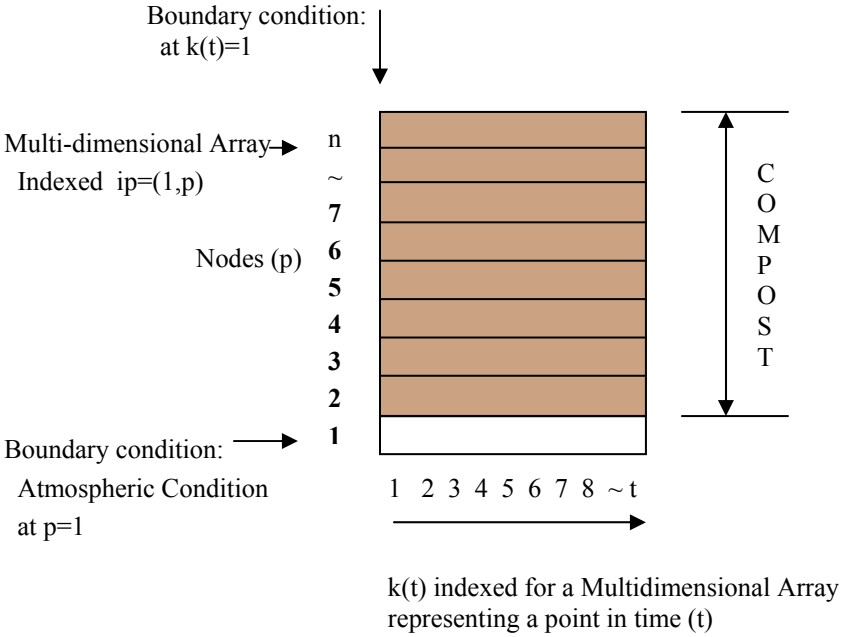

Figure 4.1 Model schematic for layers $(1\ to\ n)$ and time $(1\ to\ t)$

Experimental design

Figure 4.1 showed the model schematic for the mathematical model and the experimental model. The experimental design is presented in Figure 4.3. Target mixture contents are shown as percentage of each substrate class. The experimental units are measured and samples taken for analysis after different amounts of run time. Samples

are to be taken at node levels 2, 4, and 6. Units A1, B1, and C1 are to be taken off line and sampled at Day 3. Units A2, B2, and C2 are to be taken off line and sampled at Day 7. Units A3, B3, and C3 are to be taken off line and sampled at Day 14. Finally, at Day 28, Units A4, B4, and C4 are to be taken off line and sampled. In fact, as described later in Chapter 5, modifications were made.

	Node No.	Boundary condition at k(t)=1	Internal determinations: ⟶ at (k(t)=2 to k(t)=t, p=2 to 9)				
Multi-dimensional Array Indexed ip=(1,p)	9	(1,9)	(2,9)	(3,9)	(4,9)	~	(k,9)
	8	(1,8)	(2,8)	(3,8)	(4,8)	~	(k,8)
	7	(1,7)	(2,7)	(1,7)	(4,7)	~	(k,7)
	6	(1,6)	(2,6)	(3,6)	(4,6)	~	(k,6)
	5	(1,5)	(2,5)	(3,5)	(4,5)	~	(k,5)
	4	(1,4)	(2,4)	(3,4)	(4,4)	~	(k,4)
	3	(1,3)	(2,3)	(3,3)	(4,3)	~	(k,3)
Boundary condition: Atmospheric conditions at (k, p=1)	2	(1,2)	(2,2)	(3,2)	(4,2)	~	(k,2)
	1	(1,1)	(2,1)	(3,1)	(4,1)	~	(k,1)
	Time	1	2	3	4	~	T

k(t) indexed for a Multidimensional Array representing a point in time (t)

Figure 4.2 Nodal schematic

Mixture Identification Letter	Target Mixture Content %			Experimental Unit Identification Number			
	Soluble	Cellulose/ Hemicellulose	Lignin	Proposed Run Times			
				3 days	7 days	14 days	28 days
A Slower-to-biodegrade	25	50	25	A1	A2	A3	A4
B Resistant-to-biodegradation	25	25	50	B1	B2	B3	B4
C Readily-biodegradable	50	25	25	C1	C2	C3	C4

Figure 4.3 Proposed experimental design

Experimental equipment setup

The experimental composting unit consisted of three major parts: the reactor, the temperature-sensor system, and the air-flow system. The experimental-unit-equipment setup (Figure 4.4) shows the composting-vessel parameters (height, diameter, number of layers, volume and wall thermal resistance); the number of nodes (p), where p equals the number layers plus one. Outputs measured are: temperature, carbon-dioxide production, change in substrate weight, depth of substrate, moisture content, and change in substrate composition (percent soluble, cellulose/hemicellulose, lignin, and ash/inorganic).

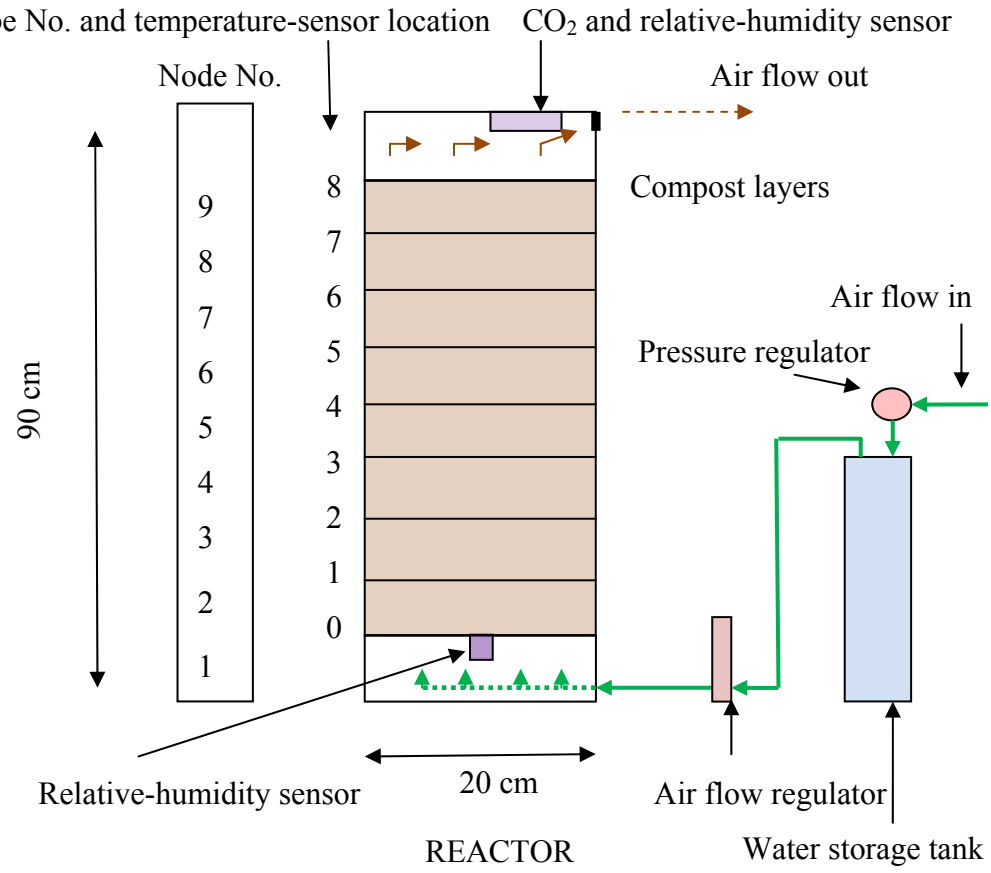

Figure 4.4 Experimental-unit-equipment setup

Reactor

Figure 4.3 illustrates that twelve reactor tubes are to be utilized. The nodal schematic, indicated in Figure 4.2, designates the placement of the temperature probes. Each composting reactor unit is constructed from 20.3-cm (8-inch) diameter Cresline ® PVC TYPE PSM SDR 35 sewer line and 20.3-cm (8-inch) sewer line caps. The pipe wall is 0.7-cm thick. The end cap wall is 0.6-cm thick. The cap has an internal depth of 10.4 cm.

The pipe was cut into 90-cm sections. Each 90-cm section was marked at 7 cm, 9 cm, 9.7 cm, and 10 cm from the bottom, then at 10-cm intervals from 10 cm up to 80 cm, and at 86 cm. At both the 7-cm and 86-cm marks, three 0.2-cm holes were drilled, 120º apart around the circumference. A number 6 x 0.95-cm stainless-steel pan-phillips head, sheet-metal screw was inserted into each of the three holes. The point of each screw that protruded through the pipe wall was removed. These screws acted as stops for both end caps. At the 9-cm and 20-cm through 80-cm marks, a 0.71-cm diameter hole was drilled. Thermocouples were to be inserted into these holes after the tubes were filled with the composting mixture. At the 9-cm mark, an additional hole, 0.40 cm in diameter, was drilled opposite from the original hole. A temperature thermocouple rod is to be inserted and fed through the second hole on the opposite side wall. The thermocouple measurement junction end was adjusted to be centered (10 cm from each pipe wall). At the 9.7-cm height, four, 0.32-cm diameter holes were drilled 90º apart around the circumference. Into each hole a number 8 x 2.54-cm hex-head, slotted, stainless-steel screw was inserted, protruding into the interior. An expanded metal plate was inserted to sit on the screws to form the base on which the compost mixture was placed. The top of the grate was at the 10-cm height. After all holes were drilled, the reactor pipe was wrapped in 2.54-cm thick fiberglass insulation with mylar outer sheet. Holes were cut to allow insertion of the thermocouple into the mixture.

A picture detailing the compost reactor pipe before and after wrapping is shown in Figure 4.5 and in Appendix B, Figure B.1. Figure B.2 details the expanded metal plate looking up from the bottom of the tube. This plate establishes the separation between the air inflow zone and the compost mixture.

A cap was placed on both the bottom and top of the pipe. The bottom cap had a 0.79-cm diameter hole drilled and threaded with a 0.95-cm tap at 8.5 cm down from the open end of the cap. A 0.64-cm hose bib was installed to allow air inflow. The top cap had a 2.86-cm hole drilled 6.4 cm away from the open end of the cap that permited air to escape from the reactor.

Figure 4.5 Compost reactor pipe after and before wrapping

Six of the compost reactors were fitted with a relative-humidity sensor. At the 7-cm mark on the pipe, an additional hole, 1.27 cm in diameter, was drilled approximately 2.54 cm to the left of the 0.32-cm hole, and a relative-humidity sensor inserted. The top cap had two additional holes drilled. One 1.27-cm hole was drilled through the top of the cap 7 cm in from the cap's edge measured from the hole drilled for the air to exit. A relative-humidity sensor is be inserted in this hole. The second hole, 0.32 cm in diameter, was drilled in line with the 1.27-cm hole but 13.5 cm from the edge of the cap. The carbon-dioxide sensor data line was fed through this hole. The carbon-dioxide sensor was attached by duct tape to the inside of the cap. A photograph of the experimental compost cap with the relative-humidity and carbon-dioxide sensors installed inside the top cap is shown in Appendix B, Figure B.3. After each reactor component was constructed, each piece was weighed to the nearest 4.5 g (one hundredth of a pound) using a balance-beam scale.

Temperature Sensor System

The temperature sensor system consisted of three parts: the thermocouple, the multiplexer, and the datalogger. All temperature points were measured using Type T, copper/constantan thermocouples. The standard temperature range is from 0 ºC to 133 ºC, the limits of error are 1 ºC. At the measurement junction the two electrical conductors were twisted together, soldered, and epoxy coated. The measurement junction end was soldered and coated with epoxy. The reference end was connected to a multiplexer that fed into a datalogger for temperature measurement. Each thermocouple, except for the one inserted into the top reactor cap, was placed on a 0.5-cm diameter wooden dowel with the measurement end sticking out beyond the end of the dowel. A piece of shrink wrap, 10.7 cm x 0.64 cm, was inserted over the thermocouple and dowel, and heat treated to shrink it. The 10.7-cm length accounted for the inside radius and pipe wall thickness of the reactor. This created a reference line as to when the thermocouple was inserted 10 cm into the substrate.

The bottom and top thermocouple supports were constructed differently. The bottom, ambient-reference-temperature-thermocouple dowel, or "0-cm" probe, penetrated the entire pipe diameter at the 9-cm mark. Starting at the end of the dowel inserted into the reactor, a mark was measured at 0.7 cm. At this mark, one end of a piece of shrink wrap, approximately 1.27-cm long, was placed and heat treated. Continuing measuring, a mark was made at 10.7 cm. At this point, the measurement junction end of the thermocouple hung down 2.54 cm from the dowel. From the 10.7-cm mark, the thermocouple wire and dowel were covered by shrink wrap for at least another 10.7 cm. For the top thermocouple wire, a 0.16-cm hole was drilled in the top of the cap. The thermocouple wire was inserted approximately 2.54 cm into the cap and taped into place. All thermocouple wires except for the "0-cm" probe for each individual reactor were taped together as a wiring harness to maintain order. Each wiring harness was color-coded and numbered.

The thermocouples were inserted horizontally into each hole to penetrate 10 cm into the mixture, i.e., to the midpoint of the reactor diameter after the reactor was filled with the compost mixture. The "0-cm" probe, which measures the incoming air temperature below the compost, was set in place before any compost mixture was added.

Each tube was turned upside down to permit the placement of the "0-m" probe. The "0-cm" probe was inserted through the entrance hole at 9 cm into the tube, the epoxy was placed on the wooden tip of the probe, and, finally, the probe end was inserted into the interior hole (Appendix B, Figure B.4). After the reactor tubes were filled and in place, the thermocouple wire was connected to the assigned multiplexer location.

Each thermocouple was connected to one of four AM32 multiplexers (Campbell Scientific, Inc., Logan, Utah), and each AM32 multiplexer had a capacity of 32 thermocouple connections. Twenty-nine thermocouple connections were made per multiplexer (three reactors with nine thermocouples each and two blank jumper connections to indicate separation between the individual reactor thermocouples). The four AM32 Multiplexers were connected to a CR10X Measurement and Control Module Datalogger (Campbell Scientific, Inc., Logan, Utah). The CR10X had the capacity for four multiplexers. Two, 12-volt car batteries connected in series were used as the power source for the CR10X. Photographs of the datalogger and multiplexers are shown in Appendix B, Figure B.5.

Air-Flow System

Each reactor was supplied with air through an air manifold which was connected to the building's compressed air system. The manifold was an 8.9-cm by 8.9-cm by 136-cm, steel-box channel with welded end plates. Two support plates, 3.2 cm x 0.6 cm by 31 cm, were welded to the bottom of the channel near each end to provide stabilization to the manifold. Nine holes were drilled into the manifold. The first hole was the air supply inlet. It was drilled and tapped with a 1.27-cm by number-14 pipe thread. A quick connect fitting was attached to which the compressed air line was attached.

The remaining holes were to supply air to the individual reactors. These air-outlet ports were drilled and tapped with a 0.64-cm by number-18 pipe thread. A flow meter was attached to each outlet port using 0.64-cm brass fittings. The flow meters are Dwyers® Series RM Rate-Master® Flowmeter, Model RMB-50 manufactured by Dwyer Instruments, Inc., Michigan City, Indiana. All flow meters were calibrated using a Dry Cal® DC-Lite primary flow meter manufactured by BIOS International Corporation, Butler, New Jersey.

The building's air compressor system is set to turn on at approximately 6.6 bar and turn off at approximately 9.7 bar. The intake to the compressor is located within the building, thus the air supply is at room temperature which varied around 24 ºC. The system has some water in its air lines. As the pressure per bar increases; the vapor pressure increases. When the vapor pressure exceeds 100 %, the excess water vapor condenses in the system. If the compressed air is released inside the reaction tubes, the compressed air will expand to atmospheric conditions with less water content than the building's ambient air, which will create a drying effect.

The amount of water air can hold at different pressures and temperatures are presented at Figure 4.5 (http://www.engineeringtoolbox.com/water-content-compressed-air-d_1275.html). This figure indicates the maximum mass of water (at 100% water content) contained in the feed air at atmospheric pressure (0 bar) and 24 ºC will be approximately 0.02 kg m^{-3}. When the air is compressed to 9.7 bar at 24 ºC, the maximum mass of water (at 100% water content) will be approximately 0.002 kg m^{-3}. All excess water (0.018 kg m^{-3}) will condense in the system. When the air pressure is reduced back to atmospheric conditions (0 bar) the air will only contain 10% of the original water content. Thus, any air flowing through the reaction tube will create a drying effect.

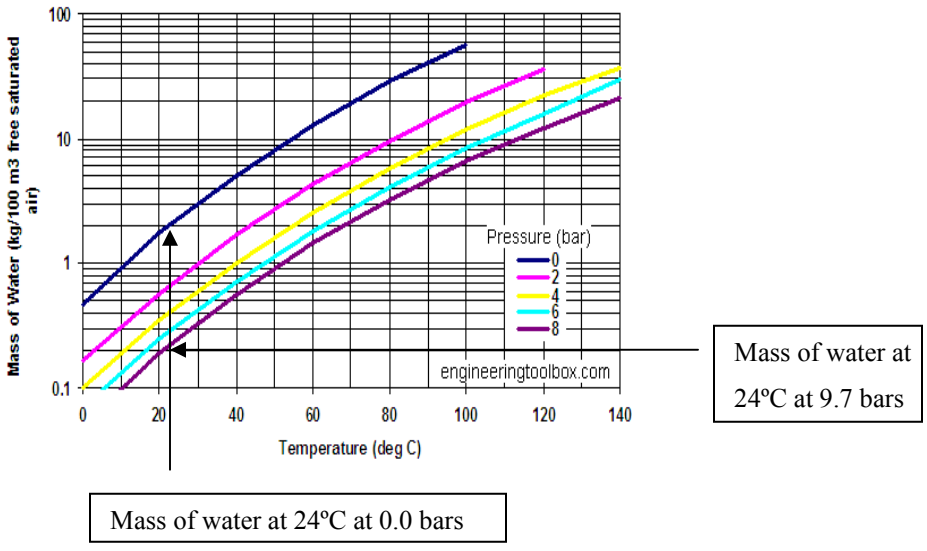

Figure 4.6 Guage pressure in bars (http://www.engineeringtoolbox.com/water-content-compressed-air-d_1275.html)

The air supply system was designed to correct this problem. The compressed air was decreased from the line pressure of 6.6 bar to 9.7 bar to approximately 0.55 bar before being fed through a column of water in a certified, pressure-worthy vessel acting as a water bath. The water content will increase to near saturation as the air passes through the water bath. The air will then flow through the air manifold to the reaction tubes where it will be released to atmospheric conditions. Psychrometric calculation indicates that when this level of compressed air is expanded to atmospheric pressure in the reactor tube, the air will contain approximately 63% of saturatation water content.

The water bath system was constructed as follows: A 284-L (75-gal) hot water heater was placed in line as the water bath and was filled approximately half full with water. The outlet side of the modular regulator was connected to the inlet (cold water) side of the water heater. The modular regulator had a maximum inlet pressure of 20.7 bar, and a reduced pressure range of 0.14 bar to 8.62 bar. The compressed air supply was connected to the regulator. A ball valve was installed on the water-heater-outlet port (hot-water side) to control air flow. A compressed-air line was utilized with quick release connectors to connect the water heater to the air manifold. The modular regulator was set to deliver an output pressure of 0.55 bar. A photograph of the water bath system and air flow manifold is shown in Appendix B, Figure B.6.

Carbon-dioxide Sensors

The carbon-dioxide sensors used to measure CO_2 concentration are non-dispersive, infrared, CO_2 sensors, Ventostat 8102, Telaire, Goleta, California. The manufacturer rated the sensor accuracy is ± 100 parts per million (ppm) or 7%, whichever is greater at 0 ºC to 50 ºC, and ± 50 ppm or 5%, whichever is greater (7% for levels over 1,500 ppm) at 15 ºC to 32 ºC. The sensor has a voltage output of 0 volts to 10 volts and readout of 0 ppm to 10,000 ppm. The sensor transmits its data to the computer via telephone wires. The six sensors used were provided by the Agricultural Research Services, U.S. Dept. of Agriculture, Manhattan, Kansas. A photograph of the carbon dioxide sensor installed in the cap is shown in at Appendix B, Figure B.3.

Relative-humidity Sensors

Six relative-humidity sensors were available with the carbon-dioxide sensors. This sensor provides the opportunity to verify the water content of the air. The sensor is an SHT75, single-chip, relative-humidity and temperature multi-sensor module. The measurement range is 0% to 100% relative humidity, with a rated accuracy of ±2.0% relative humidity between 10% to 90% relative humidity. The sensor is enclosed in a porous polymer tube, Porex Porous Products Group X-5108-60µ 1/8 inch Tube HDPE, Porex Corp., Fairburn, Georgia.

To install the relative-humidity sensor, a rubber stopper of sufficient size to plug the 1.27-cm hole had a 0.32-cm hole drilled through its center. One side of the stopper was split to expose the hole, and the sensor wire was inserted through the split into the hole. The stopper with sensor was inserted thumb tight into the 1.27-cm hole in the reactor.

System test

Prior to initiating the experiment, all systems were tested. Minor problems were detected (e.g., a loose screw or loose wire) and corrected.

Experimental procedure

Ingredients

The four ingredients chosen are pine wood shavings, wheat straw, corn silage, and cattle manure (Figure 4.6 and Appendix B, Figures B.7). The pine-wood shavings are purchased from a local pet supply store. The remaining substrates are obtained from the Animal Science Department, Kansas State University: the wheat straw from the Swine Unit, the corn silage from the Dairy Unit, and the manure from the Cattle Unit. The wheat straw was baled and stored in an open shed. The corn silage was stored in long, plastic-wrap tubes approximately two meters tall. The cattle manure was taken directly from the cattle pens, which are open on four sides and have a roof. The flooring is concrete. Periodically, the pens are cleaned with a bucket attachment on a bobcat-type loader that scrapes the wastes to the end of the pens into a sloped-concrete catchment, where the samples were collected.

Mixtures

Based on the experimental design, three mixtures were selected to best represent a wide range of inputs to test the model. The first mixture was predominately soluble with the soluble substrate content of 50%, and both the cellulose/hemicellulose and lignin substrates at 25% each. The second mixture was predominately cellulose/hemicellulose, with cellulose/hemicellulose substrate as the dominate substrate at 50%, and both the soluble and lignin substrates at 25% each. The third mixture had lignin as the dominate substrate at 50%, and both the soluble and cellulose/hemicellulose substrates at 25% each. The amount of each ingredient actually selected was based on best meeting the composition of the mixtures. The moisture content would be adjusted to equal 60% if required. The carbon/nitrogen ration would be adjusted down, if required, to 25:1 by adding ammonium sulfate.

a.

c.

b.

d.

Figure 4.7 Ingredients used: (a) pine wood shavings; (b) wheat straw; (c) corn silage; and, (d) cattle manure

Laboratory Analysis

The Analytical Services Laboratory, Animal Science Department, Weber Hall, Kansas State University, Manhattan, Kansas conducted the laboratory analyses. The procedures utilized are published by ANKOM Technologies, Macedon, New York, and by *Official Methods of Analysis of AOAC International*, by AOAC International, Gaithersburg, Maryland. Procedures used are:

- ANKOM ^{200} Technology Method Crude Fiber Analysis in Feeds, filter bag technique: determines crude fiber, which is the organic residue remaining after digesting with 0.255N H_2SO_4 and 0.313N NaOH. The compounds removed are predominantly protein, sugar, starch, lipids, and portions of both structural carbohydrates and lignin.
- ANKOM ^{200} Technology Method Neutral Detergent Fiber in Feeds, filter bag technique: determines the neutral detergent fiber, which is the residue remaining after digesting in a detergent solution. The fiber residues are predominantly hemicelluloses, celluloses, cellulose, and lignin.
- ANKOM ^{200} Technology Method Acid Detergent Fiber in feeds, filter bag technique: determines the acid detergent fiber, which is the residue remaining after digesting with H_2SO_4 and cetyl trimethlyammonium bromide (CTAB). The fiber residues are predominantly cellulose and lignin.
- ANKOM ^{200} Technology Method Acid Detergent Lignin in Beakers: determines the acid detergent fiber, which is the residue remaining after digesting with H_2SO_4, 72% by weight. The fiber residue is lignin with inorganic matter.
- ANKOM ^{200} Technology Method Ashing: determines the loss in weight after ignition (550-600ºC). The residue is the ash (inorganic matter).
- AOAC Method No. 990.03 Protein (Crude) to determine nitrogen
- AOAC Method No. 990.15 to determine moisture

Quality control for all ANKOM ^{200} procedures is accomplished through the use of standard samples obtained from the Nation Bureau of Standards. The standard is run along with the samples. The results for the samples are accepted if the standard was within its limits of error. The limits of error were ±1.5% for all tests.

Sample Collection

Sample collection was accomplished in two phases. The initial collection was done to provide material to determine the expected composition of each ingredient. Two random grab samples of manure were collected from the cattle pens. Each was placed in a 3.78-L (one-gallon) freezer Ziploc® bag. Two random grab samples were taken from the corn silage tube being utilized at that time, and they also were placed in freezer bags. The wheat straw samples were pulled from different locations, from randomly chosen bales, and also were placed in two different freezer bags. The pine shavings were obtained from the vendor, who permitted a grab sample to be taken, and they were placed in freezer bags. All bags were annotated for contents and date, and they were immediately delivered to the laboratory for analysis. The mixture's composition was determined based upon the fill results of the analyses of the first set of samples.

The second phase was to collect sufficient amounts of each ingredient to fill all of the compost reactors in the laboratory. The manure and silage were placed in two, 208-L (55-gallon) plastic containers and the lids are sealed on. These ingredients were used on the third day after collection. One bale of straw was randomly selected. The straw was pretreated by mowing it several times with a bagging-type lawn mower to reduce its particle size, and then the straw was bagged in heavy duty, black, plastic industrial strength trash bags. Two bales of pine shaving were purchased. After the ingredients were collected, two grab samples, one from each container, were taken immediately and dried at 104 ºC for 24 hours to determine the moisture content. The weight of each ingredient to satisfy the mixture requirements were then recalculated based on these new moisture-content results.

Carbon/nitrogen ratio

Prior to mixing, the carbon/nitrogen (C/N) ratio was calculated. First, the percent carbon in the soluble, cellulose/hemicellulose, and lignin substrates was calculated based on the stoichiometric equation for each particular substrate. The initial percent of nitrogen available for each ingredient had been determined by the previous analytical laboratory analysis. These nitrogen contents were then applied to the percent of soluble, cellulose/hemicellulose, and lignin contained in each ingredient. The C/N ratio for each ingredient was determined by dividing the percent carbon by the percent nitrogen. If the

calculated C/N ratio was greater then 25:1, the amount of nitrogen in the ammonium form required to decrease the C/N ratio of 25:1 was determined. The form of nitrogen added was feed-grade ammonium sulfate, a white, crystalline, granular compound used in dairy and cattle rations. Its solubility in water is 70.6 g/100 mL at 0ºC. It contains 21% nitrogen as ammonium and 24% sulfur as sulphate. Ammonium sulfate was chosen because the nitrogen, in the ammonium form, is the form of nitrogen most easily utilized by the microorganisms. The ammonium sulfate was purchased at the local Farmer's Cooperative, Manhattan, Kansas.

Mixing procedure

Prior to mixing, a grab sample of each ingredient was obtained. The samples were placed in a 3.78-L freezer Ziploc® plastic bag, and each bag was labeled with the date and identified. Each mixture was then prepared. Because the capacity of the mixer was not large enough to mix the entire batch for a mixture at one time, each mixture was weighed in two separate batches, mixed and the two batches were combined into one large container and then mixed by hand. Each ingredient was weighed to the nearest 4.5 g (0.01 lbs) on a balance beam scale, then placed in the large container and mixed. After all dry ingredients were added, the lid was placed on the container and the container was manually tumbled and turned to facilitate mixing. This was accomplished by flipping the container on to its side, rolling it, tipping it on to its top, back on its side, rolling so more, and then back in an up-right position four times.

Some of the water and manure was mixed together to form a slurry to reduce the formation of manure balls during mixing. The slurry mixture was fed proportionally into the mixer with the ingredients. After the slurry was added, the remaining water was added to the bucket to rinse the residual manure and then was fed into the mixer. The mixer ran approximately 10 minutes after all ingredients for each batch had been added. Pictures of weighing and mixing are at Figure 4.8. These and additional pictures are at Appendix B, Figures B.8.

Three grab samples were taken from each ingredient and from each mixture. One sample was dried at 104 ºC for 24 hours to determine the moisture content. A second sample was placed in a 3.87-L Ziploc® freezer bag, labeled, and frozen for later analysis.

All analyses were conducted after the termination of the experiment. The third set of samples were displayed and photographed. Pictures of the three mixtures are presented in Figure 4.9 and Appendix B, Figures B.9.

a. b.

Figure 4.8 Mixing of ingredients: (a) individual ingredient weighted on a balance beam scale; and, (b) ingredients mixed together using a cement mixer

Assembly procedure

The inside of both the bottom and top caps of each reactor was coated with wax in a 2.54-cm band around the cap's rim (Appendix B, Figure B.10). The wax is Master Plumber Bol-Wax® No.1 full size, wax toilet gasket. This wax is not supposed to harden or deteriorate. It is advertised to form a gas-tight, odor-tight and water-tight seal. The bottom caps were installed before the reactor tubes were filled. Each bottom cap was twisted as it is being pushed on to form a better seal. The tubes were filled and tapped on the outside to promote settling. Each tube was placed on the scale, substrate added to fill the tube to the brim, the probes inserted and the entire reactor weighted. Each tube was carefully placed on the floor in its final position. The top cap was placed on and lightly pressed onto the tube. The top cap was not twisted to minimize any additional settling. The remaining relative-humidity sensors were installed, the top thermocouple wire inserted into the top of the cap, and all holes sealed with the wax. All reactors were set in place, the air tubes were attached to the air manifold and the air flow set for the particular mixture. Pictures taken of the entire experimental setup are presented as Figure 4.10 and in Appendix B, Figure B.11.

a. Mixture 1

c. Mixture 3

b. Mixture 2

Figure 4.9 Three mixtures: (a) Mixture 1: predominately resistant-to-biodegradation with 25% soluble, 25% cellulose/hemicellulose, and 50% lignin; (b) Mixture 2: predominately slower-to-biodegrade with 25% soluble, 50% cellulose/hemicellulose, and 25% lignin; and, (c) Mixture 3: predominately readily-biodegradable with 50% soluble, 25% cellulose/hemicellulose, and 25% lignin.

a. b.

Figure 4.10 Experimental unit equipment setup: (a) Reactor tubes with thermocouple probes inserted and connected to datalogger with battery back-up, computer, and air supply manifold with air tube connected to each reactor; and, (b) water-bath system for saturating the supply air

Experimental run

The air flow rates were determined based on 0.312 L min^{-1} kg^{-1} of manure (dry basis) [10 ft^3 min^{-1} ton^{-1} of manure (dry basis)] (Rynk et al., 1992, p. 33). After the dry weight of each mixture was calculated and the air tubes were attached to the air manifold, the air flow was set as follows: 0.55 L min^{-1} (1.17 ft^3 hr^{-1}) for Mixture 1; 0.83 L min^{-1} (1.75 ft^3 hr^{-1}) for Mixture 2, and 1.74 L min^{-1} (3.68 ft^3 hr^{-1}) for Mixture 3. One computer system was utilized to record all data. The computer program to record the carbon dioxide and relative humidity was initiated. The datalogger program was reset and started.

On the first day, the air flow was reset to the recommended flow using a primary flow meter, Dry Cal® DC-Lite primary flow meter by the Bios Instrument Corporation. The meter was attached to each flow meter outflow. The rate was adjusted to deliver the amount of air calculated. On a daily bases, data was collected and the system was checked and any minor adjustments to the air flow were made as needed.

The first set of reactors was taken off line and sampled on Day 6. The second set of reactors was taken off line on Day 14, the third set on Day 21. The last set, to be removed on Day 28, was changed from the time-line proposed in experimental design. The last reactor for both the slower-to-biodegrade and the resistant-to-biodegradation were removed on Day 21. The slower-to-biodegrade was removed because its temperature profile had dropped to the reference-temperature level, indicating the major decomposition process was completed. The resistant-to-biodegradation was removed because it was performing just like the other three resistant-to-biodegradation reactors had, following the reference-temperature profile. The readily-biodegradable reactor that had its air supply interrupted, was chosen to remain on for additional time until its decomposition reaction indicated completion.

As each unit was taken off line, the unit was weighed, the cap removed, a picture of the mixture taken, and the distance of the mixture from the top measured and recorded. The top layer of mixture was removed down to the 70-cm probe and discarded, and the 70-cm probe was removed. At the 60-cm to 70-cm level, the entire volume was removed and placed in a clean container and mixed by hand. Three grab samples were taken; one bagged for analysis, one placed in a tin to determine moisture content, and the last to be photographed. Notes were taken about the observed characteristics of the mixture. The bagged sample was identified and frozen for later analysis. The remaining mixture was removed and discarded. Next, the 60-cm probe was removed and the mixture down to the 50-cm probe was removed and discarded. The 50-cm probe was removed, and the procedure for the mixture in the 40-cm to 50-cm interval was conducted the same as for the 60-cm to 70-cm interval. This procedure was repeated for the 20-cm to 30-cm and the 0-cm to 10-cm intervals. The samples taken for moisture content were dried at 104 ºC for 24 hours. All frozen samples were retained until all the experimental runs were completed; then they all submitted to the laboratory for analysis at the same time. Pictures of the final composted mixtures are presented in Figure 4.11. Additional pictures of looking into each reactor tube when it was removed from the system and samples of the composted material are presented in Appendix B for the readily-biodegradable, mixture 3 (Appendix B, Figures B.12, B.13, and B.14); for the slower-to-

biodegrade, mixture 1 (Appendix B, Figures B.15 and B.16); and for the resistant-to-biodegradation, mixture 2 (Appendix B, Figures B.17, B.18, and B.19).

a.

c.

b.

Figure 4.11 Three mixtures composted: (a) readily-biodegradable from Reactor C1 after Hour 552 (Mixture 3); (b) slower-to-biodegrade from Reactor B2 after Hour 550 (Mixture 2); and, (c) resistant-to-biodegradation from Reactor A2 after Hour 550.5 (Mixture 1).

Statistical analysis methodology

The goal of this research work is to develop a predictive, deterministic, mathematical, in-vessel, compost model based on substrate type(s) and microbial populations groups, and their effect on the temperature profile. The purpose of the experimental design is to provide actual operational results to the mathematical model. Each one of the three mixtures tested is separate from other mixtures. Thus, the design is a one-way design, and not a factorial experiment.

The mathematical model was written in Matlab® (The MathWorks, Version R2007a), an interactive system with a basic data element that does not require dimensioning. Technical computing problems, especially those with matrix and vector formulations, are solved in a relatively short time.

The model was initially to be validated by plotting residual differences between the model curve and the actual data ($y_{obs} - Y_{predicted}$). The residual plot is presented to magnify the differences between the model fit and the actual data so deviations between the model and data are made more obvious (Sulfita et al., 1987 *in* Schmidt, 1992). Crop projection models are validated using square error (Kastens, 2008). The $Standard\ Deviation(observed)$ is obtained for the experimental data. The $Square\ Root\left(avg\sum(predicted - observed)\right)$ is calculated. The square error is then calculated:

$\frac{SQRT\left(avg\sum(predicted - observed)\right)}{Standard\ Deviation(observed)}$. If the square is 1.0 or less the model is a good fit.

CHAPTER 5 - EXPERIMENTAL RESULTS

This chapter discusses the laboratory experimental results. It is divided into three sections: substrate analysis for mixtures, analysis of the composted mixtures and recorded temperature profiles during composting.

Substrate analysis

Initial sample analysis

The four proposed ingredients were pine wood shavings (as used for pets, horse bedding), corn silage (used as feed for dairy cattle), wheat straw, which included the entire above ground portion of the wheat plant (used as bedding in the swine unit), and cattle manure (the end product). The freshness of the cattle manure was from just being dropped up to three days old. The initial sample analysis (Tables 5.1 and 5.2) was to determine the percent dry matter, crude protein, and the percent of soluble, cellulose/hemicellulose, lignin, and ash/inorganic components of each ingredient. The laboratory report can be found in (Appendix C, Analytical Laboratory Results, Laboratory results 6321-6324 (R1) 1 Nov 07).

Table 5.1 Substrate composition by percent of each ingredient in the initial sampling.

Ingredient (Initial Sampling)	Dry Mass (% Dry Basis)				Wet Mass (% Wet Basis)				
	Soluble	Cellulose / Hemicellulose	Lignin	Ash / Inorganic	Water	Soluble	Cellulose / Hemicellulose	Lignin	Ash / Inorganic
Wheat Straw	22.4	64.5	6.1	6.0	10.1	20.1	58.0	5.5	6.3
Pine	6.1	69.6	22.5	1.8	9.9	5.5	62.7	20.3	1.6
Silage	57.8	38.8	2.0	1.4	62.7	21.6	14.5	0.8	0.5
Manure	60.3	35.7	1.8	2.2	65.1	21.0	12.5	0.6	0.8

Table 5.2 Percent crude protein and nitrogen composition of each ingredient in the initial sampling.

Ingredient (Initial Sampling)	Crude Protein (% Dry Mattert	Nitrogen (% Dry Matter)
Wheat Straw	5.4	0.864
Pine	0.6	0.096
Silage	9.3	1.487
Manure	25.9	4.137

Three targeted experimental design mixtures, as specified in Figure 4.3, were calculated from the analytical results for each ingredient. The readily-biodegradable mixture had the soluble substrate as the predominate substrate. The slower-to-biodegrade had cellulose/hemicellulose substrate as the predominate substrate. And, the resistant-to-biodegradation had cellulose/hemicellulose with higher lignin concentration as the predominate substrate. These three mixtures are presented in Table 5.3. The table lists the targeted percentage for each substrate, the possible-to-achieve level for each substrate based on the initial analysis, and the percent required of each dry ingredient to meet the possible-to-achieve level.

Table 5.3 Target and possible-to-achieve mass (% dry basis) for each substrate within each ingredient based on the initial sampling for three mixtures: (a) readily-biodegradable; (b) slower-to-biodegrade; and, (c) resistant-to-biodegradation.

(a) Readily-biodegradable: Mixture 3	Component	Soluble	Cellulose / Hemicellulose	Lignin	Ash / Inorganic
	Target Percent	60.0	30.0	10.0	0.0
	% possible-to-achieve	59.0	36.2	1.9	1.8
Ingredients	% of ingredient in the mixture	% each ingredient contributes to the particular substrate on a dry basis			
Wheat	0.0	0.0	0.0	0.0	0.0
Pine	0.0	0.0	0.0	0.0	0.0
Silage	50.0	28.9	19.4	1.0	0.7
Manure	50.0	30.1	16.8	0.9	1.1

(b) Slower-to-biodegrade: Mixture 1	Component	Soluble	Cellulose / Hemicellulose	Lignin	Ash / Inorganic
	Target Percent	30.0	60.0	10.0	0.0
	% possible-to-achieve	29.2	56.8	9.0	4.1
Ingredients	% of ingredient in the mixture	% each ingredient contributes to the particular substrate on a dry basis			
Wheat	45.0	10.1	29.0	2.8	3.1
Pine	25.0	1.5	16.4	5.6	0.4
Silage	20.0	11.6	6.8	0.4	0.3
Manure	10.0	6.0	3.6	0.2	0.2

(c) Resistant-to-biodegradation: Mixture 2	Component	Soluble	Cellulose / Hemicellulose	Lignin	Ash / Inorganic
	Target Percent	10.0	70.0	20.0	0.0
	% possible-to-achieve	9.6	66.7	20.7	2.1
Ingredients	% of ingredient in the mixture	% each ingredient contributes to the particular substrate on a dry basis			
Wheat	5.0	1.1	3.2	0.3	0.3
Pine	90.0	5.5	62.7	20.3	1.6
Silage	0.0	0.0	0.0	0.0	0.0
Manure	5.0	3.0	1.8	0.1	0.1

The issue of insufficient nitrogen was eliminated from the analysis by adding additional nitrogen where required to provide a C/N ratio of 25:1 (Rynk et al.,1992). The percent carbon for each substrate was calculated using the stoichiometric equations presented in Chapter 3. Results of the stoichiometric calculations are presented in Table 5.4. Next, the percent carbon for each ingredient was calculated by percent dry weight of each substrate contained in the ingredient (Table 5.1). The resultant C/N ratio (Table 5.5) was determined by dividing the total percent carbon in the ingredient (using Tables 5.4 and 5.1) by the percent nitrogen present in the ingredient (Table 5.2). These results were utilized to calculate the amount of ammonium sulfate to be added.

Table 5.4 Determination of the percent carbon in each substrate based on stoichiometric equation.

Type of Substrate	Molecular wt. of one mole substrate ($g\ mol^{-1}$)	Mass of Carbon present ($g\ mol^{-1}$)	Percent Carbon
Soluble	180.156	72.060	40.0
Cellulose	382.295	144.132	36.7
Lignin	180.203	120.110	66.7

The analysis from the first set of ingredient samples was utilized to calculate the mixtures. A second ingredients collection was conducted. From this ingredient collection the mixtures were made. A set of samples were taken from these ingredients two days before mixing to determine their moisture content. The amount of water added to the mixture was based on the moisture from these samples. The target moisture content was 60% (wet basis). The moisture content of mixture (Table 5.6) was determined based on the percent moisture in the individual ingredients and the percent of each ingredient in the mixture. From these results the amount of moisture required to raise the total mixture to 60% (wet basis) was calculated.

Table 5.5 Determination of the carbon/nitrogen ratios based on percent of each substrate in: (a) wheat straw; (b) pine shavings; (c) corn silage; and, (d) cattle manure.

(a) Wheat Straw	% C by wt	% N from analysis	C/N Ratio
Soluble	8.96	0.86	43.3
Cellulose / Hemicellulose	24.32		
Lignin	4.09		
Total	37.37		

(b) Pine Shavings	% C by wt	% N from analysis	C/N Ratio
Soluble	2.44	0.096	455
Cellulose / Hemicellulose	26.25		
Lignin	15.00		
Total	43.68		

(c) Corn Silage	% C by wt	% N from analysis	C/N Ratio
Soluble	23.12	1.498	26.3
Cellulose / Hemicellulose	14.63		
Lignin	1.36		
Total	39.10		

(d) Cattle Manure	% C by wt	% N from analysis	C/N Ratio
Soluble	24.11	4.14	9.38
Cellulose / Hemicellulose	13.45		
Lignin	1.22		
Total	38.79		

Table 5.6 Percent moisture in bulk samples from second sampling, used in determining water additions to mixed ingredients.

Ingredient Bulk Sample	Moisture percent
Wheat straw	6.0
Pine Shavings	6.0
Corn Silage	63.6
Cattle manure	66.0

Second sample analysis

The makeup of each of the experimental mixtures was computed based on the composition of the ingredients as given in Table 5.1. However, new ingredients were collected and the mixtures were made from these new ingredients, which had slightly defferent compositions. Table 5.7 lists the laboratory analyses of each ingredient and Table 5.8 lists the nitrogen content.

Table 5.7 Substrate composition by percent of each ingredient used in mixtures.

Ingredient (used in mixtures)	% Dry Basis				% Wet Basis				
	Soluble	Cellulose / Hemicellulose	Lignin	Ash / Inorganic	Water	Soluble	Cellulose / Hemicellulose	Lignin	Ash / Inorganic
Wheat Straw	25.3	62.3	6.1	5.3	6.9	23.6	58.0	6.4	4.9
Pine	2.0	72.8	23.7	1.5	9.8	1.8	65.7	21.4	1.3
Silage	63.2	33.4	2.0	1.5	63.2	23.3	12.3	0.7	0.5
Manure	63.1	23.4	3.7	9.8	68.1	20.1	6.5	1.2	3.1

Table 5.8 Percent crude protein and nitrogen composition of each ingredient in the second sampling.

Ingredient (Initial Sampling)	Crude Protein (% Dry Mattert	Nitrogen (% Dry Matter)
Wheat Straw	6.7	1.07
Pine	0.6	0.096
Silage	10.2	1.63
Manure	226.7	4.14

Comparison of the substrate composition of the ingredients as indicated in the initial sample results (Table 5.1) to the analysis of the ingredients used in the mixtures (Table 5.7) shows there are differences. Comparison of the nitrogen content between the initial sample (Table 5.2) and the second sample (Table 5.8) also indicate some differences. Recall that the analysis of ingredients used was not accomplished until after the composting experiment is finished. Table 5.9 indicates the percent differences. A positive number indicates the value increases from the initial sampling. A negative number indicates a decrease in value from the initial sampling. Wheat straw and the pine shavings exhibited large changes in both the soluble substrate and ash/inorganic. Wheat straw also indicates a large decrease in water content. The silage and manure indicate a decrease in the cellulose/hemicellulose substrate.

Table 5.9 Percent difference in the substrates in the ingredients between the initial sampling to the second sampling.

Ingredient (used in mixtures)	% Difference between initial and second analysis on a dry basis					Water
	Soluble	Cellulose / Hemicellulose	Lignin	Ash / Inorganic	Nitrogen	
Wheat Straw	12.9	-3.4	16.4	-24.3	24.1	-31.7
Pine	-66.2	4.6	5.3	-16.7	0.0	-1.0
Silage	9.3	-13.9	0.0	0.1	9.8	0.8
Manure	4.6	-12.3	1.9	6.6	3.3	4.6

Because of these differences, the actual substrate percentages in the three experimental design mixtures were recalculated from the second analytical results of each ingredient. The results for the three mixtures are presented in Table 5.10. The table presents the original targeted percentage, the results achieved based on the second analysis, and the percent contribution of each ingredient to the soluble, cellulose/hemicellulose, lignin, or the ash/inorganic components. Comparing Table 5.3 to Table 5.10 indicates changes to the percent achieved. The readily-biodegradable mixture increased in soluble substrate by 3.1%, from 59.0% to 63.1%; the cellulose/hemicellulose decreased by 8.8%, from 36.2% to 28.4%; the lignin content increased by 0.9%, from 1.9% to 2.8%; and the ash/inorganic increased by 3.8%, from 1.8% to 5.6%. Thus, this mixture increased slightly in the soluble content. The slower-to-biodegrade mixture has changes, but they were not as great. The soluble substrate increased by 1.6%, from 29.2% to 30.8%; the cellulose/hemicellulose decreased by 2.5%, from 56.8% to 55.3%; the lignin content increased by 0.9%, from 9.0% to 9.9%; and the ash/inorganic decreased by 0.1%, from 4.1% to 4.0%. These results show that the concentration of cellulose/hemicellulose mixture was slightly less than intended. The resistant-to-biodegradation mixture also slightly changed. The soluble substrate decreased by 3.4%, from 9.6% to 6.2%; the cellulose/hemicellulose increased by 2.1%, from 66.7% to 69.8%; the lignin content increased by 1.2%, from 20.7% to 21.9%; and the ash/inorganic remained the same at 2.1%. This mixture was slightly more resistant to decomposition than the intended target.

Table 5.10 Target and possible-to-achieve mass (% dry basis) for each substrate within each ingredient based on the second sampling for the three mixtures: (a) readily-biodegradable; (b) slower-to-biodegrade; and, (c) resistant-to-biodegradation.

(a) Readily-biodegradable: Mixture 3	Component	Soluble	Cellulose / Hemicellulose	Lignin	Ash / Inorganic
	Target Percent	60.0	30.0	10.0	0.0
	% achieved	63.1	28.4	2.8	5.6
Ingredients	% of ingredient in the mixture	% each ingredient contributes to the particular substrate on a dry basis			
Wheat	0.0	0.0	0.0	0.0	0.0
Pine	0.0	0.0	0.0	0.0	0.0
Silage	50.0	31.6	16.7	1.0	0.7
Manure	50.0	31.5	11.7	1.8	4.9

(b) Slower-to-biodegrade: Mixture 1	Component	Soluble	Cellulose / Hemicellulose	Lignin	Ash / Inorganic
	Target Percent	30.0	60.0	10.0	0.0
	% achieved	30.8	55.3	9.9	4.0
Ingredients	% of ingredient in the mixture	% each ingredient contributes to the particular substrate on a dry basis			
Wheat	45.0	11.4	28.0	3.2	2.4
Pine	25.0	0.5	18.2	5.9	0.4
Silage	20.0	12.6	6.7	0.4	0.3
Manure	10.0	9	2.3	0.4	1.0

(c) Resistant-to-biodegradation: Mixture 2	Component	Soluble	Cellulose / Hemicellulose	Lignin	Ash / Inorganic
	Target Percent	10.0	70.0	20.0	0.0
	% achieved	6.2	69.8	21.9	2.1
Ingredients	% of ingredient in the mixture	% each ingredient contributes to the particular substrate on a dry basis			
Wheat	5.0	1.3	3.1	0.4	0.3
Pine	90.0	1.8	65.6	21.3	1.3
Silage	0.0	0.0	0.0	0.0	0.0
Manure	5.0	3.2	1.2	0.2	0.5

A new C/N ratio was also determined. The percent carbon for each substrate was also recalculated using the stoichiometric equations. The new C/N ratios are presented in Table 5.11. The results show the C/N ratios decreased by 21% for the wheat straw, 70% for the corn silage and by 60% for the manure.

Table 5.11 Determination of the carbon/nitrogen ratios based on percent of each substrate in second sampling for: (a) wheat straw; (b) pine shavings; (c) corn silage; and, (d) cattle manure.

(a) Wheat Straw	% C by wt	% N from analysis	C/N Ratio
Soluble	10.13	1.07	35.8
Cellulose / Hemicellulose	23.49		
Lignin	4.75		
Total	38.37		

(b) Pine Shavings	% C by wt	% N from analysis	C/N Ratio
Soluble	0.8	0.096	459
Cellulose / Hemicellulose	24.56		
Lignin	15.79		
Total	44.05		

(c) Corn Silage	% C by wt	% N from analysis	C/N Ratio
Soluble	25.27	1.63	15.5
Cellulose / Hemicellulose	12.59		
Lignin	1.32		
Total	39.18		

(d) Cattle Manure	% C by wt	% N from analysis	C/N Ratio
Soluble	25.24	4.27	5.90
Cellulose / Hemicellulose	8.83		
Lignin	2.45		
Total	36.52		

Results based on mixtures

Samples were also taken from each mixture for analyses (Table 5.12). The comparison (Table 5.12) of initial sampling (Table 5.3), the second sampling (Table 5.10) and the mixture (Table 5.12) to the target composition of each substrate on a percent dry basis indicates, in general, an increase in the soluble substrate, and a decrease in the cellulose/hemicellulose substrate. The readily-biodegradable mixture (Table 5.13a) indicates the amount of soluble component increased even more to 9.5% greater than the target of 60%. The cellulose/hemicellulose substrate decreased more to 23.6%, 6.4% lower than the target of 30%. The percent lignin changed by 0.1% when compared to the second sampling. The ash/inorganic actually decreased from the second sampling but still greater than the initial sampling. The slower-to-biodegrade mixture (Table 5.13b) showed similar results, but the slower-to-biodegrade is not as high in the cellulose/hemicellulose as was targeted. The resistant-to-biodegradation mixture (Table 5.13c) shows a similar picture, with the soluble substrate being more than desired and the cellulose/hemicellulose and lignin substrate being less than desired.

A new C/N ratio was computed for the mixtures (Table 5.14). The results indicate all mixtures were less than the target C/N ratio of 25:1. The readily-biodegradable was 13.5:1, the slower-to-biodegrade was 10.4:1, and the resistant-to-biodegrade was 18.6:1.

Table 5.12 Percent ingredient analysis based on mixture analysis.

Mixtures	% Dry Basis					Water
	Soluble	Cellulose / Hemicellulose	Lignin	Ash / Inorganic	Nitrogen	
Readily-biodegradable Mixture 3	69.5	23.6	2.7	4.2	2.69	65.8
Slower-to-biodegrade Mixture 1	34.7	53.2	8.9	3.2	2.14	44.8
Resistant-to-biodegradation Mixture 2	22.2	58.8	16.6	1.4	3.36	32.8

Table 5.13 Comparison of initial sampling, the second sampling and the mixture to the target composition of each substrate on a percent dry basis for the three mixtures: (a) readily-biodegradable; (b) slower-to-biodegrade; and, (c) resistant-to-biodegradation.

(a) Readily-biodegradable Mixture 3	% Dry Basis				Water
	Soluble	Cellulose / Hemicellulose	Lignin	Ash / Inorganic	
Target composition	60.0	30.0	10.0	0.0	
Initial: based on grab sample	59.0	36.2	1.9	1.8	64.9
Ingredients: Based on bulk ingredients use in mixture preparation	63.1	28.4	2.8	5.6	65.8
Mixture: Based on analysis of the mixture	69.5	23.6	2.7	4.2	65.8

(b) Slower-to-biodegrade Mixture 1	% Dry Basis				Water
	Soluble	Cellulose / Hemicellulose	Lignin	Ash / Inorganic	
Target composition	30.0	60.0	10.0	0.0	
Initial: based on grab sample	29.2	56.8	9.0	4.1	48.9
Ingredients: Based on bulk ingredients use in mixture preparation	30.8	55.3	9.9	4.0	49.2
Mixture: Based on analysis of the mixture	34.7	53.2	8.9	3.2	44.9

(c) Resistant-to-biodegradation Mixture 2	% Dry Basis				Water
	Soluble	Cellulose / Hemicellulose	Lignin	Ash / Inorganic	
Target composition	10.0	70.0	20.0	0.0	
Initial: based on grab sample	9.6	66.7	20.7	2.1	41.2
Ingredients: Based on bulk ingredients use in mixture preparation	6.2	69.8	21.9	2.1	42.0
Mixture: Based on analysis of the mixture	22.2	55.8	16.6	1.4	31.4

Table 5.14 Determination of the carbon/nitrogen ratio based on percent for each mixture: (a) readily-biodegradable; (b) slower-to-biodegrade; and, (c) resistant-to-biodegradation.

(a) Readily-biodegradable: Mixture 3	% C by wt	% N from analysis	C/N Ratio
Soluble	27.80	2.85	13.5
Cellulose / Hemicellulose	8.89		
Lignin	1.79		
Total	38.48		

(b) Slower-to-biodegrade: Mixture 2	% C by wt	% N from analysis	C/N Ratio
Soluble	8.87	3.36	10.4
Cellulose / Hemicellulose	20.07		
Lignin	5.95		
Total	34.89		

(c) Resistant-to-biodegradation: Mixture 1	% C by wt	% N from analysis	C/N Ratio
Soluble	13.86	2.14	18.6
Cellulose / Hemicellulose	20.07		
Lignin	5.95		
Total	39.88		

Problems encountered

The experiment had to be run twice due to problems. The major problems encountered during the first experimental run are listed below. The corrected procedures were presented in Chapter 4.

- During mixing all the required water was added proportionally as well as the manure. The manure, however, stuck to the mixing-container sides making it difficult to ensure all the manure was actually was added. When the manure was added it formed balls, some over 2.5 cm in diameter. Smaller amounts were tried and the manure balls were broken up by hand, but as the mixture rotated in the mixer, the balls reformed. Also, when measuring out the amount of ingredients required, the volume of each ingredient was measured

separately. When combined, there was insufficient volume because the smaller particles filled in around the larger ones.

- Another problem was after the three mixtures were added to the reactor units, installing the "0 cm" probes was impossible without spilling the contents or causing more settling. The tubes had to be slanted at a 45°-angle, and while lying on the floor, the probes were inserted. Any slight movement caused the probes to pull out. This was beause the probes were set into a hole, having no substrate to help keep them in place And, because each reactor's thermocouple wires were taped together to form a wiring harness and all wires were connected to the data logger thus making it impossible to move the wire around so sufficient wire was available as the reactors were set in the proper location.
- During the initial several days, several thermocouples probes failed to provide a reading. In some cases the connection to the data logger was bad even though the entire system was tested. For some probes, reconnecting the wires did correct the problem. If the probe did not respond, other probes not being utilized were set in their place. The data logger did not recognize these connections. The probe replacement became the major problem because since the space to move was so tight, every time a connection was worked on, more connections were being disturbed than what was being fixed.
- The first experimental run was terminated when the electrical breaker to the air compressor tripped resulting in the loss of air flow for an entire day.
- When the reactors were being cleaned out after the first experimental run, the substrate at the bottom of the reactors was extremely dry. The compressing of the air resulted in the air to exceed saturation, thus liquid water came out. When the air was released back into atmospheric conditions, the relative humidity of the air decreased. The dry air dried the mixtures.

There also were several problems encountered during the second experimental run. There problems were:

- The first problem occurred with the second manure sample collection. The cattle pens are cleaned twice a week. Three days before the manure was

to be collected, a cold front came through that dropped night temperatures to -11.7 °C (11 °F). The day temperatures were 5 °C to 10.5 °C (41 °F to 51 °F). The day before the sample was collected, the day temperature only reached -2.2 °C (28 °F), with the night temperature still at -11.7 °C (11 °F). Hence, the manure was partially frozen when collected. The sample was held for two days at temperatures just above freezing. The sample was stirred twice a day to allow for a slow, uniformed thaw. When the ingredients were mixed, some ice crystals were still present in the manure. During mixing, the manure completely thawed. The readily-biodegradable mixture (Mixture 3) still was very cold. The low temperature inhibited microbial growth at the start of the experimental run.

- The second problem was that, at 1830 hours on March 3, 2008 (approximately 191 hours into the experimental run), the air hose connecting reactor C2 to the air supply was found disconnected. The air hose immediately was reconnected. Apparently, the hose accidentally was disconnected during the last equipment check, conducted at 1630 hours on March 2, 2008. As a result, no forced air was supplied to reactor C2 for 26 hours and the aerobic decomposition process began to shut down. Aaerobic microorganisms began to die and heat generatation was reduced; the decomposition population was transitioning from aerobic to anaerobic. Restoration of the air supply permitted the regrowth of the aerobic microorganisms. This effected the comparative analysis on a time line basis with the similar (Reactor C) mixtures.
- Another problem concerned the CO_2 and relative humidity sensors. Two issues occurred. First, the monitoring computer shut down several times, losing the data being collected during those particular times, thus leaving gaps in the data. Second, was the CO_2 sensers themselves because the high-humidity atmosphere corroded the sensors' prongs, which produced a constant maximun $CO_{2,}$ recorded by the sensor. The problem became apparent when temperature readings fell while the expected CO_2 reading remained at maximum. Both the relative humidity and CO_2 readings were discarded.

Analysis of composted substrate

Visual and sensory observations were recorded as the reactors were taken off line. Pictures of three reactor units, one of each mixture type, are presented as in Figure 5.1. Additional pictures of looking into each reactor tube when it was removed from the system are presented in Appendix B for the readily-biodegradable, mixture 3 (Appendix B, Figure B.12); for the slower-to-biodegrade, mixture 1 (Appendix B, Figure B.15); and for the resistant-to-biodegradation, mixture 2 (Appendix B, Figure B.17).

a.

c.

b.

Figure 5.1 Pictures inside of reactor tubes when caps were removed: (a) readily-biodegradable (Mixture 3) (note shrinkage); (b) slower-to-biodegrade (Mixture 2); and, (c) resistant-to-biodegradation (Mixture 1).

Table 5.15 Visual and sensory observations when reactor tubes were taken off-line and opened.

Reactor No.	Substrate composition	Time Reactor was removed from system and opened (h)	Visual and sensory observations
A1	Slower-to-biodegrade	550	Musty smelling when cap removed Moisture in cap Found white fungus through the mixture from approximately the 60-cm to 20-cm level Mixture at the bottom 5 cm was dusty
B1	Resistant-to-biodegradation	550	No visual change noted from initial mixture
C1	Readily-biodegradable	552	Moisture (beads) inside of cap Mixture from the 50-cm to 20-cm level very wet Mixture from the 10-cm to 0-cm level felt dry Bottom 2.54 cm hard and crusty
A2	Slower-to-biodegrade	550.5	Some moisture on inside of cap Fungus on top of mixture Mixture felt dry at the 10-cm to 0-cm level Dusty on bottom
B2	Resistant-to-biodegradation	550	When cap removed, the tape on one side of the CO_2 meter came free from cap. Meter hanging down Mixture dusty at the 10-cm to 0-cm layer
C2	Readily-biodegradable	974.5	Some cavities were found at the 40-cm to 30-cm and the 30-cm to 20-cm levels At the 20-cm to 10-cm layer, near the 10-cm level, found dried material in center of tube, could see white fungus The 10-cm to 0-cm level felt dry When removing the CO_2 meter, could not remove the meter from the back. After pulling, meter and back separated. All the prongs were corroded (green in color)
A3	Slower-to-biodegrade	328	Some water found inside cap Small amount of fungus on top of mixture Musty smelling at the 40-cm to 50-cm layer Found some lumps of manure that contained white fungus, felt dryer than the remainder of mixture
B 3	Resistant-to-biodegradation	328	Inside of cap was dry Found several lumps of manure, were dry Mixture was consistent throughout, no degradation noted
C3	Readily-biodegradable	326.5	Strong ammonia smell when cap removed Water in cap Water in bottom cap, when drained was dark brown in color Water found on floor under bottom Mass of mixture shrank, probe "70-cm" in air As mixture removed, smell dissipated White fungus started to appear at approximately the 20-cm level. Bottom of mixture was hard.
A4	Slower-to-biodegrade	164.5	Water condensed in top of cap White fungi visible on top Found some small hard lumps of manure in mixture
B4	Resistant-to-biodegradation	165.5	No water in cap No fungus visible Found some small hard lumps of manure in mixture

C4	Readily-biodegradable	163.5	Light musty smell of manure when cap removed Water in top of cap White fungi visible over top As mixture removed, composition uniform throughout Could feel heat within mixture Bottom approximately 15 cm (6 inch) came out as a plug. The bottom 1.5 cm (0.6 inch) was dried.

Analysis Comparison

The composted mixtures were sampled as the reactor tubes were taken off line, then analyzed (Appendix C, Analytical Laboratory Results, Laboratory Analysis 9921-9963 (R1) May 08). The analysis of the laboratory results were compiled (Appendix D). The results were compared within each mixture type (readily-biodegradable, slower-to-biodegrade, and resistant-to-biodegradation) and by each substrate type (soluble, cellulose/hemicellulose, lignin, and ash/inorganic). In general the results indicate major differences between the three major substrate types: the readily-biodegradable, the slower-to-biodegrade, and resistant-to-biodegradation. When applicable, each figure contains description listing the degradability of the mixture and the mixture number for tracking purposes.

Figure 5.2 presents the change in substrate mass ($kg_{dry\ substrate}\ kg^{-1}_{total\ dry\ mass}$) by reactor through time. The readily-biodegradable mixture shows a decrease in soluble substrate [Figure 5.2(a)]. The cellulose/hemicellulose showed a slight increase followed by a decrease. The lignin showed a slight increase. Humus production would occur in this organic matter category because of its resistance to biodegradation. The ash/inorganic matter indicates a change, but is believed to be due to the non-homogeneity of the sample. Reactor C2 is not included because of the aeration problem that occurd.

The slower-to-biodegrade mixture followed its expected results: a decrease in the soluble substrate [Figure 5.2(b)]. This decrease was limited by the amount of soluble substrate present. The cellulose/hemicellulose slowly decreased through time. The lignin indicated an overall increase, again possibly due to humus production. The ash/inorganic remained constant as expected. Reactor A1 was taken off-line at the same time as Reactor A2. A decision was made not to conduct any analysis on this composted material because of the similiarity of the temperature curve for Reactor A2.

The resistant-to-biodegradation remained nearly constant [Figure 5.2(c)]. The data indicated there was a slight increase in soluble substrate after the first seven days, and then there was a slight decrease. The cellulose/hemicellulose showed no change after seven days and then a decrease after 14 days. Lignin showed the opposite: no change after the first seven days and then a slight increase. Reactors B1 and B2 were taken off at Hour 550. Again a decision was made not to conduct any analysis on these reactor omposted materials because of the similiarity of the temperature curve to Reactor B3.

a. Figure 5.2

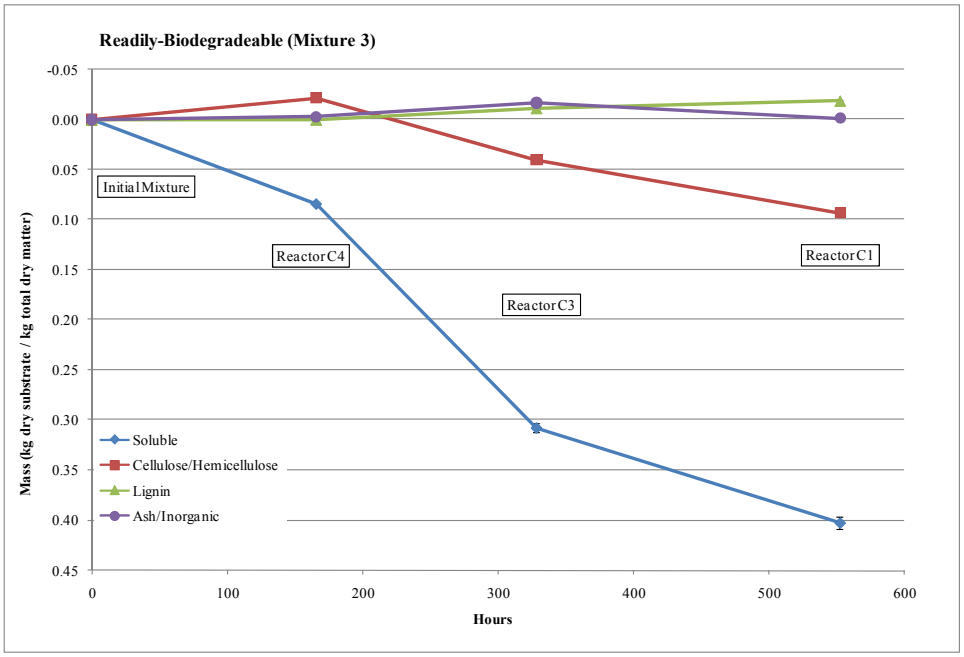

b. Figure 5.2

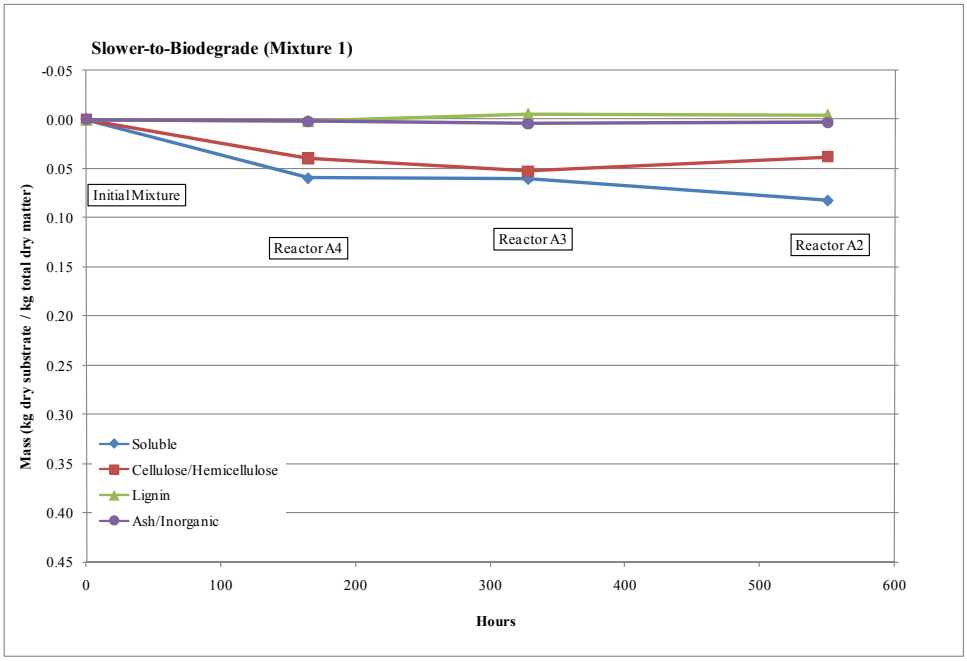

c. Figure 5.2

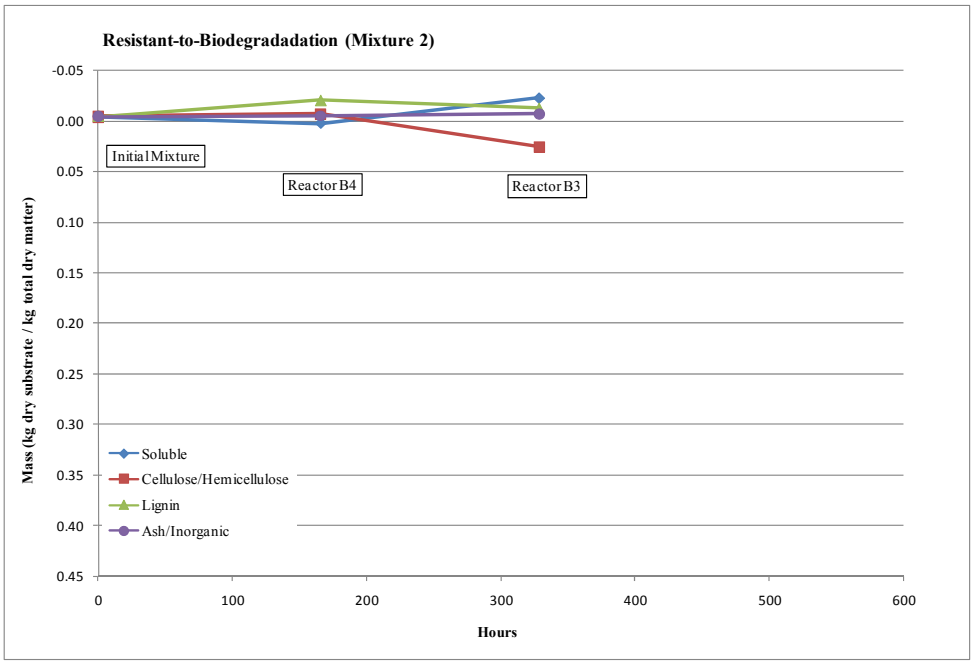

Figure 5.2 Change in substrate mass through time within a mixture by reactor for: (a) readily-biodegradable; (b) slower-to-biodegrade; and, (c) resistant-to-biodegradation.

Figure 5.3 shows the change in percent composition of substrates through time within a mixture by reactor for (a) readily-biodegradable, (b) slower-to-biodegrade, and (c) resistant-to-biodegradation. Figure 5.3 demonstrated a similar pattern to Figure 5.2. Figure 5.3(a) includes the fourth reactor, C2. This reactor shows an increase in lignin, decrease in cellulose/hemicellulose, and an increase in soluble.

In all cases, the bars on the graphs indicate the limits of error of ±1.5% for all laboratory analysis. Quality control for all ANKOM [200] procedures is accomplished through the use of standard samples obtained from the Nation Bureau of Standards. The standard is run along with the samples. The results for the samples are accepted if the standard was within its limits of error. The limits of error are ±1.5% for all tests.

a. Figure 5.3

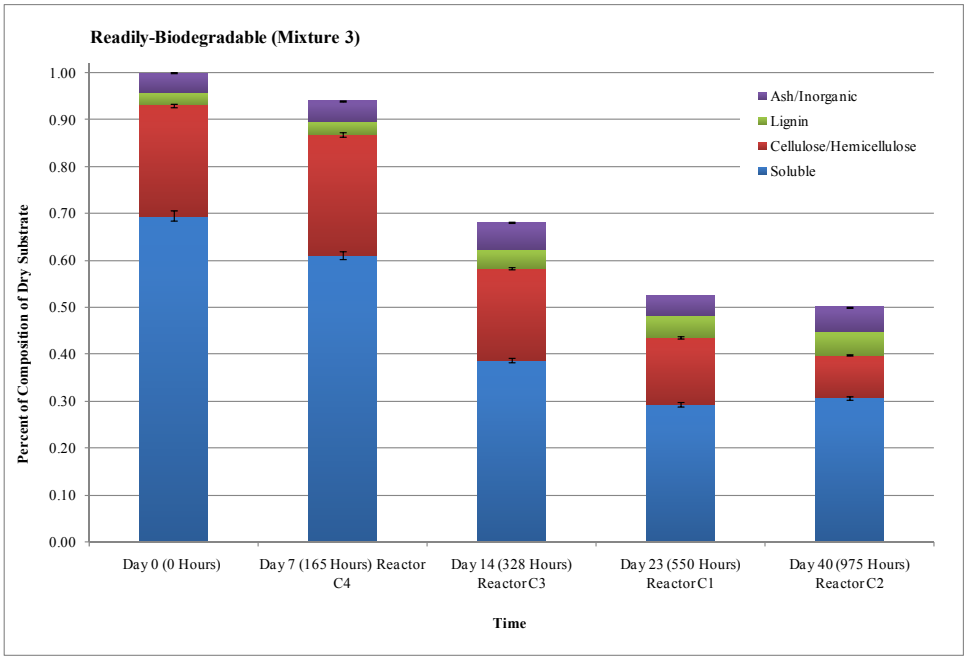

b. Figure 5.3

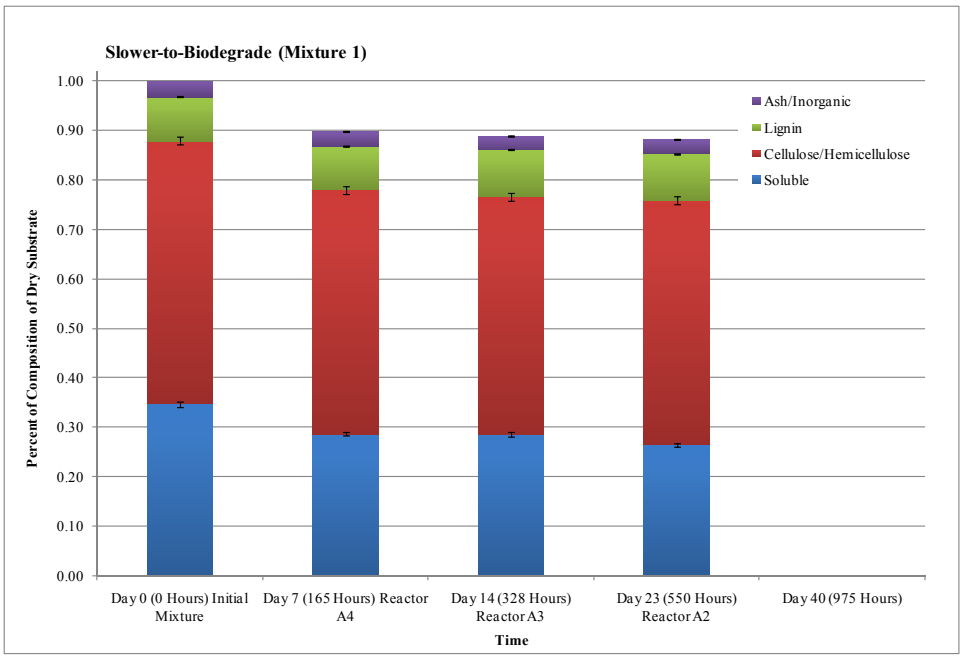

c. Figure 5.3

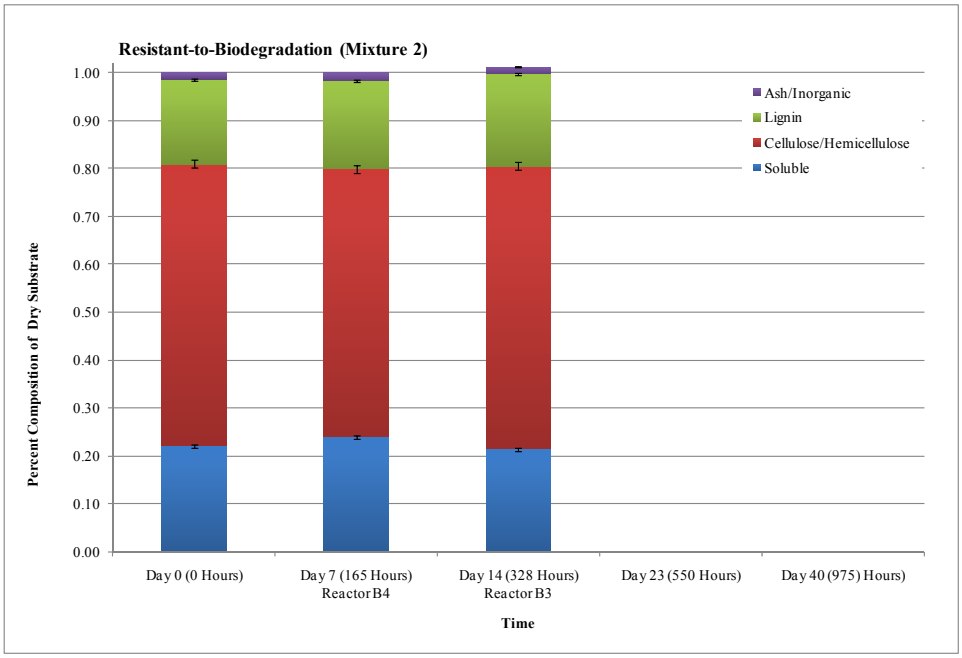

Figure 5.3 Change in percent composition of substrates through time within a mixture by reactor for: (a) readily-biodegradable; (b) slower-to-biodegrade; and, (c) resistant-to-biodegradation.

Figure 5.4 depicts the degradation of substrate mass ($kg_{dry\ substrate}\ kg^{-1}_{total\ dry\ matter}$) through time by reactor within the mixture (a) readily-biodegradable, (b) slower-to-biodegrade, and (c) resistant-to-biodegradation. The readily-biodegradable [Figure 5.4(a)] shows a reduction of the soluble substrate through time, an increase in the cellulose/hemicellulose at Day 7 then a constant reduction, and a gradual increase in lignin. The ash/inorganic appears to vary, but this was a result on a non-homogeneity of the sample. The slower-to-biodegrade [Figure 5.4(b)] shows a gradual decrease in the soluble substrate through time, a slight decrease in cellulose/hemicellulose through time, and a very slight increase in lignin through time. Ash/inorganic appears to be constant. The resistant-to-biodegradation [Figure 5.4(c)] shows an increase then a decrease in the soluble substrate. The cellulose/hemicellulose shows a decrease then increased. Lignin appears to increase, with the ash/inorganic remaining constant.

a. Figure 5.4

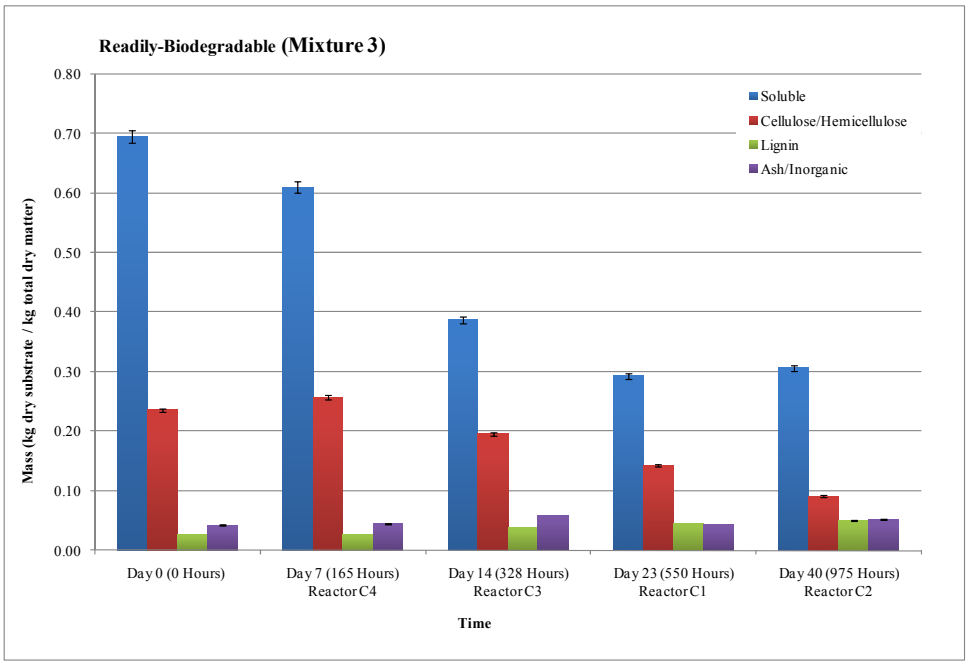

b. Figure 5.4

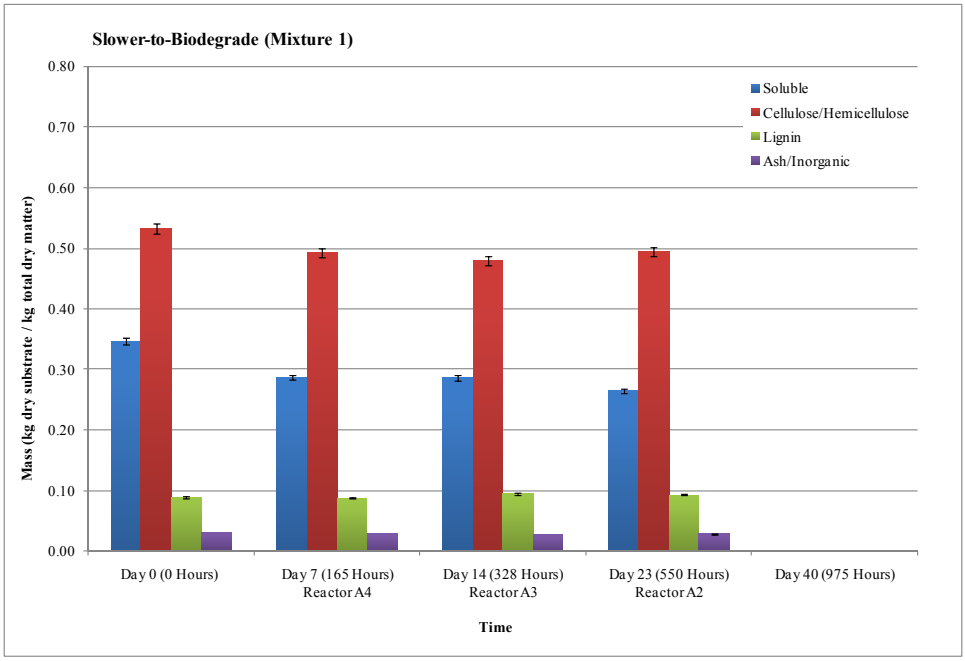

c. Figure 5.4

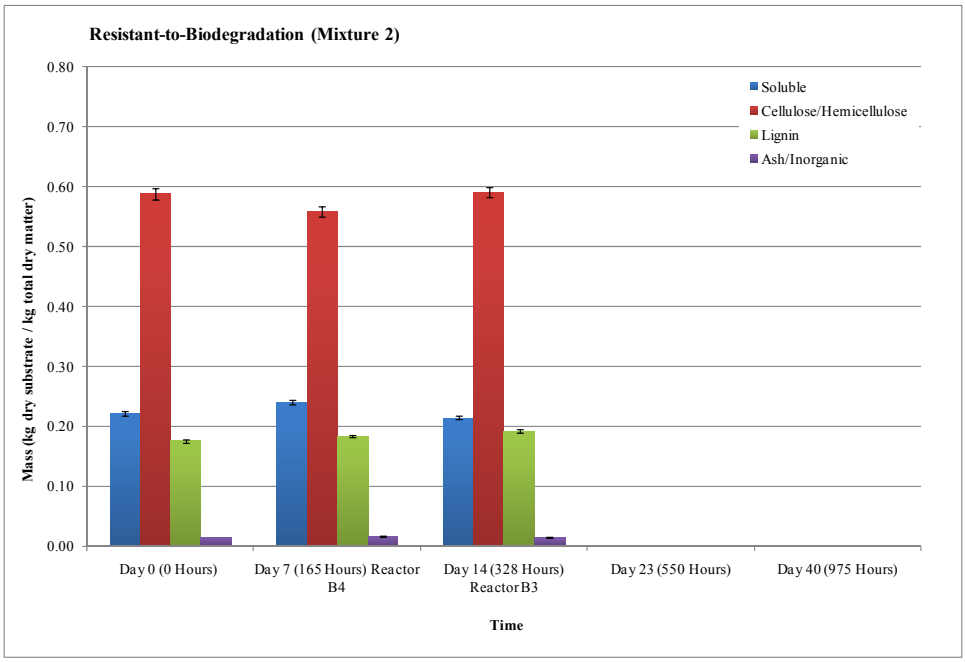

Figure 5.4 Degradation of substrate mass through time by reactor within a mixture: (a) readily-biodegradable; (b) slower-to-biodegrade; and, (c) resistant-to-biodegradation.

Figure 5.5 provides a comparison of the utilization of substrate mass by type by reactor through time within the mixture (a) readily-biodegradable, (b) slower-to-biodegrade, and (c) resistant-to-biodegradation. This figure illustrates the expected results from the three different mixtures. The readily-biodegradable [Figure 5.5(a)] showed a decrease in soluble substrate, which corresponds to a release of heat, and a lesser reduction of cellulose/hemicellulose. The increase in lignin can be accounted for by the slow destruction of lignin compounds and the production of humus (cell-wall material from expired microorganisms and fractured-lignin molecules). The slower-to-biodegrade [Figure 5.5(b)] exhibits a similar trend, but at a much reduced rate. The resistant-to-biodegradation [Figure 5.5(c)] shows very little utilization.

a. Figure 5.5

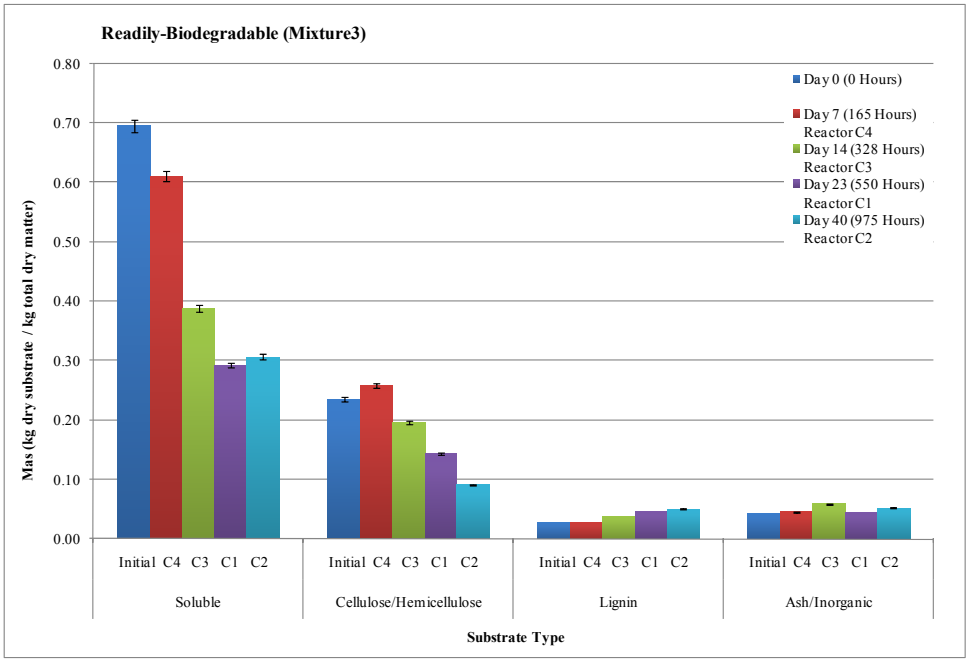

b. Figure 5.5

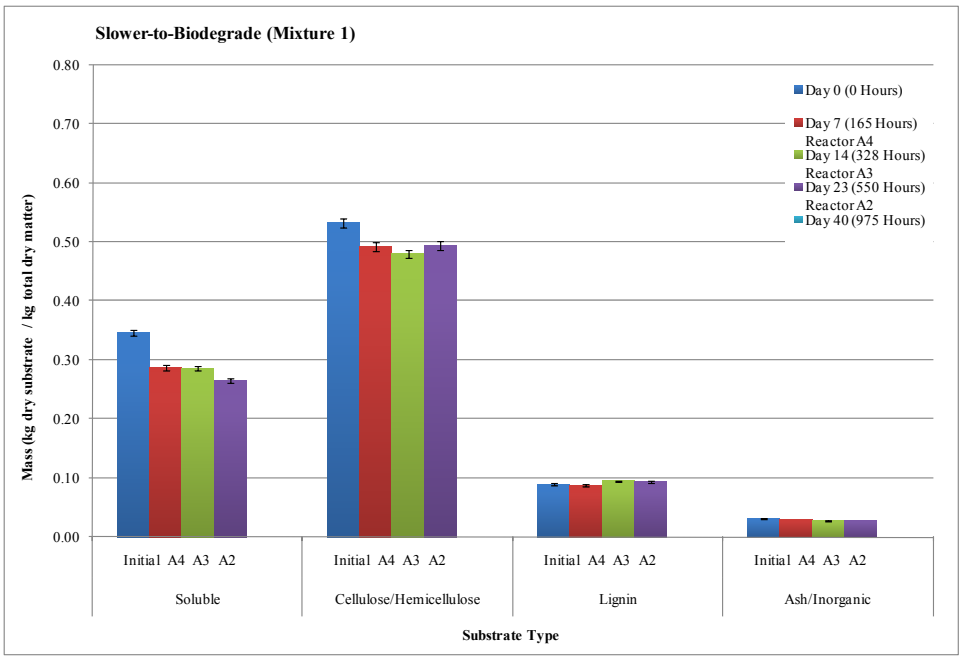

c. Figure 5.5

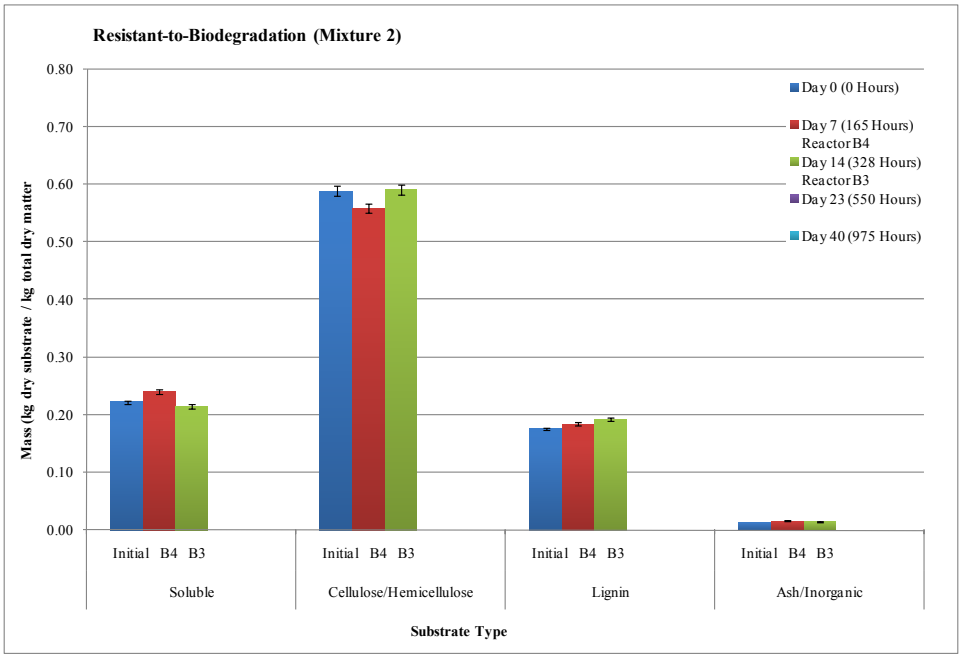

Figure 5.5 Utilization of substrate mass by type by reactor within a mixture through time for: (a) readily-biodegradable; (b) slower-to-biodegrade; and, (c) resistant-to-biodegradation.

Figure 5.6 shows the change in water mass (kg_{water} $kg^{-1}_{total\ wet\ mass}$) by reactor type within a mixture through time for (a) readily-biodegradable, (b) slower-to-biodegrade, and (c) resistant-to-biodegradation. All three mixtures have some variation but indicate a consistency within a mixture. The figure presents the problem that the target moisture content of 60% (wet basis) was not obtained for the slower-to-biodegrade and resistant-to-biodegradation mixtures. The ingredients were fed into and tumbled in the mixer for ten minutes to obtain as-close-as possible a homogeneous blend. During mixing all water appeared to be incorporated into each of the mixtures. The mixing took place outside. During the time the mixing was accomplished, the day was sunny and dry. The temperature reached a high of 5 °C (41 °F).

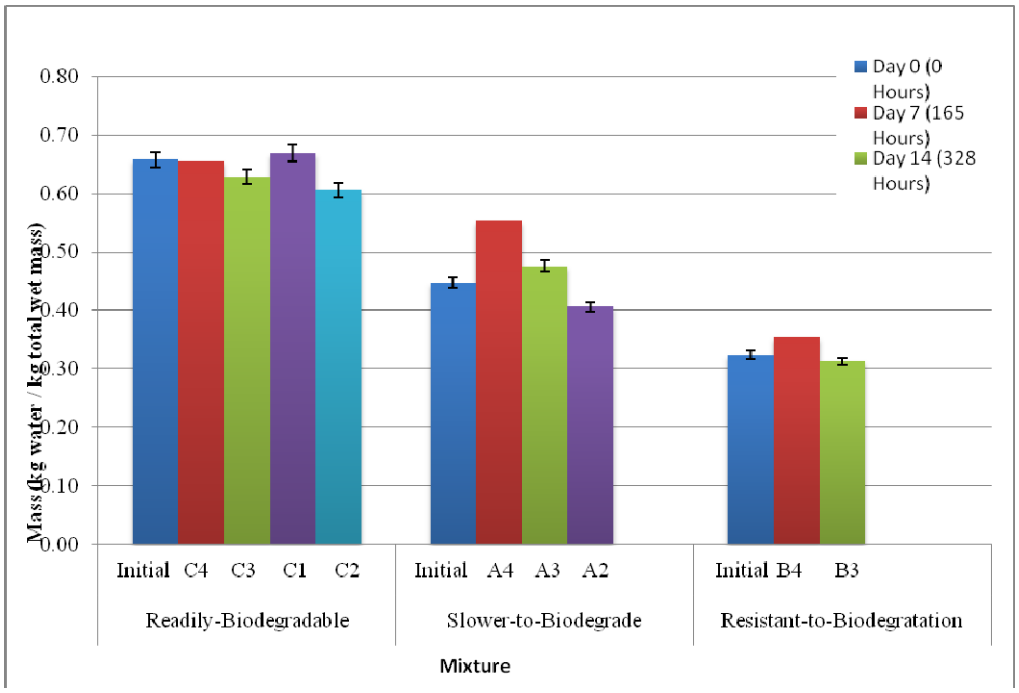

Figure 5.6 Change in water mass by reactor type within a mixture through time for: (a) readily-biodegradable; (b) slower-to-biodegrade; and, (c) resistant-to-biodegradation.

Temperature profile results

Temperature profiles of each reactor tube, as recorded by the data logger, are presented in Figures 5.7 through 5.10. The figures are divided by substrate type and then by the length of time each reactor was on line. The corrected data is attached to the electronic copy of the dissertation as Appendix F. The corrections made involved the

removal of erroneous data points, where the thermocouple reading was "out of bounds": 1) the reading was below or exceed the data points before and after in the same profile and the reading was below or exceed the data points in the temperature profile above and below; 2) the data logger registered no reading; and 3) the reading exceeded the value possible for microbial activity (> 85 °C).

Each figure displays the temperature profiles for the different levels within the reactor as specified in the experimental design (Figures 4.1 and 4.2). Each layer is defined by distance in centimeters starting from the bottom of the reactor moving by layer to the top. Profile layer "0 cm" is the first layer $(p = 1)$ and represents atmospheric conditions. Profile layer "10 cm" is the second layer $(p = 2)$. It represents the initial layer of substrate in the reactor. The reference temperature (Ref Temp) profile is the actual temperature in the enclosure in which the experimentation was accomplished. Inspection of the reference temperature indicates several degree fluctuations within the enclosure. The experimental enclosure was approximately 2.7 m (8.7 ft) wide with large double doors at one end, 3.7 m (12.3 ft) deep and 3.5 m (11.4 ft) high. The experimental enclosure was constructed in a large shop area that is approximately 11.9 m (39 ft) wide by 23.8 m (78 ft) long with a 4 m (13 ft) ceiling. A large garage door 5.7-m (18.7-ft) wide and 3.2-m (10. 4-ft) high is located at the far end from the experimental enclosure on the 11.9-m wide wall. Due to other projects, this door was opened at irregular intervals but often multiple times per day. The experimentation was conducted from February 24, 2008 to April 5, 2008. The outside temperatures varied from a maximum temperature ranging from a low of -2.2 °C to a high of 23.9 °C with an average maximum of 11.4 °C. The minimum temperatures ranged from a low of -13.3 °C to a high of 7.8 °C with an average minimum temperature of -2.2 °C. The shop cooled every time the door was open.

In general, the results indicate major differences between the three major substrate types: the readily-biodegradable, the slower-to-biodegrade, and resistant-to-biodegradation. Each figure contains a description listing the degradability of the mixture, the reactor number, and the mixture number.

Figure 5.7 presents the temperature profile for four reactors filled with the readily-biodegradable mixture. The reactors were taken off-line at different times for

destructive sampling. Reactor C4 was removed at Hour 164.5 [Figure 5.7(a)]; Reactor C3 at Hour 328 [Figure 5.7(b)]; Reactor C1 at Hour 552 [Figure 5.7(c)]; and Reactor C2 at Hour 974.5 [Figure 5.7(d)]. The profile indicates transition from the mesophilic-microorganism range to the thermophilic-microorganism range, the death of the thermophilic organisms at the peak temperature, the initial cooling with some regrowth of organisms as the temperature again increased slightly and a cooling as the readily-biodegradable material was being used up. Figure 5.7(c) indicates times when major settling events of substrate took place within the reactore tube.

The temperature profile for reactor C2 [Figure 5.7(d)] exhibits the effect of the loss of air flow starting at approximately Hour 165, March 2, 2008, when the air hose was accidently dislodged from the air supply. The figure does indicate the restoration of air approximately 28 hours later on March 3, 2008, as the temperature climbed again proceeding through the profile described above.

a. Figure 5.7

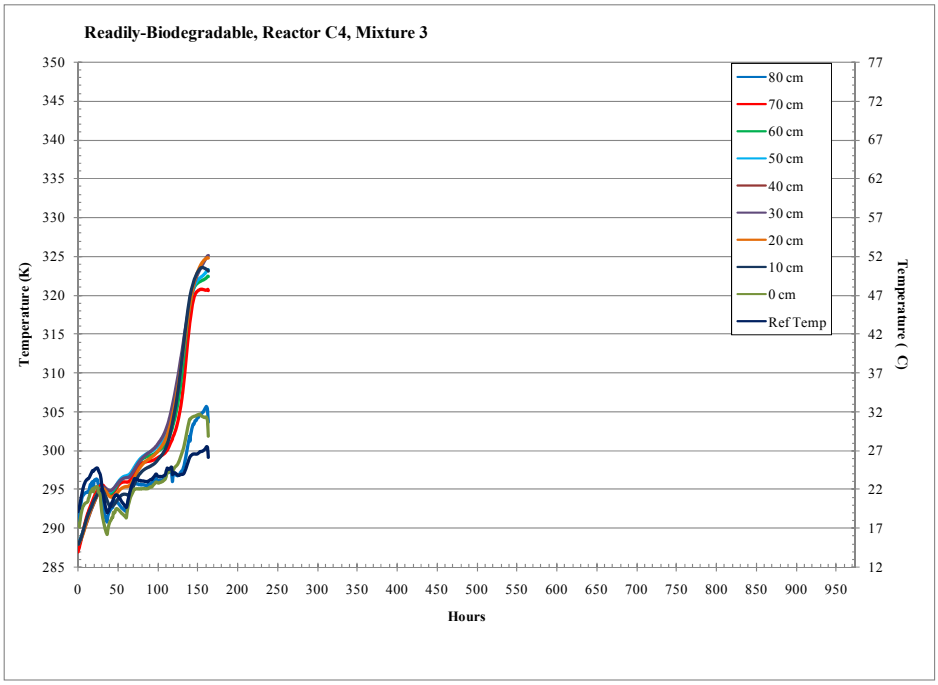

b. Figure 5.7

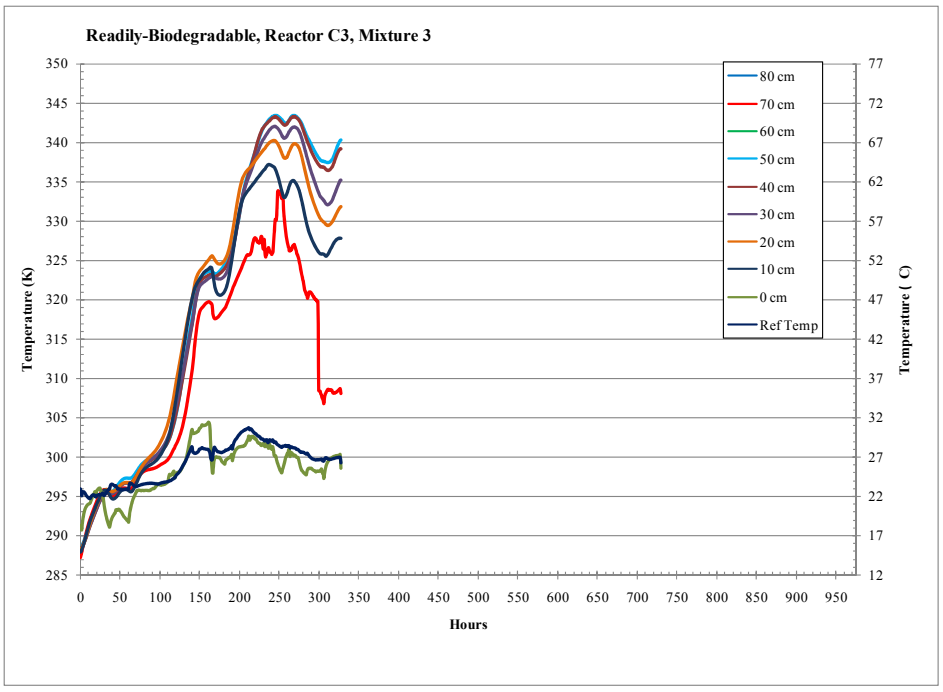

c. Figure 5.7

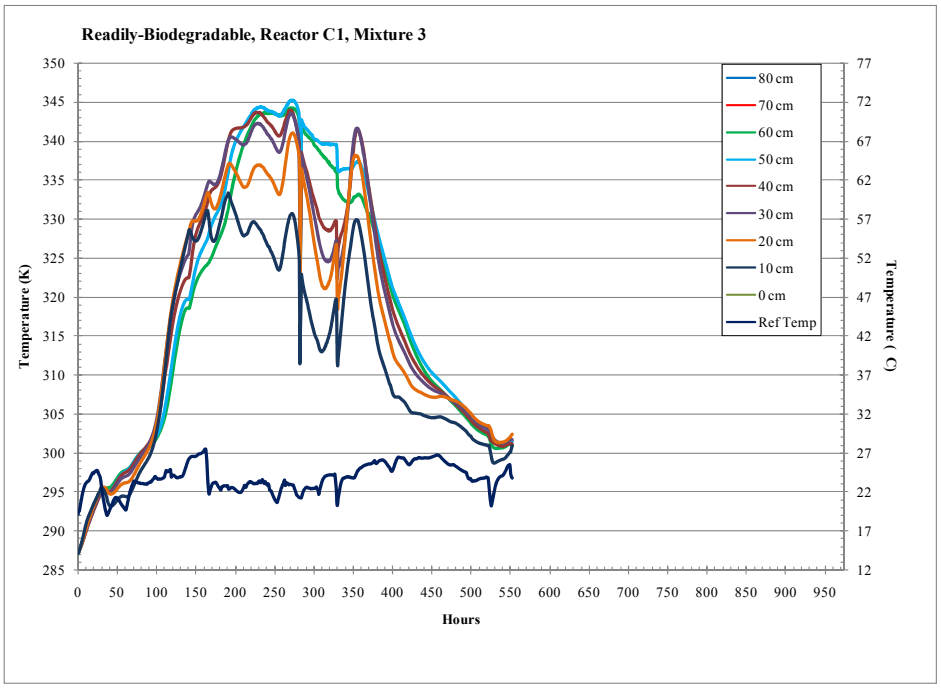

d. Figure 5.7

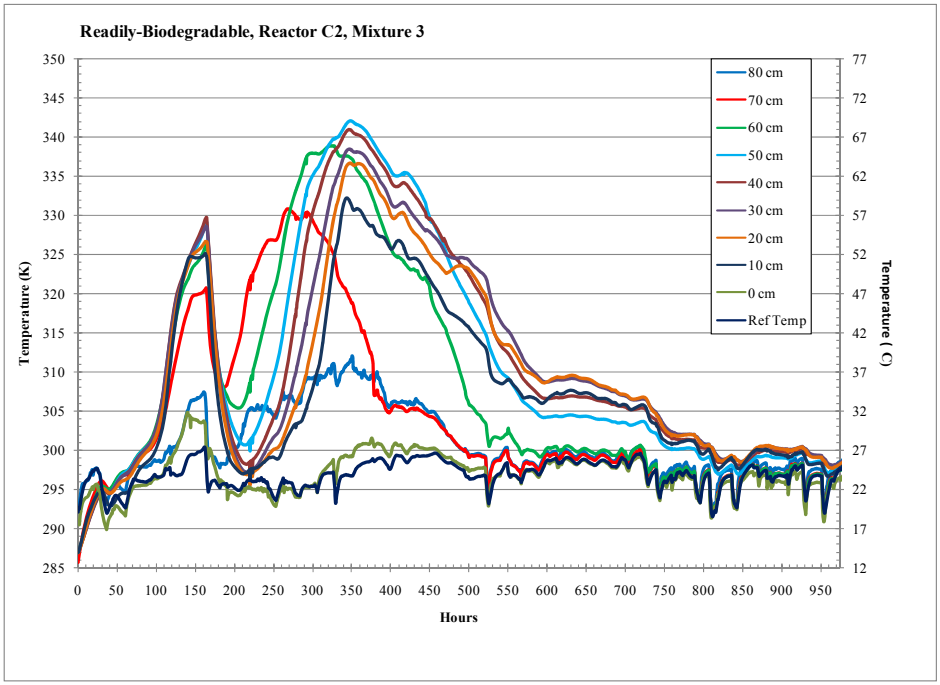

Figure 5.7 Temperature profile for four reactors filled with the readily-biodegradable mixture, removed at: (a) Hour 164.5; (b) Hour 328; (c) Hour 552; and, (d) Hour 974.5.

Figure 5.8 presents the temperature profile for four reactors filled with the slower-to-biodegrade mixture. The reactors were taken off-line at different times, except the last two, for destructive testing. Reactor A4 was removed at Hour 164.5 [Figure 5.8(a)]; Reactor A3 at Hour 328 [Figure 5.8(b)]; Reactor A2 at Hour 550.5 [Figure 5.8(c)]; and Reactor A1 at Hour 550.5 [Figure 5.8(d)]. These profiles exhibit the characteristic of sufficient soluble substrate to initiate a temperature rise, but insufficient soluble substrate to maintain it, and thus a decline in temperature.

a. Figure 5.8

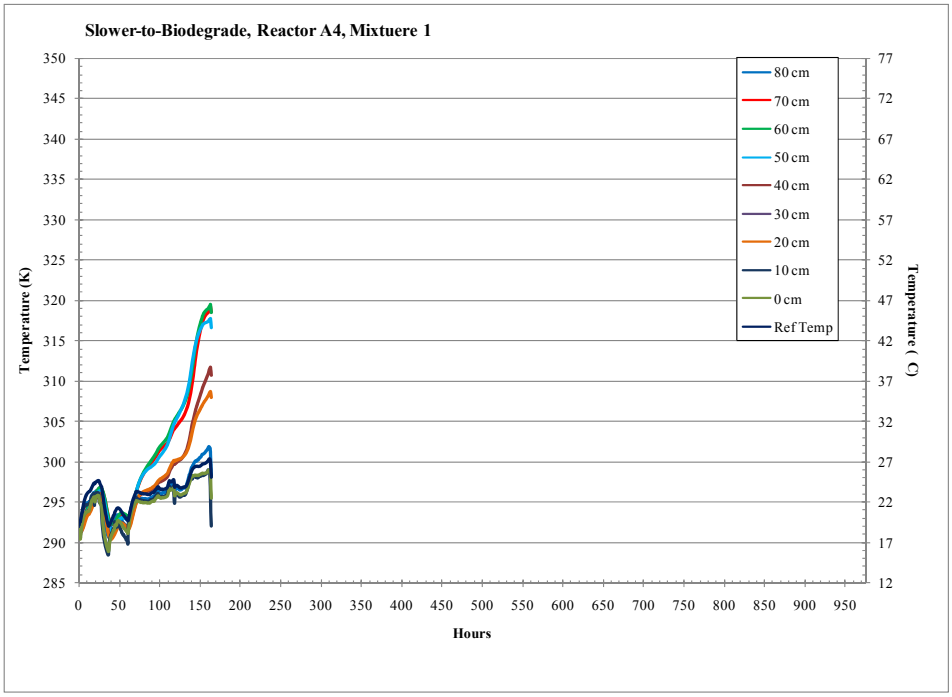

b. Figure 5.8

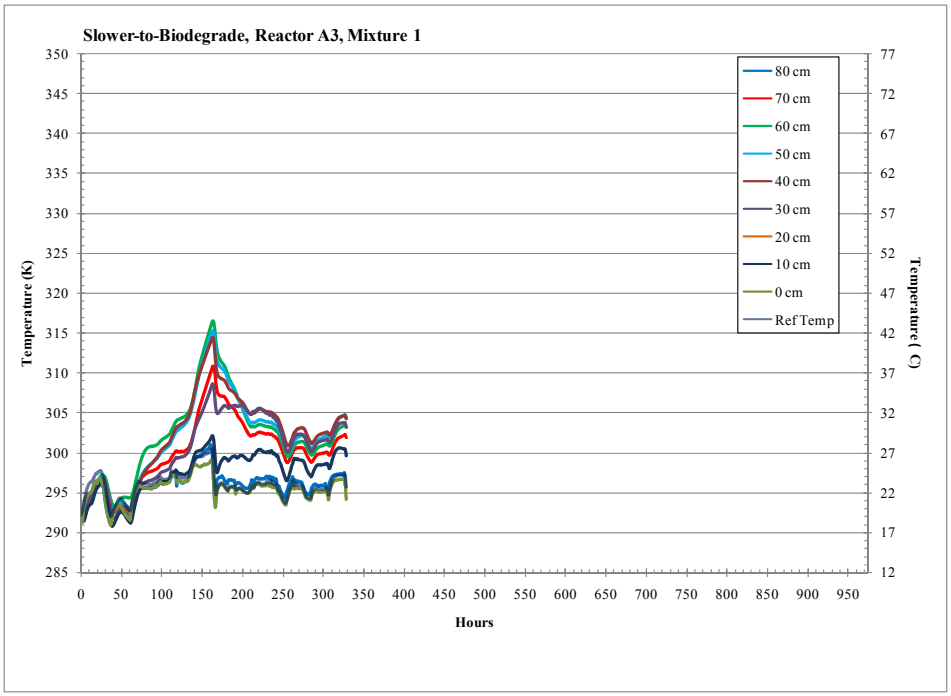

c. Figure 5.8

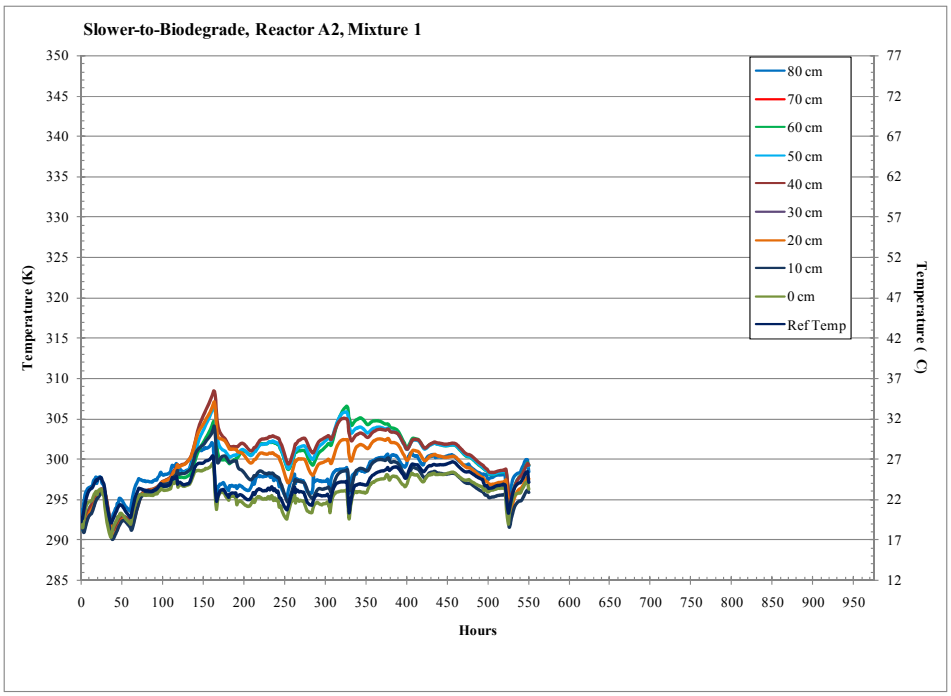

d. Figure 5.8

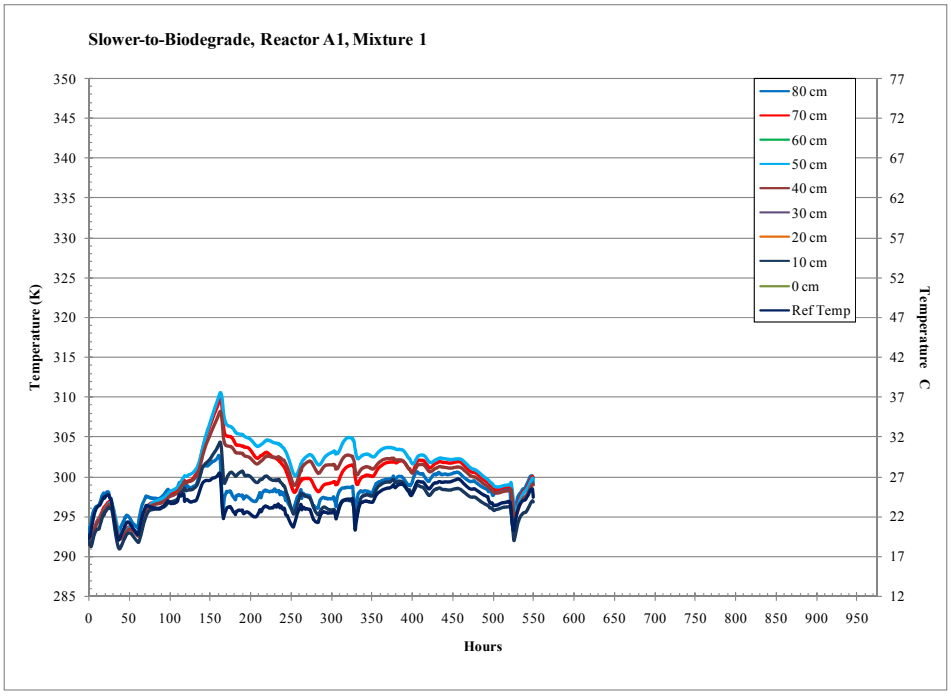

Figure 5.8 Temperature profile for four reactors filled with the slower-to-biodegrade mixture, removed at: (a) Hour 164.5; (b) Hour 328; (c) Hour 550.5; and, (d) Hour 550.5.

Figure 5.9 presents the temperature profile for four reactors filled with the resistant-to-biodegradation mixture. The reactors were also taken off-line at different times, except the last two, for destructive testing. Reactor B4 was removed at Hour 164.5 [Figure 5.9(a)]; Reactor B3 at Hour 328 [Figure 5.9(b)]; Reactor B2 at Hour 550 [Figure 5.9(c)]; and Reactor B1 at Hour 550 [Figure 5.9(d)]. These profiles followed the reference temperature profile, exhibited no temperature increase on their own. There was insufficient soluble substrate present to bring about an increase in temperature.

a. Figure 5.9

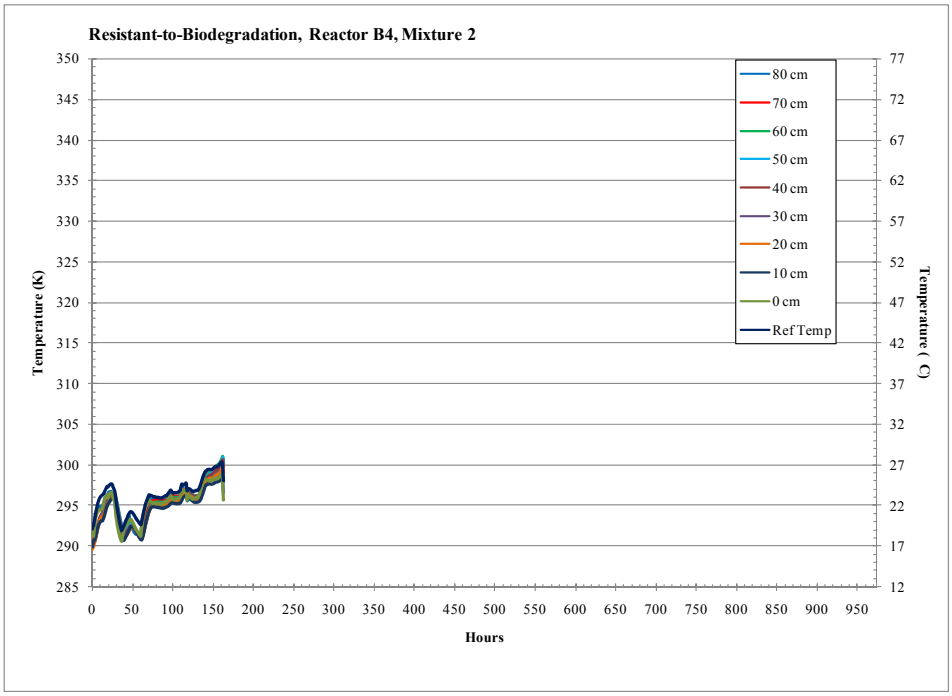

b. Figure 5.9

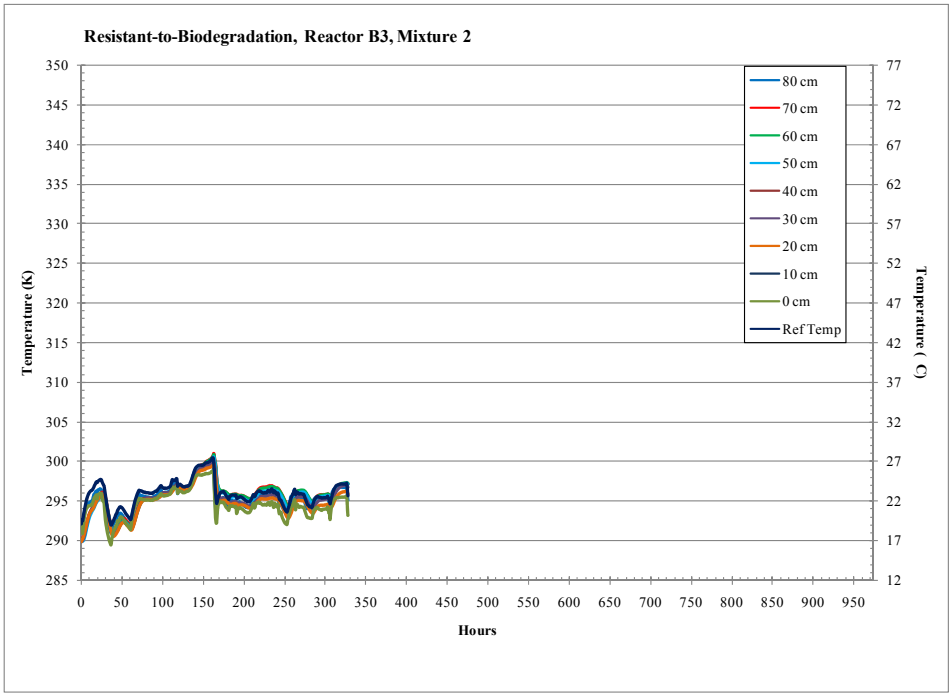

c. Figure 5.9

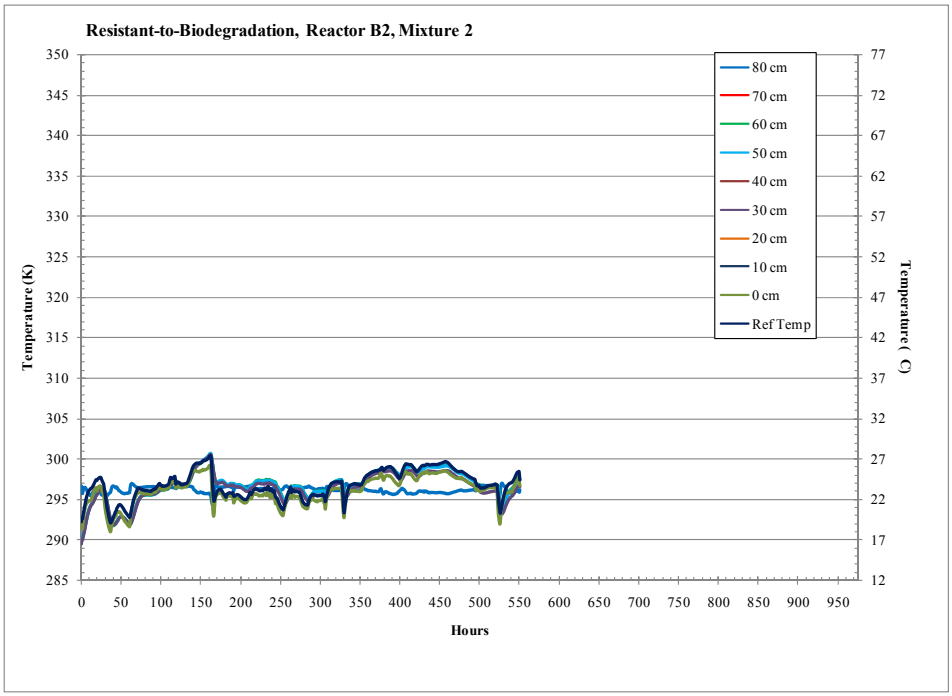

d. Figure 5.9

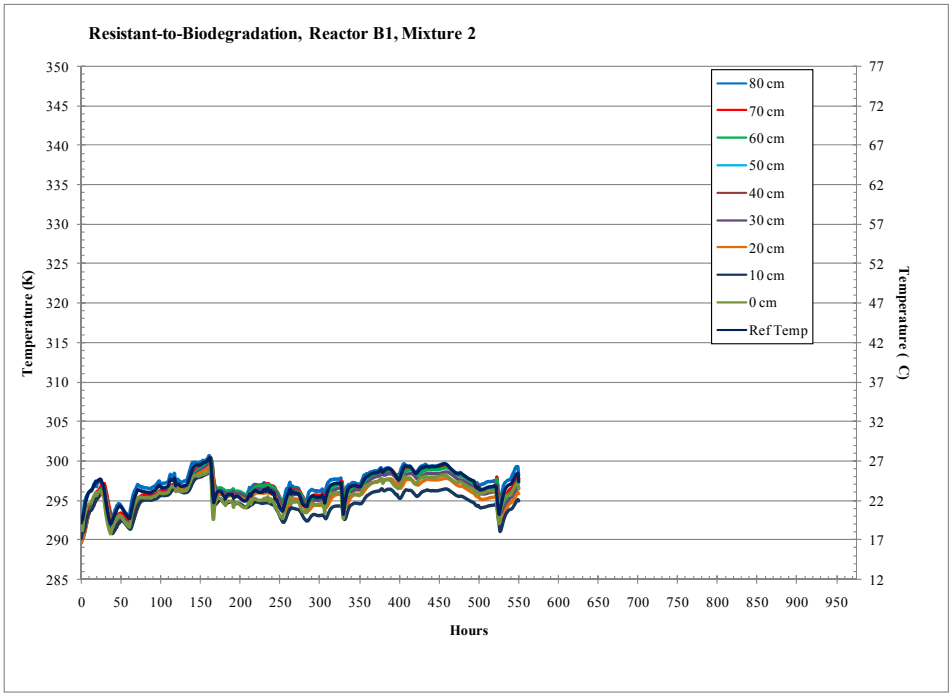

Figure 5.9 Temperature profile for four reactors filled with the resistant-to-biodegradation mixture, removed at: (a) Hour 165.5; (b) Hour 328; (c) Hour 550; and, (d) Hour 550.

The data presented above indicates the success of the experimental design. A strong matrix has been established to provide the link between the experimental design and the mathematical model. The results indicate the target mixtures established in the experimental design generally performed as expected.

CHAPTER 6 - MATHEMATICAL MODEL

The research model was based on differential equations to describe microbial growth, substrate consumption, oxygen concentration, moisture content, and temperature. The microbial process utilized Monod's growth kinetics, describing microbial growth and microbial maintenance as functions of specific growth rate or maintenance coefficient, substrate and oxygen concentrations. The equations were solved using finite differences. The computer used to run the model contained Intel® Core™ 2 Duo CPU T9300 @ 2.5 GHz 2.49GHz, 1.99GB of Ram, and the model's time step was set for minute intervals. The computers capacity permitted an approximate maximum of 2520 minute (105 day) time steps before memeory was exceeded.

The model's function was to permit a designer of a composting system to evaluate different composting mixtures mathematically by changing substrate type, moisture levels, atmospheric temperature, and vessel dimensions, prior to actual experimentation. This chapter delineates the model's mathematical relationships and the order of execution. The data value used in this case is for the readily-biodegradable substrate. The actual model operates in Matlab® (The MathWorks, Version R2007a). Appendix E contains the model coding.

The model's coding was divided into several sections based on the order the parameters are entered into the model. The initial section set the variable conditions: time, the setting of the length of run and time step interval; the composting vessel's dimensions and heat loss characteristics; and, the types and quantities of substrate selected and their respective water content, plus any additional water added. This section also set the fixed values: the heats of combustion, specific heat, and various coefficients. The second section set the array size and initializes the values to zero. The third section set all boundary conditions. The fourth section begins the actual time loop, calculating the results for each time step within the composting vessel, i.e., substrate decomposition rate, oxygen utilization, microbial growth, microbial death, carbon-dioxide and water production, and expected temperatures. The actual model can print graphs of the various

results as desired. Appendix A contains an alphabetic listing of all equation symbols, their corresponding Matlab® symbol, definition and units.

Governing Equations

There were six differential equations (Cundiff and Mankin, 2003; and Stombaugh and Nokes, 1996) governing the composting process. These equations were converted into finite difference equations to calculate the changes. The sequence of the calculations was accomplished as detailed in the nodal schematic (Fig. 4.2).

First Differential Equation

The first differential equation was the rate of change of the microbial biomass ($\frac{dX}{dt}$, $kg_x\ m^{-3}\ h^{-1}$) with respect with time,

$$\frac{dX}{dt} = \mu * X - k_d * X \tag{6.1}$$

where:

X = microbial mass concentration ($kg_x\ m^{-3}$). In this model, the total microbial biomass represented the bacteria, actinomycetes, and fungi both mesophilic and thermophilic.

μ = specific growth rate (h^{-1})

k_d = fraction of current microbial population that die each hour (h^{-1}).

The specific growth rate was defined as

$$\mu = \mu_{\max} * \left(\frac{S}{K_s + S} \right) * \left(\frac{O_2}{K_{O_2} + O_2} \right) \tag{6.2}$$

where:

$\mu_{\max}$ = maximum specific growth rate (h^{-1})

S = concentration of substrate ($kg_s\ m^{-3}$). In this model, the total substrate was composed of the soluble or readily-biodegradable, the cellulose/hemicellulose or slower-to-biodegrade, the lignin or resistant-to-biodegrade, and the inert or inorganic/minerals.

O_2 = oxygen concentration (kg_{O2} $m^{-3)}$

K_s = half velocity constant for degradable substrate (kg_s m^{-3})

K_{O_2} = half velocity constant for oxygen (kg_{O2} m^{-3}).

Second Differential Equation

The second differential equation was the rate of change in the substrate ($\frac{dS}{dt}$, kg_x m^{-3} h^{-1}) with respect with time,

$$\frac{dS}{dt} = \frac{1}{Y_{X/S}} * \left(\frac{dX}{dt} \right) + \eta * X \tag{6.3}$$

where:

$Y_{X/S}$ = yield coefficient ($kg_{x\ (cells\ produced)}$ kg_s^{-1} $_{(substrate\ consumed)}$)

η = microbial maintenance coefficient (h^{-1}).

The microbial maintenance coefficient was defined as:

$$\eta = \eta_{max} * \left(\frac{S}{K_S + S} \right) * \left(\frac{O_2}{K_{O_2} + O_2} \right) \tag{6.4}$$

where:

η_{max} = maximum microbial maintenance coefficient (h^{-1}).

Third Differential Equation

The third differential equation was the rate of change of oxygen ($\frac{dO_2}{dt}$, kg_{O2} m^{-3} h^{-1}) with respect to time,

$$\frac{dO_2}{dt} = Y_{X/O_2} * \left(\frac{dS}{dt} \right) + \frac{F_{air}}{Vol_{cb}} * \left(O_{2\,in} - O_{2\,out} \right) \tag{6.5}$$

where:

Y_{X/O_2} = yield coefficient ($kg_{O2\ (consumed)}$ kg_s^{-1} $_{(substrate\ consumed)}$)

Vol_{cb} = volume of the entire reactor (m^3)

H_{in} = oxygen in the air entering the layer from the layer below (kg_{H2O} kg_{da}^{-1})

H_{out} = oxygen in the air leaving the layer, entering the layer above (kg_{H2O} kg_{da}^{-1})

F_{air} = air flow rate into the reaction vessel ($m^3\ h^{-1}$).

Fourth Differential Equation

The fourth differential equation was the rate of change in water ($\frac{dW}{dt}$, $kg_w\ m^{-3}\ h^{-1}$) with respect to time,

$$\frac{dW}{dt} = Y_{W/S} * \left(\frac{dS}{dt}\right) - \frac{F}{Vol_{cl}} * \left(H_{in} - H_{out}\right) \tag{6.6}$$

where:

$Y_{W/S}$ = yield coefficient ($kg_{w\ (water\ produced)}\ kg_{s}^{-1}{}_{(substrate\ consumed)}$)

F = air flow rate of the entire reactor ($kg_{da\ (dry\ air)}\ m^{-3}\ h^{-1}$)

Vol_{cl} = volume of each increment within the reactor (m^3)

H_{in} = humidity ratio of the air entering the layer from the layer below ($kg_{H2O}\ kg_{da}^{-1}$)

H_{out} = humidity ratio of the air leaving the layer, entering the layer above ($kg_{H2O}\ kg_{da}^{-1}$).

Fifth differential equation

The fifth differential equation was the rate of change in the carbon dioxide ($\frac{dCO_2}{dt}$, $kg_{CO2}\ m^{-3}\ h^{-1}$) production with respect to time,

$$\frac{dCO_2}{dt} = Y_{X/CO_2} * \left(\frac{dS}{dt}\right) \tag{6.7}$$

where:

Y_{X/CO_2} = yield coefficient ($kg_{CO2\ (produced)}\ kg_{s}^{-1}{}_{(substrate\ consumed)}$).

Sixth Differential Equation

The sixth differential equation was the rate of change in temperature ($\frac{dT}{dt}$, $K\ h^{-1}$) with respect to time,

$$q_m \frac{dT}{dt} = \left[\Delta h_{C_s}{}^{T} * \frac{dC_S}{dt} - \frac{F_{air}}{Vol_{cl}} * \left(h_{out} - h_{in} \right) - \frac{Q_l}{Vol_{cl}} \right] \tag{6.8}$$

where

$\Delta h_{C_s}{}^{T}$ = heat of combustion (heat released when substrate is decomposed by the microorganisms (kJ kg_s^{-1})

h_{out} = enthalpy of air leaving the layer, entering the layer above (kJ kg_{da}^{-1})

h_{in} = enthalpy of the air entering the layer from the layer below (kJ kg_{da}^{-1})

Q_l = conductive heat loss through the reactor wall (kJ h^{-1})

q_m = sensible heat stored in the substrate within the layer of the reactor per degree temperature rise above a given reference temperature (kJ m^{-3} K^{-1}).

The sensible heat was defined as,

$$q_m = c_W * W + c_{S_{ss}} * S \tag{6.9}$$

where:

c_W = specific heat of water (kJ K^{-1})

c_{S_s} = specific heat of all substrate types (kJ K^{-1}).

Section 1: Setting Initial Parameters

Time

The initial parameter was time. The length of time the program will run before terminating (t_{stop}, h) and the time step increments (t_{step}, h) when each step was to be calculated were chosen and entered into the program,

$$t_{step} = 1/60 \tag{6.10}$$

$$t_{stop} = 975 \tag{6.11}$$

The simulated run time (t, h) was calculated from these parameters,

$$t = [0 : t_{step} : t_{stop}] \tag{6.12}$$

Composting Vessel

Next, the composting vessel's parameters wee established and the nodal scheme applied. The values given were the size of the experimental reactor utilized in the experimentation. Depth of compost bed ($Depth_{cb}$, m), which was the actual depth of the substrate to be composted, was set.

$$Depth_{cb} = 0.8 \tag{6.13}$$

The number of increments (d , no units) within the compost vessel was set based on the nodal scheme.

$$d = 8 \tag{6.14}$$

The depth of each compost layer ($Depth_{cl}$, m) was determined,

$$Depth_{cl} = \frac{Depth_{cb}}{d} \tag{6.15}$$

The number of nodes (p , no units) was calculated. Based on the nodal scheme, the number of nodes is always one greater than the depth to account for the atmospheric layer below the substrate. The layer below the substrate is the lower boundary condition,

$$p = d + 1 \tag{6.16}$$

The diameter of the vessel (Dia , m) was established, set by the diameter of the experimental reactor,

$$Dia = 0.203 \tag{6.17}$$

The cross sectional area (V_{csa} , m^2) and the volume of the compost bed layer (Vol_{cl} , m^3) were calculated. The volume of the bed layer was the smallest unit for which all concentration calculations were based,

$$V_{csa} = \pi * \left(\frac{Dia}{2} \right)^2 \tag{6.18}$$

$$Vol_{cl} = V_{csa} * Depth_{cl} \tag{6.19}$$

The volume of the compost bed (total volume) (Vol_{cb} , m^3) was determined.

$$Vol_{cb} = Depth_{cb} * V_{csa} \tag{6.20}$$

The wall area (A_{wall} , m^2) was determined to account for heat loss through the vessel walls,

$$A_{wall} = 2 * \pi * \left(\frac{Dia}{2} \right) * Depth_{cb} \quad (6.21)$$

Thermal resistance (R_T , K m^{-2} h^{-1} J^{-1}) was based on two parts. First, the experimental reactor walls were insulated with 2.5 cm of fiber glass insulation incased in a mylar sheet. The reactor wall themselves had esentially no resistance. The resistance value of the insulation was calculated at 0.21. Second, the additional thermal resistance that was provided by the thickness of compost the probe was inserted into the substrate. Curve fitting indicated the total thermal resistance should be approximately 0.45. Therefore, the thermal resistance was set at

$$R_T = 0.45 \quad (6.22)$$

Atmospheric Parameter

The atmospheric pressure (P_{atm} , Pa or kg m^{-1} sec^{-2}) was the pressure at sea level (Zumdahl, 1993).

$$P_{atm} = 101325 \quad (6.23)$$

Substrate/Water Parameters

The substrate parameters were entered based on the laboratory report which reported the weight of the dry matter and water weight of each ingredient and the total weight utilized in the mixture. The four substrates dry matter were calculated and entered into the program. The entries were: soluble substrate (S_s , kg_{ss}), where 'ss' indicates soluble substrate; cellulose substrate (S_c , kg_{sc}), lignin substrate (S_l , kg_{sl}); and, inert substrate (S_i , kg_{si}). The values entered for example purposes were for the readily-biodegradable substrate utilized in experimental work,

$$S_s = 3.79 \quad (6.24)$$

$$S_c = 1.28 \quad (6.25)$$

$$S_l = 0.146 \quad (6.26)$$

$$S_i = 0.231 \quad (6.27)$$

From these values, the total amount of substrate (S_t , kg_s) was determined,

$$S_t = S_s + S_c + S_l + S_i \tag{6.28}$$

The water parameter indicated the total amount of water (W_s, kg_w) present in the substrate utilized, the amount of water added (W_{add}, kg_w) to the substrate as it was being mixed, and the total water (W_t, kg_w) present,

$$W_s = 10.47 \tag{6.29}$$

$$W_{add} = 0.00 \tag{6.30}$$

$$W_t = W_s + W_{add} \tag{6.31}$$

The air flow rate (F_{air}, L h^{-1}) feeding the substrate was entered,

$$F_{air} = 104.0 \tag{6.32}$$

Temperature Parameters

This next set of parameters set all temperature requirements. The initial dry bulb or ambient temperature (T_C, ºC) and the wet bulb temperature ($T_{C_{wb}}$, ºC) were entered. The dry bulb temperature was the temperature of the air supply connected to the experimental reactor. Again, the values entered for example purposes were from the experimental work. The initial dry bulb temperature was the average feed air temperature. The wet bulb temperature was determined from the psychometric chart using initial experimental readings,

$$T_C = 23.7 \tag{6.33}$$

$$T_{C_{wb}} = 15 \tag{6.34}$$

Next was the setting of the temperature ranges in which the mesophilic and thermophilic microorganisms survive. It was important to overlap the mesophilic and thermophilic ranges. It was within this overlapping band both types of organisms survive. The lower limit for mesophilic range ($T_{C_{t\min}}$, ºC), the upper limit for the mesophilic range ($T_{C_{t\max}}$, ºC) were entered and then converted to degrees Kelvin for the lower mesophilic range limit ($T_{t\min}$, K) and upper mesophilic range ($T_{t\max}$, K),

$$T_{C_{m\min}} = 15 \tag{6.35}$$

$$T_{C_{m\max}} = 55 \tag{6.36}$$

$$T_{m\min} = T_{C_{m\min}} + 273.16 \tag{6.37}$$

$$T_{m\max} = T_{C_{m\max}} + 273.16 \tag{6.38}$$

The lower limit for the thermophilic range ($T_{C_{m\min}}$, ºC) and the upper limit thermophilic range ($T_{C_{t\max}}$, ºC) were entered and converted to degrees Kelvin for the lower thermophilic range limit ($T_{t\min}$, K) and the upper thermophilic range limit ($T_{t\max}$, K),

$$T_{C_{t\min}} = 40 \tag{6.39}$$

$$T_{C_{t\max}} = 70 \tag{6.40}$$

$$T_{t\min} = T_{C_{t\min}} + 273.16 \tag{6.41}$$

$$T_{t\max} = T_{C_{t\max}} + 273.16 \tag{6.42}$$

Heat of Combustion, Specific Heat, and Coefficients

The heat of combustion for the soluble substrate ($\Delta h_{C_{ss}}{}^{T}$, kJ kg_{ss}^{-1} K^{-1}), the cellulose substrate ($\Delta h_{C_{sc}}{}^{T}$,kJ kg_{sc}^{-1} K^{-1}), and the lignin substrate ($\Delta h_{C_{sl}}{}^{T}$,kJ kg_{sl}^{-1} K^{-1}) were entered,

$$\Delta h_{C_{ss}}{}^{T} = 19100 \tag{6.43}$$

$$\Delta h_{C_{sc}}{}^{T} = 19100 \tag{6.44}$$

$$\Delta h_{C_{sl}}{}^{T} = 19100 \tag{6.45}$$

The specific heat for water (c_w,kJ kg_w^{-1} K^{-1}), soluble substrate (c_{ss}, kJ kg_{ss}^{-1} K^{-1}), cellulose substrate (c_{sc},kJ kg_{sc}^{-1} K^{-1}), lignin substrate (c_{sl},kJ kg_{sl}^{-1} K^{-1}), and inert substrate (c_{si}, kJ kg_{si}^{-1} K^{-1}) were entered,

$$c_w = 4.18 \tag{6.46}$$

$$c_{ss} = 1.48 \tag{6.47}$$

$$c_{sc} = 1.48 \tag{6.48}$$

$$c_{sl} = 1.48 \tag{6.49}$$

$$c_{si} = 0.84 \tag{6.50}$$

Next, the 'half-velocity' coefficient for substrate (K_S , $kg_s\ m^{-3}$), the 'half-velocity' coefficient for oxygen (K_{O_2} , $kg_{O2}\ m^{-3}$) were entered,

$$K_S = 62 \tag{6.51}$$

$$K_{O_2} = 0.07 \tag{6.52}$$

There were four sets of yield coefficients. They were all based on the stoichiometric equation for the particular substrate and the particular microorganism assigned to that substrate. The first set of yield coefficients was for the amount of carbon-dioxide generated per unit soluble substrate utilized ($Y_{CO_2/S_{ss}}$, $kg_{CO2}\ kg_{ss}^{-1}$); per cellulose substrate utilized ($Y_{CO_2/S_{sc}}$, $kg_{CO2}\ kg_{sc}^{-1}$), and per lignin substrate utilized ($Y_{CO_2/S_{sl}}$, $kg_{CO2}\ kg_{sl}^{-1}$),

$$Y_{CO_2/S_{ss}} = 0.4478 \tag{6.53}$$

$$Y_{CO_2/S_{sc}} = 0.0535 \tag{6.54}$$

$$Y_{CO_2/S_{sl}} = 0.7695 \tag{6.55}$$

The second set of yield coefficients was for the amount of oxygen consumed per unit soluble substrate utilized ($Y_{O_2/S_{ss}}$, $kg_{O2}\ kg_{ss}^{-1}$); per cellulose substrate utilized ($Y_{O_2/S_{sc}}$, $kg_{O2}\ kg_{sc}^{-1}$), and per lignin substrate utilized ($Y_{O_2/S_{sl}}$, $kg_{O2}\ kg_{sl}^{-1}$),

$$Y_{O_2/S_{ss}} = 0.3570 \tag{6.56}$$

$$Y_{O_2/S_{sc}} = 0.7156 \tag{6.57}$$

$$Y_{O_2/S_{sl}} = 0.8374 \tag{6.58}$$

The third set of yield coefficients was for the amount of water generated per unit soluble substrate utilized ($Y_{W/S_{ss}}$, $kg_w\ kg_{ss}^{-1}$); per cellulose substrate utilized ($Y_{W/S_{sc}}$, $kg_w\ kg_{sc}^{-1}$), and per lignin substrate utilized ($Y_{W/S_{sl}}$, $kg_w\ kg_{sl}^{-1}$),

$$Y_{W/S_{ss}} = 0.4312 \tag{6.59}$$

$$Y_{W/S_{sc}} = 0.3898 \tag{6.60}$$

$$Y_{W/S_{sl}} = 0.2520 \tag{6.61}$$

The forth set of yield coefficients was for the amount of bacteria biomass generated per unit soluble substrate utilized ($Y_{X_b/S_{ss}}$, $kg_{xb}\ kg_{ss}^{-1}$); the amount of actinomycetes biomass generated per unit per cellulose substrate utilized ($Y_{X_a/S_{sc}}$, $kg_{xa}\ kg_{sc}^{-1}$), and the amount of fungi biomass generated per unit per lignin substrate utilized ($Y_{X_f/S_{sl}}$, $kg_{xf}\ kg_{sl}^{-1}$),

$$Y_{X_b/S_{ss}} = 0.5782 \tag{6.62}$$

$$Y_{X_a/S_{sc}} = 0.3281 \tag{6.63}$$

$$Y_{X_f/S_{sl}} = 0.9160 \tag{6.64}$$

Section 2: Arrays and Initialized

The multidimensional array was established and initialized to zero to facilitate data collection for all variable parameters. Each array had an identifier (k, p). The 'k' was the index for the multidimensional array to represent a point at time 't'. The 'k' was the x-axis. For the array 'k' equals the '$length(t)$' where t was calculated in the equation $t = [0 : t_{increment} : t_{stop}]$ (Equation 6.12). The 'p' was the index for the multidimensional array to represent each increment of the compost vessel at 'k'. The 'p' was the y-axis. If this step was not accomplished the program would require each array to be expanded at each step before a calculation is performed and then enter the calculated value. This step permited the MATLAB® program to operate efficiently otherwise each time the program ran it would take hours.

Section 3: External Boundary and Internal Vessel Conditions Initialized

This step established and initialized the external and internal boundary conditions. To accomplish this the identifier (k, p) was adjusted for programming purposes to (k, ip) where,

$$ip = (1 : p) \tag{6.65}$$

When $p = 1$, the increment was below the actual compost substrate. This was the atmospheric layer from which air was drawn to aerate the compost bed. The value $p = 2$

represented the bottom increment or first layer of the actual composting substrate. The program continued calculating the values for each node until the value of ' p ' was reached. This was the top of the composting substrate as established in the first section [the number of increments (d) the compost reactor was divided into plus one for a layer below the compost representing atmospheric or lower boundary conditions].

The initial step was to set the parameters that were common to the lower external boundary layer and internal boundary at $k = 1$ for $ip = 1 : p$. This included the ambient temperature (T , K), wet bulb temperature (T_{wb} , K), atmospheric oxygen concentration (C_{O_2} , kg_{O2} m^{-3}), and volume of inflowing air (V_{air} , m^3 h^{-1}),

$$T_{(1,ip)} = T_C + 273.16 \tag{6.66}$$

$$T_{wb(1,ip)} = T_{C_{wb}} + 273.16 \tag{6.67}$$

$$C_{O_2\,(1,ip)} = 0.2992 \tag{6.68}$$

$$V_{air\,(1,ip)} = 0.001 * F_{air} \tag{6.69}$$

Next a series of calculations that was executed to determine the enthalpy, which was utilized to determine the drying effect the air supply had on the moisture content of the substrate. First, the saturation vapor pressure at atmospheric (P_{sa} , Pa or kg m^{-1} sec^{-2}) (ASAE D271.2) and the saturation vapor pressure at wet bulb temperature (P_{swb} , Pa or kg m^{-1} sec^{-2}) (ASAE D271.2) were calculated by

$$P_{sa\,(k,ip)} = R * \exp\left(\frac{A + BT_{(k,ip)} + CT_{(k,ip)}{}^2 + DT_{(k,ip)}{}^3 + ET_{(k,ip)}{}^4}{FT_{(k,ip)} - GT_{(k,ip)}{}^2} \right) \tag{6.70}$$

where,

$R = 22{,}105{,}649.5$

$A = -27{,}405.526$

$B = 97.5413$

$C = -0.146244$

$D = 0.12558 * 10^{-3}$

$E = -0.48502 * 10^{-7}$

$F = 4.34903$

$G = 0.39381 * 10^{-2}$

$$P_{swb\,(k,ip)} = R * \exp\left(\frac{A + BT_{wb\;(k,ip)} + CT_{wb\,(k,ip)}{}^{2} + DT_{wb\,(k,ip)}{}^{3} + ET_{wb\,(k,ip)}{}^{4}}{FT_{wb\;(k,ip)} - GT_{wb\,(k,ip)}{}^{2}} \right) \quad (6.71)$$

The coefficients for this equation were the same as Eq. 6.70.

Next, the latent heat of vaporization (h'_{fg}, kJ kg^{-1}) (ASAE D271.2) at wet bulb temperature was calculated by

$$h'_{fg\;(k,ip)} = 2502.535259 - 2.38576424 * \left(T_{wb\,(k,ip)} - 273.16 \right) \quad (6.72)$$

Based on latent heat vaporization, the partial vapor pressure (Pv, Pa or kg m^{-1} sec^{-2}) (ASAE D271.2), was calculated,

$$P_{v(k,ip)} = \frac{.62194 * h'_{fg\,(k,ip)} * P_{swb\,(k,ip)} - 1.0069254 * \left(P_{swb\,(k,ip)} - P_{atm} \right) * \left(T_{wb\,(k,ip)} - T_{(k,ip)} \right)}{0.62194 * h'_{fg\,(k,ip)} + \dfrac{0.15684877 * \left(P_{swb(k,ip)} - P_{atm} \right) * \left(T_{wb\,(k,ip)} - T_{(k,ip)} \right)}{P_{atm}}} \quad (6.73)$$

The partial vapor pressure was used to determine the dew point temperature (T_{dp}, K) (ASAE D271.2),

$$T_{dp(k,ip)} = 255.38 + \sum_{i=0}^{8} A_i \left[\ln\left(0.00145 P_{v\,(k,ip)} \right) \right]^{i} \quad (6.74)$$

where,

$A_0 = 19.5322$
$A_1 = 13.6626$
$A_2 = 1.17678$
$A_3 = -0.189693$
$A_4 = 0.087453$
$A_5 = -0.0174053$
$A_6 = 0.00214768$
$A_7 = -0.000138343$
$A_8 = 0.0000038$

Next, the latent heat of vaporization (h''_{fg}, kJ kg^{-1}) (ASAE D271.2) at dew point temperature was determined by

$$h''_{fg\,(k,ip)} = 2502535.259 - 2385.76424 * \left(T_{dp\,(k,ip)} - 273.16 \right) \quad (6.75)$$

The humidity ratio (H, kg-w kg-da^{-1}) (ASAE D271.2) was calculated by

$$H_{(k,ip)} = \frac{0.6219 * P_{v\,(k,ip)}}{P_{atm} - P_{v\,(k,ip)}} \tag{6.76}$$

With the humidity value established, the enthalpy (h , J kg_{DA}^{-1}) (ASAE D271.2) of the air-vapor mixture was determined by

$$h_{(k,ip)} = 1006.9254 * \left(T_{(k,ip)} - 273.16\right) + 4186.8 * H_{(k,ip)} * \left(T_{dp\,(k,ip)} - 273.16\right) ...$$
$$+ h"_{fg\,(k,ip)} * H_{(k,ip)} + 1875.6864 * H_{(k,ip)} * \left(T_{(k,ip)} - T_{dp\,(k,ip)}\right) \tag{6.77}$$

The next step was to establish the initial conditions within the vessel only. This was at $k = 1$ but with $ip = 2 : p$ only. First, the mass of substrate in each increment within the vessel for the soluble substrate (S_{ss} , kgs_{ss}), cellulose substrate (S_{sc} , kg_{sc}), lignin substrate (S_{sl} , kg_{sl}), inert substrate (S_{si} , kg_{si}) and for the total amount of substrate (S_t , kg_{st}) was calculated by

$$S_{ss(k,ip)} = \frac{S_s}{d} \tag{6.78}$$

$$S_{sc(k,ip)} = \frac{S_c}{d} \tag{6.79}$$

$$S_{sl(k,ip)} = \frac{S_l}{d} \tag{6.80}$$

$$S_{si(k,ip)} = \frac{S_i}{d} \tag{6.81}$$

$$S_{st(k,ip)} = S_{ss(k,ip)} + S_{sc(k,ip)} + S_{sl(k,ip)} + S_{si(k,ip)} \tag{6.82}$$

Next, the mass of water (W_{st} , kg_w) was determined by

$$W_{st\ (k,ip)} = \frac{W_w}{d} \tag{6.83}$$

With the total amount of substrate and water determined per increment, the moisture content (W_{mc} , $kg_w\ kg_S^{-1}$) (wet basis) of the compost substrate was computed. This was the fraction of water to the total mass (water and substrate).

$$W_{mc(k,ip)} = \frac{W_{st(k,ip)}}{\left(W_{st(k,ip)} + S_{st(k,ip)}\right)} \tag{6.84}$$

Microbial growth is affected by the amount of moisture present. To adjust the microbial growth, a weighted moisture coefficient (k_{H_2O}, no units) was calculated based on the moisture content.

$$\text{If } 0.00 \geq W_{mc(k,ip)} < 0.10 \tag{6.85}$$

$$\text{then } k_{H_2O(k,ip)} = 0.00$$

$$\text{If } 0.10 \geq W_{mc(k,ip)} < 0.20 \tag{6.86}$$

$$\text{then } k_{H_2O(k,ip)} = -0.0759 + 0.9011 * W_{mc(k,ip)}$$

$$\text{If } 0.20 \geq W_{mc(k,ip)} < 0.60 \tag{6.87}$$

$$\text{then } k_{H_2O(k,ip)} = -0.3482 + 2.2597 * W_{mc(k,ip)}$$

$$\text{If } W_{mc(k,ip)} = 0.60 \tag{6.88}$$

$$\text{then } k_{H_2O(k,ip)} = 1.00$$

$$\text{And, if } 0.60 > W_{mc(k,ip)} \leq 1.00 \tag{6.89}$$

$$\text{then } k_{H_2O(k,ip)} = 7.5844 - 20.5315 * W_{mc(k,ip)} + 19.8468 * W_{mc(k,ip)}^{\ 2} \ldots$$

$$-6.5147 * W_{mc(k,ip)}^{\ 3}$$

The concentration of substrate per increment volume was determined for the soluble substrate ($C_{S_{ss}}$, kg_{ss} m^{-3}), the cellulose substrate ($C_{S_{sc}}$, kg_{sc} m^{-3}), the lignin substrate ($C_{S_{sl}}$, kg_{sl} m^{-3}) and the inert substrate ($C_{S_{si}}$, kg_{si} m^{-3}). The concentration of water (C_w, kg_w m^{-3}) was also calculated by

$$C_{S_{ss}(k,ip)} = \frac{S_{ss\,(k,ip)}}{Vol_{cl}} \tag{6.90}$$

$$C_{S_{sc}(k,ip)} = \frac{S_{sc\,(k,ip)}}{Vol_{cl}} \tag{6.91}$$

$$C_{S_{sl}(k,ip)} = \frac{S_{sl\,(k,ip)}}{Vol_{cl}} \tag{6.92}$$

$$C_{S_{si}(k,ip)} = \frac{S_{si\,(k,ip)}}{Vol_{cl}} \tag{6.93}$$

$$C_{w(k,ip)} = \frac{W_{st(k,ip)}}{Vol_{cl}} \tag{6.94}$$

The microbial seed population for the mesophilic bacteria ($C_{X_{mb}}$, $kg_{Xmb}\ m^{-3}$), actinomycetes ($C_{X_{ma}}$, $kg_{Xma}\ m^{-3}$), and fungi ($C_{X_{mf}}$, $kg_{Xmf}\ m^{-3}$), and the thermophilic bacteria ($C_{X_{tb}}$, $kg_{Xtb}\ m^{-3}$), actinomycetes ($C_{X_{ta}}$, $kg_{Xta}\ m^{-3}$) and fungi ($C_{X_{tf}}$, $kg_{Xtf}\ m^{-3}$) were established to initiate microbial growth,

$$C_{X_{mb}(k,ip)} = 0.008 \tag{6.95}$$

$$C_{X_{mb}(k,ip)} = 0.008 \tag{6.96}$$

$$C_{X_{mf}(k,ip)} = 0.008 \tag{6.97}$$

$$C_{X_{tb}(k,ip)} = 0.008 \tag{6.98}$$

$$C_{X_{ta}(k,ip)} = 0.008 \tag{6.99}$$

$$C_{X_{tf}(k,ip)} = 0.008 \tag{6.100}$$

Section 4: Begin Time loop

With both external and internal boundary conditions set, the next a series of calculations were executed to calculate the reactions occurring within the composting vessel through time. The initial step was to initiate the time loop where 'k' equals each time step starting at time step '2' through the last time step which equals '$length(t)$'

$$k = 2 : length(t) \tag{6.101}$$

and

$$t(k) \tag{6.102}$$

The finite difference (dt) was determined by calculating the difference between each time step by

$$\Delta t = t(k) - t(k-1) \tag{6.103}$$

In each time loop step (k, ip) the lower external boundary layer parameters were calculated first for $(ip = 1)$. These parameters were set equal to the previous time set which was equal to the initial values determined for $k = 1$,

$$T_{(k,ip)} = T_{(k-1,ip)} \tag{6.104}$$

$$T_{wb(k,ip)} = T_{wb(k-1,ip)} \tag{6.105}$$

$$C_{O_2\,(k,ip)} = C_{O_2\,(k-1,ip)} \tag{6.106}$$

$$P_{sa(k,ip)} = P_{sa(k-1,ip)} \tag{6.107}$$

$$P_{swb(k,ip)} = P_{swb(k-1,ip)} \tag{6.108}$$

$$h'_{fg\,(k,ip)} = h'_{fg(k-1,ip)} \tag{6.109}$$

$$P_{v(k,ip)} = P_{v(k-1,ip)} \tag{6.110}$$

$$T_{dp(k,ip)} = T_{dp(k-1,ip)} \tag{6.111}$$

$$h''_{fg\,(k,ip)} = h''_{fg(k-1,ip)} \tag{6.112}$$

$$H_{(k,ip)} = H_{(k-1,ip)} \tag{6.113}$$

$$h_{(k,ip)} = h_{(k-1,ip)} \tag{6.114}$$

The mass flow of air was handled differently. For every loop the mass flow of air was referenced back to $k = 1$ where,

$$V_{air(k,ip)} = V_{air(1,ip)} \tag{6.115}$$

This procedure permited the mass flow of air to be turned off for any given span of time. The following equations were utilized to turn the air flow off and then back on. This procedure could be used to fluctuate the air flow. In this example the air flow was turned off at hour 114 and turned back on at hour 140 into the simulation,

if $k \geq 114/\Delta t \; and \; k \leq 140/\Delta t$ (6.116)

$$V_{air(k,ip)} = 0.00$$

else (otherwise)

$$V_{air(k,ip)} = V_{air(1,ip)}$$

The specific volume of dry air (V_{sa}, $m^3\ kg_{da}^{-1}$) and the mass flow of dry air (m_{fda}, $kg_{da}\ h^{-1}$) were calculated by

$$V_{sa(k,ip)} = \frac{287 + T_{(k-1,ip)}}{P_{atm} - P_{v(k,ip)}} \tag{6.117}$$

$$m_{fda} = \frac{V_{air(k,ip)}}{V_{sa(k,ip)}} \tag{6.118}$$

After all the parameters for the external boundary condition where $(ip = 1)$ for the time step were calculated, the parameters within the composting vessel are then calculated. First, the psychometric parameters were recalculated using the temperature value calculated from the previous time step. The same equations were utilized to determine the saturation vapor pressure at ambient temperature (P_{sa}) (Eq.6.70), the saturation vapor pressure at wet bulb temperature (P_{swb}) (Eq. 6.71), and the latent heat of vaporization (h'_{fg}) (Eq. 6.72). The partial vapor pressure (P_v) however was determined differently because the wet bulb reading cannot be calculated. With the assumption the air is saturated, a best fit equation was developed using EXCEL, 2007, from psychrometric chart listing the temperature (T_C) and vapor pressure (P_v) data (Wilhelm, et al. 2005. p 223). Thus, based on the ambient temperature, the partial vapor pressure was determined by

$$P_{v(k,ip)} = \left(0.0007 * \left(T_{(k-1,ip)} - 273.16\right)^4\right) - \left(0.001 * \left(T_{(k-1,ip)} - 273.16\right)^3\right) \ldots$$
$$+2.1126 * \left(T_{(k-1,ip)} - 273.16\right)^2 + \left(38.161 * \left(T_{(k-1,ip)} - 273.16\right)\right) + 623.37 \quad (6.119)$$

The dew point temperature (T_{dp}) was calculated as previously (Eq. 6.74). The latent heat of vaporization (h''_{fg}) (ASAE D271.2), which was based on the value of T_{dp}, was calculated by

if $T_{dp(k,ip)} <= 338.72$ (6.120)

$$h''_{fg\,(k,ip)} = 2502.535259 - 2.38576424 * \left(T_{dp\,(k,ip)} - 273.16\right) \text{ (Eq. 6.75)}$$

else (otherwise),

$$h''_{fg\,(k,ip)} = 7329155978.00 - 15995.96408 * \left(T_{dp\,(k,ip)} - 273.16\right)^{0.5} \quad (6.121)$$

The humidity ratio (H) (Eq.6.76) and enthalpy (h) (Eq. 6.77) were determined as described previously.

Next, the mass flow of air flowing into the reactor was calculated by taking its value from the node below,

$$V_{air(k,ip)} = V_{air(k,ip-1)} \quad (6.122)$$

From V_{air} the new values for specific volume of dry air and the mass flow of dry air were calculated as before (Eq. 6.117 and (Eq. 6.118).

The cell maintenance requirements for the mesophilic microorganisms ($\eta_{\max m}$, $kg_s\ kg_{Xm}^{-1}\ h^{-1}$) and thermophilic microorganisms ($\eta_{\max t}$, $kg_s\ kg_{Xt}^{-1}\ h^{-1}$) were entered as

$$\eta_{\max m(k,ip)} = 0.48 \tag{6.123}$$

$$\eta_{\max t(k,ip)} = 0.48 \tag{6.124}$$

The fraction of the mesophilic microbial population which expired each hour (k_{dm}, $kg_{Xm}\ kg_{Xm}^{-1} h^{-1}$) and fraction of the thermophilic microbial population which expired each hour (k_{dt}, $kg_{Xt}\ kg_{Xt}^{-1} h^{-1}$) were set at

$$k_{dm(k,ip)} = 0.025 \tag{6.125}$$

$$k_{dt(k,ip)} = 0.025 \tag{6.126}$$

These values applied as long as the temperature remained within the appropriate temperature range for the respective microorganism. The values changed when the temperature fell below or exceeded their appropriate temperature range.

Microbial growth rate

The next step in the time loop was to compute microbial growth. Two actions were taking place; one for the mesophilic microorganisms and the other for the thermophilic microorganism. These actions occurred separately or concurrently depending on the temperature. A temperature range was established for each group. These ranges were specified above. If the ambient temperature was equal to or greater than the required minimum and less than the maximum mesophilic temperature, $\left(T_{(k-1,ip)} \geq T_{m\min}\ and\ T_{(k-1,ip)} \leq T_{m\max}\right)$ the maximum growth rate for mesophilic bacteria ($\mu_{max\,mb}$, h^{-1}), the actinomycetes ($\mu_{max\,ma}$, h^{-1}) and fungi ($\mu_{max\,mf}$, h^{-1}) were set at

$$\mu_{\max mb(k,ip)} = 0.23 \tag{6.127}$$

$$\mu_{\max ma(k,ip)} = 0.06 \tag{6.128}$$

$$\mu_{\max mf(k,ip)} = 0.02 \tag{6.129}$$

The microbial growth rate was determined for the mesophilic bacteria (μ_{mb} , $kg_{ss}\ kg_{Xmb}^{-1}$), the actinomycetes (μ_{ma} , $kg_{sc}\ kg_{Xma}^{-1}$) and fungi (μ_{mf} , $kg_{sl}\ kg_{Xmf}^{-1}$) by

$$\mu_{mb(k,ip)} = \mu_{\max\, mb(k,ip)} * \frac{C_{S_{ss}(k-1,ip)}}{K_S + C_{S_{ss}(k-1,ip)}} * \frac{C_{O_2(k-1,ip)}}{K_{O_2} + C_{O_2(k-1,ip)}} * k_{H_2O(k-1,ip)} \tag{6.130}$$

$$\mu_{ma(k,ip)} = \mu_{\max\, ma(k,ip)} * \frac{C_{S_{sc}(k-1,ip)}}{K_S + C_{S_{sc}(k-1,ip)}} * \frac{C_{O_2(k-1,ip)}}{K_{O_2} + C_{O_2(k-1,ip)}} * k_{H_2O(k-1,ip)} \tag{6.131}$$

$$\mu_{mf(k,ip)} = \mu_{\max\, mf(k,ip)} * \frac{C_{S_{sl}(k-1,ip)}}{K_S + C_{S_{sl}(k-1,ip)}} * \frac{C_{O_2(k-1,ip)}}{K_{O_2} + C_{O_2(k-1,ip)}} * k_{H_2O(k-1,ip)} \tag{6.132}$$

If required, the microbial spore /seed condition was reintroduced. This was accomplished by checking to determine if the microbial populations for the mesophilic bacteria, actinomycetes, and/or fungi were equal to zero. If the populations were equal to zero, the microbial populations were reset to equal the initial seed conditions (Eq. 6.95, Eq.6.96 and Eq. 6.97). If the population was greater than zero, the population equaled the population from the previous time step.

For the mesophilic bacteria,

$$\text{If } C_{X_{mb}(k,ip)} = 0.00 \tag{6.133}$$

$$C_{X_{mb}(k,ip)} = C_{X_{mb}(1,ip)}$$

$$\text{else (otherwise)}\, C_{X_{mb}(k,ip)} = C_{X_{mb}(k-1,ip)}$$

For the mesophilic actimomycetes,

$$\text{If } C_{X_{ma}(k,ip)} = 0.00 \tag{6.134}$$

$$C_{X_{ma}(k,ip)} = C_{X_{ma}(1,ip)}$$

$$\text{else (otherwise)}\, C_{X_{ma}(k,ip)} = C_{X_{ma}(k-1,ip)}$$

and, for the mesophilic fungi,

$$\text{If } C_{X_{mf}(k,ip)} = 0.00 \tag{6.135}$$

$$C_{X_{mf}(k,ip)} = C_{X_{mf}(1,ip)}$$

$$\text{else (otherwise)}\, C_{X_{mf}(k,ip)} = C_{X_{mf}(k-1,ip)}$$

Similar calculations were performed for the thermophilic microorganisms. If the ambient temperature was equal to or greater than the required minimum and less than the maximum thermophilic temperature, $\left(T_{(k-1,ip)} \geq T_{t\min} \; and \; \mathrm{T}_{(k-1,ip)} \leq T_{t\max}\right)$, the maximum growth rate for thermophilic bacteria ($\mu_{\max tb}$, h^{-1}), the actinomycetes ($\mu_{\max ta}$, h^{-1}) and fungi ($\mu_{\max tf}$, h^{-1}) were set at,

$$\mu_{\max tb(k,ip)} = 0.23 \tag{6.136}$$

$$\mu_{\max ta(k,ip)} = 0.06 \tag{6.137}$$

$$\mu_{\max tf(k,ip)} = 0.02 \tag{6.138}$$

The microbial growth rate for the thermophilic bacteria (μ_{tb}, $kg_{ss}\ kg_{Xtb}^{-1}$), the actinomycetes (μ_{ta}, $kg_{sc}\ kg_{Xta}^{-1}$) and fungi (μ_{tf}, $kg_{sl}\ kg_{Xtf}^{-1}$) were determined in the same manner as for the mesophilic microorganisms:

$$\mu_{tb(k,ip)} = \mu_{\max tb(k,ip)} * \frac{C_{S_{ss}(k-1,ip)}}{K_S + C_{S_{ss}(k-1,ip)}} * \frac{C_{O_2(k-1,ip)}}{K_{O_2} + C_{O_2(k-1,ip)}} * k_{H_2O(k-1,ip)} \tag{6.139}$$

$$\mu_{tb(k,ip)} = \mu_{\max ta(k,ip)} * \frac{C_{S_{sc}(k-1,ip)}}{K_S + C_{S_{sc}(k-1,ip)}} * \frac{C_{O_2(k-1,ip)}}{K_{O_2} + C_{O_2(k-1,ip)}} * k_{H_2O(k-1,ip)} \tag{6.140}$$

$$\mu_{tb(k,ip)} = \mu_{\max tf(k,ip)} * \frac{C_{S_{sl}(k-1,ip)}}{K_S + C_{S_{sl}(k-1,ip)}} * \frac{C_{O_2(k-1,ip)}}{K_{O_2} + C_{O_2(k-1,ip)}} * k_{H_2O(k-1,ip)} \tag{6.141}$$

Again, if required, the microbial spore /seed condition was reintroduced. This was accomplished by checking to determine if the microbial populations for the thermophilic bacteria, actinomycetes, and/or fungi were equal to zero. If the populations were equal to zero, the microbial populations were reset to equal the initial seed conditions (Eq. 6.98, Eq.6.99 and Eq. 6.100). If the population was greater than zero, the population equaled the population from the previous time step.

For the thermophilic bacteria,

If $C_{X_{tb}(k,ip)} = 0.00$ (6.142)

$$C_{X_{tb}(k,ip)} = C_{X_{tb}(1,ip)}$$

else (otherwise) $C_{X_{tb}(k,ip)} = C_{X_{tb}(k-1,ip)}$

For the thermophilic actinomycetes,

If $C_{X_{ta}(k,ip)} = 0.00$ (6.143)

$C_{X_{ta}(k,ip)} = C_{X_{ta}(1,ip)}$

else (otherwise) $C_{X_{ta}(k,ip)} = C_{X_{ta}(k-1,ip)}$

and, for the thermophilic fungi,

If $C_{X_{tf}(k,ip)} = 0.00$ (6.144)

$C_{X_{tf}(k,ip)} = C_{X_{tf}(1,ip)}$

else (otherwise) $C_{X_{tf}(k,ip)} = C_{X_{tf}(k-1,ip)}$

As stated above, there was a fraction of the mesophilic and thermophilic microbial populations which expired per hour while the population was growing. If the temperature fell outside their respective growth range, the population died. To account for this, the following equations were utilized:

If $T_{(k-1,ip)} > T_{m\min}$ *and* $\mathrm{T}_{(k-1,ip)} < T_{t\min}$ (6.145)

$k_{dt(k,ip)} = 0.40$

If $T_{(k-1,ip)} > T_{m\max}$ *and* $\mathrm{T}_{(k-1,ip)} < T_{t\max}$ (6.146)

$k_{dm(k,ip)} = 0.40$

Microbial Maintenance and Growth

The microbial cell maintenance requirement was considered. The same Monod equation utilized for cellular growth rate was used for cellular maintenance. A maximum cell maintenance rate was entered in place of the maximum growth rate. In this model the rate was the same for all microorganisms,

$\eta_{\max m\,(k,ip)} = 0.48$ (6.147)

$\eta_{\max t\,(k,ip)} = 0.48$ (6.148)

These calculations were divided into mesophilic and thermophilic. Cell maintenance rate was determined for the mesophilic bacteria (η_{mb}, $kg_{ss}\ kg_{Xmb}^{-1}$), the actinomycetes (η_{ma}, $kg_{sc}\ kg_{Xma}^{-1}$) and fungi (η_{mf}, $kg_{sl}\ kg_{Xmf}^{-1}$),

$$\eta_{mb(k,ip)} = \eta_{\max m(k,ip)} * \frac{C_{S_{ss}(k-1,ip)}}{K_S + C_{S_{ss}(k-1,ip)}} * \frac{C_{O_2(k-1,ip)}}{K_{O_2} + C_{O_2(k-1,ip)}} \tag{6.149}$$

$$\eta_{ma(k,ip)} = \eta_{\max m(k,ip)} * \frac{C_{S_{sc}(k-1,ip)}}{K_S + C_{S_{sc}(k-1,ip)}} * \frac{C_{O_2(k-1,ip)}}{K_{O_2} + C_{O_2(k-1,ip)}} * k_{H_2O(k-1,ip)} \tag{6.150}$$

$$\eta_{mf(k,ip)} = \eta_{\max m(k,ip)} * \frac{C_{S_{sl}(k-1,ip)}}{K_S + C_{S_{sl}(k-1,ip)}} * \frac{C_{O_2(k-1,ip)}}{K_{O_2} + C_{O_2(k-1,ip)}} * k_{H_2O(k-1,ip)} \tag{6.151}$$

The rate of change in the microbial concentrations due to growth for mesophilic bacteria ($dC_{X_{g\,mb}}$, $kg_{Xmb}\ m^{-3}\ h^{-1}$), actinomycetes ($dC_{X_{g\,ma}}$, $kg_{Xma}\ m^{-3}\ h^{-1}$) and fungi ($dC_{X_{g\,mf}}$, $kg_{Xmf}\ m^{-3}\ h^{-1}$) were determined by

$$dC_{X_{g\,mb}(k-1,ip)} = \mu_{mb(k-1,ip)} * C_{X_{mb}(k-1,ip)} \tag{6.152}$$

$$dC_{X_{g\,ma}(k-1,ip)} = \mu_{ma(k-1,ip)} * C_{X_{ma}(k-1,ip)} \tag{6.153}$$

$$dC_{X_{g\,mf}(k-1,ip)} = \mu_{mf(k-1,ip)} * C_{X_{mf}(k-1,ip)} \tag{6.154}$$

Next, the rate of change in concentrations of microorganisms due to that portion of the population which were dying was calculated for the mesophilic bacteria ($dC_{X_{kd\,mb}}$, $kg_{Xmb}\ m^{-3}\ h^{-1}$), actinomycetes ($dC_{X_{kd\,ma}}$, $kg_{Xma}\ m^{-3}\ h^{-1}$) and fungi ($dC_{X_{kd\,mf}}$, $kg_{Xmf}\ m^{-3}\ h^{-1}$) were calculated by

$$dC_{X_{kd\,mb}(k,ip)} = k_{dm(k,ip)} * C_{X_{mb}(k,ip)} \tag{6.155}$$

$$dC_{X_{kd\,ma}(k,ip)} = k_{dm(k,ip)} * C_{X_{ma}(k,ip)} \tag{6.156}$$

$$dC_{X_{kd\,mf}(k,ip)} = k_{dm(k,ip)} * C_{X_{mf}(k,ip)} \tag{6.157}$$

From these calculations, the rate of change for the mesophilic bacteria ($dC_{X_{mb}}$, $kg_{Xmb}\ m^{-3}\ h^{-1}$), actinomycetes ($dC_{X_{ma}}$, $kg_{Xma}\ m^{-3}\ h^{-1}$) and fungi ($dC_{X_{mf}}$, $kg_{Xmf}\ m^{-3}\ h^{-1}$) were calculated by

$$dC_{X_{mb}(k,ip)} = dC_{X_{g\,mb}(k,ip)} - dC_{X_{kd\,mb}(k,ip)} \tag{6.158}$$

$$dC_{X_{ma}(k,ip)} = dC_{X_{g\,ma}(k,ip)} - dC_{X_{kd\,ma}(k,ip)} \tag{6.159}$$

$$dC_{X_{mf}(k,ip)} = dC_{X_{g\,mf}(k,ip)} - dC_{X_{kd\,mf}(k,ip)} \tag{6.160}$$

The new concentrations of mesophilic microorganisms were now determined from the previous step's concentration and the change in concentration due to death and growth. Mathematically, it was possible that the change could make the final concentration a negative number. Since this does not occur in nature, an adjustment could be required. If the resulting concentration was less than zero, the concentration was set to equal zero,

$$C_{X_{mb}(k,ip)} = C_{X_{mb}(k-1,ip)} - dC_{X_{mb}(k,ip)} * \Delta t \tag{6.161}$$

if $C_{X_{mb}(k,ip)} < 0.00$

then $C_{X_{mb}(k,ip)} = 0.00$

$$C_{X_{ma}(k,ip)} = C_{X_{ma}(k-1,ip)} - dC_{X_{ma}(k,ip)} * \Delta t \tag{6.162}$$

if $C_{X_{ma}(k,ip)} < 0.00$

then $C_{X_{ma}(k,ip)} = 0.00$

$$C_{X_{mf}(k,ip)} = C_{X_{mf}(k-1,ip)} - dC_{X_{mf}(k,ip)} * \Delta t \tag{6.163}$$

if $C_{X_{mf}(k,ip)} < 0.00$

then $C_{X_{mf}(k,ip)} = 0.00$

The same process was repeated for the thermophilic microorganisms. The cell maintenance rates were determined for the thermophilic bacteria (η_{tb}, $kg_{ss}\ kg_{Xtb}^{-1}$), the actinomycetes (η_{ta}, $kg_{sc}\ kg_{Xta}^{-1}$) and fungi (η_{tf}, $kg_{sl}\ kg_{Xtf}^{-1}$) by

$$\eta_{tb(k,ip)} = \eta_{\max t(k,ip)} * \frac{C_{S_{ss}(k-1,ip)}}{K_S + C_{S_{ss}(k-1,ip)}} * \frac{C_{O_2(k-1,ip)}}{K_{O_2} + C_{O_2(k-1,ip)}} * k_{H_2O(k-1,ip)} \tag{6.164}$$

$$\eta_{ta(k,ip)} = \eta_{\max t(k,ip)} * \frac{C_{S_{sc}(k-1,ip)}}{K_S + C_{S_{sc}(k-1,ip)}} * \frac{C_{O_2(k-1,ip)}}{K_{O_2} + C_{O_2(k-1,ip)}} * k_{H_2O(k-1,ip)} \tag{6.165}$$

$$\eta_{tf(k,ip)} = \eta_{\max t(k,ip)} * \frac{C_{S_{sl}(k-1,ip)}}{K_S + C_{S_{sl}(k-1,ip)}} * \frac{C_{O_2(k-1,ip)}}{K_{O_2} + C_{O_2(k-1,ip)}} * k_{H_2O(k-1,ip)} \tag{6.166}$$

The rate of change in the microbial concentrations due to growth for thermophilic bacteria ($dC_{X_{g\,tb}}$, $kg_{Xtb}\ m^{-3}\ h^{-1}$), actinomycetes ($dC_{X_{g\,ta}}$, $kg_{Xta}\ m^{-3}\ h^{-1}$) and fungi ($dC_{X_{g\,tf}}$, $kg_{Xtf}\ m^{-3}\ h^{-1}$) were calculated by

$$dC_{X_{g\,tb}(k-1,ip)} = \mu_{tb(k-1,ip)} * C_{X_{tb}(k-1,ip)} \quad (6.167)$$

$$dC_{X_{g\,ta}(k-1,ip)} = \mu_{ta(k-1,ip)} * C_{X_{ta}(k-1,ip)} \quad (6.168)$$

$$dC_{X_{g\,tf}(k-1,ip)} = \mu_{tf(k-1,ip)} * C_{X_{tf}(k-1,ip)} \quad (6.169)$$

Next, the rate of change in the concentrations of microorganisms due to that portion of the population which were dying was calculated for the thermophilic bacteria ($dC_{X_{kd\,tb}}$, $kg_{Xtb}\ m^{-3}\ h^{-1}$), actinomycetes ($dC_{X_{kd\,ta}}$, $kg_{Xta}\ m^{-3}\ h^{-1}$) and fungi ($dC_{X_{kd\,tf}}$, $kg_{Xtf}\ m^{-3}\ h^{-1}$) by

$$dC_{X_{kd\,tb}(k,ip)} = k_{dt(k,ip)} * C_{X_{tb}(k,ip)} \quad (6.170)$$

$$dC_{X_{kd\,ta}(k,ip)} = k_{dt(k,ip)} * C_{X_{ta}(k,ip)} \quad (6.171)$$

$$dC_{X_{kd\,tf}(k,ip)} = k_{dt(k,ip)} * C_{X_{tf}(k,ip)} \quad (6.172)$$

From these calculations, the rates of change in the thermophilic bacteria ($dC_{X_{tb}}$, $kg_{Xtb}\ m^{-3}\ h^{-1}$), actinomycetes ($dC_{X_{ta}}$, $kg_{Xta}\ m^{-3}\ h^{-1}$) and fungi ($dC_{X_{tf}}$, $kg_{Xtf}\ m^{-3}\ h^{-1}$) were calculated by

$$dC_{X_{tb}(k,ip)} = dC_{X_{g\,tb}(k,ip)} - dC_{X_{kd\,tb}(k,ip)} \quad (6.173)$$

$$dC_{X_{ta}(k,ip)} = dC_{X_{g\,ta}(k,ip)} - dC_{X_{kd\,ta}(k,ip)} \quad (6.174)$$

$$dC_{X_{tf}(k,ip)} = dC_{X_{g\,tf}(k,ip)} - dC_{X_{kd\,tf}(k,ip)} \quad (6.175)$$

The new concentrations of thermophilic microorganisms were now determined from the previous step's concentration and the change in concentration due to death and growth. Again, mathematically it was possible the change could make the final concentration a negative number. Again, an adjustment could be required. If resulting concentration was less than zero, the concentration was set to equal zero,

$$C_{X_{tb}(k,ip)} = C_{X_{tb}(k-1,ip)} - dC_{X_{tb}(k,ip)} * \Delta t \quad (6.176)$$

if $C_{X_{tb}(k,ip)} < 0.00$

then $C_{X_{tb}(k,ip)} = 0.00$

$$C_{X_{ta}(k,ip)} = C_{X_{ta}(k-1,ip)} - dC_{X_{ta}(k,ip)} * \Delta t \quad (6.177)$$

if $C_{X_{ta}(k,ip)} < 0.00$

then $C_{X_{ta}(k,ip)} = 0.00$

$$C_{X_{tf}(k,ip)} = C_{X_{tf}(k-1,ip)} - dC_{X_{tf}(k,ip)} * \Delta t \tag{6.178}$$

if $C_{X_{tf}(k,ip)} < 0.00$

then $C_{X_{tf}(k,ip)} = 0.00$

Substrate Utilization

The next step in the time loop was to compute the change in substrate. The substrate sources were utilized by both the mesophilic and thermophilic microorganisms. The rates of change in the concentration of substrate due to consumption was determine for the soluble ($dC_{S_{ss}}$, kg_{ss} m^{-3} h^{-1}), cellulose/hemicellulose ($dC_{S_{sc}}$, kg_{sc} m^{-3} h^{-1}), and lignin ($dC_{S_{sl}}$, kg_{sl} m^{-3} h^{-1}) substrates by

$$dC_{S_{ss}(k,ip)} = \left(\frac{dC_{X_{g\,mb}(k-1,ip)}}{Y_{X_b/S_{ss}}} + \left(C_{X_{mb}(k,ip)} * \eta_{mb(k,ip)} \right) \right) + \left(\frac{dC_{X_{g\,tb}(k-1,ip)}}{Y_{X_b/S_{ss}}} + \left(C_{X_{tb}(k,ip)} * \eta_{tb(k,ip)} \right) \right) \tag{6.179}$$

$$dC_{S_{sc}(k,ip)} = \left(\frac{dC_{X_{g\,ma}(k-1,ip)}}{Y_{X_a/S_{sc}}} + \left(C_{X_{ma}(k,ip)} * \eta_{ma(k,ip)} \right) \right) + \left(\frac{dC_{X_{g\,ta}(k-1,ip)}}{Y_{X_a/S_{sc}}} + \left(C_{X_{ta}(k,ip)} * \eta_{ta(k,ip)} \right) \right) \tag{6.180}$$

$$dC_{S_{sl}(k,ip)} = \left(\frac{dC_{X_{g\,mf}(k-1,ip)}}{Y_{X_f/S_{sl}}} + \left(C_{X_{mf}(k,ip)} * \eta_{mf(k,ip)} \right) \right) + \left(\frac{dC_{X_{g\,tf}(k-1,ip)}}{Y_{X_f/S_{sl}}} + \left(C_{X_{tf}(k,ip)} * \eta_{tf(k,ip)} \right) \right) \tag{6.181}$$

At the same time while substrate was being consumed, the rate of change in the microbial population due to death produced new substrate. The rate of change the new substrate was produced ($dC_{S_s} C_{X_{kd}}$, kg_s m^{-3} h^{-1}) was calculated by

$$\begin{aligned} dC_{S_s} C_{X_{kd}} &= dC_{X_{kd\,mb}(k,ip)} + dC_{X_{kd\,ma}(k,ip)} + dC_{X_{kd\,mf}(k,ip)} \cdots \\ &\quad + dC_{X_{kd\,tb}(k,ip)} + dC_{X_{kd\,ta}(k,ip)} + dC_{X_{kd\,tf}(k,ip)} \end{aligned} \tag{6.182}$$

The concentration of the substrate remaining was computed. The new substrate generated as the result of microbial death was proportionally divided: 95% as soluble and 5% as resistant organic material. Thus, 95% was added to the soluble substrate concentration and 5% was added to the lignin substrate concentration,

$$C_{S_{ss}(k,ip)} = C_{S_{ss}(k-1,ip)} - dC_{S_{ss}(k,ip)} * \Delta t + 0.95 * dC_{S_s} C_{X_{kd}} * \Delta t \quad (6.183)$$

$$C_{S_{sc}(k,ip)} = C_{S_{sc}(k-1,ip)} - dC_{S_{sc}(k,ip)} * \Delta t \quad (6.184)$$

$$C_{S_{sl}(k,ip)} = C_{S_{sl}(k-1,ip)} - dC_{S_{sl}(k,ip)} * \Delta t + 0.05 * dC_{S_s} C_{X_{kd}} * \Delta t \quad (6.185)$$

The inert material had no utilization, thus the concentration remained the same as in the previous step,

$$C_{S_{si}(k,ip)} = C_{S_{si}(k-1,ip)} \quad (6.186)$$

Oxygen Consumption and Carbon Dioxide Production

Oxygen concentration changed due to two actions: the amount of oxygen consumed due to microbial activities (, $dC_{O_2 consumed}$ kg_{O2} m^{-3} h^{-1}) and the amount of oxygen added due to mass air flow ($dC_{O_2 aeration}$, kg_{O2} m^{-3} h^{-1}) through the reactor vessel. The change in oxygen due to microbial activities was computed by

$$dC_{O_2 comsumed} = Y_{O_2/S_{ss}} * dC_{S_{ss}(k,ip)} + Y_{O_2/S_{sc}} * dC_{S_{sc}(k,ip)} + Y_{O_2/S_{sl}} * dC_{S_{sl}(k,ip)} \quad (6.187)$$

The change in oxygen concentration due to aeration was computed by

$$dC_{O_2 aeration(k,ip)} = \frac{V_{air(k,ip)}}{Vol_{cl}} * \left(C_{O_2(k-1,ip-1)} - C_{O_2\ (k-1,ip)} \right) \quad (6.188)$$

In the model, the above two equation were multiplied by Δt during this step rather than later (Eq. 6.190). This prevented the computed values from exceeding the oxygen concentration available for that particular time step, which in return resulted in an oxygen concentration of 0.0 kg_{O2} m^{-3}. If Eq. 6.187 and Eq. 6.188 were not multiplied by Δt, the following step would compute no microbial activity because the previous step indicated no oxygen available, thus no substrate would be consumed resulting in no oxygen being consumed and the air flow would replenish the oxygen concentration back up to the maximum limit of 0.2992 kg_{O2} m^{-3}. The model would continue computing these extreme swings until substrate consumption was reduced to a point where the oxygen consumption was within the range of oxygen availability.

The rate of change in the oxygen concentration was calculated by

$$dC_{O_2(k,ip)} = dC_{O_2 aeration(k-1,ip)} - dC_{O_2 consumed(k,ip)} \quad (6.189)$$

The new oxygen concentration was calculated by

$$C_{O_2(k,ip)} = C_{O_2(k-1,ip)} - dC_{O_2(k,ip)} * \Delta t \quad (6.190)$$

As before, due to the mathematics, the calculation could indicate a negative oxygen concentration. An adjustment would be required since this was not possible. If the resulting concentration was less than zero, the concentration was corrected to equal zero,

$$\text{If } C_{O_2(k,ip)} < 0.00 \quad (6.191)$$

$$\text{then } C_{O_2(k,ip)} = 0.00$$

$$\text{otherwise } C_{O_2(k,ip)} = C_{O_2(k,ip)}$$

The rate of carbon dioxide production ($C_{CO_2(k,ip)}$, kg_{CO2} m^{-3} h^{-1}) was calculated by

$$dC_{CO_2(k,ip)} = Y_{CO_2/S_{ss}} * dC_{S_{ss}(k,ip)} + Y_{CO_2/S_{sc}} * dC_{S_{sc}(k,ip)} + Y_{CO_2/S_{sl}} * dC_{S_{sl}(k,ip)} \quad (6.192)$$

The total concentration of carbon dioxide produced (C_{CO_2}, kg_{CO2} m^{-3}) was determined by

$$C_{CO_2(k,ip)} = C_{CO_2(k-1,ip)} - dC_{CO_2(k,ip)} * \Delta t \quad (6.193)$$

Water Content

Next the change in water concentration was calculated. Similar to oxygen, water concentration changed due to two actions: the amount of water produced due to microbial activities ($dC_{W\ produced}$, kg_{H2O} m^{-3} h^{-1}) and the amount of water change due to mass air flow ($dC_{W\ aeration}$, kg_{H2O} m^{-3} h^{-1}) through the reactor vessel. The rate of change in water produced due to microbial activities was computed by

$$dC_{W\ produced(k,ip)} = Y_{W/S_{ss}} * dC_{S_{ss}(k,ip)} + Y_{W/S_{sc}} * dC_{S_{sc}(k,ip)} + Y_{W/S_{sl}} * dC_{S_{sl}(k,ip)} \quad (6.194)$$

The rate of change in water lost due to aeration was computed by

$$dC_{W\ aeration(k,ip)} = \frac{F_{air\ (k,ip)}}{Vol_{cb}} * \left(H_{(k,ip-1)} - H_{(k,ip)} \right) \quad (6.195)$$

As was done with the change of oxygen, the above two change of water equations were multiplied by Δt during this step rather than later (Eq. 6.197). This prevented the computed values from negatively affecting the weighted moisture coefficient (k_{H_2O}). If Eq. 6.194 and Eq. 6.195 were not multiplied by Δt, the moisture content could increase

to a point where k_{H_2O} would reduce microbial activity, thus substrate consumption would be reduced and eventually reducing the water production. After k_{H_2O} corrected itself, microbial activity would return. The model would continue computing these extreme swings until substrate consumption was reduced to a point where k_{H_2O} was within the range of substrate availability that did not negatively affect the overall process.

The rate of change in the water concentration was calculated by

$$dC_{W(k,ip)} = dC_{W\,produced(k,ip)} + dC_{W\,aeration(k,ip)} \tag{6.196}$$

The new water concentration was calculated by

$$C_{W(k,ip)} = C_{W(k-1,ip)} - dC_{W(k,ip)} * \Delta t \tag{6.197}$$

A new weighted moisture coefficient was required for the next time step. This was accomplished by converting the water and substrate concentrations back into the mass now present. Mathematically, it was possible to generate negative water and substrate concentrations. To prevent this from occurring the following equations were added to bring to mass to zero if a negative number was generated:

$$W_{st(k,ip)} = C_{w(k,ip)} * Vol_{cl} \tag{6.198}$$

if $W_{st(k,ip)} < 0.00$

then $W_{st(k,ip)} = 0.00$

$$S_{ss(k,ip)} = C_{S_{ss}(k,ip)} * Vol_{cl} \tag{6.199}$$

if $S_{ss(k,ip)} < 0.00$

then $S_{ss(k,ip)} = 0.00$

$$S_{sc(k,ip)} = C_{S_{sc}(k,ip)} * Vol_{cl} \tag{6.200}$$

if $S_{sc(k,ip)} < 0.00$

then $S_{sc(k,ip)} = 0.00$

$$S_{sl(k,ip)} = C_{S_{sl}(k,ip)} * Vol_{cl} \tag{6.201}$$

if $S_{sl(k,ip)} < 0.00$

then $S_{sl(k,ip)} = 0.00$

$$S_{si(k,ip)} = C_{S_{si}(k,ip)} * Vol_{cl} \tag{6.202}$$

Next, the total substrate mass ($S_{st(k,ip)}$) (Eq. 6.81), the moisture content ($W_{mc(k,ip)}$) (wet basis) (Eq. 6.84), and the weighted moisture coefficient (k_{H_2O}) (Eq. 6.74) were recomputed for the next time step.

Energy balance

The energy balance was computed. First, the sensible heat (q_m , kJ K^{-1} m^{-3}) stored in the composting material was determined by

$$q_{m(k,ip)} = c_W * C_{W(k,ip)} + c_{S_{ss}} * C_{S_{ss}(k,ip)} + c_{S_{ss}} * C_{S_{sc}(k,ip)} \ldots + c_{S_{sl}} * C_{S_{sl}(k,ip)} + c_{S_{si}} * C_{S_{si}(k,ip)} \tag{6.203}$$

Next, the change in temperature that would be caused by the heat produced due to substrate consumption (dT_P , kJ K^{-1} m^{-3}), the heat lost due to aeration (dT_A , kJ K^{-1} m^{-3}), and heat lost through the reactor walls (dT_Q , kJ K^{-1} m^{-3}) were calculated by

$$dT_{produced\,(k,ip)} = \Delta h_{C_{ss}}{}^{T} * dC_{S_{ss}(k,ip)} + \Delta h_{C_{sc}}{}^{T} * dC_{S_{sc}(k,ip)} + \Delta h_{C_{sl}}{}^{T} * dC_{S_{sl}(k,ip)} \tag{6.204}$$

$$dT_{aeration(k,ip)} = \frac{m_{fda(k,ip)}}{Vol_{cl}} * \left(h_{(k,ip)} - h_{(k-1,ip-1)} \right) \tag{6.205}$$

$$dT_{loss(k,ip)} = \frac{\dfrac{A_{wall} * \left(T_{(k-1,ip)} - T_{(1,1)} \right)}{R_T}}{Vol_{cl}} \tag{6.206}$$

Finally, the weighted temperature change was determined by

$$dT_{(k,ip)} = \frac{\left(dT_{produced\,(k,ip)} - dT_{aeration(k,ip)} - dT_{loss(k,ip)} \right)}{q_{m(k,ip)}} \tag{6.207}$$

and the new temperatures per node were computed by

$$T_{(k,ip)} = T_{(k-1,ip)} + dT_{(k,ip)} * \Delta t \tag{6.208`}$$

This time loop was now completed and the execution continued until t_{stop} was reached.

CHAPTER 7 - RESULTS AND DISCUSSION

This chapter is divided into three sections: 1) model results, that is, a) comparison of dividing the basic microbial approach into three parts (bacteria, actimomycetes, and fungi), b) the two temperature ranges, and, c) comparing the modeled results using the different experimental data; 2) comparisons of results, that is, evaluating the model and experimental results using the residual differences between the model curve and the actual data; and, 3) model sensitivity, that is, how the model results were effected by adjusting selected parameter values. For the model results, the actual mixture values for substrates and water content, based on analysis, were used in the comparisons.

Model Results

The objective of this research was to present a comprehensive mathematical composting model that predicts outcomes based on the selected parameters. A major feature is that all ingredients can be dissected to four basic composition types: soluble, cellulose/hemicellulose, lignin, and mineral/inorganic. All composting materials are now comparable at the fundamental level. Additionally, the model looks at the three microorganism types (bacteria, actinomycetes, and fungi), and two microbial temperature range types (mesophilic and thermophilic). The model allows repeated runs to be made. Each run can concentrate on a particular issue by varying amounts and types of substrates, moisture, aeration rate, and reactor size and its heat loss to predict the decomposition of the waste(s) before any pilot work is initiated.

The experimental work had three target mixtures based on percentage of each substrate. The three target mixtures are readily-biodegradable (predominately soluble substrate), slower-to-biodegrade (predominately cellulose/hemicellulose), and resistant-to-biodegradation (predominately cellulose/hemicellulose and lignin). The inert is considered because it part of the overall total substrate which in turn effects moisture content.

Temperature

Three scenarios were run: readily-biodegradable, slower-to-biodegrade, and resistant-to-biodegradation. The first scenario was the readily-biodegradable mixture. Three runs were made. The first run [Figure 7.1(a)] did not differentiate between the microorganism types (bacteria, actinomycetes, and fungi), nor between the mesophilic and thermophilic microorganisms. This run mirrors current models, which use use only one general microorganism type that extends over the entire composting temperature range. The second run [Figure 7.1(b)] differentiated between the microorganism types, but did not differentiate between the mesophilic and thermophilic microorganisms. The third run had two parts. The first run [Figure 7.1(c)] differentiated between the three microorganism types, and between the mesophilic and thermophilic microorganisms. The second run, reflected in Figure 7.1(d), shows the differentiation between the three microorganism types, and between the mesophilic and thermophilic microorganisms, as well as the simulated result of a 26-hour loss of aeration.

There was no difference between the first run [Figure 7.1(a)] and the second run [Figure 7.1(b)]. This is because of the maximum-growth rate used for the general microorganism was equal to the bacteria's maximum-growth rate, which was set at 0.22 h^{-1}. This maximum-growth rate is the dominate contributor. The actinomycters maximum-growth rate was set at 0.06 h^{-1}, which is 3.7 times slower than the bacteria's maximum-growth rate. The fungi maximum-growth rate was set at 0.02 h^{-1}, which is 11 times slower than the bacteria's maximum-growth rate. Thus, the similarity of the two curves.

The third run [Figure 7.1(c)] clearly indicated the transition between the mesophilic and thermophilic microorganisms. Figure 7.1(c) also shows the difference in the temperature between the layers. These changes can be explained by the difference in the oxygen concentration between the layers. Since there is a qualitative relationship between the microbial and the oxygen concentration, as the oxygen concentration decreases, the microbial growth rate decreases. This relationship reduces the amount of substrate consumed, reducing the heat output, thus reducing the temperature. This is similar to what the experimental data graphs for the readily-biodegradable mixture show.

Figure 7.1(c) indicates an apparent problem with the model exhibited in the steepness of the initial increase in temperature and the flatness of the transition. These features are due to the maximum-growth rate. The model relies on a linear, maximum-growth rate. Figure 3.2 and Figure 3.4 indicates the characteristics of a growth curve: the maximum growth rate has an initial lag phase and a decline phase, in which there is a reduction in the growth rate as the microorganisms experience a reduction in food availability. Such a rate would allow the model to simulate an actual temperature curve.

Figure 7.1(d) mirrors the experimental data for Reactor C2, in which the air hose was disconnected for 26 hours.

All figures display an informational code for tracking purposes. The code lists the type of mixture. The number in the first position and the letter in the second position refer to the number of organism types in the mesophilic range. The second set of number and letter refer to the number of microorganisms in the thermophilic range. If the code reads '1m0t', it represents one general microorganism in the mesophilic range that covers the entire temperature range since there are no thermophilic microorganisms. The code '3m0t' represents all three microorganisms but only one temperature range. The code '3m3t' represents all three microorganisms for both mesophilic and thermophilic temperature ranges.

The second scenario was the slower-to-biodegrade mixture. Only the '3m3t' run was made (Figure 7.2). This run differentiated between both the microorganism types, and the mesophilic and thermophilic microorganisms. There was sufficient microbial activity elevate the temperature to 326 °K (53 °C), to the upper limit set for the mesophilic range. This peak occurred at Hour 328. The moisture content for the mixture was low at 45% (wet basis). The initial weighted moisture coefficient (k_{H_2O}, no units) equaled 0.65. During the composting process there was sufficient microbial activity to raise the mixture to a moisture content of 0.59 (wet basis). This increased k_{H_2O} to 0.99. The maximum value for k_{H_2O} is 1.0. This figure does show the difference in temperature layers which is, as above, due to the effect of the oxygen concentration and of the weighted moisture coefficient. The graph does appear to be similar to the experimental data graphs for the slower-to-biodegrade mixture.

a. Figure 7.1

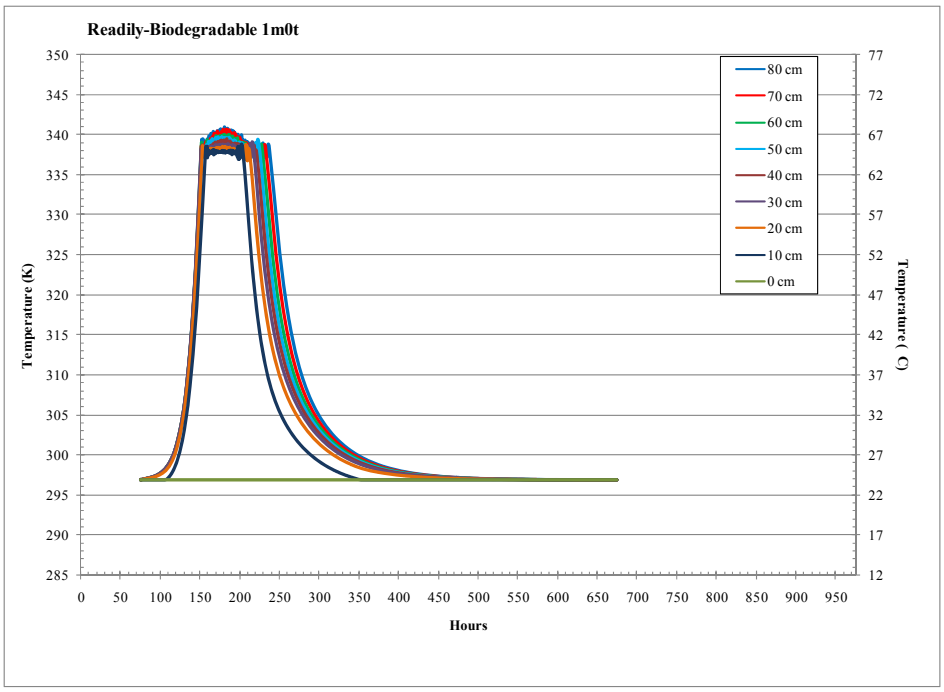

b. Figure 7.1

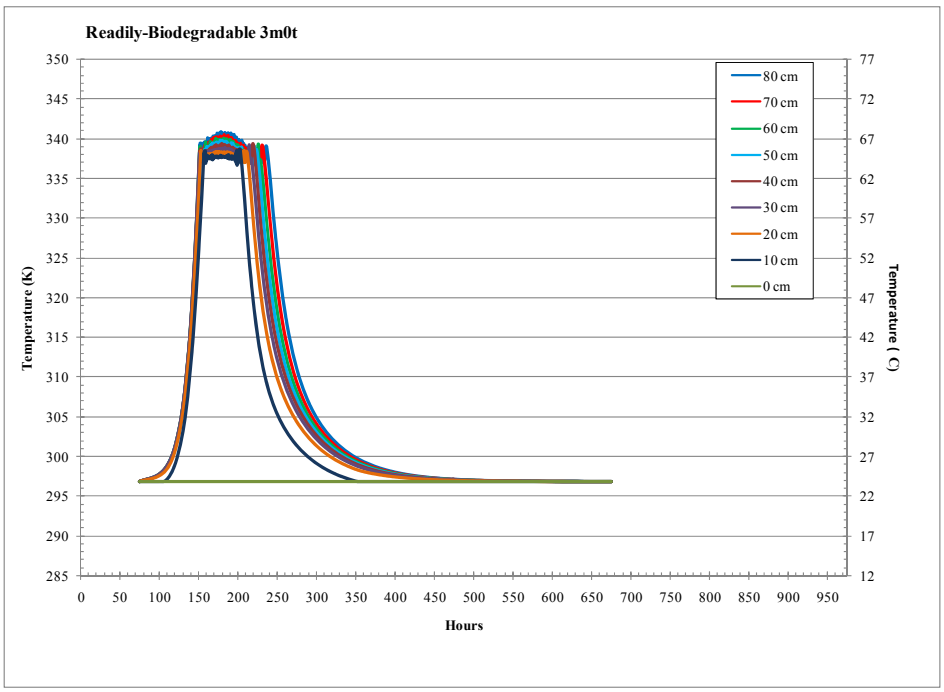

c. Figure 7.1

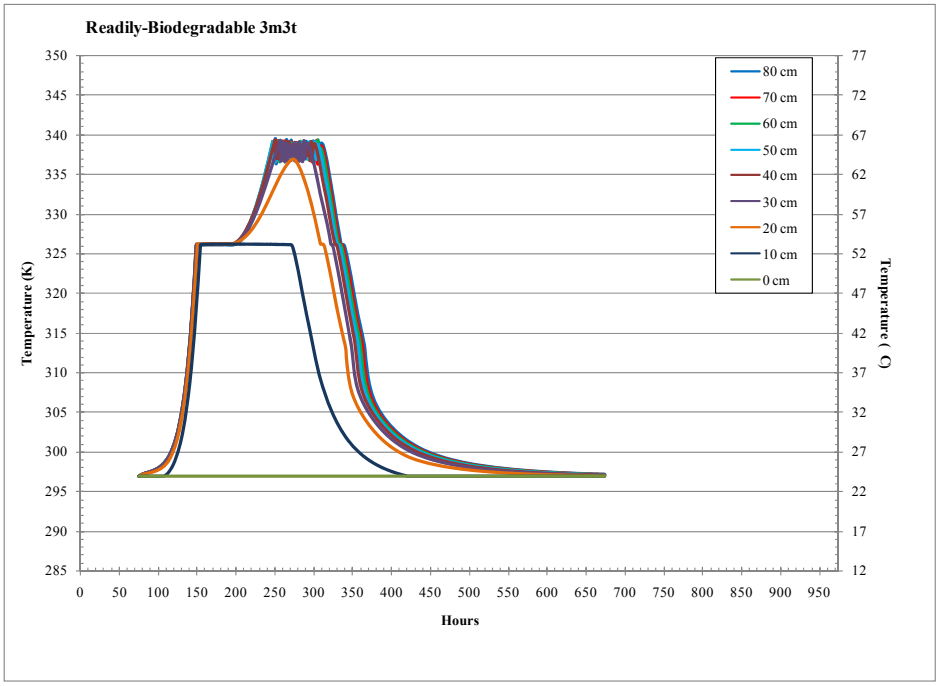

d. Figure 7.1

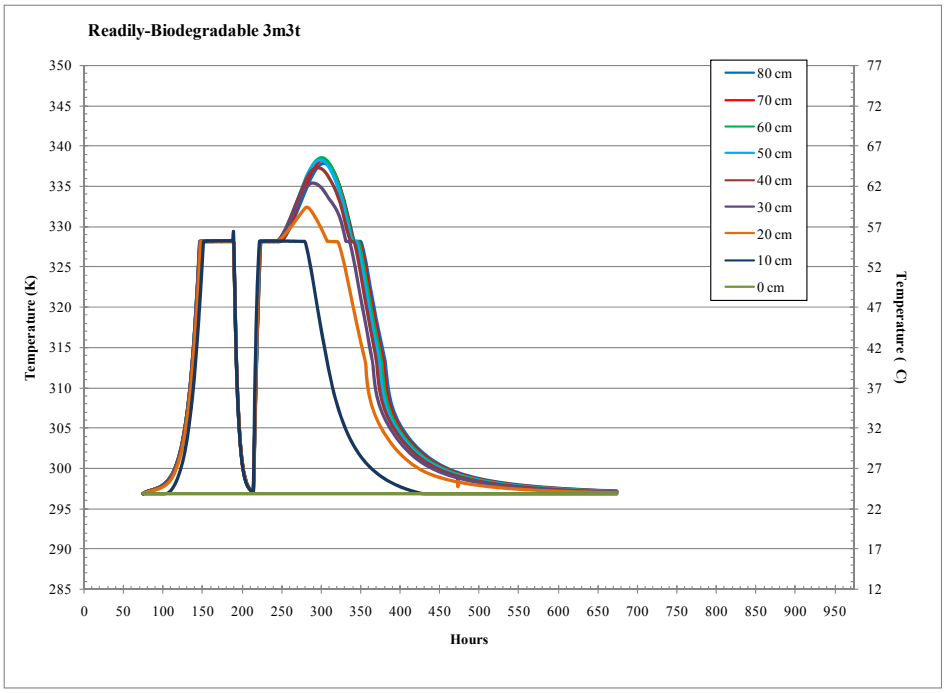

Figure 7.1 Modeled temperature profile for readily-biodegradable mixture for: (a) one microorganism type, one temperature range; (b) three microorganism types, one temperature range; (c) three microorganism types, two temperature ranges; and, (d) same as (c) but with aeration terminated for 26 hours.

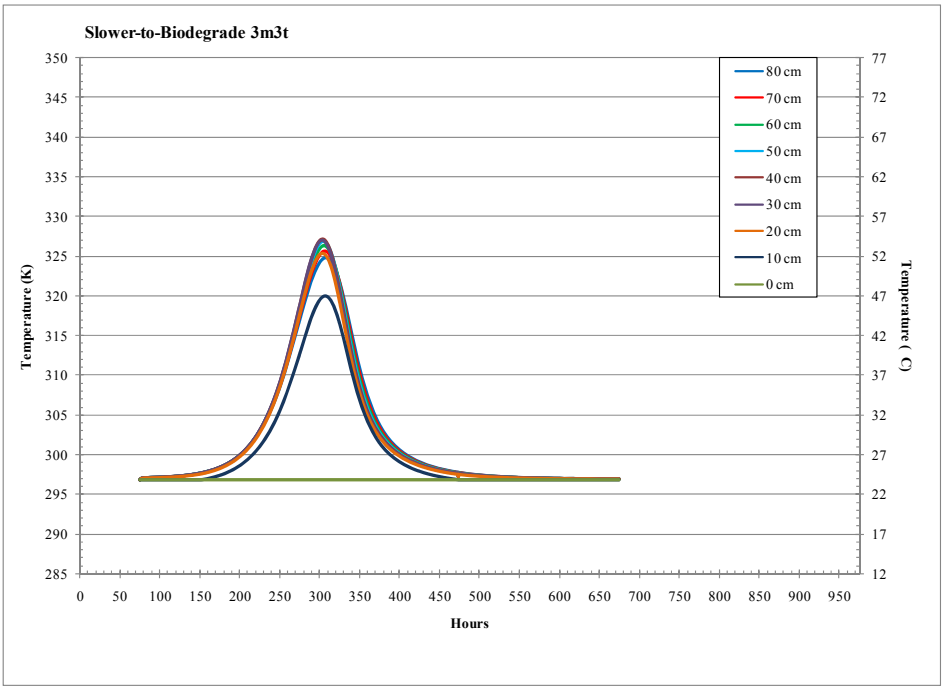

Figure 7.2 Modeled temperature profile for the slower-to-biodegrade mixture for three microorganism types and two temperature ranges.

The third scenario was the resistant-to-biodegradation mixture. Only the '3m3t' run was made (Figure 7.3). This run did differentiate between both the microorganism types, and the mesophilic and thermophilic microorganisms. However the temperature profile indicates that insufficient heat was generated to raise the temperature level. The reason for this is there was an insufficient amount of the readily-biodegradable material for the bacteria to raise the temperature. The actinomycetes, which decomposes the cellulose/hemicellulose and have a smaller maximum-growth rate then the bacteria, were insufficient to provide any substantial heat. Finally, the fungi, which decompose the lignin and have even a smaller maximum-growth rate, were very insufficient to provide any amount of heat. The graph is similar to the experimental data graphs for the resistant-to-biodegradation mixture. The difference is the experimental work reflected the influence in the room temperature variation.

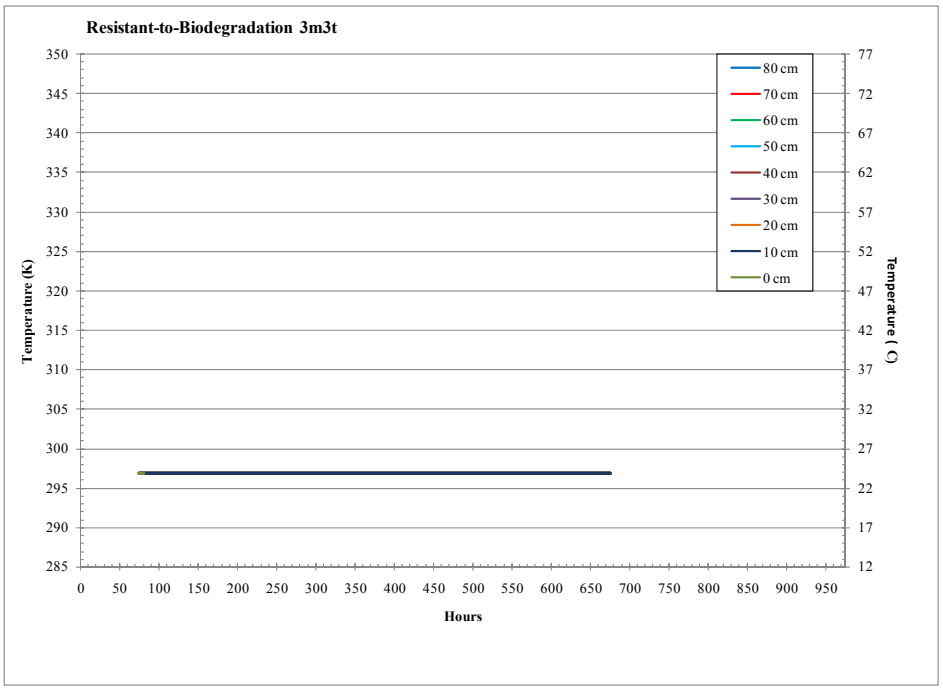

Figure 7.3 Modeled temperature profile for the resistant-to-biodegradation mixture for three microorganism types and two temperature ranges.

Oxygen Concentration

Graphs that depict the changes in the oxygen concentration for the same three scenarios described previously are below. The first scenario is the readily-biodegradable mixture. Three runs were made. The first run [Figure 7.4(a)] did not differentiate between the microorganism types, nor between the mesophilic and thermophilic microorganisms. The second run [Figure 7.4(b)] differentiated between the microorganism types but not between the mesophilic and thermophilic microorganisms. The third run had two parts. First, the run [Figure 7.4(c)] differentiated between both the microorganism types and the mesophilic and thermophilic microorganisms. Second, the run [Figure 7.4(d)] shows the differentiation, as well as the simulated result of a 26-hour loss of aeration.

Three factors influenced oxygen consumption: first, availability of the substrate for microbial consumption; second, the rate of air flow entering the reactor vessel; and third, division of the microbial population between mesophilic and thermophilic. Figures 7.4(a), (b), (c), and (d) are all the readily-biodegradable mixture. They received the

greatest rate of air flow. Figures 7.4(a) and (b) show a rapid decrease in oxygen concentration as the substrate was consumed followed by an increase in oxygen concentration levels as substrate consumption slowed. Figure 7.4(c) shows the influence of the transition zone between the mesophilic and thermophilic microorganisms. Initially, oxygen utilization was rapid. The consumption rate then leveled during the transition period between the mesophilic and thermophilic microorganisms. When the thermophilic microorganisms became dominant, utilization increased until the substrate supply was diminished. Finally, the utilization rate decreased as the system cooled. Figure 7.4(d) shows the drop in oxygen when the air flow was temporarily removed. In nature, there would have been a reduction in available oxygen, but not as abrupt as the model predicted.

Figures 7.5 and 7.6 show the impact of slower-to-biodegrade and resistant-to-biodegrade substrates on decomposition. The slower-to-biodegrade utilizes oxygen, but, because of the slow consumption of oxygen and the aeration effect, a lower reduction of oxygen concentration was exhibited. The resistant-to-biodegradation simulation showed no change in oxygen concentration throughout the run because there was almost no utilization of substrate.

a. Figure 7.4

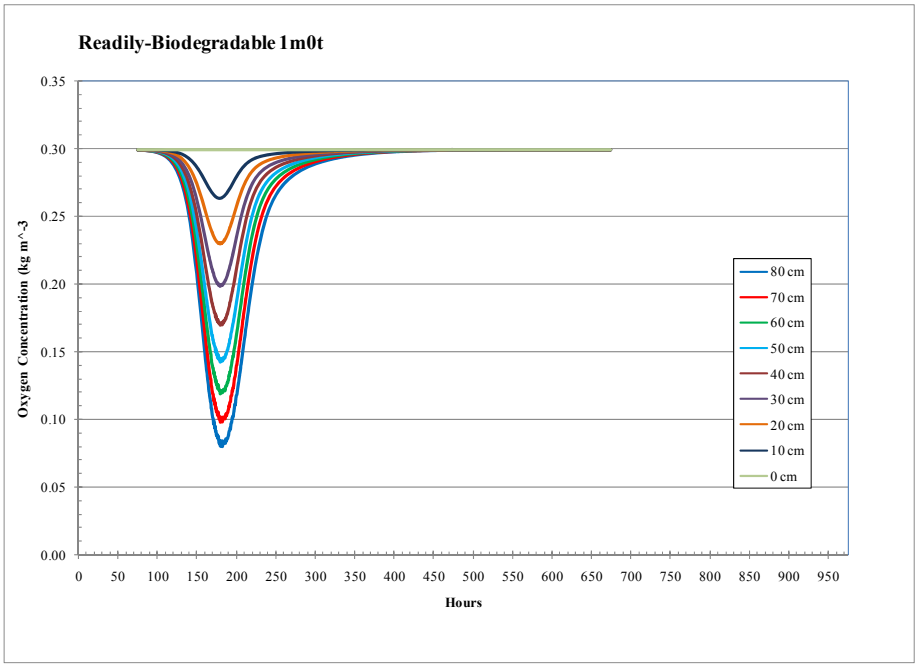

b. Figure 7.4

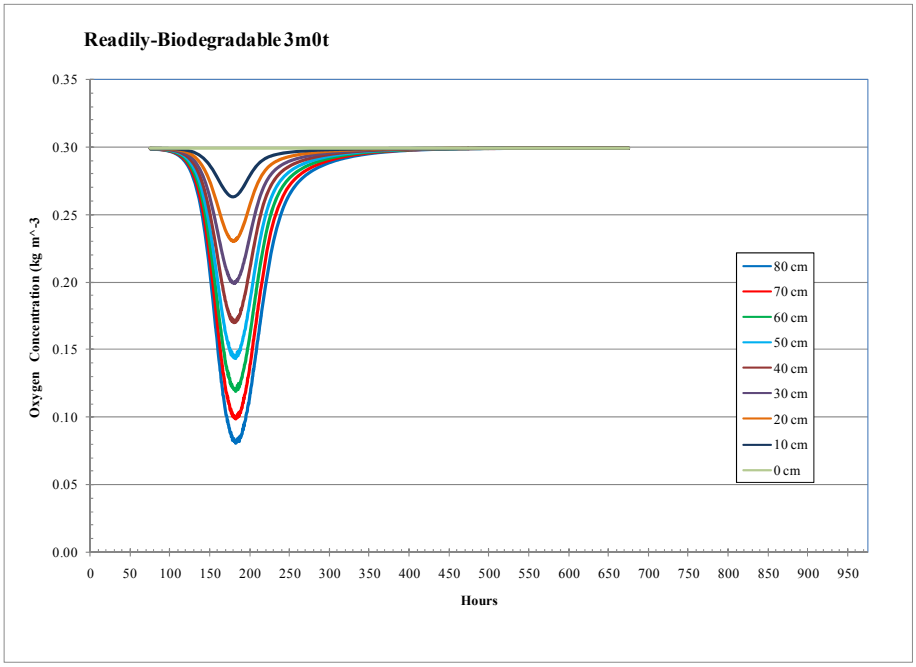

c. Figure 7.4

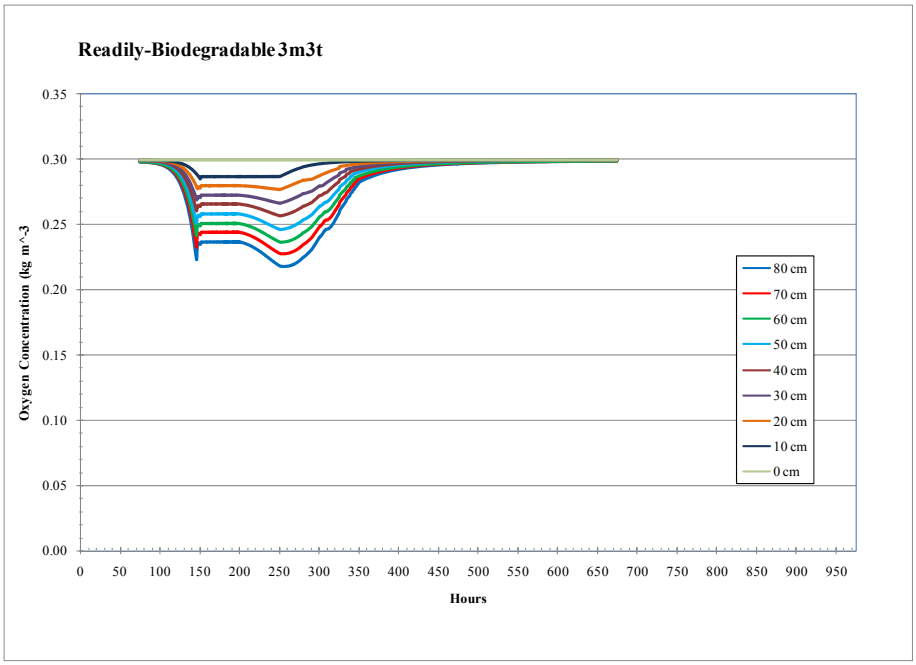

d. Figure 7.4

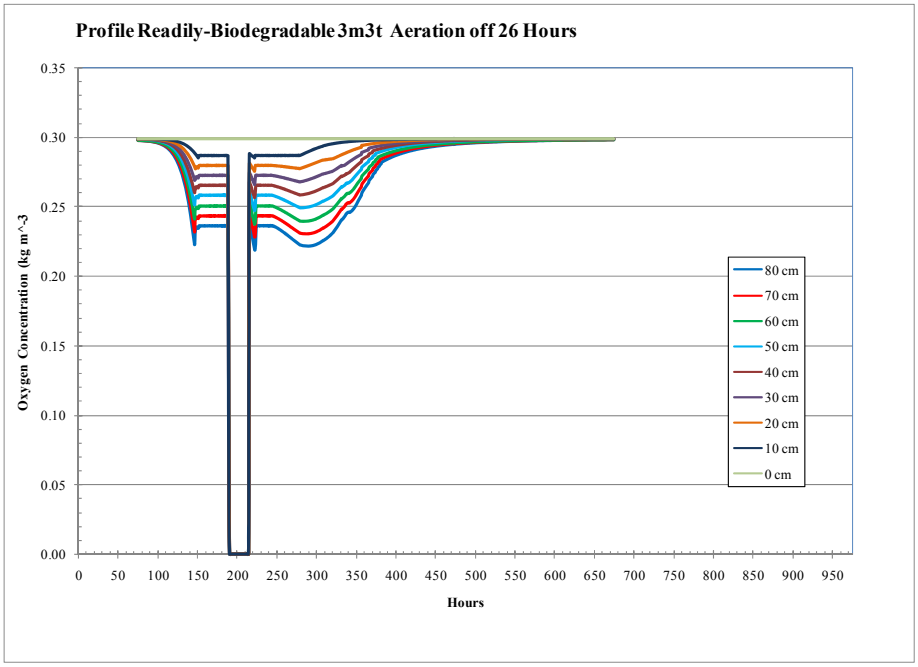

Figure 7.4 Modeled oxygen concentration profile for readily-biodegradable mixture for: (a) one microorganism type, one temperature range; (b) three microorganism types, one temperature range; (c) three microorganism types, two temperature ranges; and, (d) same as (c) but with aeration terminated for 26 hours.

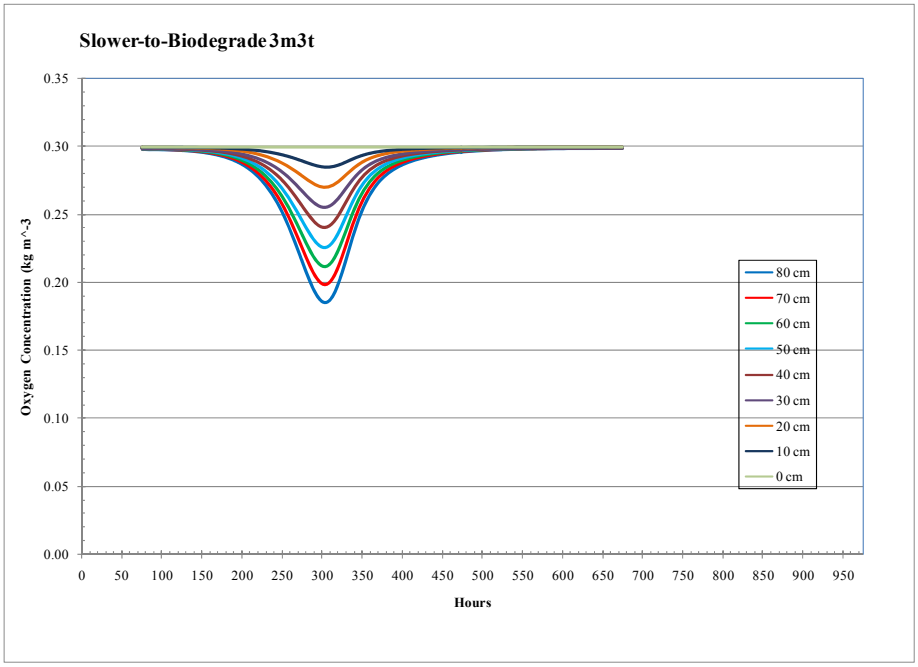

Figure 7.5 Modeled oxygen concentration profile for the slower-to-biodegrade mixture for three microorganism types and two temperature ranges.

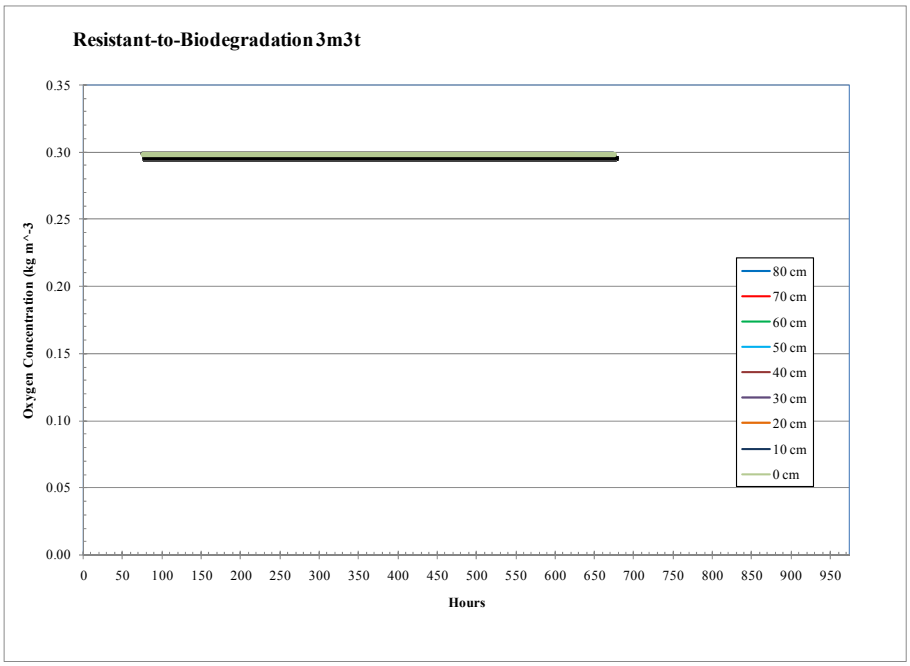

Figure 7.6 Modeled oxygen concentration profile for the resistant-to-biodegradation mixture for three microorganism types and two temperature ranges.

Water Concentration

Graphs depicting the changes in the simulated water concentration for the same three different scenarios that were run as for temperature and oxygen concentration profiles are below. Several factors influenced water concentration: first, the quantity of water present at the start of the decomposition; second, the amount of substrate available for microbial consumption; third, the air flow rate and water content entering the reactor vessel; and, fourth, the temperatures reached and the resultant enthalpy of the air moving through the reactor. Figures 7.7(a), (b), (c), and (d) reflect the readily-biodegradable mixture. The initial water content present was 65.8% (wet basis). Figures 7.7(a) and (b) show identical water concentration through time. Initially, water was produced through the decomposition process in all increments. After a period of time, water was removed from the bottom level of composting matter, causing it to begin to dry. Figure 7.7(c) shows the same, although a greater rate of drying occurred. Figure 7.7(d) appears similar to Figure 7.7(c), except, there was a deflection in which aeration was reduced for a 26-hour period. The slower-to-biodegrade mixture started with a substantially lower concentration of water at 44.8% (wet basis). The profile (Figure 7.8) is similar to Figure

7.4, but not as pronounced. The resistant-to-biodegradation mixture started at a very low water concentration of 33.4 % (wet basis). Its profile (Figure 7.9) shows little change in water content.

a. Figure7.7

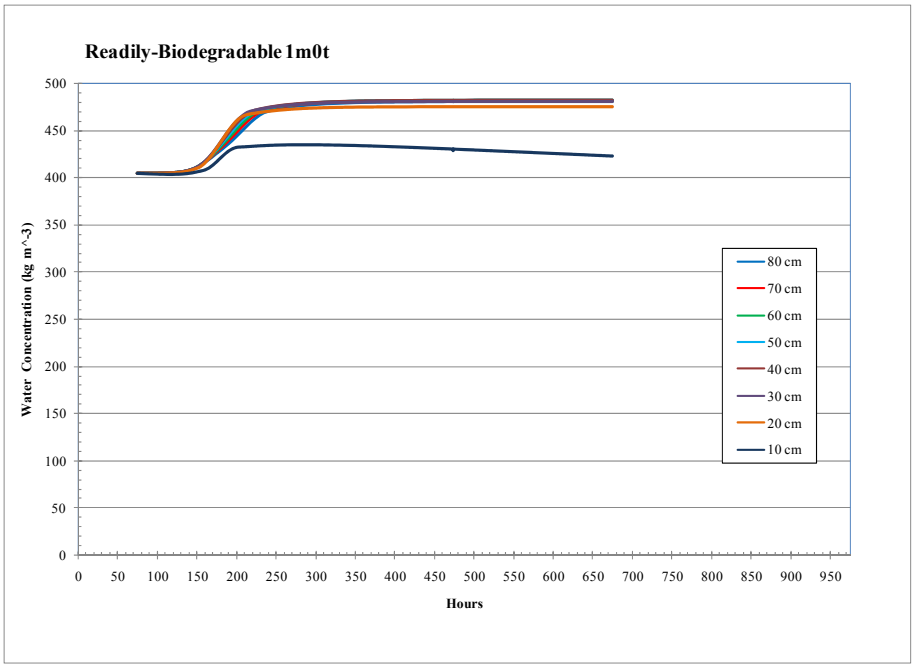

b. Figure 7.7

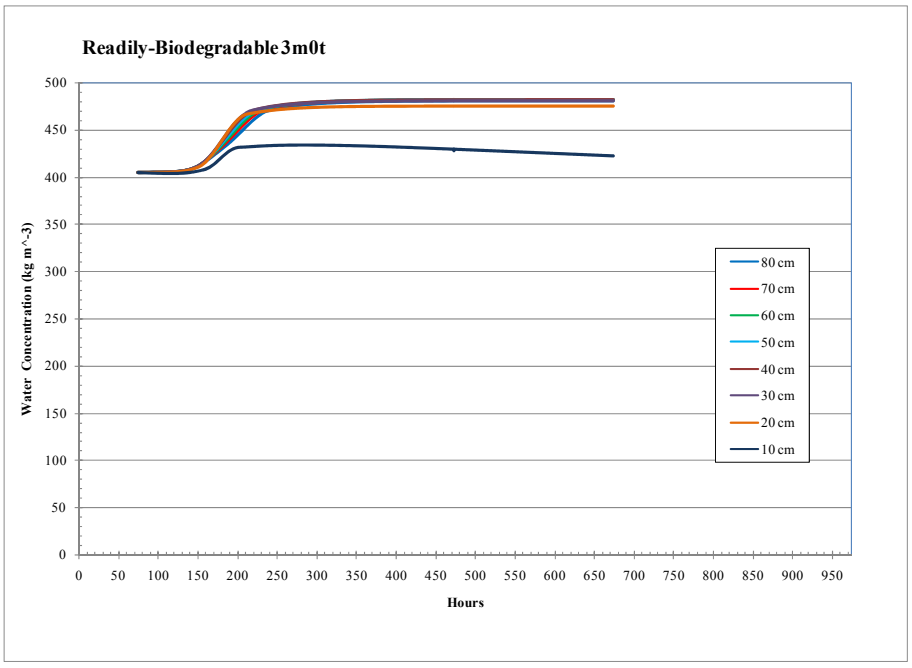

c. Figure 7.7

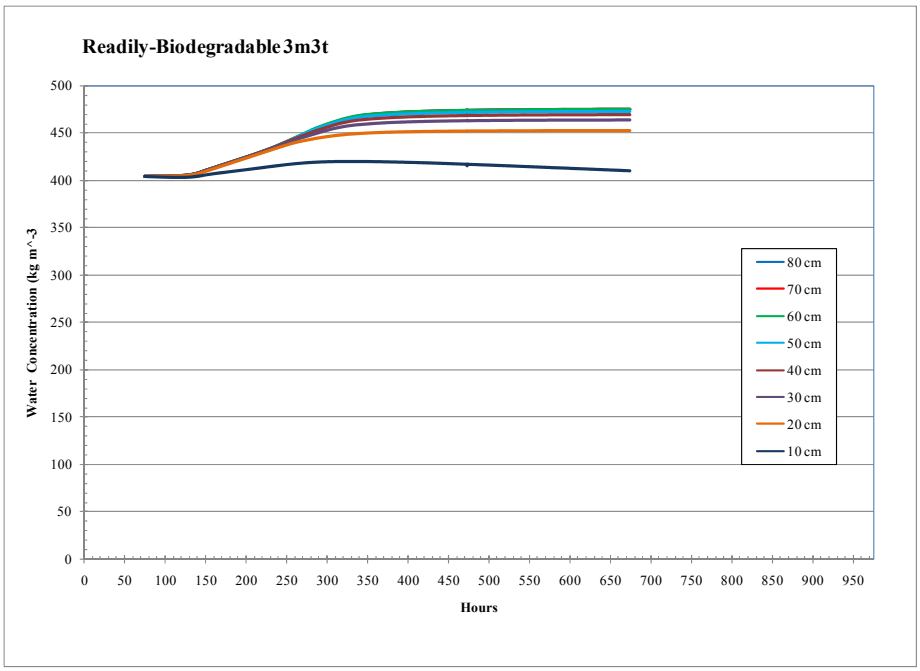

d. Figure 7.7

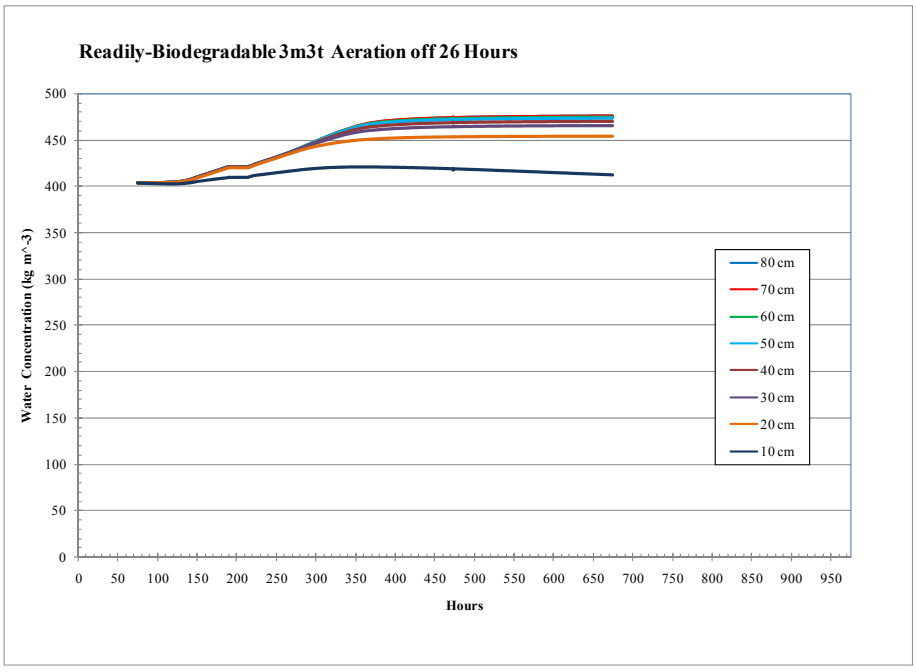

Figure 7.7 Modeled water concentration profile for readily-biodegradable mixture for: (a) one microorganism type, one temperature range; (b) three microorganism types, one temperature range; (c) three microorganism types, two temperature ranges; and, (d) same as (c) but with aeration terminated for 26 hours.

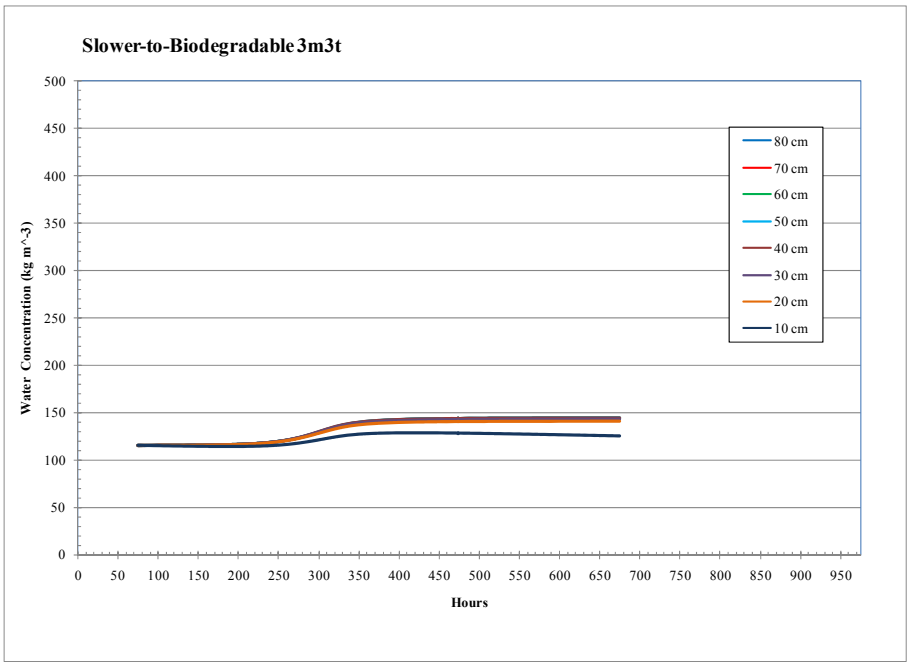

Figure 7.8 Modeled water concentration profile for the slower-to-biodegrade mixture for three microorganism types and two temperature ranges.

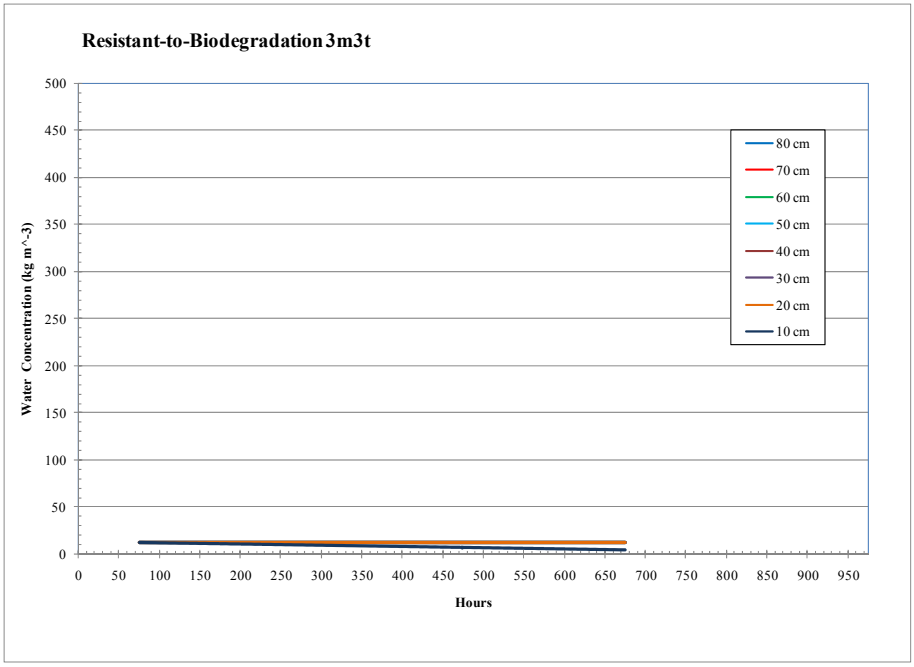

Figure 7.9 Model water concentration profile for the resistant-to-biodegradation mixture for three microorganism types and two temperature ranges.

Substrate

The simulation model results indicate major differences between the three major substrate types: the readily-biodegradable, the slower-to-biodegrade, and resistant-to-biodegradation. Figure 7.10 presents the change in substrate mass (kg $_{\text{dry substrate}}$ kg^{-1} $_{\text{total dry mass}}$) of the four substrate types through time.

The simulated data for the readily-biodegradable [Figure 7.10(a)] compared to the experimental data [Figure 5.2(a), inserted below the figure 7.10(a) for reference] indicates a major difference between the amount of substrate the model predicts to be consumed by Hour 552 (0.69 kg $_{\text{dry substrate}}$ kg^{-1} $_{\text{total dry mass}}$) versus the experimental data (0.40 kg $_{\text{dry substrate}}$ kg^{-1} $_{\text{total dry mass}}$). The maximum-growth rate was decreased to align the two points at Hour 552, but the model generated insufficient heat to move the temperature out of the mesophilic range. The model predicts a smaller decrease to the cellulose/hemicellulose substrate than the experimental data. To align the two points at Hour 552, the maximum-growth rate had to be increased from 0.06 h^{-1} to 0.21h^{-1}. This change made the temperature curve broader. The model predicted a lignin value of - 0.005 kg $_{\text{dry substrate}}$ kg^{-1} $_{\text{total dry mass}}$ at Hour 552 versus to the experimental data's value of -0.02 kg $_{\text{dry substrate}}$ kg^{-1} $_{\text{total dry mass}}$ at Hour 552 The model's lignin value can be increased by increasing the percentage of dead microbial mass that becomes lignin substrate. As for the inert substrate, the model did not utilize or add substrate to this pool, thus there was no change in its mass. The experimental data indicated a change to the inert, but this is believed to be due to the non-homogeneity within the mixture.

The simulated data for the slower-to-biodegrade [Figure 7.10(b)] when compared to the experimental data [Figure 5.2(b), inserted below the figure 7.10(b) for reference], indicated similar results. The soluble again was utilized too quickly over the entire run time of 552 hours, 0.33 kg $_{\text{dry substrate}}$ kg^{-1} $_{\text{total dry mass}}$ for the model versus 0.08 kg $_{\text{dry substrate}}$ kg^{-1} $_{\text{total dry mass}}$ for the experimental data. This explains the height of the temperature curve obtained by the model. The model also predicted insufficient utilization of the cellulose/hemicellulose slower-to-biodegrade mixture (0.006 kg $_{\text{dry substrate}}$ kg^{-1} $_{\text{total dry mass}}$) compared to the experimental data (0.04 kg $_{\text{dry substrate}}$ kg^{-1} $_{\text{total dry mass}}$). Lignin utilization was approximately the same.

For the resistant-to-biodegradation, the simulated model predicted a very slight change [Figure 7.10(c)]. Compared to the experimental data [Figure 5.2(c), inserted below the figure 7.10(c) for reference], the three substrate in the resistant-to-biodegradation mixture remained nearly constant. The data indicated there was a slight increase in soluble substrate after the first seven days, and then there was a slight decrease. The cellulose/hemicellulose showed no change after seven days and then a decrease after 14 days. Lignin showed the opposite; no change after the first seven days and then a slight increase. These differences are within the range of experimental analysis uncertainty.

Summary of Model Simulation

Results demonstrate the model did simulate, as predicted, temperature, oxygen concentration and water concentration. The model has the capability of comparing the response a composting mixture would have to a multitude of different parameters. This model contains 91 arrays. Each array is multi-dimensional and established to facilitate data collection for all variable parameters. The list of variables is presented in the model under the heading "SET ARRAYS."

a. Figure 7.10

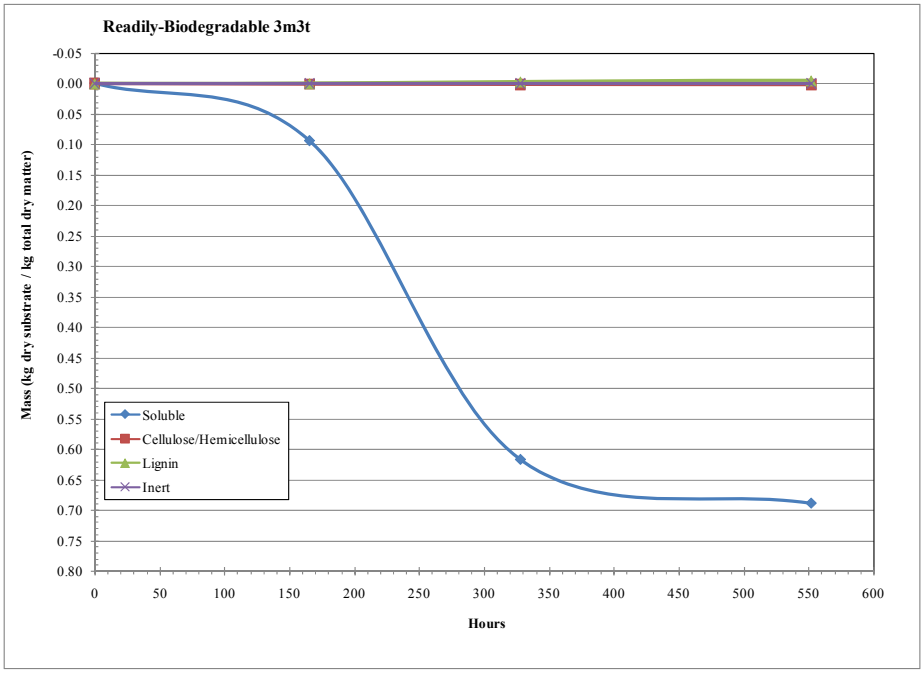

Inserted for reference: Experimental data Figure 5.2(a).

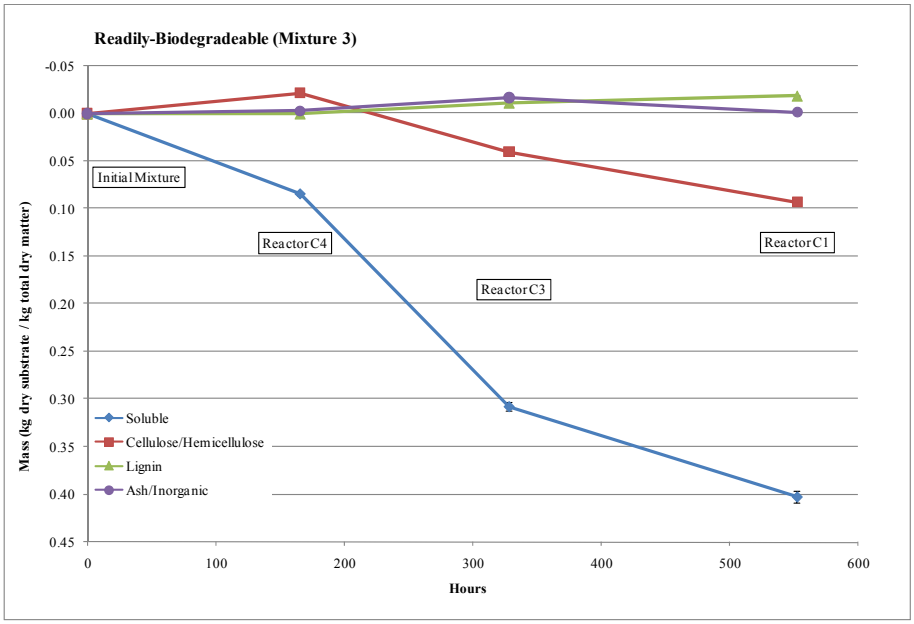

b. Figure 7.10

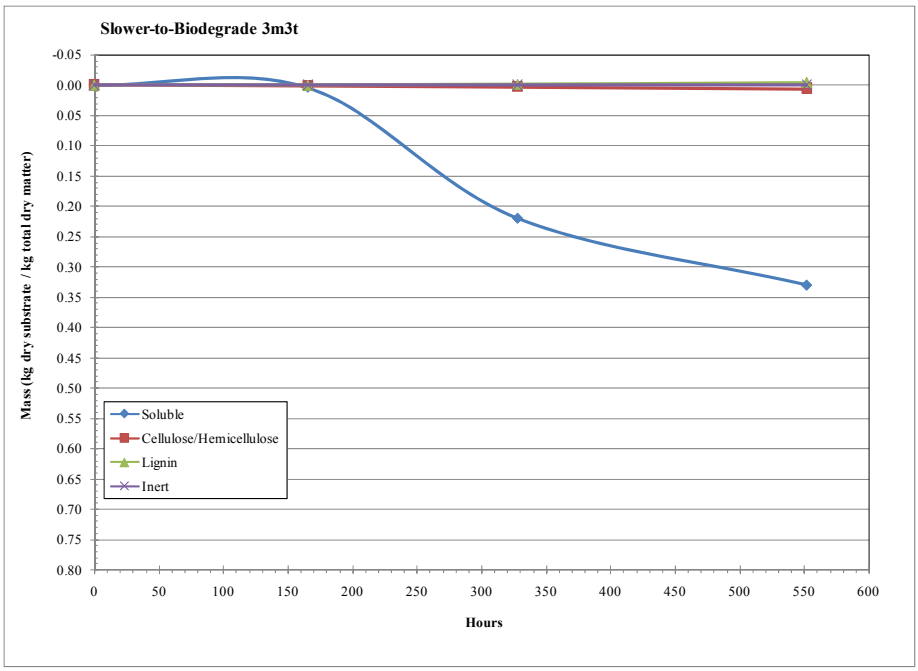

Inserted for reference: Experimental data Figure 5.2(b).

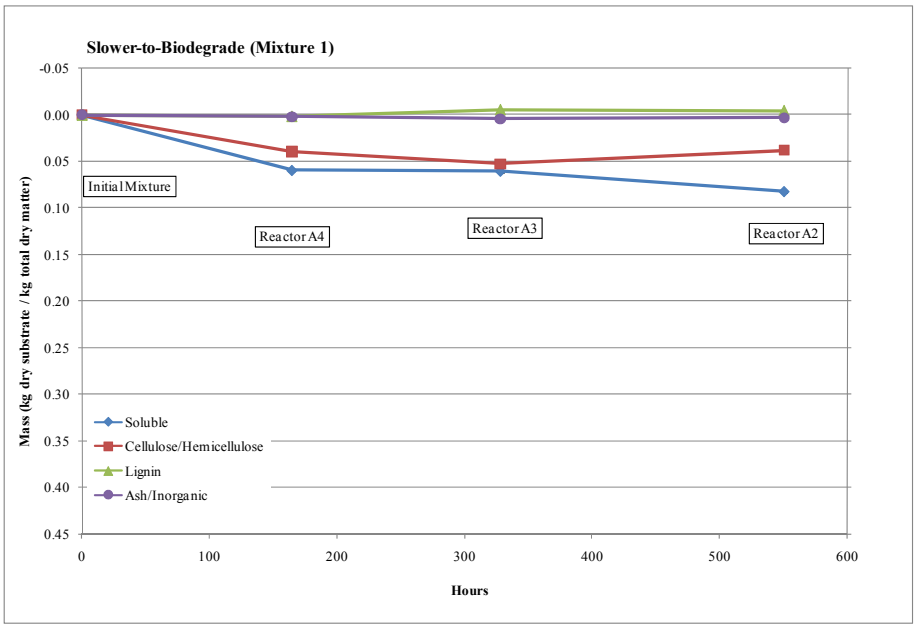

c. Figure 7.10

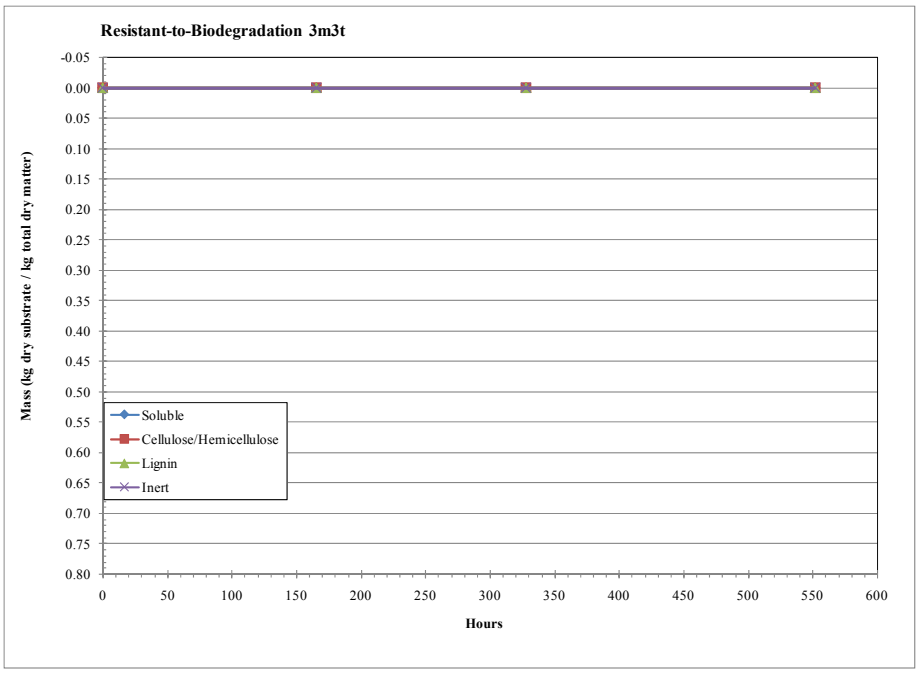

Inserted for reference: Experimental Data Figure 5.2(c).

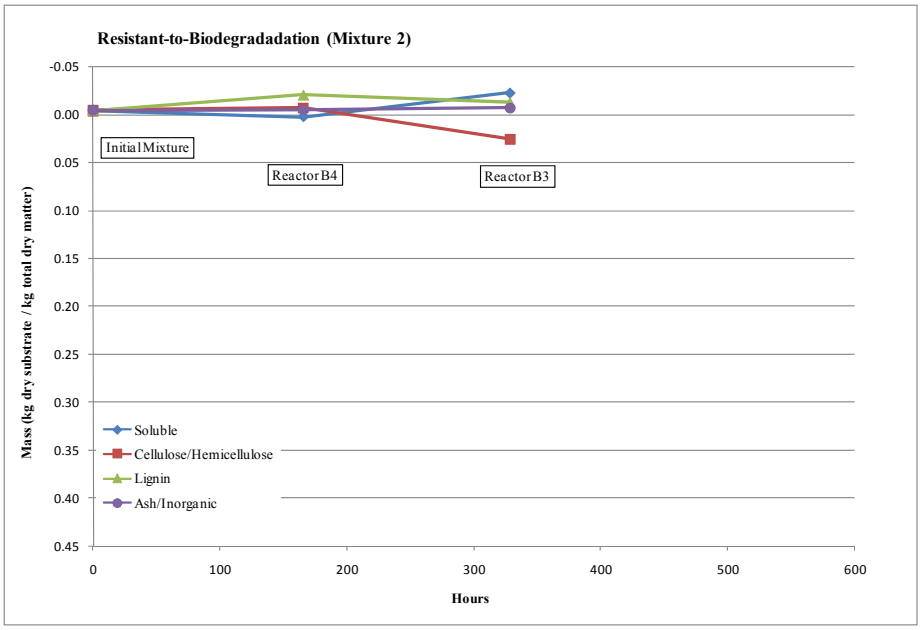

Figure 7.10 Model change in substrate mass through time within a mixture by reactor for: (a) readily-biodegradable; (b) slower-to-biodegrade; and, (c) resistant-to-biodegradation.

Comparison of Results

The experimental laboratory temperature profiles are compared to the results of the mathematical model's simulation temperature profiles to examine the model's ability to predict measured results. Since the model is not capable of accounting for volume reduction as the substrate is utilized during the composting process, the experimental results are adjusted to eliminate those layers that indicated volume reduction occurred to a point that those data were not comparable. Therefore, the '70-cm' and '80-cm' layers were eliminated.

The square error (Kastens, 2008) is the standard deviation of the experimental temperature profile [$Standard\ Deviation\left(observed\right)$] results divided by square root of the averaged square error of the simulated model [$SQRT\left(avg\sum\left(predicted-observed\right)\right)$] results. The square error is calculated for each layer. If the result is a number less than one, the model is judged to reasonably predict the observed result.

Reactor C1's experimental results are used to compare the readily-biodegradable model predictive results because the temperature data indicated the experimental run had good definition and appeared to have completed the active composting phase. The results for Reactors C3 and C4 had similar temperature profiles but shorted run hours by design, thus were not used for comparison., similar to the two partial runsit indicated it. The manure had ice crystals when the mixture was being mixed, and, so, the simulation model was adjusted by 75 hours to account for the lag time the experimental temperatures took to reach room temperature. The results (Table 7.1) indicate the model square errors are slightly greater than 1.00, just exceeding the threshold to predict the observed data. Figure 7.11 shows the visual fit for each layer. The figure reflects that the predicted values lagged the experimental values for part of the time. Neither the lag acceleration nor the decline phases are well defined (Figure 3.2). Monod's equation may be correct, but the maximum growth rate used is linear. The use of a linear maximum-growth rate is not appropriate for the model during the transitions from one phase to the next. An equation reflecting the lag, accerleration and decline phases is appropriate.

Table 7.1 Square error results for the readily-biodegradable

Comparison Tests	Layer					
	10-cm	20-cm	30-cm	40-cm	50-cm	60-cm
Experimental data: $Standard\ Deviation(observed)$	3.06	5.38	6.71	7.03	7.67	9.98
Square root: $SQRT\left(avg\sum(predicted-observed)\right)$	5.23	6.90	7.59	7.86	9.74	8.71
Square error: $\frac{SQRT\left(avg\sum(predicted-observed)\right)}{Standard\ Deviation(observed)}$	1.17	1.10	1.05	1.05	1.12	1.10

a. Figure 7.11

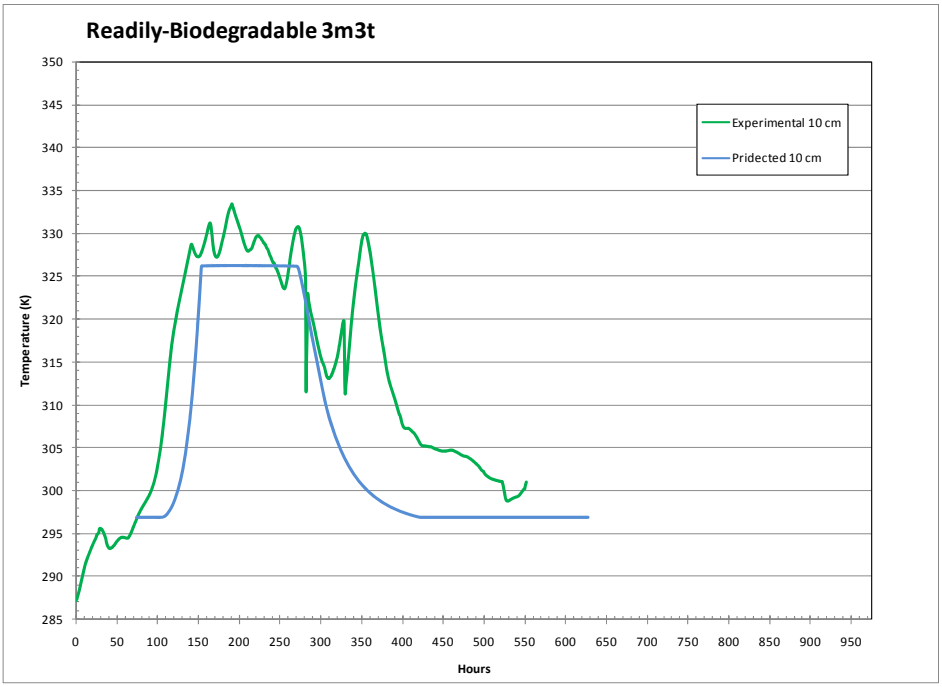

b. Figure 7.11

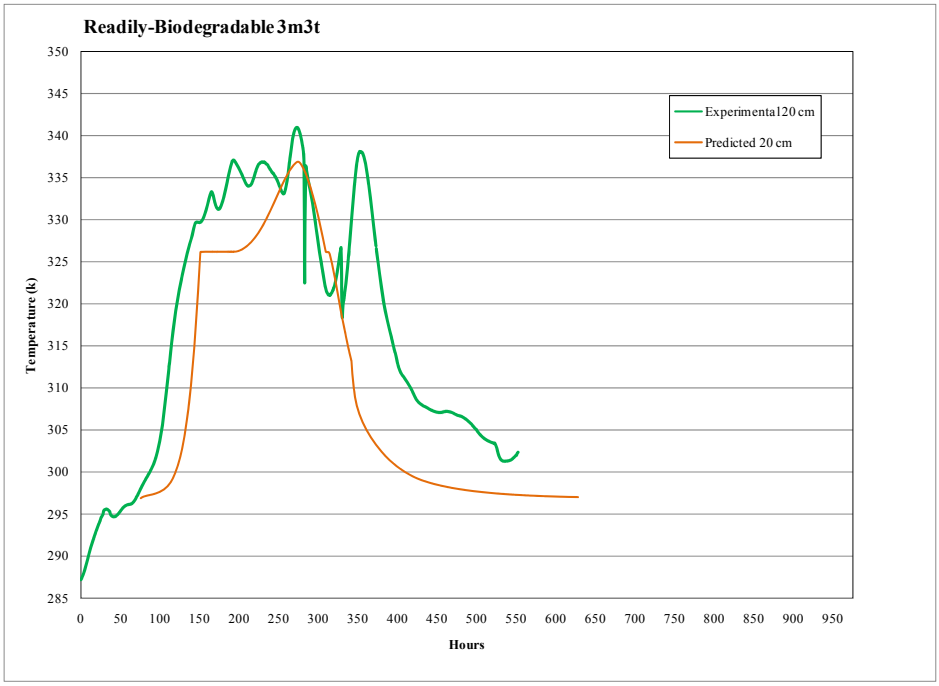

c. Figure 7.11

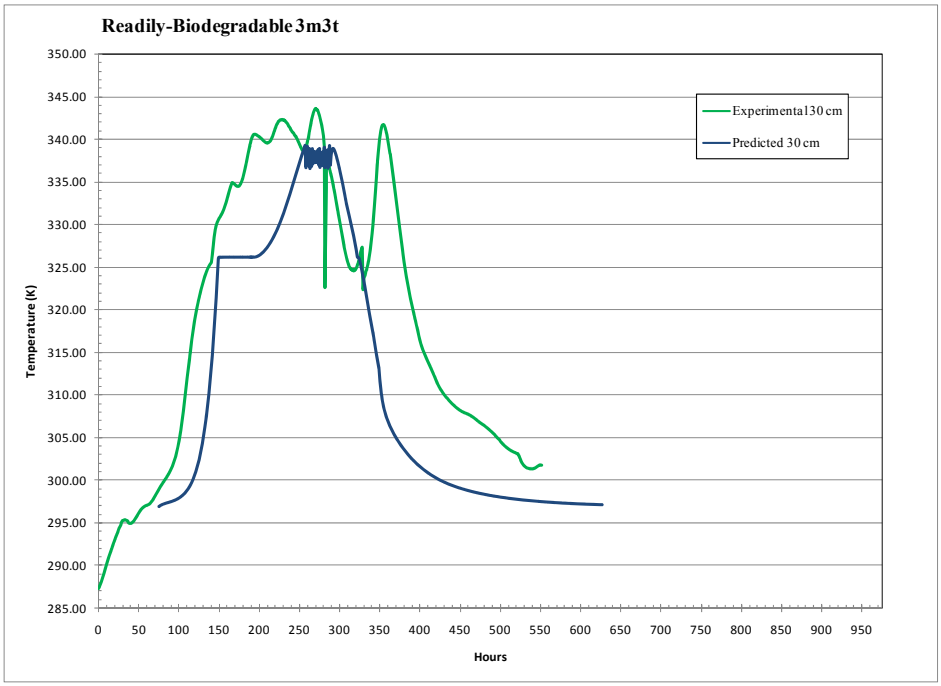

d. Figure 7.11

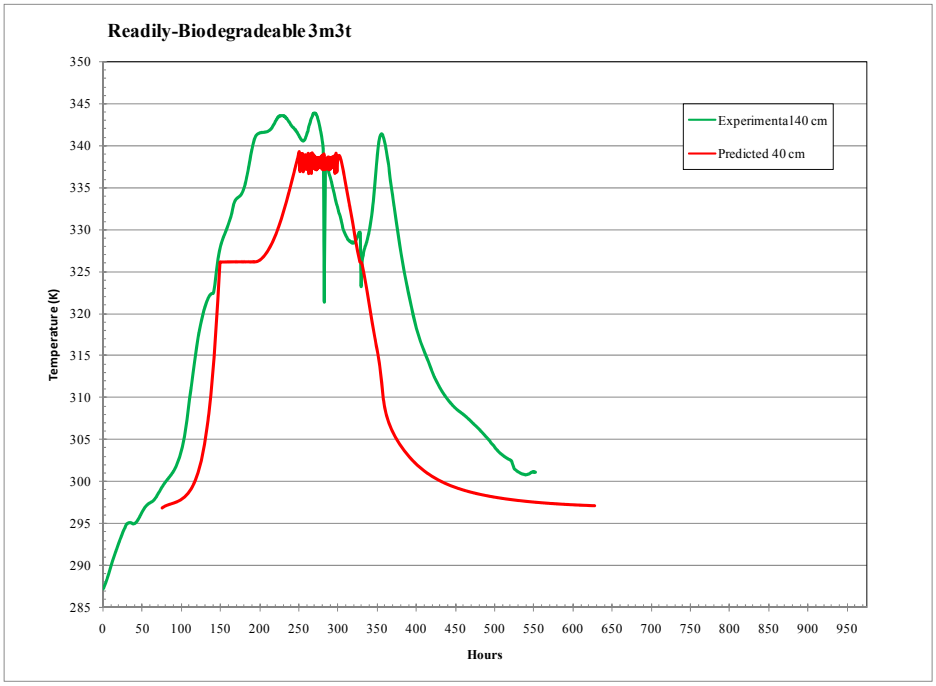

e. Figure 7.11

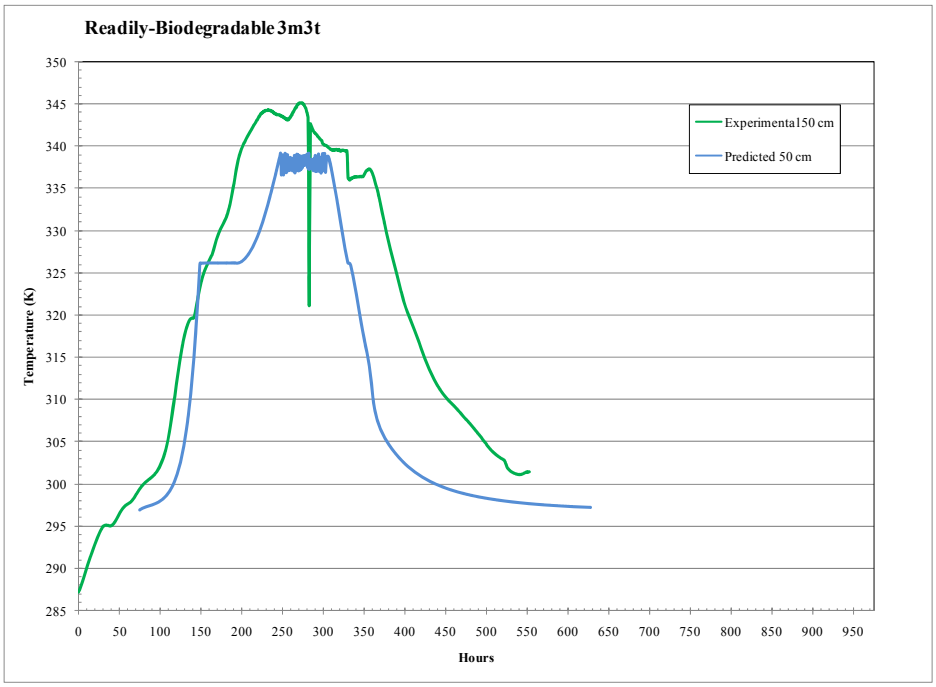

f. Figure 7.11

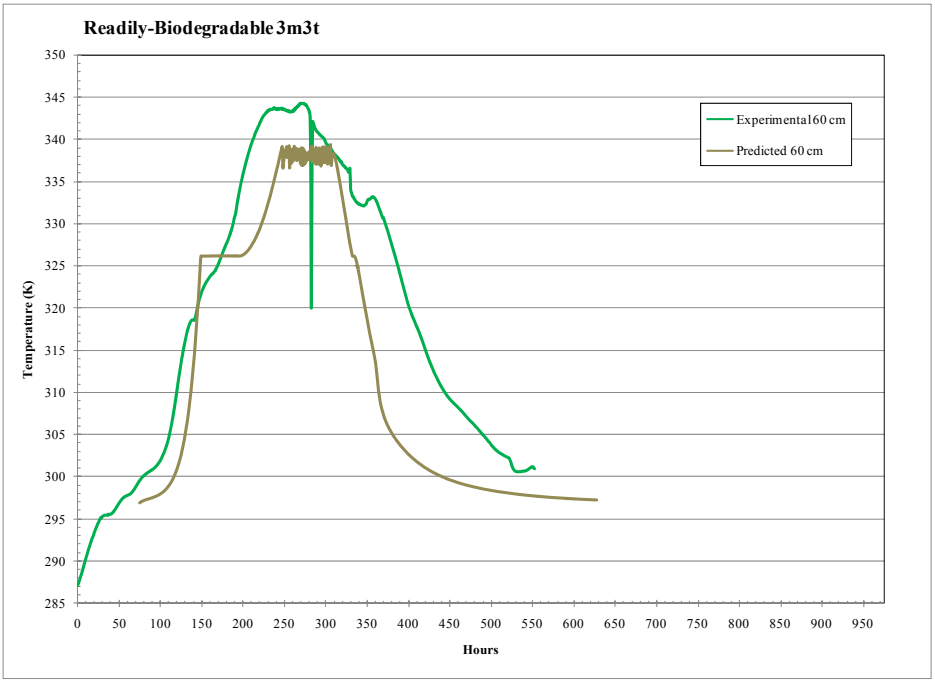

Figure 7.11 Comparison of the readily-biodegradable material experimental temperature profile with the predicted temperature profile layer-by-layer: (a) 10-cm layer; (b) 20-cm layer; (c) 30-cm layer; (d) 40-cm layer; (e) 50-cm layer; and, (f) 60-cm layer.

Reactor A3's experimental results were used to make the same comparisons for the slower-to-biodegrade material. The results (Table 7.2) indicate the model does not do a reasonable job of predicting the experimental results, even after adjusting the time profile to align the curves for a better fit. The experimental data at the 20-cm layer was deleted because large data gaps occurred when the data was cleaned. Again, the general temperature profile pattern of the experimental data was present. Figure 7.12 shows the visual fit for each layer of the slower-to-biodegrade material.

Table 7.2 Square error results for the slower-to-biodegrade

Comparison Tests	Layer					
	10-cm	20-cm	30-cm	40-cm	50-cm	60-cm
Experimental data: $Standard\ Deviation(observed)$	2.79	No value	4.67	5.44	5.45	5.43
Square root: $SQRT\left(avg\sum(predicted-observed)\right)$	9.51	No value	10.19	10.43	10.98	11.45
Square error: $\frac{SQRT\left(ave\sum(predicted-observed)\right)}{Standard\ Deviation(observed)}$	3.41	No value	2.18	1.92	2.01	2.11

a. Figure 7.12

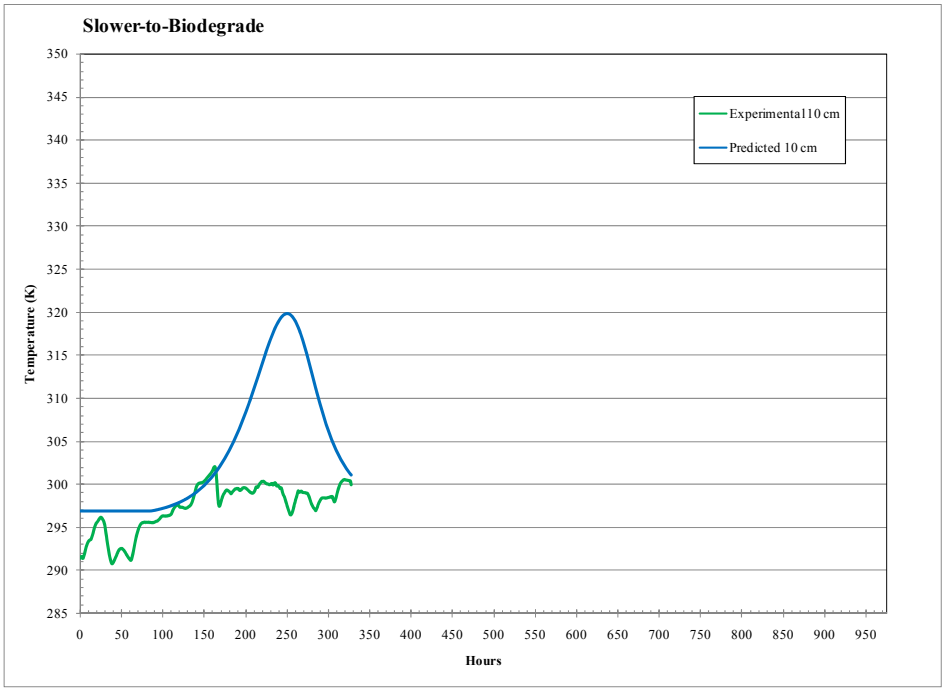

b. Figure 7.12

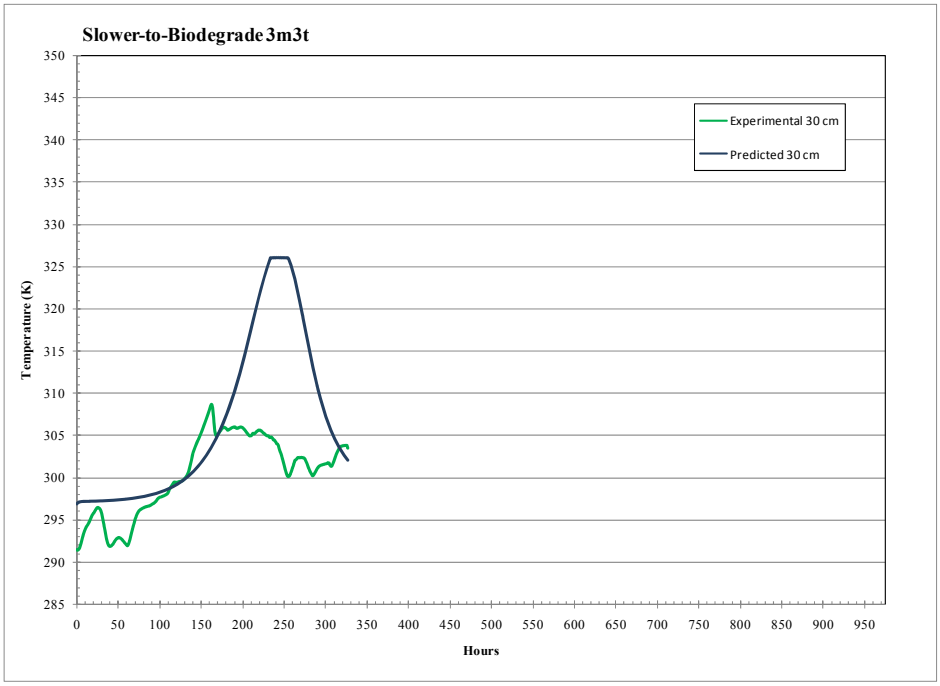

c. Figure 7.12

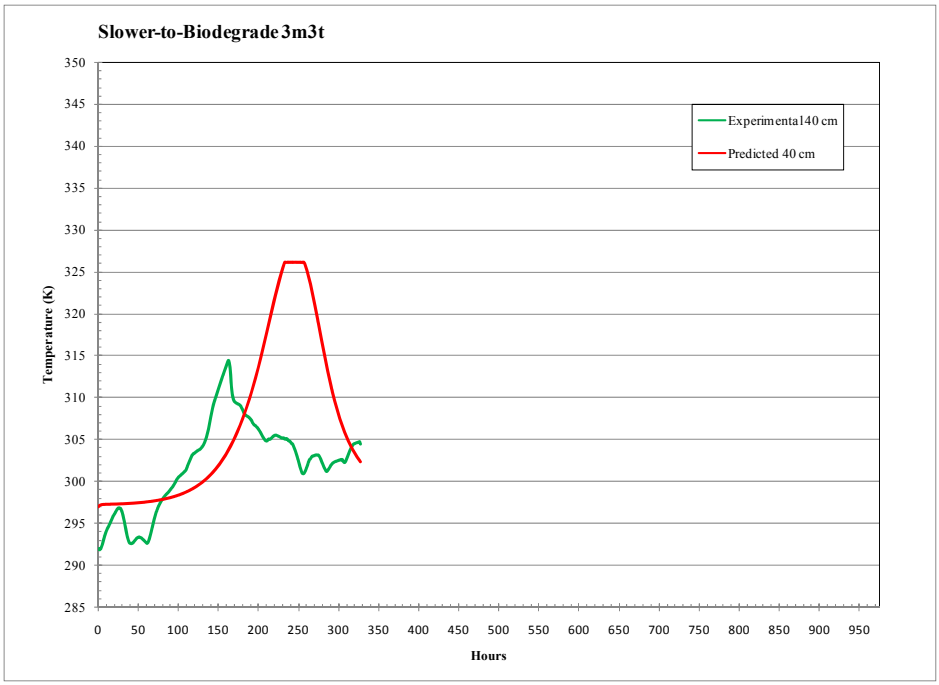

d. Figure 7.12

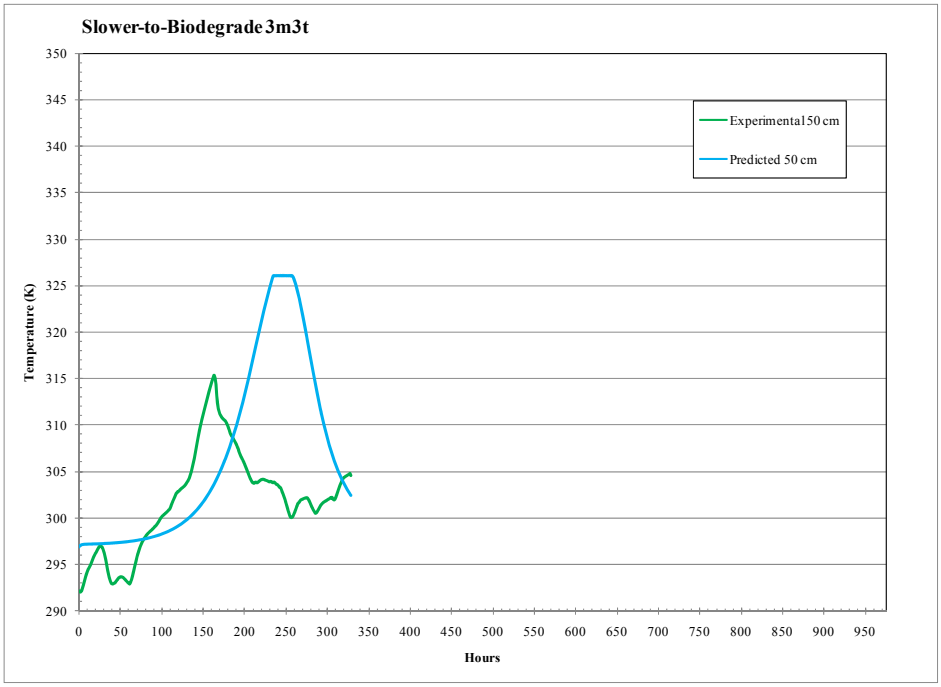

e. Figure 7.12

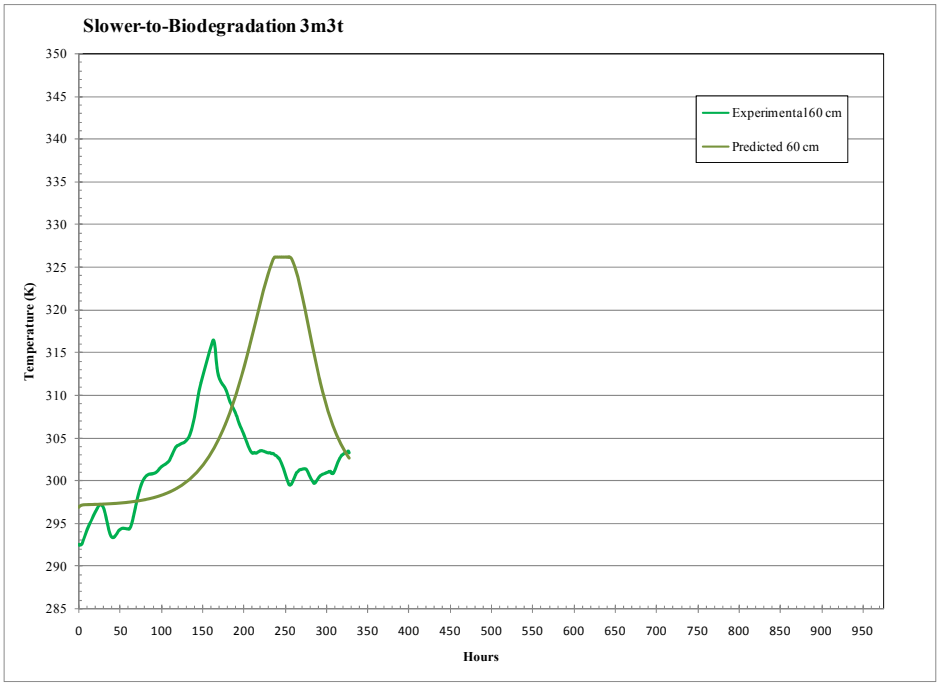

Figure 7.12 Comparison of the slower-to-biodegrade material experimental temperature profile with the predicted temperature profile data by: (a) 10-cm layer; (b) 30-cm layer; (c) 40-cm layer; (d) 50-cm layer; and, (e) 60-cm layer. There was no 20-cm layer.

Reactor B1's experimental temperature profile results were used to make the same comparisons for the resistant-to-biodegradation material. The square error results (Table 7.3) indicated the model does not reasonably predict the observed data. However, the general pattern of the data is that all the experimental data follows the variation exhibited by the reference temperature profile and the "0-cm" profile temperature as seen in Figure 5. 9. The reference temperature is the room temperature. The "0-cm" profile is the temperature of the air flowing into the reactor tube just below the first layer of composting material. The model has no capability to adjust for this type of fluctuation because it assumed a constant reference temperature throughout the simulation run. The simulation model predicted no activity, and, in fact, no activity was observed.

The observed data for the 40-cm and 50-cm layers was deleted when the data was cleaned. Figure 7.13 show the visual fit for each layer for the resistant-to-biodegradation data.

Table 7.3 Square error results for the resistant-to-biodegradation

Comparison Tests	Layer					
	10-cm	20-cm	30-cm	40-cm	50-cm	60-cm
Experimental data: $Standard\ Deviation(observed)$	1.54	1.68	1.78	No value	No value	1.85
Square root: $SQRT\left(avg\sum(predicted-observed)\right)$	2.63	2.09	1.91	No value	No value	1.88
Square error: $\frac{SQRT\left(avg\sum(predicted-observed)\right)}{Standard\ Deviation(observed)}$	1.71	1.24	1.07	No value	No value	1.02

a. Figure 7.13

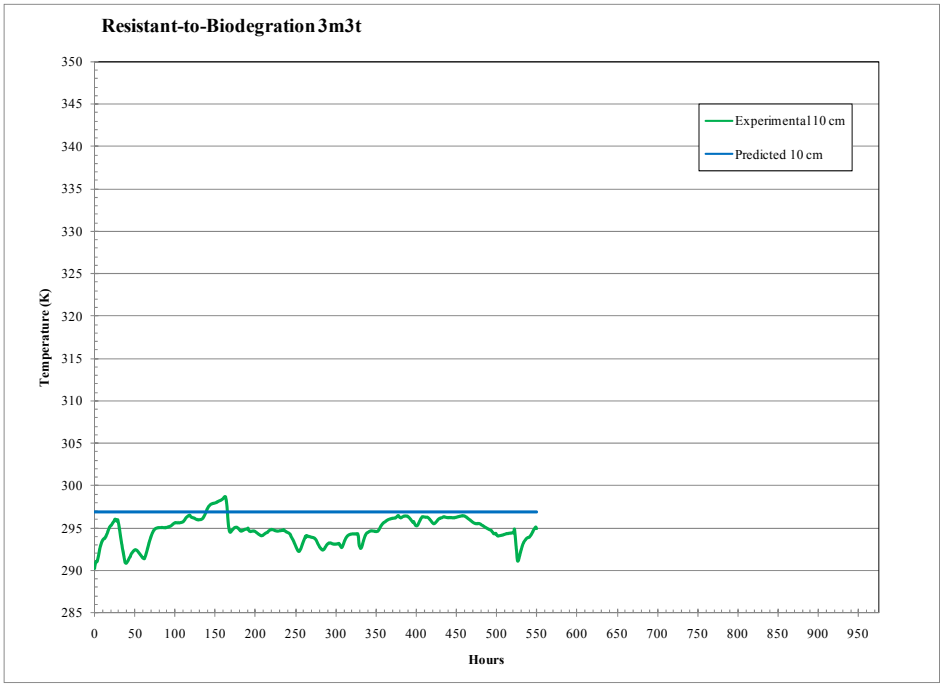

b. Figure 7.13

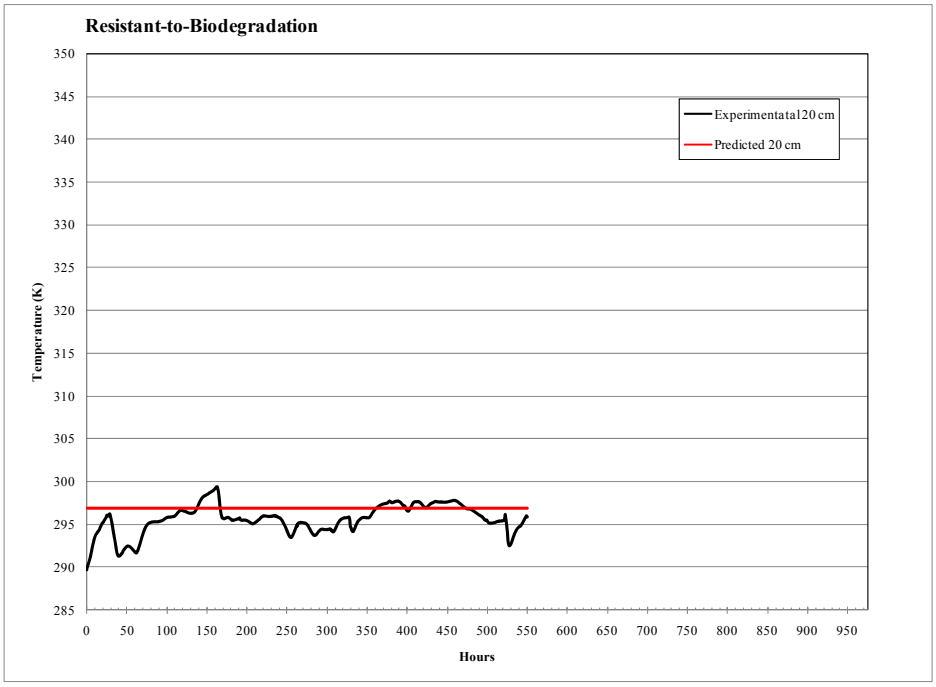

c. Figure 7.13

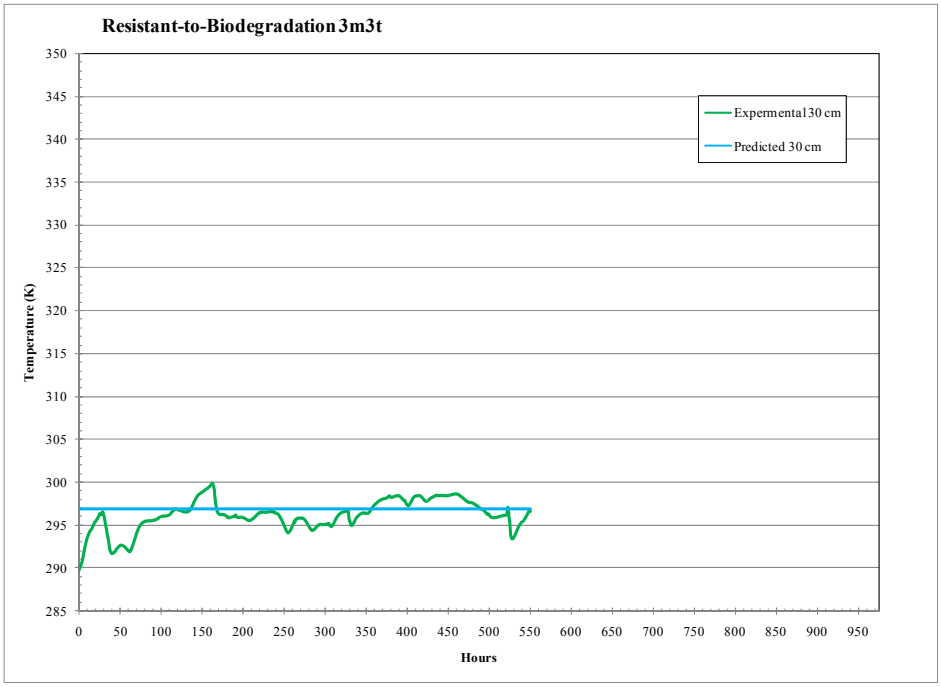

d. Figure 7.13

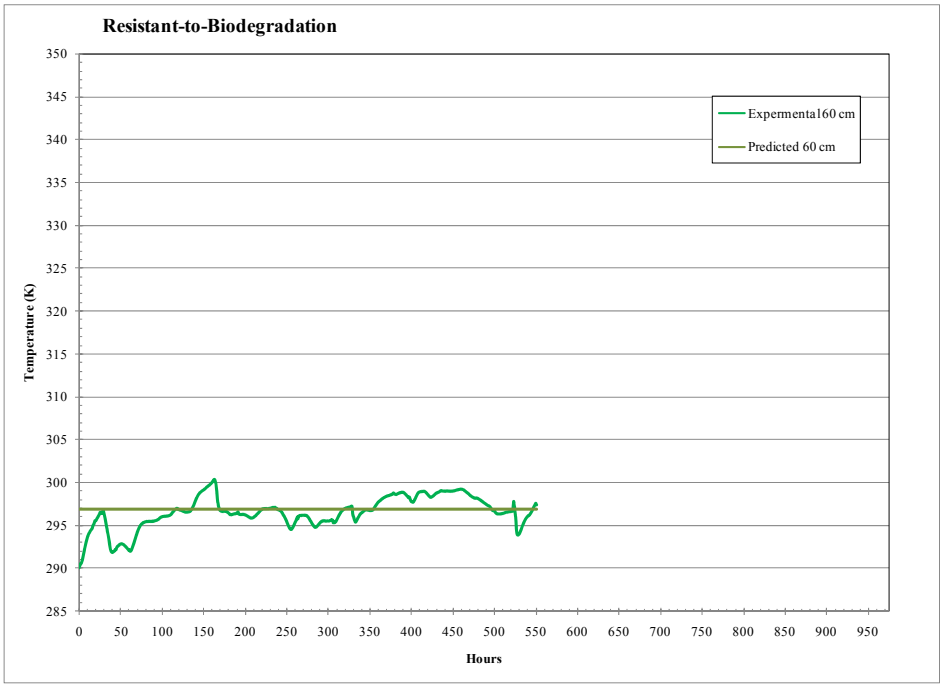

Figure 7.13 Comparison of the resistant-to-biodegradation material experimental temperature profile with the predicted temperature profile layer-by-layer: (a) 10-cm layer; (b)20-cm layer; (c) 30-cm layer; and, (d) 60-cm layer. There were no 40-cm and 50 cm layers.

Model Sensitivity

A simulation model should be robust to account for changes. The "standard" simulation from which comparison changes were made is the readily-biodegradable simulation model that utilized the three microorganism types and two temperature ranges [Figure 7.1 (c)]. Figures 7.14 through 7.17 illustrate simulated results due to changes in: 1) the minimum temperature for the threshold for thermophilic microorganisms; 2) the heat loss factor from the reactor vessel; 3) starting moisture content; and 4) maximum growth rate. Inadditions to the comparison to a "standard" simulation, two simulations (Figures 7.18 and 7.19) were run to observe the changes to the slower-to-biodegrade and the resistant-to-biodegradable simulatation if the moisture content was 60% (wet basis). The experimental runs showed the moisture content for the slower-to-biodegrade at 45% (wet basis) and for the resistant-to-biodegradation at 31% (wet basis).

Figures 7.14 through 7.19 display an additional informational code for tracking purposes. The code 'TKXX' is utilized. The 'TK' refers to thermophilic Kelvin, the temperature value at which the thermophilic temperature range begins. The 'RTXX' refers to thermal resistance, the amount of heat loss through the reactor's walls. The 'WmcXX' refers to the water moisture content of the initial mixture. And 'MGR' refers to the maximum growth rate assigned to the bacteria microbial group. The 'XX' refers to the values used in the particular run.

The minimum temperature for growth of thermophilic microorganisms is set at 325.16 K (53 °C) in the "standard" simulation [Figure 7.1(c)] based on the literature, as discussed in Chapter 3, and from comparisons with the experimental data. But, what if the minimum temperature should be lower or higher? What effects would be seen? First, the minimum temperature was set to 323.16 K (50 °C) [Figure 7.14(a)]. Next, the minimum temperature was set to 328.16 K (55 °C) [Figure 7.14(b)]. The most noticeable effect was the shift of the transition zone where the microorganism type went from the mesophilic to thermophilic microorganisms. The shift in the 323.16 K run occurred at approximately 323 K. In the 328.16 K run, the shift occurred at approximately 328 K. Thus the selection of the minimum temperature for thermophilic microorganism resulted in what temperature the transition zone would occur.

a. Figure 7.14

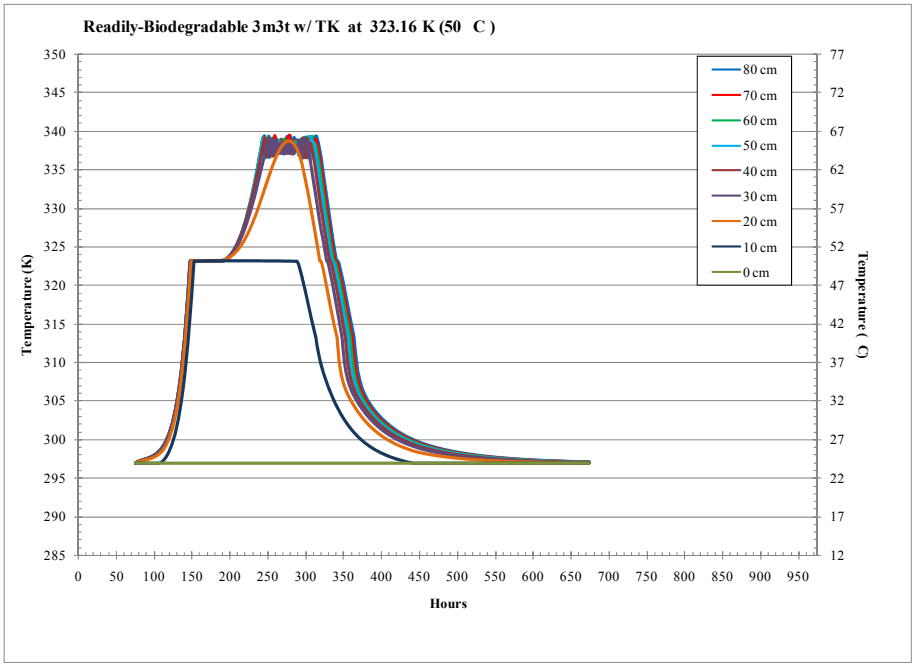

b. Figure 7.14

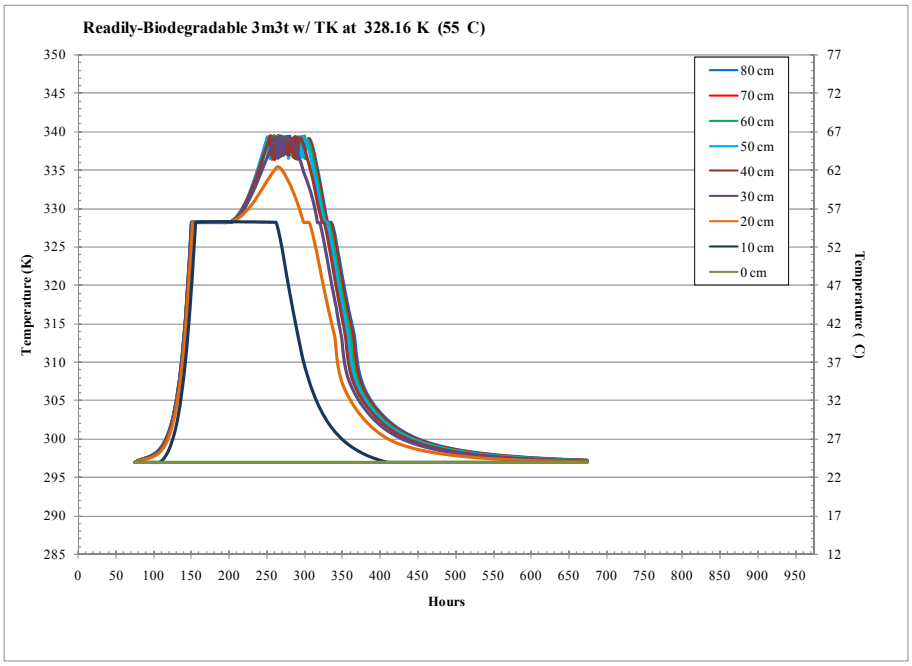

Figure 7.14 Modeled temperature profile changes due to change in thermophilic minimum temperature from 326.16 K to (a) 323.16 K and (b) 328.16 K.

Next, the change in the heat loss from the reactor vessel for the "standard" simulation was made by changing the R_T value. It was set at 0.45 K m^{-2} h J^{-1} h^{-1}. Initially, this value was based on calculating the thermal resistance of the insulation wrap. The experimental data indicated the value was too low. Thus, the heat loss number was determined on a best-fit base. If a lower value was utilized ($R_T = 0.40$), the length of time the maximum temperature values were maintained before decreasing [Figure 7.15(a)] was short. Conversely, if a higher value was used ($R_T = 0.50$), the period of time the maximum temperature were maintained increased [Figure 7.15(b)]. All three simulations reached a temperature greater than 335 K (62 °C). The simulation utilizing the R_T value of 0.40 had the 40-cm, and above, layers over 335 K (62 °C) for 42 hours, with the 50-cm layer first exceeding the temperature starting at Hour 258 and continued until Hour 300. The "standard" simulation utilized a R_T value of 0.45. The 50-cm and 60-cm layers exceeded the 335 K (62 °C) mark at Hour 237. The temperature fell below 335 K (62 °C) 83 hours later at Hour 320. The simulation utilizing a R_T value of 0.50 had all layers except the 10-cm layer exceeding 335 K (62 °C). The 50-cm and the 60-cm layers exceeded the temperature at Hour 227.5 and remained above until Hour 327.5 when the top two layers fell below. The length of time was 100 hours. Clearly, the heat loss characteristics are important to know and account for in composting.

a. Figure 7.15

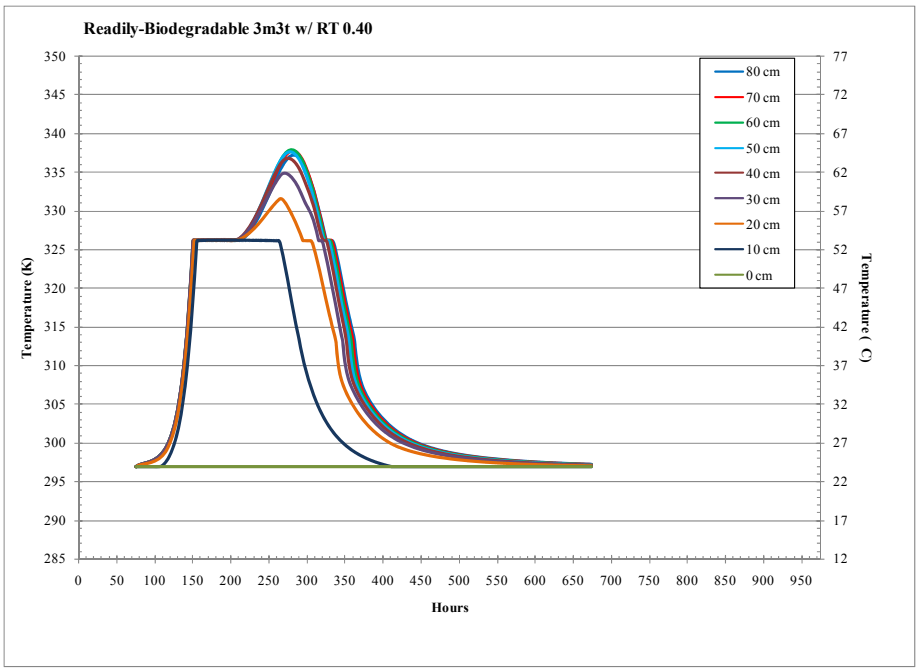

b. Figure 7.15

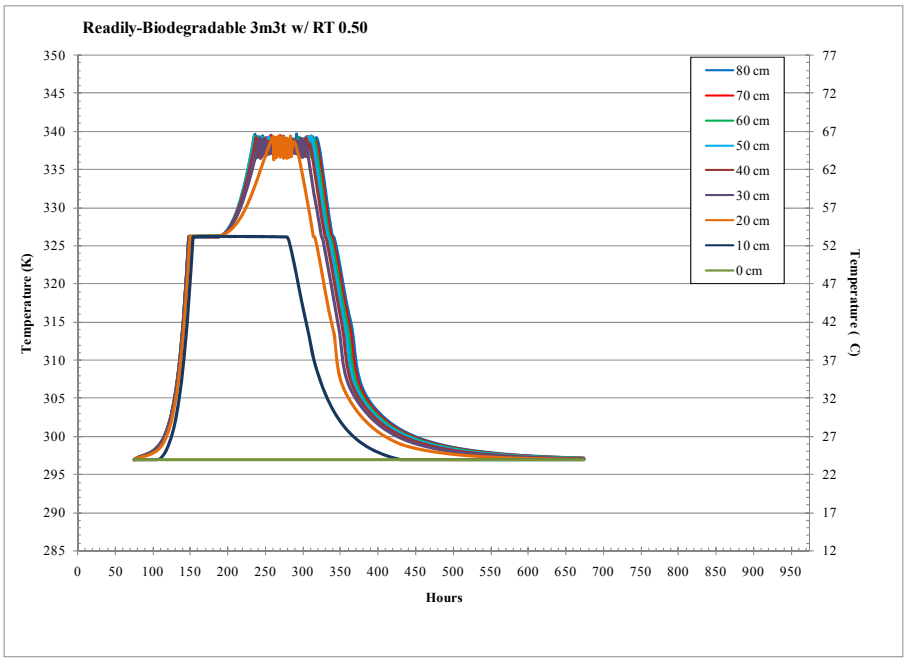

Figure 7.15 Modeled temperature profile changes due to change in thermal resistance (R_T) from 0.45 K m^{-2} h J^{-1} h^{-1} to (a) 0.40 K m^{-2} h J^{-1} h^{-1} and (b) 0.50 K m^{-2} h J^{-1} h^{-1} .

The third change was the starting water moisture content (Wmc) (wet basis). This value initially was determined based on the measured water content 0.67 kg_w $kg_{s\&w}^{-1}$ (wet basis). In all runs, the air feeding the reactors was from a low of 291.6 K (18.4°C) at Hour 808.0 to a high of 300.5 K (27.3°C) at Hour 161.5, with an average feed temperature of 296.9 K (23.7°C) and an average relative humidity set at 60%. Figure 7.6(a) indicated the model's "standard" prediction if the initial moisture content was 0.41 kg_w $kg_{s\&w}^{-1}$ (wet basis). In this "standard" run the initial weighted moisture coefficient (k_{H_2O}, no units) equaled 0.57. During the composting process, k_{H_2O} rose to 1.0, the maximum value. This indicated that, although the initial moisture content was low, the in-flowing air supplied some moisture, and the decomposition process supplied additional moisture. When the initial moisture content was set at 0.751 kg_w $kg_{s\&w}^{-1}$ (wet basis), k_{H_2O} started at 0.44 and increased to a maximum value of 0.60. This simulation clearly indicates too much moisture was a problem because it did not permit the aerobic decomposition process to proceed. The maximum temperature reached was only about 327 K (54 ° C) (Figure 7.16), which was not high enough to allow thermophilic microorganisms to grow. Thermophilic temperatures are critical to destroy pathogenic organisms; therefore, initial water content is critical to the composting process.

a. Figure 7.16

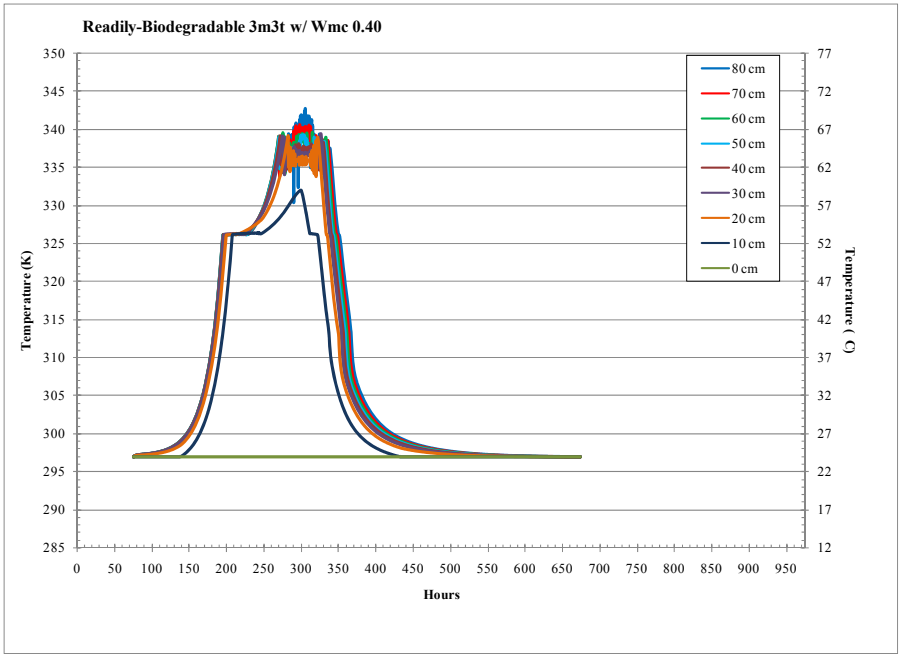

b. Figure 7.16

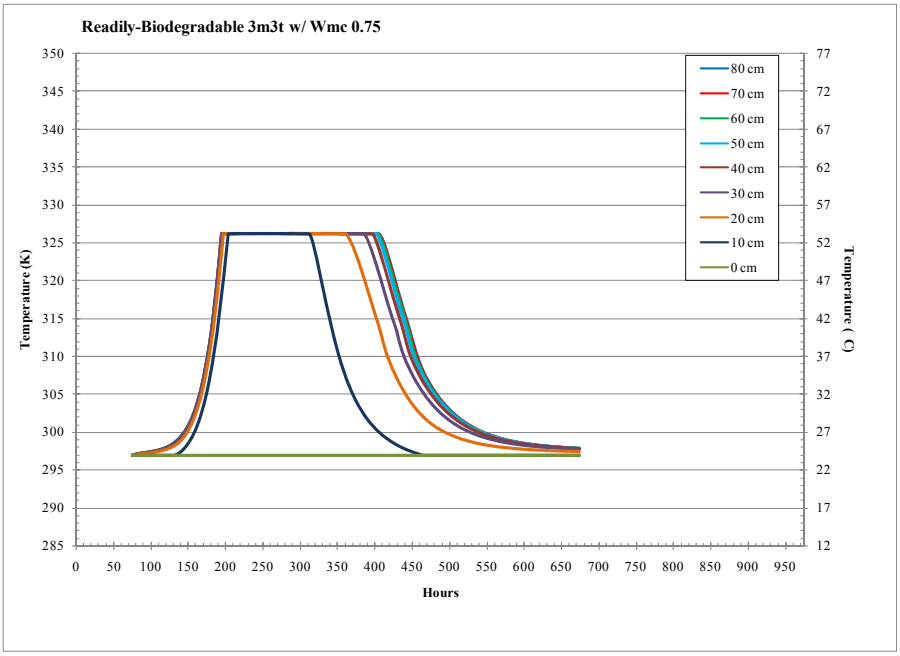

Figure 7.16 Modeled temperature profile changes due to change in initial moisture content from 0.66 kg_w $kg_{s\&w}^{-1}$ to (a) 0.41 kg_w $kg_{s\&w}^{-1}$ and (b) 0.75 kg_w $kg_{s\&w}^{-1}$.

The next change was made to examine the effect of the maximum growth rate (μ_{max} h^{-1}) for both the mesophilic and thermophilic bacteria. The maximum growth initially was based on literature values, discussed in Chapter 3, and from comparisons to the experimental data. The "standard" simulation value is $\mu_{max} = 0.22$. Setting $\mu_{max} = 0.20$ [Figure 7.17(a)] produced a distinct slowing of the microbial process. The temperature transition between the mesophilic and thermophilic microorganisms was not as high [328 K verses 326 K (55 °C verses 53 °C)], the length of time at the transition temperature was greater, and the peak temperature only reached 336 K (63 °C) versus the "standard" that reached almost 340 K (67 °C). With $\mu_{max} = 0.23$, the microbial process is faster. The slopes of the temperature profiles are steeper, the temperature remains at its peak longer, and then drops off faster [Figure 7.17(b)]. The maximum growth rate, that is, the speed at which the biological reaction occurs, is important. If the proper value is not selected, the simulation model will not generate sufficient heat, and the necessary maximum temperatures are not reached.

a. Figure 7.17

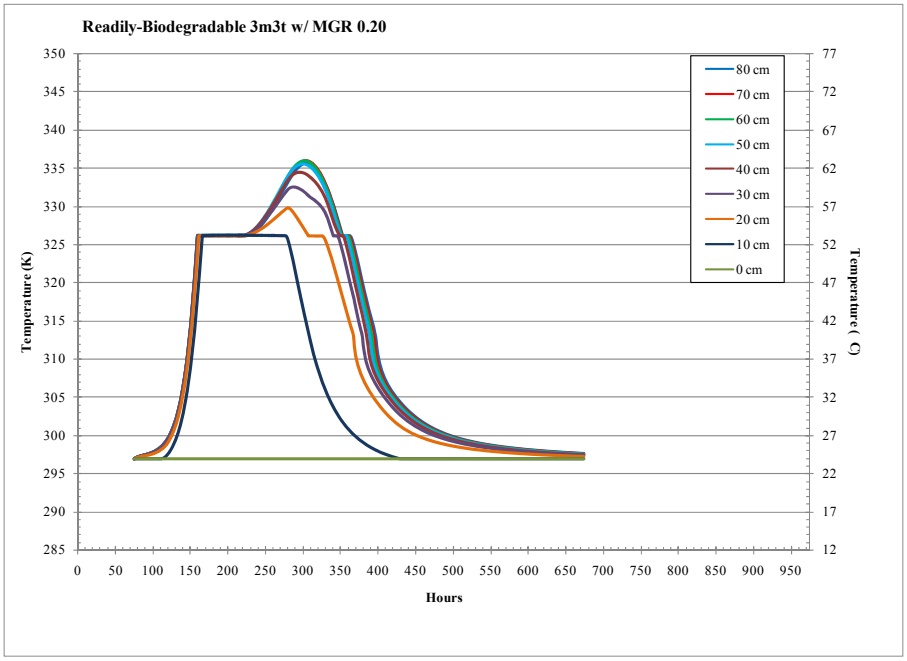

b. Figure 7.17

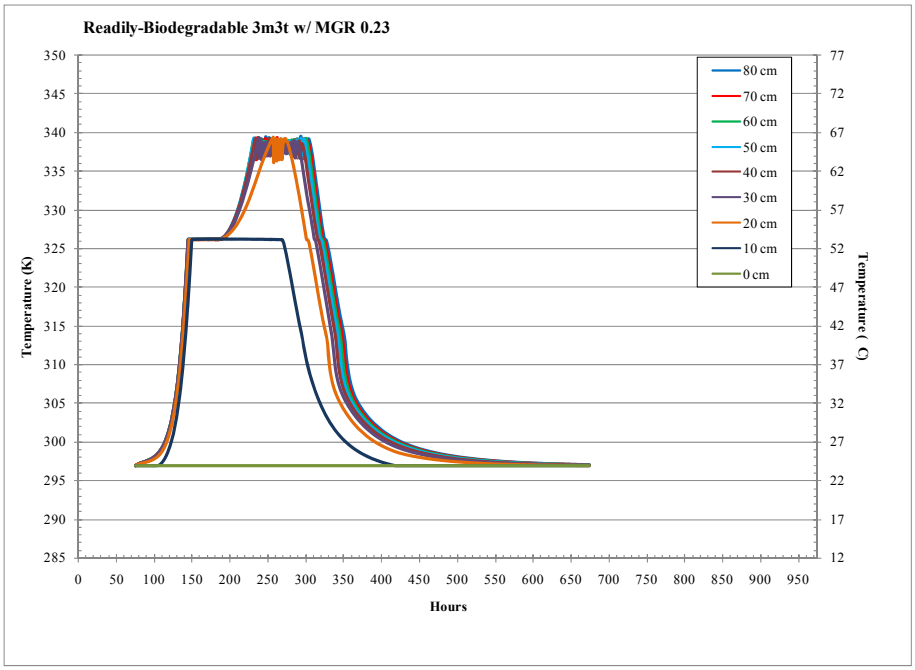

Figure 7.17 Modeled temperature profile changes due to maximum growth rate for both the mesophilic and thermophilic bacteria from 0.22 h^{-1} to (a) 0.20 h^{-1} and (b) 0.23 h^{-1}.

The final change was made to examine the effect to the temperature curve for both the slower-to-biodegrade and to the resistant-to-biodegradation curves if the initial moisture content was 60% (wet basis). For the slower-to-biodegrade mixture, the temperature profile rose to 326 K (53 °C) (Figure 7.18). This is the same temperature profile as shown in Figure 7.2, except the peak temperature was reached at Hour 225. The weighted moisture coefficient (k_{H_2O}, no units) started at 1.0, but eventually dropped to 0.78 when the peak temperature was reached.

For the resistant-to-biodegrade mixture, the temperature profile rose to 318 K (45 °C) (Figure 7.19). This temperature profile is completely different from the experimental data (Figure 5.9) and the simulation (Figure 7.3) temperature profiles. In this temperature profile (Figure 7.19), a peak temperature of 318 K (45 °C) was reached at Hour 240. The weighted moisture coefficient (k_{H_2O}, no units) started at 1.0 but eventually dropped to 0.88 at the time the peak temperature was reached. The moisture content increased to 63% (wet basis).

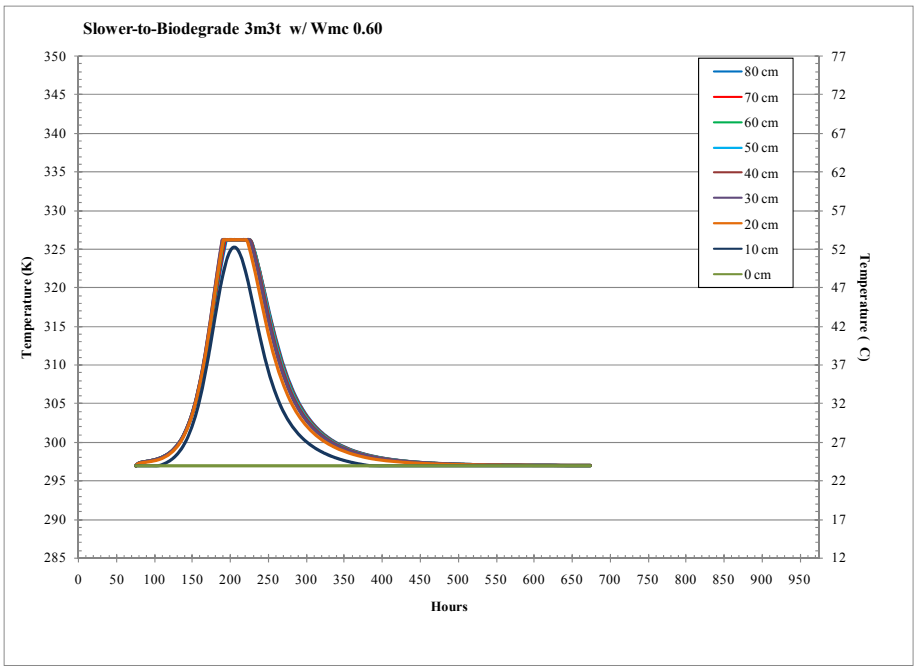

Figure 7.18 Modeled temperature profile changes due to change in initial moisture content from 0.45 kg_w $kg_{s\&w}^{-1}$ to 0.60 kg_w $kg_{s\&w}^{-1}$ for the slower-to-biodegrade mixture.

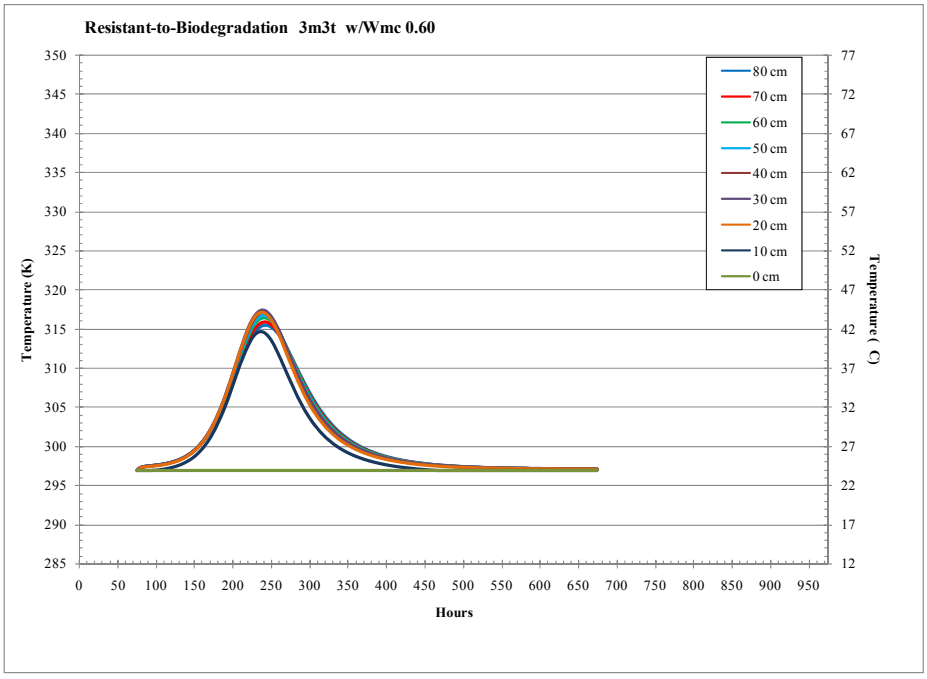

Figure 7.19 Modeled temperature profile changes due to change in initial moisture content from 0.31 kg_w $kg_{s\&w}^{-1}$ to 0.60 kg_w $kg_{s\&w}^{-1}$ for the resistant-to-biodegradation mixture.

CHAPTER 8 - CONCLUSION

The goal of this research was to move toward a more comprehensive mathematical, computer-simulation model that predicts outcome based on different substrates available or chosen. This was accomplished. Repeated runs can be made, concentrating on a particular issue of interest. Predictions can be reviewed by varying the amounts and types of substrates, moisture, aeration rate, reactor size, and heat loss, before pilot work is initiated. The simulation is based on the methodology utilized by Stombaugh and Nokes (1996), employing the Monod equation for biomass production, and it used stoichiometric equations to develop yield coefficients for substrate consumption, oxygen consumption, water production, and carbon-dioxide production.

The objectives were met. This model advances compost modeling as follows:

- It accounts for the division of the substrate into four parts: soluble substrate, cellulose/hemicellulose substrate, lignin/lignocellulose substrate, and inert (ash/inorganic) substrate. This component establishes a common level that all materials to be composted can be broken into the common basic building blocks that microorganisms utilize for energy. All organic materials can be analyzed and partitioned into the four substrate parts.
- It accounts for the division of the basic microbiological approach into three parts: bacteria, actinomycetes, and fungi, to reflect the different major decomposers substrate preferences and the time required to decompose the different substrates. This component establishes that modeling needs to focus on the microorganism predominately responsible for a substrate's biodegradation.
- It separates the microbiological organism processes into mesophilic and thermophilic temperature ranges. This component solves the problem of assigning all microorganisms to just one temperature range. The model considers the dynamics between mesophilic and thermophilic microorganisms.

- Three stoichiometric equations were developed, in which each equation reflects a specific microbial type and their major substrate type. Each equation considers the substrate type, the amount of oxygen required based on substrate type and on microorganism type, the growth of the specific microorganism type, and carbon dioxide and water produced.
- The dead microorganisms are considered. Ninety-five percent were added back into the soluble substrate to be reutilized. The remaining five percent were added into the resistant-to-biodegrade category. This component allows a more accurate capture of the effect of microbial death on the substrate availability.
- A more exact moisture coefficient was developed. This component accounts for the effects of moisture content on the bacterial population, from desiccation at to low moisture, to the lack of oxygen diffusion at high moisture levels. This coefficient demonstrated the effect water production has on the composting process.

In addition to the objectives above, this model also advanced compost modeling concerning the partial vapor pressure. The wet bulb reading is required to calculate the partial vapor pressure; however the wet bulb reading cannot be calculated. Instead of assuming the air is saturated and making the partial vapor pressure equal to the saturated vapor pressure, a best fit equation was developed using EXCEL 2007, from the psychrometric chart listing the ambient temperature and vapor pressure data. The equation was introduced and used in the mathematical model, Chapter 6. This advance allows a more accurate measure of the effect the moisture content has on the composting process.

Several different conditions were run using the mathematical-simulation model. Comparisons were made between: 1) microorganism types; 2) two temperature scenarios (that is, the one temperature profile versus the mesophilic and thermophilic profile); and 3) substrate types. The model results were compared to the experimental results, and, the experimental portion of this research focused on providing data to evaluate the model's prediction capability. Three mixtures were prepared utilizing four different ingredients.

The mixtures represented the range of compostable materials from the readily-biodegradable, through the slower-to-biodegrade, to the resistant-to-biodegradation.

The findings indicated the simulation model improved the overall capability to more accurately predict the outcome. The general differences between the different substrate types followed the experimental results. However, goodness-of-fit using the square error were all greater "1," and, for a good fit, the square error should be less than "1." The simulation for the readily-biodegradable substrate was slightly greater than "1." Likely, the problem was the value utilized for the maximum-growth rate. The linear value did not mirror what occurs in nature over the entire microbial growth curve.

The slower-to-degrade had a square error that exceeded a value of two. The simulation projected a higher temperature peak. However, the general pattern was presented. The resistant-to-biodegradation had a square error that exceeded "1". The model predicted no increase in temperature. The experimental results showed minimal temperature increase; it reflected the temperature pattern of the incoming feed air.

Additional research is needed to address the influence of volume reduction, to develop a better microbial growth curve, to include particle size influence, to add temporal temperature fluctuations to the external boundary conditions, to incorporate pH and nitrogen availability, and to develop a three-dimensional model.

CHAPTER 9 - REFERENCES

Adl, S.M. 2003. *The Ecology of Soil Decomposition*. CABI Publishing Cambridge, MA.

Aiba, S., A.E. Humphery, and N.F. Millis. 1973. *Biochemical Engineering.* 2nd ed. Tokyo, Japan: University of Tokyo Press.

Alexander, M. 1977. *Introduction to Soil Microbiology*, 2nd ed. John Wiley & Sons., NY.

ANKOM Technologies, Macedon, NY.

AOAC International. 2005. *Official Methods of Analysis of AOAC International*, 18th.ed., current through Revision 1, 2006. AOAC International, Gaithersburg, MD.

ASABE. 2006. Standards. ASAE D271.2 APR1979 (R2005), Psychrometric Data. ASABE, St. Joseph, MI.

Bagstam, G. 1978. Population changes in microorganisms during composting of spruce-bark. I Influence of temperature control. European J. Appl. Microbiol. Biotechnol. 5:315-330.

Bagstam, G. 1979. Population changes in microorganisms during composting of spruce-bark. II. Mesophilic and thermophilic microorganisms during controlled composting European J. Appl. Microbiol. Biotechnol. 6:279-288.

Berry, D.R. 1988. *Physiology of Industrial Fungi.* Blackwell Scientific Publications. Cambridge, MA.

Bear, J. and Y. Bachmat. 1991. *Introduction to Modeling of Transport Phenomena in Porous Media.* Dorderecht, Netherlands: Kluwer Academic Publishers.

Brock, T.D. 1978. *Thermophilic Microorganisms and Life at High Temperatures*. Springer_Verlag, NY.

Brock, T.D. and M.T. Madigan. 1988. *Biology of Microorganisms*, 5th ed. Prentice Hall, Englewood Cliffs, NJ.

Chang, Y. and N.J. Hudson. 1967. The fungi of wheat straw compost I. Ecological studies. Trans. Br. Mycol. Soc. 50(4):649-666.

Chefetz, B., F. Adani and P. Genevini. 1998. Humic-acid transformation during composting of municipal solid waste. J. Environ. Quality 27(4):794-800.

Chino, M., S. Kanazawa, T. Mori, M. Araragi, and B. Kanke. 1983. Biochemical studies on composting of municipal sewage sludge mixed with rice hull. Soil Sci. Plant Nutr. 29(2):159-173.

Clapp, C.E. and M.H.B. Hayes. 1999. Sizes and shape of humic substances. Soil Sci. 164(11) 777-789.

Cooney, D.G. and R. Emerson. 1964. *Thermophilic Fungi, Eumycota.* .W. H. Freeman Publ. Co., San Franscisco, CA.

Cundiff, J.S. and K.R. Mankin. 2003. *Dynamics of Biological Systems*, The Society for engineering in agricultural, foods, and biological systems, St. Joseph, MI.

Das, K. and H.M. Keener. 1997. Numerical model for the dynamic simulation of a large scale composting systems. Trans. of the ASAE 40(4):1179-1189.

De Bertoldi, M., U. Citernesi, and M. Griselli. 1980. Bulking agents in sludge composting. Compost Sci./Land Util. 21(1): 32-35,41.

De Bertoldi, M., G. Vallini, A. Pera, and F. Zucconi. 1982. Comparison of three windrow compost systems. BioCycle 23(2):45-50.

Ekinci, K., H.M. Keener, D.L. Elwell, and F.C. Michel, Jr. 2005. Effects of aeration strategies on the composting process: part II. numerical modeling and simulation. Trans. of the ASAE 48(3):1203-1215.

Elwell, D.L., H.M. Keener, M.C. Wiles, D.C. Borger, and L.B. Willett. 2001. Odorous emissions and odor control in composting swine manure/sawdust mixes using continuous and intermittent aeration. Trans. of the ASAE 44(5):1307-1316.

Engineering Tool Box.com. 2008. (http://www.engineeringtoolbox.com/water-content-compressed-air-d_1275.html).

Epstein, E. 1997. *The Science of Composting*. Technomic Publishing Co., Inc., Lancaster, PA.

Fergus, C.L., and J.W. Sinden. 1969. A new thermophilic fungus from mushroom compost: *Thielavia thermophila,* sp. Nov. Can. J. Bot. 47:1635-1637.

Fermor, T.R., J.F. Smith, and D.M. Spencer. 1979. The microflora of experimental mushroom composts. J. Horticult. Sci. 54:137-147.

Fingers, S.M., R.T. Hatch, and T.M. Regan. 1976. Aerobic microbial growth in semisolid matrices: Heat and mass transfer limitation. Biotechnology and Bioengineering 18: 1193-1218.

Finstein, M.S. 1980. Composting microbial ecosystem: implications for process design and control. Compost Sci./Land Util. 21(4): 25-39.

Finstein, M.S., F.C. Miller, J.A. Hogan, and P.F. Strom. 1987. Analysis of EPA guidance on composting sludge. Part III. Oxygen, moisture, odor, pathogens. Biocycle 28(3): 38-44.

Finstein, M.S. and M.L. Morris. 1975. Microbiology of solid waste composting, in D. Perlman (ed.). Adv. Appl. Microbiol. 19:113-149, Academic Press, NY.

Fuijita, K. 1993. *Compost Engineering*. Toyko, Japan: Gihoudo,Shuppan.

Glasser, W.G. 2000. Classification of lignin according to chemical and molecular structure, *In* W.G. Glasser, R.A. Northey, and T.P. Schultz (eds.), *Lignin: Historical, Biological, and Materials Perspectives.* Am. Chem. Soc. Symp. series: 742. Distributed by Oxford Univ. Press.

Golueke, C.G. 1972. *Composting: A Study of the Process and its Principles*. Rodale Press, Inc., Emmaus, PA.

Golueke, C.G. 1977. *Biological Reclamation of Solid Wastes*. Rodale Press, Emmaus, PA

Grant, R.F. and P. Rochette. 1994. Soil microbial respiration at different water potentials and temperatures: theory and mathematical modeling. Soil Sci. Soc. Am. J. 58: 1681-1690.

Gray, K.R., K. Sherman, and A.J. Biddleston. 1971. A review of composting-Part 2. The practical process. Process Biochemistry 6(6):22-28.

Griffin., D.H. 1994. *Fungal Physiology* 2nd ed. Wiley-Liss, Inc, NY.

Hamelers, H.V.M. 1993. A theoretical model of composting kinetics, *In* H.A.J. Hoitink and H.M. Keener (eds.), *Science and Engineering of Composting: Design, Environmental, Microbiological and Utilization Aspects*, pp. 36-58. Worthington, Ohio: Renaissance Publications.

Hamelers, B.V.M. 2001. The effect of dry matter on the composting rate: theoretical analysis and practical implications. ASAE Meeting Paper No. 01-7004, St. Joseph, MI.

Hankin, L., R.P. Poincelot, and S.L. Angnostakis. 1976. Microorganisms from composting leaves: ability to produce extracellular degradative enzymes. Microbial Ecol. 2:296-308.

Haug, R.T. 1993. *The Practical Handbook of Composting Engineering*. Lewis Publishers, CRC Press, Inc. Boca Raton, FL.

Herrmann, R.F and J.F. Shann. 1996. Microbial community changes during the composting of municipal solid waste. Microbial Ecol. 33:78-85.

Iglesias-Jimenez, E. and V. Perez-Garcia. 1992. Composting of domestic refuse and sewage sludge. II. Evolution of carbon and some "humification" indexes. Resour. Conserv. Recycl. 8:45-60.

Iiyama, K., B.A. Stone, and B.J. Macauley. 1994. Compositional changes in compost during composting and growth of *Agaricus bisporus.* Appl. Environ. Microgbiol. 60:1538-1546.

Jeris, J.S. and R.W. Regan. 1973. Controlling environmental parameters for optimum composting; II: Moisture, free air space and recycle. Compost Sci. 14(2): 8-15.

Joshua, R.S., B.J. Macauley, and C.R. Hudson. 1994. Recycling grease trap sludges. Biocycle 35: 46-47.

Kaiser, J. 1996. Modelling composting as a microbial ecosystem: a simulation approach. Ecological Modeling 91:25-36.

Kane, B.E. and J.T. Mullins. 1973. Thermophilic fungi in a municipal waste composting system. Mycologia 65:1087-1100.

Kastens, J. 2008. Personal communications. Kansas Applied Remote Sensing (KARS) Program. Univ. of KS.

Keener, H.M., C. Marugg, R.C. Hansen and H.A.J. Hoitink, 1993. Optimizing the efficiency of the composting process, *In* H.A.J. Hoitink and H.M. Keener (eds.), *Science and Engineering of Composting: Design, Environmental, Microbiological and Utilization Aspects*. Worthington, Ohio: Renaissance Publications, pp. 59-94.

Lengeler, J.W., G. Drews, and H.G. Schlegel. 1999. *Biology of the Prokaryotes*. Blackwell Science, Inc. Malden, MA.

Lilly, V.G. 1965. Volume 1 the fungal cell, *In* G.C. Ainsworth and A. S. Sussman (eds.), *The Fungi An Advanced Treatise*. Academic Press Inc. NY.

Linn, D.M. and J.W. Doran. 1984. Effects of water-filled pores on carbon dioxide and nitrous oxide production in tilled and nontilled soils. Soil Sci. Soc. Am. J. 50:344-348.

Lynch, N.J. and R.S. Cherry. 1995. Design of passively aerated compost piles: Vertical air velocities between pipes. Presented at the European Commission Int. Conf. "The Science of Composting", 30 May-2 June 1995, Bologna, Italy. Glasgow, UK: Blackie A&P.

Macauley, B.J., B. Stone, K. Iiyama, E.R. Harper, and F.C. Miller. 1993. Composting research runs "hot" and "cold" at LaTrobe University. Compost Sci./Land Util. 1: 6-12.

Mader, S.S. 1998. *Biology*, 6th ed. WCB/McGraw-Hill, Boston, MA.

Mason, I.G. 2006. Mathematical modeling of the composting process: A review. Waste Mgmt. 26:3-21.

Mathews, C.K. and K.E. Van Holde. 1996. *Biochemistry*, 2nd ed. The Benjamin/Cummings Publishing Co. Inc., Menlo Park, CA.

McKinley, V.L. and J.R. Vestal. 1985a. Effects of different temperature regimes on microbial activity and biomass in composting municipal sewage sludge. Can. J. Microbiol. 31:919-925.

McKinley, V.L. and J.R. Vestal. 1985b. Physical and chemical correlates of microbial activity and biomass in composting municipal sewage sludge. Applied and Environ. Microbiol. 50(6): 1395-1403.

Miller, F.C., E.B. Harper, B.J. Macauley, and A. Gulliver. 1990. Composting based on moderately thermophilic and aerobic conditions for the production of mushroom compost. Aust. J. Exp. Agric. 30:287-296.

Miller, F.C. 1991. Biodegradation of solid wastes by composting, *In* A.M. Martin (ed.), *Biological Degradation of Wastes*. Elsevier Science Publishing Co., Inc. NY.

Miller, F.C., B.J. Macauley, and E.B. Harper. 1991. Investigation of various gases, pH and redox potential in mushroom composting Phase I. Aust. J. Exp. Agric. 30:415:425.

Miller, F.C. 1996. Composting of municipal solid waste and its components, *In* A.C. Palmisano and M.A. Barlaz (eds.), *Microbiology of Solid Waste*. CRC Press Inc., Baco Raton, FL, pp. 115-154.

Morrison, R.T. and R.N. Boyd. 1970. *Organic Chemistry*, 2nd ed. Allyn and Bacon, Inc. Boston, MA.

Myers, R.G. and S.J. Thien. 1998. Organic matter solubility and soil reaction in an ammonium and phosphorous zone. Soil Sci. Soc. of Am. J., 52:516-522.

Nakasaki, K., J. Kato, T. Akiyama, and H. Kubota. 1987. A new composting model and assessment of optimum operating for effective drying of composting materials. J. Fermentation Technol. 65(4):441-447.

Nakasaki, K., N. Aoki, and H. Kubota. 1994. Accelerated composting of grass clippings by controlling moisture level. Waste Mgmt. Res. 12:12-20.

Nommik, H. 1965. Ammonia fixation and other reactions involving a nonenzymatic immobilization of mineral nitrogen on soil. *In* W.V. Bartholomew and F.E. Clark (eds.), *Soil Nitrogen*. Am. Soc. of Agron., Madison, WI, pp. 98-258.

Nommik, H. 1970. Non-exchangeable binding of ammonium and amino nitrogen by Norway spruce raw humus. Plant and Soil 33: 581-595.

North Dakota State University Extension Office. 2004, Forage Nutrition for Ruminants, Pub. AS-1250, Fargo, ND.

Palmisano, A.C. and M.A. Barlaz. 1996. Introduction to solid waste decomposition, *In* A.C. Palmisano and M.A. Barlaz (eds.), *Microbiology of Solid Waste*. CRC Press, Inc. Boca Raton, FL, pp. 1-30.

Paul, E.A. and F.E. Clark. 1996. *Soil Microbiology and Biochemistry*, 2nd ed. Academic Press, Inc., San Diego, CA.

Qin, Xiaosheng, Guohe Huang, Guangming Zeng, Amit Chakma, and Beidou Xi. 2007. A fuzzy composting process model. J Air & Waste Mmgt. Assoc. 56(5): 535-551.

Ratkowsky, D.A., J. Olley, T.A. McMeekin, and A. Ball. 1982. Relationship between temperature and growth rate of bacterial cultures. J. Bacteriol. 149:1-5.

Rynk, R., M. van de Kamp, G.B. Willson, M.E. Singley, T.L. Richard, J.J. Kolega, F.R. Gouin, L. Laaliberty, Jr., D. Kay, D.W. Murphy, H.A.J. Hoitink, and W.F. Brinton. 1992. *On-Farm Composting Handbook*. ed. R. Rynk. Northeast Regional Agricultural Engineering Service, Cooperative Extension, Ithaca, NY.

Safwat, M.S.A. 1980. Composting cottonseed wastes. Compost Sci./Land Util. 21(3): 27-29.

Schmidt, S.K. 1992. Models for studying the population ecology of microorganisms in natural systems. *In* C.J. Hurst (ed.). *Modeling the metabolic and physiologic activities of microorganisms.* John Wiley and Sons, Inc. NY.

Seki, H. 2000. Stochastic modeling of composting processes with batch operation by the Fokker-Plank equation. Trans. of the ASAE. 43(1): 169-179.

Seki, H. 2002. A new deterministic model for forced-aeration composting processes with batch operation. Trans of the ASAE. 45(4): 1239-1250.

Sexstone, A.J., N.P. Revsbech, T.B. Parkin, and J.M. Tiedje. 1985. Direct measurement of oxygen profiles and denitrification rates in soil aggregates. Soil Sci. Soc. Am. J. 49:645-651.

Singer, M.J. and D.N. Munns. 1999. *Soils: an Introduction* 4th ed. Prentice-Hall Inc. Upper Saddle River, NJ.

Smith, R. and R.G. Eilers. 1980. *Numerical Simulation of Aerated Sludge Composting*. U.S. Environmental Protection Agency, Cincinnati, OH.

Strom, P.F. 1985a. Effect of temperature on bacterial species diversity in thermophilic solid-waste composting. Applied and Environ. Microbiology, 50(4): 899-905.

Strom , P.F. 1985b. Identification of thermophilic bacteria in solid-waste composting. Appl. and Environ. Microbiol. 50(4): 906-913.

Stentiford, E.I. 1993. Diversity of composting systems, *In* H.A.J. Hoitink and H.M. Keener (eds.), *Science and Engineering of Composting: Design, Environmental, Microbial and Utilization Aspects*. Renaissance Pub., Worthington, OH. pp 95-110.

Stevenson, F.J. and M.A. Cole. 1999. *Cycles of Soil: Carbon, Nitrogen, Phosphorous, Sulfur, Micronutrients*, 2nd ed. John Wiley & Sons, Inc., NY.

Stombaugh, D.P. and S.E. Nokes. 1996. Development of a biologically based aerobic composting simulation model. Trans of the ASAE. 39(1): 239-250.

Straatsma, G., R.A. Samson, T.W. Olijnsma, H.J.M. Op den Camp, J.P.G. Gerrits, and L.J.L.D. Van Griensven. 1994. Ecology of thermophilic fungi in mushroom compost, with emphasis on *Scytalidium thermophilum* and growth stimulation of *Agaricus bisporus* mycelium. Appl. Environ. Microbiol. 50: 899-905.

Sylvia, D.M., J.J. Fuhrmann, P.G. Hartel, and D.A. Zuberer. 1998. *Principles and Applications of Soil Microbiology*. Prentice-Hall Inc., Upper Saddle River, NJ.

Tseng, D.Y, R.Vir, and S.J. Traina. 1995. A Fourier-transform infrared spectroscopic analysis of organic matter degradation in a bench-scale solid substrate fermentation (composting) system. Biotechnology and Bioengineering, 52(12): 661-671.

U.S. Environmental Protection Agency. 1994. *Composting Yard Wastes and Municipal Solid Waste*. EPAA530-R-94-003.

VanderGheynst, J.S., L.P. Walker, and J. Parlange. 1997. Energy transport in a high-solids aerobic degradation process: mathematical modeling and analysis. Biotehnol. Prog. 13: 238-248.

Voet, D and J.G. Voet. 2004. *Biochemistry*, 3rd ed. John Wiley & Sons, Inc., Hoboken, NJ.

Waksman, S.A. and T.C. Cordon. 1939. Thermophilic decomposition of plant residues in compost by pure and mixed cultures of micro-organisms. Soil Sci. 47:217-225.

Waksman, S.A., T.C. Cordon, and N. Hulpoi. 1939. Influence of temperature on the microbial population and decomposition process in composts of stable manure. Soil Sci. 47:83-114.

Walke, R.H. 1975. The preparation, characterization and agricultural use of bark-sewage compost. Ph.D. Disseration. Univ. of New Hampshire, Durham, NH.

Wilhelm, L.R., D.A. Suter, and G.H. Brusewitz. 2004. Psychrometrics. Chapter 9 *In Food & Process Engineering Technology*, 213-257. St. Joseph, MI. ASAE. © American Society of Agricultural Engineers. (Rev. Aug. 2005.))

Wu, L., L.Q. Ma, and G.A. Martinez. 2000. Comparison of methods for evaluating stability and maturity of biosolids compost. J. Environ. Quality. 29(2): 424-429.

Zumdahl, S.S. 1993. *Chemistry*, 3rd ed. D.C. Heath and Co., Lexington, MA.

Zwietering, M.H., J. Jongenburger, F.M. Rombouts, and K, van't Riet. 1990. Modeling of the bacterial growth curve. Appl. and Environ. Microbiol. 56(4): 1875-1881.

Zwietering, M.H., J.T. de Koos, B.E. Hasenack, J.C. de Wit, and K, van't Riet. 1991. Modeling of bacterial growth as a function of temperature. Appl. and Environ. Microbiol. 57(4): 1094-1101.

Appendix A - Symbols

EQUATION SYMBOL	MATLAB® SYMBOL	DEFINITION	UNITS
A_{wall}	Awall	Area of compost vessel wall	m^2
c_{sc}	CHsc	Specific heat of cellulose/hemicellulose substrate	kJ kg_{sc}^{-1} K^{-1}
c_{si}	CHsi	Specific heat of inert substrate	kJ kg_{si}^{1} K^{-1}
c_{sl}	CHsl	Specific heat of lignin substrate	kJ kg_{sl}^{-1} K^{-1}
c_{ss}	CHss	Specific heat of soluble substrate	kJ kg_{ss}^{-1} K^{-1}
c_{w}	CHw	Specific heat of water	kJ kg_{w}^{-1} K^{-1}
C_{CO_2}	C_CO2	Concentration of carbon dioxide	kg_{CO2} m^{-3}
C_{O_2}	C_O2	Concentration of oxygen	kg_{O2} m^{-3}
$C_{S_{sc}}$	CSsc	Concentration of cellulose/hemicellulose substrate per increment volume	kg_{sc} m^{-3}
$C_{S_{si}}$	CSsi	Concentration of inert substrate per increment volume	kg_{si} m^{-3}
$C_{S_{sl}}$	CSsl	Concentration of lignin substrate per increment volume	kg_{sl} m^{-3}
$C_{S_{ss}}$	CSss	Concentration of soluble substrate per increment volume	kg_{ss} m^{-3}
C_{W}	CWs	Concentration of water per increment volume	kg_{w} m^{-3}
$C_{X_{ma}}$	CXma	Concentration of mesophilic actinomycetes	$kg_{X\ ma}$ m^{-3}

$C_{X_{mb}}$	CXmb	Concentration of mesophilic bacteria	$kg_{X\ mb}\ m^{-3}$
$C_{X_{mf}}$	CXmf	Concentration of mesophilic fungi	$kg_{X\ mf}\ m^{-3}$
$C_{X_{ta}}$	CXta	Concentration of thermophilic actinomycetes	$kg_{X\ ta}\ m^{-3}$
$C_{X_{tb}}$	CXtb	Concentration of thermophilic bacteria	$kg_{X\ tb}\ m^{-3}$
$C_{X_{tf}}$	CXtf	Concentration of thermophilic fungi	$kg_{X\ tf}\ m^{-3}$
d	d	Number of increments or layers the compost bed is sectioned into for analysis	(no units)
dC_{CO_2}	dC_CO2	Rate of change in concentration of carbon dioxide produced due to consumption of substrate	$kg_{CO2}\ m^{-3}\ hr^{-1}$
dC_{O_2}	dC_O2	Rate of change in the concentration of oxygen	$kg_{O2}\ m^{-3}\ hr^{-1}$
$dC_{O_2\ aeration}$	dC_O2a	Rate of change in the concentration of oxygen due to aeration	$kg_{O2}\ m^{-3}\ hr^{-1}$
$dC_{O_2\ consumed}$	dC_O2c	Rate of change in the concentration of oxygen due to substrate consumption	$kg_{O2}\ m^{-3}\ hr^{-1}$
$dC_{S_{sc}}$	dCSsc	Rate of change in the concentration of cellulose/hemicellulose substrate	$kg_{sc}\ m^{-3}\ h^{-1}$
$dC_{S_s}C_{X_{kd}}$	dCSsCXkd	Rate of change in the substrate concentration generated due to death of microorganisms	$kg_{s}\ m^{-3}\ h^{-1}$
$dC_{S_{sl}}$	dCSsl	Rate of change in the concentration of lignin substrate	$kg_{sl}\ m^{-3}\ h^{-1}$
$dC_{S_{ss}}$	dCSss	Rate of change in the concentration of soluble substrate	$kg_{ss}\ m^{-3}\ h^{-1}$
dC_W	dCWs	Rate of change in the concentration of water	$kg_{w}\ m^{-3}\ h^{-1}$
$dC_{W\ aeration}$	dCWsa	Rate of change in the concentration of water due to aeration	$kg_{w}\ m^{-3}\ h^{-1}$

$dC_{W\ produced}$	dCWsp	Rate of change in the concentration of water produced due to substrate consumption	$kg_w\ m^{-3}\ h^{-1}$
$dC_{X_{g\ ma}}$	dCXgma	Rate of change in the concentration of mesophilic actinomycetes due to growth	$kg_{X\ ma}\ m^{-3}\ h^{-1}$
$dC_{X_{g\ mb}}$	dCXgmb	Rate of change in the concentration of mesophilic bacteria due to growth	$kg_{X\ mb}\ m^{-3}\ h^{-1}$
$dC_{X_{g\ mf}}$	dCXgmf	Rate of change in the concentration of mesophilic fungi due to growth	$kg_{X\ mf}\ m^{-3}\ h^{-1}$
$dC_{X_{g\ ta}}$	dCXgta	Rate of change in the concentration of thermophilic actinomycetes due to growth	$kg_{X\ ta}\ m^{-3}\ h^{-1}$
$dC_{X_{g\ tb}}$	dCXgtb	Rate of change in the concentration of thermophilic bacteria due to growth	$kg_{X\ tb}\ m^{-3}\ h^{-1}$
$dC_{X_{g\ tf}}$	dCXgtf	Rate of change in the concentration of thermophilic fungi due to growth	$kg_{X\ tf}\ m^{-3}\ h^{-1}$
$dC_{X_{kd\ ma}}$	CXkdma	Rate of change in the concentration of mesophilic actinomycetes due to that portion of the population which are dying	$kg_{X\ ma}\ m^{-3}\ h^{-1}$
$dC_{X_{kd\ mb}}$	CXkdmb	Rate of change in the concentration of mesophilic bacteria due to that portion of the population which are dying	$kg_{X\ mb}\ m^{-3}\ h^{-1}$
$dC_{X_{kd\ mf}}$	CXkdmf	Rate of change in the concentration of mesophilic fungi due to that portion of the population which are dying	$kg_{X\ mf}\ m^{-3}\ h^{-1}$
$dC_{X_{kd\ ta}}$	CXkdta	Rate of change in the concentration of thermophilic actinomycetes due to that portion of the population which are dying	$kg_{X\ ta}\ m^{-3}$
$dC_{X_{kd\ tb}}$	CXkdtb	Rate of change in the concentration of thermophilic bacteria due to that portion of the population which are dying	$kg_{X\ tb}\ m^{-3}$
$dC_{X_{kd\ tj}}$	CXkdtf	Rate of change in the concentration of thermophilic fungi due to that portion of the population which are dying	$kg_{X\ tf}\ m^{-3}$
$dC_{X_{ma}}$	dCXma	Rate of change in the concentration of mesophilic actinomycetes	$kg_{X\ ma}\ m^{-3}\ h^{-1}$

$dC_{X_{mb}}$	dCXmb	Rate of change in the concentration of mesophilic bacteria	$kg_{X\ mb}\ m^{-3}\ h^{-1}$
$dC_{X_{mb}}$	dCXmf	Rate of change in the concentration of mesophilic fungi	$kg_{X\ mf}\ m^{-3}\ h^{-1}$
$dC_{X_{ta}}$	dCXta	Rate of change in the concentration of thermophilic actinomycetes	$kg_{X\ ta}\ m^{-3}\ h^{-1}$
$dC_{X_{tb}}$	dCXtb	Rate of change in the concentration of thermophilic bacteria	$kg_{X\ tb}\ m^{-3}\ h^{-1}$
$dC_{X_{tf}}$	dCXtf	Rate of change in the concentration of thermophilic fungi	$kg_{X\ tf}\ m^{-3}\ h^{-1}$
$Depth_{cb}$	DepthCB	Depth of compost bed	m
$Depth_{cl}$	DepthCL	Depth of each increment in the compost bed	m
Dia	Dia	Inside diameter of compost vessel	m
dT	dT	Rate of change of temperature	$K\ h^{-1}$
$dT_{aeration}$	dTa	Rate of change in heat due to aeration	$K\ h^{-1}$
dT_{loss}	dTq	Rate of change in heat a result of heat loss through compost vessel wall	$K\ h^{-1}$
$dT_{produced}$	dTp	Rate of change in heat produced as a result of decomposition	$K\ h^{-1}$
$dWst$	dWst	Total mass of water per increment of substrate	$kg_w\ kg_s^{-1}$
F_{air}	Fair	Volume of air flowing into the reactor	$L\ h^{-1}$
H	H	Humidity ratio	$kg_w\ kg_{da}^{-1}$
h	h	Enthalpy of air-vapor mixture	$kJ\ kg_{da}^{-1}$
h'_{fg}	hprimefg	Latent heat of vaporization at T_{wb}	$J\ kg^{-1}$
h''_{fg}	h2primefg	Latent heat of vaporization T_{dp}	$J\ kg^{-1}$

ip	ip	Indexing notation representing all nodes from 1 to p [ip=(1,p)]. Is part of the cell reference number (k,ip) identifying the cell's location: k equals the time step whose length is defined by Δt, and ip equals the different levels within the composter reactor. Increment $ip = 1$ represents the increment below the compost vessel, the atmospheric layer from which air is drawn to aerate the compost bed. Increment $ip = 2$ represents the bottom increment or first layer of compost in the vessel.	(no units)
k	k	Indexing notation representing the time step. Is part of the cell reference number (k,ip) identifying the cell's location: k equals the time step whose length is defined by Δt, and ip equals the different levels within the composter reactor.	(no units)
k_{dm}	kdma	Fraction of mesophilic population which die each hour	$kg_{X\,m}\ kg_X^{-1}\ h^{-1}$
k_{dt}	kdmb	Fraction of mesophilic bacteria population which die each hour	$kg_{X\,t}\ kg_X^{-1}\ h^{-1}$
K_S	KS	'Half-velocity' coefficient for substrate	$kg_s\ m^{-3}$
K_{O_2}	KO2	'Half-velocity' coefficient for oxygen	$kg_{O2}\ m^{-3}$
k_{H_2O}	k_H20	Moisture factor: factor that weights the effect of moisture present on microbial growth	(no units)
$Mfda$	Mfda	Mass flow of dry air	$kg_{da}\ h^{-1}$
p	p	Number of nodes. Number of nodes equal the number of increments or layers the compost bed is sectioned into for analysis (d) plus 1 for increment below container.	(no unit)
P_{atm}	Patm	Atmospheric pressure at sea level	Pa *or* $kg\ m^{-1}\ sec^{-2}$
P_{sa}	Psa	Saturation vapor pressure at atmospheric pressure	Pa *or* $kg\ m^{-1}\ sec^{-2}$
P_{swb}	Pswb	Saturation vapor pressure at wet bulb temperature	Pa *or* $kg\ m^{-1}\ sec^{-2}$

P_v	Pv	Partial vapor pressure	Pa *or* kg m^{-1} sec^{-2}
q_m	qm	Sensible heat stored in compost material	kJ m^{-3}
R_T	RT	Thermal resistance of compost vessel wall	K m^{-2} h J^{-1} h^{-1}
S_c	Sc	Mass of cellulose/hemicellulose substrate	kg_{sc}
S_i	Si	Mass of inert substrate	kg_{si}
S_l	Sl	Mass of lignin substrate	kg_{sl}
S_s	Ss	Mass of soluble substrate	kg_{ss}
S_{sc}	Ssc	Total mass of cellulose/hemicellulose substrate per layer	kg_{sc}
S_{si}	Ssi	Total mass of inert substrate per layer	kg_{si}
S_{sl}	Ssl	Total mass of lignin substrate per layer	kg_{sl}
S_{ss}	Sss	Total mass of soluble substrate per layer	kg_{ss}
S_{st}	St	Total mass of all substrate per layer	kg_s
S_t	St	Total mass of all substrate	kg_s
T	T	Temperature in degrees Kelvin (K=ºC+273.16)	K
t	t	Time. Time is required to be in hours. If minutes are required need to use fraction i.e.(45/60)or 0.75 hours	h
T_C	Tc	Dry bulb (ambient) temperature in degrees Celsius	ºC
$T_{C_{m\max}}$	Tcmmax	Maximum temperature for mesophilic organisms in degrees Celsius	ºC
$T_{C_{m\min}}$	Tcmmin	Minimum temperature for mesophilic organisms in degrees Celsius	ºC

$T_{C_{t\max}}$	Tctmax	Maximum temperature for thermophilic organisms in degrees Celsius	ºC
$T_{C_{t\min}}$	Tctmin	Minimum temperature for thermophilic organisms in degrees Celsius	ºC
$T_{C_{wb}}$	Tcwb	Initial wet bulb temperature in degrees Celsius	ºC
T_{dp}	Tdp	Dew point temperature in degrees Kelvin	K
$T_{m\max}$	Tmmax	Maximum temperature for mesophilic organisms in degrees Kelvin	K
$T_{m\min}$	Tmmin	Menuhin temperature for mesophilic organisms in degrees Kelvin	K
t_{step}	Time_Step	Increment of time for each time step	h
t_{stop}	Time_Stop	Time at which the run will terminate	h
$T_{t\max}$	Ttmax	Maximum temperature for thermophilic organisms in degrees Kelvin	K
$T_{t\min}$	Ttmin	Minimum temperature for thermophilic organisms in degrees Kelvin	K
T_{wb}	Twb	Wet bulb temperature in degrees Kelvin	K
V_{air}	Vair	Volume flow of air	$m^3\ h^{-1}$
V_{csa}	Vcsa	Cross sectional area of volume of compost bed: for a cylinder vessel ($\pi * r^2$)	m^2
Vol_{cb}	VolCB	Total volume of compost bed ($\pi * r^2 * h$)	m^3
Vol_{cl}	VolCL	Volume of compost in each layer	m^3
V_{sa}	Vsa	Specific volume of dry air (ideal gas equation)	$m^3\ kg_{da}^{-1}$

W_{add}	Wadd	Mass of water added to the substrate	kg_w
W_{mc}	Mcw	Moisture content (wet bases) the fraction of mass of water compared to the mass of all ingredients, both water and substrate. Is measured by drying the substrate at 104 ºC for 24 hours.	$kg_w\ kg_{w\&s}^{-1}$
W_s	Wss	Mass of water present in substrate initially	kg_w
W_{st}	Wst	Mass of water per increment of substrate	kg_w
W_t	Wt	Total mass of water ($W_s + W_{add}$)	kg_w
$Y_{CO_2/S_{sc}}$	YCO2Ssc	Yield coefficient: amount of carbon dioxide produced per unit mass of cellulose/hemicellulose substrate utilized (decomposed)	$kg_{CO2}\ kg_{sc}^{-1}$
$Y_{CO_2/S_{sl}}$	YCO2Ssl	Yield coefficient: amount of carbon dioxide produced per unit mass of lignin substrate utilized (decomposed)	$kg_{CO2}\ kg_{sl}^{-1}$
$Y_{CO_2/S_{ss}}$	YCO2Sss	Yield coefficient: amount of carbon dioxide produced per unit mass of soluble substrate utilized (decomposed)	$kg_{CO2}\ kg_{ss}^{-1}$
$Y_{O_2/S_{sc}}$	YO2Ssc	Yield coefficient: amount of oxygen consumed per mass of cellulose/hemicellulose substrate utilized	$kg_{O2}\ kg_{sc}^{-1}$
$Y_{O_2/S_{sl}}$	YO2Ssl	Yield coefficient: amount of oxygen consumed per mass of lignin substrate utilized	$kg_{O2}\ kg_{sl}^{-1}$
$Y_{O_2/S_{ss}}$	YO2Sss	Yield coefficient: amount of oxygen consumed per mass of soluble substrate utilized	$kg_{O2}\ kg_{ss}^{-1}$
$Y_{W/S_{sc}}$	YWSsc	Yield coefficient: amount of water generated per unit mass of cellulose/hemicellulose substrate utilized (decomposed)	$kg_w\ kg_{sc}^{-1}$
$Y_{W/S_{sl}}$	YWSsl	Yield coefficient: amount of water generated per unit mass of lignin substrate utilized (decomposed)	$kg_w\ kg_{sl}^{-1}$
$Y_{W/S_{ss}}$	YWSss	Yield coefficient: amount of water generated per unit mass of soluble substrate utilized (decomposed)	$kg_w\ kg_{ss}^{-1}$

$Y_{X_a/S_{sc}}$	YXaSsc	Yield coefficient: amount of actinomycetes-biomass produced per unit mass of cellulose/hemicellulose substrate utilized (decomposed)	$kg_{Xa}\ kg_{sc}^{-1}$
$Y_{X_b/S_{ss}}$	YXbSss	Yield coefficient: amount of bacteria-biomass produced per unit mass of soluble substrate utilized (decomposed)	$kg_{Xb}\ kg_{ss}^{-1}$
$Y_{X_f/S_{sl}}$	YXfSsl	Yield coefficient: amount of fungi-biomass produced per unit mass of lignin substrate utilized (decomposed)	$kg_{Xf}\ kg_{sl}^{-1}$
$\Delta h_{C_{sc}}^{T}$	HCsc	Heat of combustion of cellulose/hemicellulose substrate consumed	$kJ\ kg_{sc}^{-1}$
$\Delta h_{C_{sl}}^{T}$	HCsl	Heat of combustion of lignin substrate consumed	$kJ\ kg_{sl}^{-1}$
$\Delta h_{C_{ss}}^{T}$	HCss	Heat of combustion of soluble substrate consumed	$kJ\ kg_{ss}^{-1}$
Δt	Delta_t	Time increments between each time step	h
μ_{ma}	muma	Specific growth rate for mesophilic actinomycetes	hr^{-1}
$\mu_{\max ma}$	mumaxma	Maximum specific growth rate for mesophilic actinomycetes	hr^{-1}
$\mu_{\max mb}$	mumaxmb	Maximum specific growth rate for mesophilic bacteria	hr^{-1}
$\mu_{\max mf}$	mumaxmf	Maximum specific growth rate for mesophilic fungi	hr^{-1}
$\mu_{\max ta}$	mumaxta	Maximum specific growth rate for thermophilic actinomycetes	hr^{-1}
$\mu_{\max tb}$	mumaxtb	Maximum specific growth rate for thermophilic bacteria	hr^{-1}
$\mu_{\max tf}$	mumaxtf	Maximum specific growth rate for thermophilic fungi	hr^{-1}
μ_{mb}	mumb	Specific growth rate for mesophilic bacteria	hr^{-1}

μ_{mf}	muma	Specific growth rate for mesophilic fungi	hr^{-1}
μ_{ta}	mutb	Specific growth rate for thermophilic bacteria	hr^{-1}
μ_{tb}	mutb	Specific growth rate for thermophilic bacteria	hr^{-1}
μ_{tf}	muta	Specific growth rate for thermophilic fungi	hr^{-1}
η_{ma}	numa	Microbial maintenance coefficient for mesophilic actinomycetes	h^{-1}
$\eta_{\max m}$	numaxm	Maximum microbial maintenance coefficient for mesophilic microorganisms	h^{-1}
$\eta_{\max t}$	numaxt	Maximum microbial maintenance coefficient for thermophilic microorganisms	h^{-1}
η_{ma}	numb	Microbial maintenance coefficient for mesophilic bacteria	h^{-1}
η_{ma}	numf	Microbial maintenance coefficient for mesophilic fungi	h^{-1}
η_{ta}	nuta	Microbial maintenance coefficient for thermophilic actinomycetes	h^{-1}
η_{ta}	nutb	Microbial maintenance coefficient for thermophilic bacteria	h^{-1}
η_{ta}	nutf	Microbial maintenance coefficient for thermophilic fungi	h^{-1}

Appendix B - Pictures

Figure B.1 Reactor tubes wrapped and unwrapped.

Figure B.2 Support plate for composting material. View from bottom.

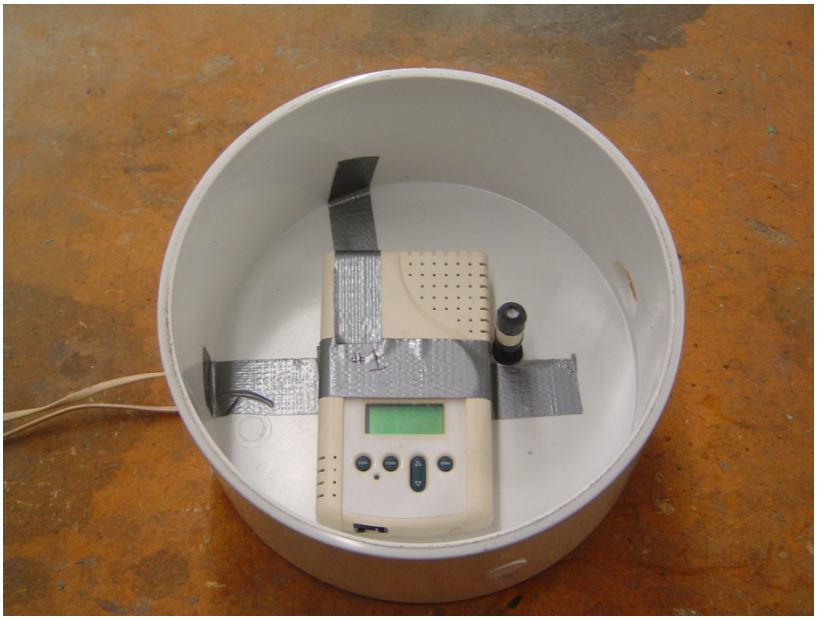

Figure B.3 Inside the top reactor cap displaying the carbon dioxide and relative humidity sensors.

Figure B.4 View inside the reactor tube from the bottom with the 0-cm thermocouple probe installed.

Figure B.5 The datalogger (center) and four multiplexers with thermocouples connected.

Figure B.6 Water bath was set up to provide 60% relative humidity air.

The water bath is a hot water heater. Yellow hose is connected to shop air compressor and to the pressure reducing valve. Air is fed into cold water port and out the hot water port. Red hose is connected the hot water port and to the air manifold (shown on table during test).

a.

b.

c.

d.

Figure B.7 The four ingredients: (a) pine shavings; (b) wheat straw; (c) silage (corn); and, (d) manure (cattle).

a.

b.

c.

d.

Figure B.8 Mixing of the ingredients: (a) weighting out each ingredient; (b) mixing the mixture and pouring into container; (c) reactor tube ready for placement of mixture; and, (d) view into reactor tube.

a.

b.

c.

Figure B.9 The three mixtures: (a) Mixture 1: slower-to-biodegrade; (b) Mixture 2: resistant-to-biodegradation; and (c) Mixture 3: readily-biodegradable.

Figure B.10 Top end cap with wax applied. Exit air hole is visible.

Figure B.11 Experimental setup.

Each reactor is in place with thermocouple probes installed, and its air supply hose connected to inlet port at base of reactor and to air supply meter on manifold. Thermocouple wires are connected to multiplex which is connected to data logger. Power supply for data logger, located on floor under table, is connected. Power supply is two, 12-volt car batteries connected in series. Data logger, relative-humidity sensors and CO_2 sensors are connected to the computer. Air supply hose (red) is connected to air manifold.

a.

c.

b.

d.

Figure B.12 Readily-biodegradable. View into Mixture 3 reactor tubes at time each was removed from the system and sampled: (a) Reactor C4 at Hour 163.5; (b) Reactor C3 at Hour 326.5; (c) Reactor C1 at Hour 552; and, (d) Reactor C2 at Hour 974.5.

View shows the amount of volume reduction. Cause was due to substrate reduction. Some volume reduction could be due to movement of tube causing settling.

a.

b.

c.

d.

Figure B.13 Readily-biodegradable. Mixture 3 reactor tube C1, removed at Hour 552, shows the results of volume reduction, temperature, and moisture: (a) Side view of Reactor C1 showing the position of the thermocouple probes. Probes were inserted to be in a horizontal position. Probes moved to approximately 45° to the horizontal. (b) View into reactor tube showing volume reduction. (c) A closer view into tube showing thermocouple probe bent. (d) Thermocouple probes laid out for inspection. Probe for 10-cm layer is at bottom.

a.

b.

c.

Figure B.14 Readily-biodegradable. Mixture 3 composted material consistency when removed: (a) Reactor C4 at Hour 163.5; (b) Reactor C3 at Hour 326.5; and, (c) Reactor C1 at Hour 552.

a.

c.

b.

d.

Figure B.15 Slower-to-biodegrade: View into Mixture 1 reactor tubes at time each was removed from the system and sampled: (a) Reactor A4 at Hour 164.5; (b) Reactor A3 at Hour 328; (c) Reactor A2 at Hour 550.5; and, (d) Reactor A1 at Hour 550.

View shows the amount of volume reduction. Reduction was probably as a result of both substrate reduction and settling due to movement of tube.

a.

b.

c.

Figure B.16 Slower-to-biodegrade. Mixture 1 composted material consistency when removed: (a) Reactor A4 at Hour 164.5; (b) Reactor A3 at Hour 328; and, (c) Reactor A2 at Hour 550.5.

a.

c.

b.

d.

Figure B.17 Resistant-to-biodegradation. View into Mixture 2 reactor tubes at time each was removed from the system and sampled: (a) Reactor B4 at Hour 164.5; (b) Reactor B3 at Hour 328; (c) Reactor B2 at Hour 550; and, (d) Reactor B1 at Hour 550.

View shows the amount of volume reduction. Causes could be due to substrate reduction. More likely due to movement of tube caused settling.

Figure B.18 Resistant-to-biodegradation. Side view of Reactor B2 just before removal from system at Hour 550.

All thermocouple probes were inserted into each tube in a horizontal position. Note the thermocouple probes on left side this tube are not quite in the horizontal position. This change in position is likely due to settling of the mixture.

a.

b.

c.

Figure B.19 Resistant-to-biodegradation. Mixture 2 composted material consistency when removed: (a) Reactor B4 at Hour 164.5; (b) Reactor B3 at Hour 328; and, (c) Reactor B2 at Hour 550.

Appendix C - Analytical Laboratory Results

Laboratory results 6321-6324 (R1) 1 Nov 07

Analytical Services Lab												
202 Weber												
Kansas State University												
Results for:	Phil Woodford											11/1/2007
			% Dry	% Crude			%AD	%	%	%		
Sample#	Sample ID		Matter	Protein **	%NDF	%ADF	Lignin	Cellulose	Hemicellulose	Lignin		
6321	Wheat Straw		89.9	5.4	76.6	56.6	13.1	44.5	20.0	6.1		
6322	Pine Shavings		90.1	0.6	93.9	80.1	24.3	55.8	13.9	22.5		
6323	Corn Silage		36.3	9.3	42.2	24.3	3.4	20.8	18.0	2.0		
6324	Manure # 2		34.9	25.9	39.7	14.9	4.0	11.0	24.7	1.8		
			**A 6.25 conversion factor is used to calculate % Crude Protein.									
			Results are reported on a 100% Dry Matter Basis.									

Laboratory Analysis 9921-9963 (R1) May 08

Analytical Services Lab												
202 Weber												
Kansas State University												
Results for:	Phil Woodford											5/15/2008
			% Dry	% Crude			%AD	%	%	%		
Sample#	Sample ID		Matter	Protein **	%NDF	%ADF	Lignin	Cellulose	Hemicellulose	Lignin		
9921	Substrate 1 Manure		31.9	26.7	36.9	23.0	13.5	9.5	13.9	3.7		
	24-Feb-08											
9922	# 9 40-50 cm		23.2	19.2	49.9	40.5	18.9	21.6	9.4	6.9		
	9-Mar-08											
9923	# 9 0-10 cm		34.4	18.4	40.4	29.9	13.6	16.3	10.5	5.7		
	9-Mar-08											
9924	C1 30-40 cm		16.7	21.0	51.2	46.0	19.5	26.5	4.1	9.7		
	18-Mar-08											
9925	# 9 60-70 cm		22.7	16.8	42.1	32.1	12.1	20.0	10.0	5.6		
	9-Mar-08											
9926	# 6 0-10 cm		28.3	22.9	36.3	33.4	18.2	15.3	3.9	9.1		
	5-Apr-08											
9927	# 6 40-50 cm		19.4	19.3	44.4	41.1	15.5	25.6	3.3	6.9		
	5-Apr-08											
9928	# 6 10-20 cm		21.4	21.5	39.3	35.2	19.3	16.0	4.1	10.0		
	5-Apr-08											
9929	# 6 20-30 cm		18.9	22.4	38.9	38.2	24.3	13.9	0.7	11.1		
	5-Apr-08											

9930	C1 0-10 cm		35.9	21.0	38.4	30.7	14.6	16.1	6.7	6.7		
	18-Mar-08											
9931	C1 10-20 cm		19.3	19.9	41.8	41.5	16.2	24.3	0.3	9.0		
	18-Mar-08											
9932	C1 50-60 cm		19.3	18.8	45.6	38.9	13.9	25.0	6.7	6.2		
	18-Mar-08											
9933	Mixture 1 Initial		55.2	13.4	65.3	46.7	12.1	35.5	16.7	8.9		
	24-Feb-08											
9934	Substrate 4 Pine Shavings		90.2	0.6	98.0	78.9	25.2	53.8	19.1	23.7		
	24-Feb-08											
9935	Substrate 3 Wheat Straw		93.1	6.7	74.7	53.1	12.4	40.7	21.6	6.1		
	24-Feb-08											
9936	Substrate 2 Silage		36.8	10.2	36.8	23.0	3.4	19.5	13.8	2.0		
	24-Feb-08											
9937	Mixture 3 Initial		34.2	16.8	30.5	20.1	6.9	13.2	10.4	2.7		
	24-Feb-08											
9938	# 9 20-30 cm		29.7	16.5	38.6	29.9	11.2	18.7	8.7	4.3		
	9-Mar-08											
9939	Tube 12 0-10 cm		34.7	18.5	36.6	25.1	8.7	16.5	12.5	3.4		
	2-Mar-08											
9940	Tube 12 60-70 cm		32.7	18.8	34.0	20.7	6.7	14.0	13.3	2.7		
	2-Mar-08											
9941	Tube 12 20-30 cm		31.7	18.9	33.0	20.8	6.7	14.1	12.2	2.7		
	2-Mar-08											
9942	Tube 12 40-50 cm		33.4	19.8	36.1	23.3	8.7	14.5	12.8	2.7		
	2-Mar-08											
9943	# 7 20-30 cm		48.4	16.6	69.3	50.8	13.9	36.9	18.5	10.4		
	9-Mar-08											
9944	# 8 60-70 cm		65.1	21.1	75.2	63.4	20.4	43.0	11.8	18.3		
	9-Mar-08											

9945	#10 40-50 cm		50.3	16.9	70.9	51.9	13.3	38.7	19.0	9.6		
	2-Mar-08											
9946	# 7 0-10 m		64.1	16.8	68.8	52.3	13.7	38.6	16.6	10.7		
	9-Mar-08											
9947	Mixture 2 Initial		66.6	21.0	76.8	58.8	19.0	39.8	19.0	16.6		
	24-Feb-08											
9948	# 7 60-70 cm		49.8	18.6	64.4	46.5	13.7	33.8	16.9	10.6		
	9-Mar-08											
9949	# 8 0-10 cm		78.6	23.0	74.8	60.1	19.3	40.8	14.7	18.1		
	9-Mar-08											
9950	A2 20-30 cm		52.0	16.1	73.0	53.3	14.5	38.8	19.7	11.1		
	18-Mar-08											
9951	A2 40-50 cm		50.3	16.3	69.0	50.2	13.4	36.8	18.8	10.1		
	18-Mar-08											
9952	# 11 60-70 cm		64.2	16.5	78.6	64.3	20.4	43.9	14.3	18.9		
	2-Mar-08											
9953	# 8 20-30 cm		68.4	20.3	76.4	63.8	20.5	43.3	13.6	19.0		
	9-Mar-08											
9954	# 7 40-50 cm		46.7	16.7	69.2	52.5	14.0	38.5	16.7	11.0		
	9-Mar-08											
9955	# 11 40-50 cm		65.6	16.3	78.6	66.6	20.6	46.0	12.0	19.2		
	2-Mar-08											
9956	# 10 20-30 cm		50.0	14.9	66.4	50.4	13.6	36.8	16.9	10.0		
	2-Mar-08											
9957	# 8 40-50 cm		65.8	20.5	76.4	61.7	19.8	41.9	14.7	18.2		
	9-Mar-08											
9958	# 10 60-70 cm		46.6	15.0	68.0	48.9	13.6	35.3	19.1	9.9		
	2-Mar-08											
9959	# 10 0-10 cm		58.0	15.0	65.0	48.2	11.7	36.4	16.9	9.5		
	2-Mar-08											
9960	A2 60-70 cm		50.7	15.1	69.8	53.2	14.2	38.9	16.7	10.9		
	18-Mar-08											

9961	A2 0-10 cm		76.9	16.1	66.5	52.1	13.5	38.7	15.4	10.2		
	18-Mar-08											
9962	# 11 20-30 cm		65.3	18.7	79.1	66.5	21.1	45.4	12.7	19.7		
	2-Mar-08											
9963	# 11 0-10 cm		70.1	16.5	78.9	61.1	19.2	42.0	16.7	16.6		
	2-Mar-08											
			**A 6.25 conversion factor is used to calculate % Crude Protein.									
			Results are reported on a 100% Dry Matter Basis.									

Appendix D - Data Analysis by Reactor

Slower-to-Degrade **Analysis: By Layer**
Lab Results, 15 May 08
A2 Reactor 4 p. 1 of 3
Mixture 1
Run time: 550.5 hr

		Dry Basis Soluble	Cell / Hemi	Lignin	Ash / Inorganic	Wet Basis Water	Soluble	Cell / Hemi	Lignin	Ash / Inorganic
A2 0-10 cm		32.5%	54.1%	10.2%	3.3%	23.13	24.95	41.56	7.85	2.50
A2 20-30 cm		27.0%	58.5%	11.1%	3.3%	47.97	14.04	30.45	5.80	1.73
A2 40-50 cm		31.0%	55.6%	10.1%	3.3%	49.67	15.60	27.98	5.11	1.64
A2 60-70 cm		30.2%	55.6%	10.9%	3.3%	49.30	15.30	28.19	5.54	1.67
Mixture 1	initial	34.7%	53.2%	8.9%	3.2%	44.77	19.14	29.39	4.93	1.76

Layer		conversion factor dry to wet	percent composition	wet weight per unit of dry	% of water	water present per unit	Layer	Wet Weght per X **kg** of dry	Dry Weight per X kg	Water Weight per X **kg** of Substrate
0-10 cm	SOLUBLE	1.301	0.325	0.4223	0.231	0.098	0-10 cm	**0.422**	**0.325**	**0.098**
	CELL/HEMI	1.301	0.541	0.7034	0.231	0.163		**0.703**	**0.541**	**0.163**
	LIGNIN	1.301	0.102	0.1329	0.231	0.031		**0.133**	**0.102**	**0.031**
	ASH/INORG	1.301	0.033	0.0423	0.231	0.010		**0.042**	**0.033**	**0.010**
20-30	SOLUBLE	1.922	0.270	0.5187	0.480	0.249	20-30	**0.519**	**0.270**	**0.249**
	CELL/HEMI	1.922	0.585	1.1250	0.480	0.540		**1.125**	**0.585**	**0.540**
	LIGNIN	1.922	0.111	0.2143	0.480	0.103		**0.214**	**0.111**	**0.103**
	ASH/INORG	1.922	0.033	0.0640	0.480	0.031		**0.064**	**0.033**	**0.031**
40-50	SOLUBLE	1.987	0.310	0.6160	0.497	0.306	40-50	**0.616**	**0.310**	**0.306**
	CELL/HEMI	1.987	0.556	1.1045	0.497	0.549		**1.105**	**0.556**	**0.549**
	LIGNIN	1.987	0.101	0.2016	0.497	0.100		**0.202**	**0.101**	**0.100**
	ASH/INORG	1.987	0.033	0.0649	0.497	0.032		**0.065**	**0.033**	**0.032**
60-70	SOLUBLE	1.972	0.302	0.5950	0.493	0.293	60-70	**0.595**	**0.302**	**0.293**
	CELL/HEMI	1.972	0.556	1.0966	0.493	0.541		**1.097**	**0.556**	**0.541**
	LIGNIN	1.972	0.109	0.2156	0.493	0.106		**0.216**	**0.109**	**0.106**
	ASH/INORG	1.972	0.033	0.0650	0.493	0.032		**0.065**	**0.033**	**0.032**

Slower-to-Degrade
Lab Results, 15 May 08
A2 Reactor 4 p. 2 of 3
Mixture 1
Run time: 550.5 hr

Multiplication Factor
No. of times unit values are multiplied
1.5485 to equal substrate weight in reactor
2.84 Final Weight

Actual / Projected Values

Layer		Wet Weight per X **kg** of d	Dry Weight per X kg	Water Weight X **kg** of Substrate	weighted value cm in layer / 10
0-10 cm	Soluble	0.654	0.503	0.151	1.00
	Cell/Hemic	1.089	0.837	0.252	
	Lignin	0.206	0.158	0.048	
	Ash/Inorga	0.065	0.050	0.015	
10-20 cm	Soluble	0.729	0.460	0.268	1.00
	Cell/Hemic	1.416	0.872	0.544	
	Lignin	0.269	0.165	0.103	
	Ash/Inorga	0.082	0.051	0.031	
20-30 cm	Soluble	0.803	0.418	0.385	1.00
	Cell/Hemic	1.742	0.906	0.836	
	Lignin	0.332	0.173	0.159	
	Ash/Inorga	0.099	0.052	0.048	
30-40 cm	Soluble	0.879	0.449	0.430	1.00
	Cell/Hemic	1.726	0.884	0.843	
	Lignin	0.322	0.165	0.157	
	Ash/Inorga	0.100	0.051	0.049	
40-50 cm	Soluble	0.954	0.480	0.474	1.00
	Cell/Hemic	1.710	0.861	0.850	
	Lignin	0.312	0.157	0.155	
	Ash/Inorga	0.101	0.051	0.050	
50-60 cm	Soluble	0.938	0.474	0.464	1.00
	Cell/Hemic	1.704	0.861	0.843	
	Lignin	0.323	0.163	0.160	
	Ash/Inorga	0.101	0.051	0.050	
60-70 cm	Soluble	0.921	0.467	0.454	1.00
	Cell/Hemic	1.698	0.861	0.837	
	Lignin	0.334	0.169	0.165	
	Ash/Inorga	0.101	0.051	0.050	
70-80 cm	Soluble	0.921	0.467	0.454	0.81
	Cell/Hemic	1.698	0.861	0.837	
	Lignin	0.334	0.169	0.165	
	Ash/Inorga	0.101	0.051	0.050	
Total Weight		22.763	12.388	10.375	7.81

Weighted Values
Times Number of cm present

Wet Weight per X **kg** of dr	Dry Weight per X kg	Water Weight X **kg** of Substrate	Moisture fraction
0.654	0.503	0.151	
1.089	0.837	0.252	
0.206	0.158	0.048	
0.065	0.050	0.015	
2.014	1.549	0.466	0.231
0.729	0.460	0.268	
1.416	0.872	0.544	
0.269	0.165	0.103	
0.082	0.051	0.031	
2.495	1.549	0.947	0.379
0.803	0.418	0.385	
1.742	0.906	0.836	
0.332	0.173	0.159	
0.099	0.052	0.048	
2.976	1.549	1.428	0.480
0.879	0.449	0.430	
1.726	0.884	0.843	
0.322	0.165	0.157	
0.100	0.051	0.049	
3.027	1.549	1.478	0.488
0.954	0.480	0.474	
1.710	0.861	0.850	
0.312	0.157	0.155	
0.101	0.051	0.050	
3.077	1.549	1.528	0.497
0.938	0.474	0.464	
1.704	0.861	0.843	
0.323	0.163	0.160	
0.101	0.051	0.050	
3.065	1.549	1.517	0.495
0.921	0.467	0.454	
1.698	0.861	0.837	
0.334	0.169	0.165	
0.101	0.051	0.050	
3.054	1.549	1.505	0.493
0.746	0.378	0.368	
1.375	0.697	0.678	
0.270	0.137	0.133	
0.082	0.041	0.040	
2.474	1.254	1.219	0.493
22.183	12.094	10.089	0.455
2.840	1.549	1.292	

Total Weight
kg 2.840 Dry kg 1.549 Water kg 1.292

Moisture (fraction) 0.455

Soluble

Layer	wet	dry	water
0-10 cm	0.654	0.503	0.151
10-20 cm	0.729	0.460	0.268
20-30 cm	0.803	0.418	0.385
30-40 cm	0.879	0.449	0.430
40-50 cm	0.954	0.480	0.474
50-60 cm	0.938	0.474	0.464
60-70 cm	0.921	0.467	0.454
70-80 cm	0.746	0.378	0.368
subtotal	6.623	3.629	2.994
Ave	0.848	0.465	0.383

Cellulose / Hemicellulose

	wet	dry	water
0-10 cm	1.089	0.837	0.252
10-20 cm	1.416	0.872	0.544
20-30 cm	1.742	0.906	0.836
30-40 cm	1.726	0.884	0.843
40-50 cm	1.710	0.861	0.850
50-60 cm	1.704	0.861	0.843
60-70 cm	1.698	0.861	0.837
70-80 cm	1.375	0.697	0.678
subtotal	12.461	6.779	5.682
Average	1.596	0.868	0.728

Lignin

	wet	dry	water
0-10 cm	0.206	0.158	0.048
10-20 cm	0.269	0.165	0.103
20-30 cm	0.332	0.173	0.159
30-40 cm	0.322	0.165	0.157
40-50 cm	0.312	0.157	0.155
50-60 cm	0.323	0.163	0.160
60-70 cm	0.334	0.169	0.165
70-80 cm	0.270	0.137	0.133
subtotal	2.368	1.288	1.080
Aveage	0.303	0.165	0.138

Ash / Inorganic

	wet	dry	water
0-10 cm	0.065	0.050	0.015
10-20 cm	0.082	0.051	0.031
20-30 cm	0.099	0.052	0.048
30-40 cm	0.100	0.051	0.049
40-50 cm	0.101	0.051	0.050
50-60 cm	0.101	0.051	0.050
60-70 cm	0.101	0.051	0.050
70-80 cm	0.082	0.041	0.040
subtotal	0.730	0.398	0.332
Aveage	0.094	0.051	0.043
ckeck on total	22.183	12.094	10.089
TOTAL	2.840	1.549	1.292

Slower-to-Degrade
Lab Results, 15 May 08
A2 Reactor 4 p. 3 of 3
Mixture 1
Run time 550.5 hours

	Total Wt	Water	Dry Matter	Soluble	Cell / Hemi	Lignin	Ash / Inorganic
		Dry Basis					
Initial		44.8%	55.2%	34.7%	53.2%	8.9%	3.2%
Final		45.48%	54.5%	30.0%	56.1%	10.6%	3.3%
Initial weight (kg)	3.18	1.42	1.76	0.61	0.93	0.157	0.06
Final weight (kg)	2.84	1.29	1.55	0.46	0.87	0.165	0.05
Difference (kg)	0.34	0.13	0.21	0.14	0.07	-0.008	0.01
Percent Change	10.7%	9.3%	11.8%	23.7%	7.1%	-5.1%	9.2%

Total Weight adjusted to 1.0

	Total Wt	Water	Dry Matter	Soluble	Cell / Hemi	Lignin	Ash / Inorganic
						Dry Basis	
Initial weight (kg)	1.00	0.45	0.55	0.19	0.29	0.05	0.02
Final weight (kg)	0.89	0.41	0.49	0.15	0.27	0.05	0.02
Difference (kg)	0.11	0.04	0.07	0.05	0.02	0.00	0.00
Percent Change	10.7%	9.3%	11.8%	23.7%	7.1%	-5.1%	9.2%

Slower-to-Degrade **Analysis: By Layer**
Lab Results, 15 May 08
A3 Reactor 7 **p. 1 of 3**
Mixture 1
Run time 328 hours

		Dry Basis Soluble	Cell / Hemi	Lignin	Ash	Wet Basis Water	Soluble	Cell/Hemi	Lignin	sh / Inorganic
# 7 0-10 m		31.2%	55.2%	10.7%	3.0%	35.91	19.96	35.35	6.85	1.92
# 7 20-30 cm		30.7%	55.4%	10.4%	3.4%	51.59	14.87	26.83	5.05	1.66
# 7 40-50 cm		30.8%	55.2%	11.0%	3.0%	53.25	14.41	25.81	5.14	1.39
# 7 60-70 cm		35.6%	50.8%	10.6%	3.1%	50.19	17.71	25.28	5.28	1.54
Mixture 1	initial	34.7%	53.2%	8.9%	3.2%	44.77	19.14	29.39	4.93	1.76

Layer		conversion factor dry to wet	percent composition	wet weight per unit of dry	% of water	water present per unit
0-10 cm	SOLUBLE	1.560	0.312	0.4861	0.359	0.175
	CELL/HEMI	1.560	0.552	0.8607	0.359	0.309
	LIGNIN	1.560	0.107	0.1667	0.359	0.060
	ASH/INORG	1.560	0.030	0.0469	0.359	0.017
20-30 cm	SOLUBLE	2.066	0.307	0.6345	0.516	0.327
	CELL/HEMI	2.066	0.554	1.1448	0.516	0.591
	LIGNIN	2.066	0.104	0.2156	0.516	0.111
	ASH/INORG	2.066	0.034	0.0708	0.516	0.037
40-50 cm	SOLUBLE	2.139	0.308	0.6592	0.533	0.351
	CELL/HEMI	2.139	0.552	1.1812	0.533	0.629
	LIGNIN	2.139	0.110	0.2352	0.533	0.125
	ASH/INORG	2.139	0.030	0.0635	0.533	0.034
60-70 cm	SOLUBLE	2.008	0.356	0.7137	0.502	0.358
	CELL/HEMI	2.008	0.508	1.0188	0.502	0.511
	LIGNIN	2.008	0.106	0.2129	0.502	0.107
	ASH/INORG	2.008	0.031	0.0620	0.502	0.031

Layer	Wet Weght per X **kg** of dry	Dry Weight per X kg	Water Weight per X **kg** of Substrate
0-10 cm	**0.486**	**0.312**	**0.175**
	0.861	**0.552**	**0.309**
	0.167	**0.107**	**0.060**
	0.047	**0.030**	**0.017**
20-30 cm	**0.634**	**0.307**	**0.327**
	1.145	**0.554**	**0.591**
	0.216	**0.104**	**0.111**
	0.071	**0.034**	**0.037**
40-50 cm	**0.659**	**0.308**	**0.351**
	1.181	**0.552**	**0.629**
	0.235	**0.110**	**0.125**
	0.063	**0.030**	**0.034**
60-70 cm	**0.714**	**0.356**	**0.358**
	1.019	**0.508**	**0.511**
	0.213	**0.106**	**0.107**
	0.062	**0.031**	**0.031**

Slower-to-Degrade
Lab Results, 15 May 08
A3 Reactor 7 p. 2 of 3
Mixture 1
Run time 328 hours

Multiplication Factor
1.772 No. of times unit values are multiplied
3.490 Final Weight

Actual / Projected Values

Layer		Wet Weight per X **kg** of d	Dry Weight per X kg	Water Weight X **kg** of Substrate	weighted value cm in layer / 10
0-10 cm	Soluble	0.861	0.552	0.309	1.00
	Cell/Hemic	1.525	0.977	0.548	
	Lignin	0.295	0.189	0.106	
	Ash/Inorgani	0.083	0.053	0.030	
10-20 cm	Soluble	0.993	0.548	0.445	1.00
	Cell/Hemic	1.777	0.980	0.797	
	Lignin	0.339	0.187	0.152	
	Ash/Inorgani	0.104	0.057	0.047	
20-30 cm	Soluble	1.124	0.544	0.580	1.00
	Cell/Hemic	2.029	0.982	1.047	
	Lignin	0.382	0.185	0.197	
	Ash/Inorgani	0.126	0.061	0.065	
30-40 cm	Soluble	1.146	0.545	0.601	1.00
	Cell/Hemic	2.061	0.980	1.081	
	Lignin	0.399	0.190	0.210	
	Ash/Inorgani	0.119	0.057	0.062	
40-50 cm	Soluble	1.168	0.546	0.622	1.00
	Cell/Hemic	2.093	0.978	1.115	
	Lignin	0.417	0.195	0.222	
	Ash/Inorgani	0.113	0.053	0.060	
50-60 cm	Soluble	1.216	0.588	0.628	1.00
	Cell/Hemic	1.949	0.939	1.010	
	Lignin	0.397	0.191	0.206	
	Ash/Inorgani	0.111	0.054	0.058	
60-70 cm	Soluble	1.265	0.630	0.635	1.00
	Cell/Hemic	1.805	0.899	0.906	
	Lignin	0.377	0.188	0.189	
	Ash/Inorgani	0.110	0.055	0.055	
70-80 cm	Soluble	1.265	0.630	0.635	0.70
	Cell/Hemic	1.805	0.899	0.906	
	Lignin	0.377	0.188	0.189	
	Ash/Inorgani	0.110	0.055	0.055	
Total Weight		27.943	14.176	13.767	7.70

Weighted Values
Times Number of cm present

Wet Weght per X **kg** of dr	Dry Weight per X kg	Water Weight X **kg** of Substrate	Moisture fraction
0.861	0.552	0.309	
1.525	0.977	0.548	
0.295	0.189	0.106	
0.083	0.053	0.030	
2.765	1.772	0.993	0.359
0.993	0.548	0.445	
1.777	0.980	0.797	
0.339	0.187	0.152	
0.104	0.057	0.047	
3.213	1.772	1.441	0.448
1.124	0.544	0.580	
2.029	0.982	1.047	
0.382	0.185	0.197	
0.126	0.061	0.065	
3.660	1.772	1.888	0.516
1.146	0.545	0.601	
2.061	0.980	1.081	
0.399	0.190	0.210	
0.119	0.057	0.062	
3.725	1.772	1.953	0.524
1.168	0.546	0.622	
2.093	0.978	1.115	
0.417	0.195	0.222	
0.113	0.053	0.060	
3.790	1.772	2.018	0.533
1.216	0.588	0.628	
1.949	0.939	1.010	
0.397	0.191	0.206	
0.111	0.054	0.058	
3.674	1.772	1.902	0.518
1.265	0.630	0.635	
1.805	0.899	0.906	
0.377	0.188	0.189	
0.110	0.055	0.055	
3.557	1.772	1.785	0.502
0.885	0.441	0.444	
1.264	0.630	0.634	
0.264	0.132	0.133	
0.077	0.038	0.039	
2.490	1.240	1.250	0.502
26.876	13.644	13.231	0.492
3.490	1.772	1.718	

Total Weight kg 3.490 Dry kg 1.772 Water kg 1.718

Moisture (fraction) 0.492

Soluble

Layer	wet	dry	water
0-10 cm	0.861	0.552	0.309
10-20 cm	0.993	0.548	0.445
20-30 cm	1.124	0.544	0.580
30-40 cm	1.146	0.545	0.601
40-50 cm	1.168	0.546	0.622
50-60 cm	1.216	0.588	0.628
60-70 cm	1.265	0.630	0.635
70-80 cm	0.885	0.441	0.444
subtotal	8.659	4.395	4.265
Average	1.125	0.571	0.554

Cellulose / Hemicellulose

Layer	wet	dry	water
0-10 cm	1.525	0.977	0.548
10-20 cm	1.777	0.980	0.797
20-30 cm	2.029	0.982	1.047
30-40 cm	2.061	0.980	1.081
40-50 cm	2.093	0.978	1.115
50-60 cm	1.949	0.939	1.010
60-70 cm	1.805	0.899	0.906
70-80 cm	1.264	0.630	0.634
subtotal	14.503	7.366	7.137
Average	1.884	0.957	0.927

Lignin

Layer	wet	dry	water
0-10 cm	0.295	0.189	0.106
10-20 cm	0.339	0.187	0.152
20-30 cm	0.382	0.185	0.197
30-40 cm	0.399	0.190	0.210
40-50 cm	0.417	0.195	0.222
50-60 cm	0.397	0.191	0.206
60-70 cm	0.377	0.188	0.189
70-80 cm	0.264	0.132	0.133
subtotal	2.871	1.457	1.414
Average	0.373	0.189	0.184

Ash / Inorganic

Layer	wet	dry	water
0-10 cm	0.083	0.053	0.030
10-20 cm	0.104	0.057	0.047
20-30 cm	0.126	0.061	0.065
30-40 cm	0.119	0.057	0.062
40-50 cm	0.113	0.053	0.060
50-60 cm	0.111	0.054	0.058
60-70 cm	0.110	0.055	0.055
70-80 cm	0.077	0.038	0.039
subtotal	0.842	0.427	0.415
Average	0.109	0.055	0.054
ckeck on total	26.876	13.644	13.231
TOTAL	3.490	1.772	1.718

Slower-to-Degrade
Lab Results, 15 May 08
A3 Reactor 7 p. 3 of 3
Mixture 1
Run time 328 hours

	Total Wt	Water	Dry Matter	Soluble	Cell / Hemi	Lignin	Ash / Inorganic
		Dry Basis					
Initial		44.8%	55.2%	34.7%	53.2%	8.9%	3.2%
Final		49.2%	50.8%	32.2%	54.0%	10.7%	3.1%
Initial weight (kg)	3.61	1.62	1.99	0.69	1.06	0.178	0.064
Final weight (kg)	3.49	1.72	1.77	0.57	0.96	0.189	0.055
Difference (kg)	0.12	-0.10	0.22	0.12	0.10	-0.011	0.008
Percent Change	3.3%	-6.3%	11.1%	17.4%	9.8%	-6.3%	12.9%

Total Weight adjusted to 1.0

	Total Wt	Water	Dry Matter	Soluble	Cell / Hemi	Lignin	Ash / Inorganic
					Dry Basis		
Initial weight (kg)	1.00	0.45	0.55	0.19	0.29	0.049	0.018
Final weight (kg)	0.97	0.48	0.49	0.16	0.26	0.052	0.015
Difference (kg)	0.03	-0.03	0.06	0.03	0.03	-0.003	0.002
Percent Change	3.3%	-6.3%	11.1%	17.4%	9.8%	-6.3%	12.9%

Slower-to-Degrade **Analysis: By Layer**
Lab Results, 15 May 08
A4 Reactor 10 p. 1 of 3
Mixture 1
Run time: 164.5 hr

		Dry Basis Soluble	Cell / Hemi	Lignin	Ash / Inorganic	Wet Basis Water	Soluble	Cell / Hemi	Lignin	Ash / Inorganic
# 10 0-10 cm		35.0%	53.3%	9.5%	2.2%	41.96	20.29	30.94	5.53	1.28
# 10 20-30 cm		32.6%	53.8%	10.0%	3.6%	49.98	16.32	26.90	5.02	1.78
#10 40-50 cm		29.1%	57.6%	9.6%	3.6%	49.68	14.65	29.00	4.85	1.83
# 10 60-70 cm		32.0%	54.4%	9.9%	3.7%	53.37	14.91	25.39	4.62	1.72
Mixture 1	initial	34.7%	53.2%	8.9%	3.2%	44.77	19.14	29.39	4.93	1.76

Layer		conversion factor dry to wet	percent composition	wet weight per unit of dry	% of water	water present per unit		Wet Weght per X **kg** of dry	Dry Weight per X kg	Water Weight per X **kg** of Substrate
0-10 cm	SOLUBLE	1.723	0.350	0.6024	0.420	0.253	0-10 cm	**0.602**	**0.350**	**0.253**
	CELL/HEMI	1.723	0.533	0.9184	0.420	0.385		**0.918**	**0.533**	**0.385**
	LIGNIN	1.723	0.095	0.1642	0.420	0.069		**0.164**	**0.095**	**0.069**
	ASH/INORG	1.723	0.022	0.0379	0.420	0.016		**0.038**	**0.022**	**0.016**
20-30 cm	SOLUBLE	1.999	0.326	0.6523	0.500	0.326	20-30 cm	**0.652**	**0.326**	**0.326**
	CELL/HEMI	1.999	0.538	1.0748	0.500	0.537		**1.075**	**0.538**	**0.537**
	LIGNIN	1.999	0.100	0.2006	0.500	0.100		**0.201**	**0.100**	**0.100**
	ASH/INORG	1.999	0.036	0.0713	0.500	0.036		**0.071**	**0.036**	**0.036**
40-50 cm	SOLUBLE	1.987	0.291	0.5786	0.497	0.287	40-50 cm	**0.579**	**0.291**	**0.287**
	CELL/HEMI	1.987	0.576	1.1451	0.497	0.569		**1.145**	**0.576**	**0.569**
	LIGNIN	1.987	0.096	0.1914	0.497	0.095		**0.191**	**0.096**	**0.095**
	ASH/INORG	1.987	0.036	0.0722	0.497	0.036		**0.072**	**0.036**	**0.036**
60-70 cm	SOLUBLE	2.145	0.320	0.6855	0.534	0.366	60-70 cm	**0.686**	**0.320**	**0.366**
	CELL/HEMI	2.145	0.544	1.1675	0.534	0.623		**1.168**	**0.544**	**0.623**
	LIGNIN	2.145	0.099	0.2123	0.534	0.113		**0.212**	**0.099**	**0.113**
	ASH/INORG	2.145	0.037	0.0791	0.534	0.042		**0.079**	**0.037**	**0.042**

Slower-to-Degrade
Lab Results, 15 May 08
A4 Reactor 10 p. 2 of 3
Mixture 1
Run time: 164.5 hr

Multiplication Factor
1.8892 No. of times unit values are multiplied
3.750 Final Weight

		Actual / Projected Values			weighted value	**Weighted Values** Times Number of cm present				
Layer		Wet Weght per X **kg** of d	Dry Weight per X kg	Water Weight X **kg** of Substrate	cm in layer / 10	Wet Weght per X **kg** of dr	Dry Weight per X kg	Water Weight X **kg** of Substrate	Moisture fraction	
0-10 cm	Soluble	1.138	0.661	0.477	1.00	1.138	0.661	0.477		
	Cell/Hemic	1.735	1.007	0.728		1.735	1.007	0.728		
	Lignin	0.310	0.180	0.130		0.310	0.180	0.130		
	Ash/Inorga	0.072	0.042	0.030		0.072	0.042	0.030		
						3.255	1.889	1.366	0.420	
10-20 cm	Soluble	1.185	0.639	0.547	1.00	1.185	0.639	0.547		
	Cell/Hemic	1.883	1.011	0.871		1.883	1.011	0.871		
	Lignin	0.345	0.185	0.160		0.345	0.185	0.160		
	Ash/Inorga	0.103	0.054	0.049		0.103	0.054	0.049		
						3.516	1.889	1.627	0.463	
20-30 cm	Soluble	1.232	0.616	0.616	1.00	1.232	0.616	0.616		
	Cell/Hemic	2.031	1.016	1.015		2.031	1.016	1.015		
	Lignin	0.379	0.190	0.189		0.379	0.190	0.189		
	Ash/Inorga	0.135	0.067	0.067		0.135	0.067	0.067		
						3.777	1.889	1.887	0.500	
30-40 cm	Soluble	1.163	0.583	0.579	1.00	1.163	0.583	0.579		
	Cell/Hemic	2.097	1.052	1.045		2.097	1.052	1.045		
	Lignin	0.370	0.186	0.185		0.370	0.186	0.185		
	Ash/Inorga	0.136	0.068	0.068		0.136	0.068	0.068		
						3.765	1.889	1.876	0.498	
40-50 cm	Soluble	1.093	0.550	0.543	1.00	1.093	0.550	0.543		
	Cell/Hemic	2.163	1.089	1.075		2.163	1.089	1.075		
	Lignin	0.362	0.182	0.180		0.362	0.182	0.180		
	Ash/Inorga	0.136	0.069	0.068		0.136	0.069	0.068		
						3.754	1.889	1.865	0.497	
50-60 cm	Soluble	1.194	0.577	0.617	1.00	1.194	0.577	0.617		
	Cell/Hemic	2.185	1.059	1.126		2.185	1.059	1.126		
	Lignin	0.381	0.184	0.197		0.381	0.184	0.197		
	Ash/Inorga	0.143	0.069	0.074		0.143	0.069	0.074		
						3.903	1.889	2.014	0.516	
60-70 cm	Soluble	1.295	0.604	0.691	1.00	1.295	0.604	0.691		
	Cell/Hemic	2.206	1.029	1.177		2.206	1.029	1.177		
	Lignin	0.401	0.187	0.214		0.401	0.187	0.214		
	Ash/Inorga	0.149	0.070	0.080		0.149	0.070	0.080		
						4.051	1.889	2.162	0.534	
70-80 cm	Soluble	1.295	0.604	0.691	0.75	0.971	0.453	0.518		
	Cell/Hemic	2.206	1.029	1.177		1.654	0.771	0.883		
	Lignin	0.401	0.187	0.214		0.301	0.140	0.161		
	Ash/Inorga	0.149	0.070	0.080		0.112	0.052	0.060		
						3.039	1.417	1.622	0.534	
Total Weight		30.073	15.114	14.959	7.75	29.060	14.641	14.419	0.496	
						3.750	1.889	1.860		

Total Weight kg	Dry kg	Water kg
3.750	1.889	1.860

Moisture (fraction) 0.496

Soluble

Layer	wet	dry	water
0-10 cm	1.138	0.661	0.477
10-20 cm	1.185	0.639	0.547
20-30 cm	1.232	0.616	0.616
30-40 cm	1.163	0.583	0.579
40-50 cm	1.093	0.550	0.543
50-60 cm	1.194	0.577	0.617
60-70 cm	1.295	0.604	0.691
70-80 cm	0.971	0.453	0.518
subtotal	9.272	4.683	4.589
Ave	1.196	0.604	0.592

Cellulose / Hemicellulose

Layer	wet	dry	water
0-10 cm	1.735	1.007	0.728
10-20 cm	1.883	1.011	0.871
20-30 cm	2.031	1.016	1.015
30-40 cm	2.097	1.052	1.045
40-50 cm	2.163	1.089	1.075
50-60 cm	2.185	1.059	1.126
60-70 cm	2.206	1.029	1.177
70-80 cm	1.654	0.771	0.883
subtotal	15.953	8.034	7.920
Average	2.058	1.037	1.022

Lignin

Layer	wet	dry	water
0-10 cm	0.310	0.180	0.130
10-20 cm	0.345	0.185	0.160
20-30 cm	0.379	0.190	0.189
30-40 cm	0.370	0.186	0.185
40-50 cm	0.362	0.182	0.180
50-60 cm	0.381	0.184	0.197
60-70 cm	0.401	0.187	0.214
70-80 cm	0.301	0.140	0.161
subtotal	2.849	1.434	1.415
Aveage	0.368	0.185	0.183

Ash / Inorganic

Layer	wet	dry	water
0-10 cm	0.072	0.042	0.030
10-20 cm	0.103	0.054	0.049
20-30 cm	0.135	0.067	0.067
30-40 cm	0.136	0.068	0.068
40-50 cm	0.136	0.069	0.068
50-60 cm	0.143	0.069	0.074
60-70 cm	0.149	0.070	0.080
70-80 cm	0.112	0.052	0.060
subtotal	0.986	0.491	0.495
Aveage	0.127	0.063	0.064

ckeck on total	29.060	14.641	14.419
TOTAL	3.750	1.889	1.860

Slower-to-Degrade
Lab Results, 15 May 08
A4 Reactor 10 p. 3 of 3
Mixture 1
Run time: 164.5 hr

	Total Wt	Water	Dry Matter	Soluble	Cell / Hemi	Lignin	Ash / Inorganic
		Dry Basis					
Initial		44.8%	55.2%	34.7%	53.2%	8.9%	3.2%
Final		49.6%	50.4%	32.0%	54.9%	9.8%	3.4%
Initial weight (kg)	3.81	1.71	2.10	0.73	1.12	0.188	0.067
Final weight (kg)	3.75	1.86	1.89	0.60	1.04	0.185	0.063
Difference (kg)	0.06	-0.15	0.21	0.13	0.08	0.003	0.004
Percent Change	1.6%	-9.1%	10.2%	17.2%	7.4%	1.5%	5.7%

Total Weight adjusted to 1.0

	Total Wt	Water	Dry Matter	Soluble	Cell / Hemi	Lignin	Ash / Inorganic
					Dry Basis		
Initial weight (kg)	1.00	0.45	0.55	0.19	0.29	0.049	0.018
Final weight (kg)	0.98	0.49	0.50	0.16	0.27	0.049	0.017
Difference (kg)	0.02	-0.04	0.06	0.03	0.02	0.001	0.001
Percent Change	1.6%	-9.1%	10.2%	17.2%	7.4%	1.5%	5.7%

Resistant-to-Biodegradation Analysis: By Layer
Lab Results, 15 May 08
B3 Reactor 8 p. 1 of 3
Mixture 2
Run time: 328 hr

		Dry Basis Soluble	Cell / Hemi	Lignin	Ash / Inorganic	Wet Basis Water	Soluble	Cell / Hemi	Lignin	Ash / Inorganic
# 8 0-10 cm		25.2%	55.5%	18.1%	1.2%	21.43	19.81	43.59	14.19	0.98
# 8 20-30 cm		22.6%	56.9%	19.0%	1.5%	31.61	15.43	38.93	12.98	1.05
# 8 40-50 cm		23.6%	56.6%	18.2%	1.6%	34.18	15.54	37.23	12.01	1.04
# 8 60-70 cm		24.8%	54.8%	18.3%	2.1%	34.87	16.17	35.69	11.90	1.36
Mixture 2	initial	22.2%	58.8%	17.6%	1.4%	32.39	14.99	39.78	11.90	0.94

Layer		conversion factor dry to wet	percent composition	wet weight per unit of dry	% of water	water present per unit	Layer	Wet Weght per X **kg** of dry	Dry Weight per X kg	Water Weight per X **kg** of Substrate
0-10 cm	SOLUBLE	1.273	0.252	0.3209	0.214	0.069	0-10 cm	**0.321**	**0.252**	**0.069**
	CELL/HEMI	1.273	0.555	0.7061	0.214	0.151		**0.706**	**0.555**	**0.151**
	LIGNIN	1.273	0.181	0.2298	0.214	0.049		**0.230**	**0.181**	**0.049**
	ASH/INORG	1.273	0.012	0.0159	0.214	0.003		**0.016**	**0.012**	**0.003**
20-30 cm	SOLUBLE	1.462	0.226	0.3300	0.316	0.104	20-30 cm	**0.330**	**0.226**	**0.104**
	CELL/HEMI	1.462	0.569	0.8322	0.316	0.263		**0.832**	**0.569**	**0.263**
	LIGNIN	1.462	0.190	0.2776	0.316	0.088		**0.278**	**0.190**	**0.088**
	ASH/INORG	1.462	0.015	0.0224	0.316	0.007		**0.022**	**0.015**	**0.007**
40-50 cm	SOLUBLE	1.519	0.236	0.3588	0.342	0.123	40-50 cm	**0.359**	**0.236**	**0.123**
	CELL/HEMI	1.519	0.566	0.8594	0.342	0.294		**0.859**	**0.566**	**0.294**
	LIGNIN	1.519	0.182	0.2772	0.342	0.095		**0.277**	**0.182**	**0.095**
	ASH/INORG	1.519	0.016	0.0240	0.342	0.008		**0.024**	**0.016**	**0.008**
60-70 cm	SOLUBLE	1.535	0.248	0.3813	0.349	0.133	60-70 cm	**0.381**	**0.248**	**0.133**
	CELL/HEMI	1.535	0.548	0.8414	0.349	0.293		**0.841**	**0.548**	**0.293**
	LIGNIN	1.535	0.183	0.2806	0.349	0.098		**0.281**	**0.183**	**0.098**
	ASH/INORG	1.535	0.021	0.0321	0.349	0.011		**0.032**	**0.021**	**0.011**

Resistant-to-Biodegradation
Lab Results, 15 May 08
B3 Reactor 8 p. 2 of 3
Mixture 2
Run time: 328 hr

Multiplication Factor
2.953 No. of times unit values are multiplied
4.320 Final Weight

		Actual / Projected Values				**Weighted Values** Times Number of cm present			
Layer		Wet Weight per X **kg** of d	Dry Weight per X kg	Water Weight X **kg** of Substrate	weighted value cm in layer / 10	Wet Weight per X **kg** of dr	Dry Weight per X kg	Water Weight X **kg** of Substrate	Moisture fraction
0-10 cm	Soluble	0.948	0.745	0.203	1.00	0.948	0.745	0.203	
	Cell/Hemic	2.085	1.638	0.447		2.085	1.638	0.447	
	Lignin	0.679	0.533	0.145		0.679	0.533	0.145	
	Ash/Inorga	0.047	0.037	0.010		0.047	0.037	0.010	
						3.758	2.953	0.805	0.214
10-20 cm	Soluble	0.961	0.705	0.256	1.00	0.961	0.705	0.256	
	Cell/Hemic	2.271	1.660	0.612		2.271	1.660	0.612	
	Lignin	0.749	0.547	0.202		0.749	0.547	0.202	
	Ash/Inorga	0.057	0.041	0.015		0.057	0.041	0.015	
						4.038	2.953	1.085	0.269
20-30 cm	Soluble	0.974	0.666	0.308	1.00	0.974	0.666	0.308	
	Cell/Hemic	2.458	1.681	0.777		2.458	1.681	0.777	
	Lignin	0.820	0.561	0.259		0.820	0.561	0.259	
	Ash/Inorga	0.066	0.045	0.021		0.066	0.045	0.021	
						4.318	2.953	1.365	0.316
30-40 cm	Soluble	1.017	0.682	0.335	1.00	1.017	0.682	0.335	
	Cell/Hemic	2.498	1.676	0.822		2.498	1.676	0.822	
	Lignin	0.819	0.550	0.269		0.819	0.550	0.269	
	Ash/Inorga	0.068	0.046	0.023		0.068	0.046	0.023	
						4.402	2.953	1.449	0.329
40-50 cm	Soluble	1.060	0.697	0.362	1.00	1.060	0.697	0.362	
	Cell/Hemic	2.538	1.670	0.867		2.538	1.670	0.867	
	Lignin	0.819	0.539	0.280		0.819	0.539	0.280	
	Ash/Inorga	0.071	0.047	0.024		0.071	0.047	0.024	
						4.487	2.953	1.534	0.342
50-60 cm	Soluble	1.093	0.715	0.377	1.00	1.093	0.715	0.377	
	Cell/Hemic	2.511	1.644	0.867		2.511	1.644	0.867	
	Lignin	0.824	0.539	0.284		0.824	0.539	0.284	
	Ash/Inorga	0.083	0.054	0.029		0.083	0.054	0.029	
						4.510	2.953	1.557	0.345
60-70 cm	Soluble	1.126	0.733	0.393	1.00	1.126	0.733	0.393	
	Cell/Hemic	2.485	1.618	0.866		2.485	1.618	0.866	
	Lignin	0.828	0.540	0.289		0.828	0.540	0.289	
	Ash/Inorga	0.095	0.062	0.033		0.095	0.062	0.033	
						4.534	2.953	1.581	0.349
70-80 cm	Soluble	1.126	0.733	0.393	0.90	1.013	0.660	0.353	
	Cell/Hemic	2.485	1.618	0.866		2.236	1.456	0.780	
	Lignin	0.828	0.540	0.289		0.746	0.486	0.260	
	Ash/Inorga	0.095	0.062	0.033		0.085	0.056	0.030	
						4.081	2.658	1.423	0.349
Total Weight		34.581	23.624	10.957	7.90	34.128	23.329	10.799	0.316
						4.320	2.953	1.367	

Total Weight kg	Dry kg	Water kg
4.320	2.953	1.367

Moisture (fraction) 0.316

Soluble

Layer	wet	dry	water
0-10 cm	0.948	0.745	0.203
10-20 cm	0.961	0.705	0.256
20-30 cm	0.974	0.666	0.308
30-40 cm	1.017	0.682	0.335
40-50 cm	1.060	0.697	0.362
50-60 cm	1.093	0.715	0.377
60-70 cm	1.126	0.733	0.393
70-80 cm	1.013	0.660	0.353
subtotal	8.192	5.604	2.587
Ave	1.037	0.709	0.327

Cellulose / Hemicellulose

	wet	dry	water
0-10 cm	2.085	1.638	0.447
10-20 cm	2.271	1.660	0.612
20-30 cm	2.458	1.681	0.777
30-40 cm	2.498	1.676	0.822
40-50 cm	2.538	1.670	0.867
50-60 cm	2.511	1.644	0.867
60-70 cm	2.485	1.618	0.866
70-80 cm	2.236	1.456	0.780
subtotal	19.082	13.043	6.038
Average	2.415	1.651	0.764

Lignin

	wet	dry	water
0-10 cm	0.679	0.533	0.145
10-20 cm	0.749	0.547	0.202
20-30 cm	0.820	0.561	0.259
30-40 cm	0.819	0.550	0.269
40-50 cm	0.819	0.539	0.280
50-60 cm	0.824	0.539	0.284
60-70 cm	0.828	0.540	0.289
70-80 cm	0.746	0.486	0.260
subtotal	6.283	4.294	1.989
Aveage	0.795	0.544	0.252

Ash / Inorganic

	wet	dry	water
0-10 cm	0.047	0.037	0.010
10-20 cm	0.057	0.041	0.015
20-30 cm	0.066	0.045	0.021
30-40 cm	0.068	0.046	0.023
40-50 cm	0.071	0.047	0.024
50-60 cm	0.083	0.054	0.029
60-70 cm	0.095	0.062	0.033
70-80 cm	0.085	0.056	0.030
subtotal	0.572	0.387	0.185
Aveage	0.072	0.049	0.023

ckeck on total	34.128	23.329	10.799
TOTAL	4.320	2.953	1.367

Resistant-to-Biodegradation
Lab Results, 15 May 08
B3 Reactor 8 p. 3 of 3
Mixture 2
Run time: 328 hours

	Total Wt	Water	Dry Matter	Soluble	Cell / Hemi	Lignin	Ash / Inorganic
		Dry Basis					
Initial		32.4%	67.6%	22.2%	58.8%	17.6%	1.4%
Final		31.6%	68.4%	24.0%	55.9%	18.4%	1.7%
Initial weight (kg)	4.37	1.42	2.95	0.66	1.74	0.520	0.041
Final weight (kg)	4.32	1.37	2.95	0.71	1.65	0.544	0.049
Difference (kg)	0.05	0.05	0.00	-0.05	0.09	-0.024	-0.008
Percent Change	1.1%	3.4%	0.1%	-8.3%	5.0%	-4.5%	-19.2%

Total Weight adjusted to 1.0

	Total Wt	Water	Dry Matter	Soluble	Cell / Hemi	Lignin	Ash / Inorganic
					Dry Basis		
Initial weight (kg)	1.00	0.32	0.68	0.15	0.40	0.119	0.009
Final weight (kg)	0.99	0.31	0.68	0.16	0.38	0.124	0.011
Difference (kg)	0.01	0.01	0.00	-0.01	0.02	-0.005	-0.002
Percent Change	1.1%	3.4%	0.1%	-8.3%	5.0%	-4.5%	-19.2%

Resistant-to-Biodegradation Analysis: By Layer
Lab Results, 15 May 08
B4 Reactor 11 p. 1 of 3
Mixture 2
Run time: 165.5 hr

		Dry Basis Soluble	Cell / Hemi	Lignin	Ash / Inorganic	Wet Basis Water	Soluble	Cell / Hemi	Lignin	Ash / Inorganic
# 11 0-10 cm		21.1%	59.7%	17.6%	1.5%	29.94	14.81	41.81	12.35	1.08
# 11 20-30 cm		20.9%	58.0%	19.7%	1.4%	34.66	13.62	37.91	12.88	0.92
# 11 40-50 cm		21.4%	57.9%	19.2%	1.5%	34.35	14.07	38.03	12.60	0.95
# 11 60-70 cm		21.4%	58.2%	18.9%	1.5%	35.84	13.74	37.33	12.15	0.94
Mixture 2	initial	22.2%	58.8%	17.6%	1.4%	32.39	14.99	39.78	11.90	0.94

Layer		conversion factor dry to wet	percent composition	wet weight per unit of dry	% of water	water present per unit
0-10 cm	SOLUBLE	1.427	0.211	0.3018	0.299	0.090
	CELL/HEMI	1.427	0.597	0.8520	0.299	0.255
	LIGNIN	1.427	0.176	0.2516	0.299	0.075
	ASH/INORG	1.427	0.015	0.0220	0.299	0.007
20-30 cm	SOLUBLE	1.531	0.209	0.3191	0.347	0.111
	CELL/HEMI	1.531	0.580	0.8881	0.347	0.308
	LIGNIN	1.531	0.197	0.3017	0.347	0.105
	ASH/INORG	1.531	0.014	0.0215	0.347	0.007
40-50 cm	SOLUBLE	1.523	0.214	0.3264	0.344	0.112
	CELL/HEMI	1.523	0.579	0.8824	0.344	0.303
	LIGNIN	1.523	0.192	0.2923	0.344	0.100
	ASH/INORG	1.523	0.015	0.0221	0.344	0.008
60-70 cm	SOLUBLE	1.559	0.214	0.3338	0.358	0.120
	CELL/HEMI	1.559	0.582	0.9067	0.358	0.325
	LIGNIN	1.559	0.189	0.2952	0.358	0.106
	ASH/INORG	1.559	0.015	0.0228	0.358	0.008

Layer	Wet Weght per X **kg** of dry	Dry Weight per X kg	Water Weight per X **kg** of Substrate
0-10 cm	**0.302**	**0.211**	**0.090**
	0.852	**0.597**	**0.255**
	0.252	**0.176**	**0.075**
	0.022	**0.015**	**0.007**
20-30 cm	**0.319**	**0.209**	**0.111**
	0.888	**0.580**	**0.308**
	0.302	**0.197**	**0.105**
	0.022	**0.014**	**0.007**
40-50 cm	**0.326**	**0.214**	**0.112**
	0.882	**0.579**	**0.303**
	0.292	**0.192**	**0.100**
	0.022	**0.015**	**0.008**
60-70 cm	**0.334**	**0.214**	**0.120**
	0.907	**0.582**	**0.325**
	0.295	**0.189**	**0.106**
	0.023	**0.015**	**0.008**

Resistant-to-Biodegradation
Lab Results, 15 May 08
B4 Reactor 11 p. 2 of 3
Mixture 2
Run time: 165.5 hr

Multiplication Factor
2.834 No. of times unit values are
4.30 Final Weight

		Actual / Projected Values				**Weighted Values** Times Number of cm present			
Layer		Wet Weght per X **kg** of d	Dry Weight per X kg	Water Weight X **kg** of Substrate	weighted value cm in layer / 10	Wet Weght per X **kg** of dr	Dry Weight per X kg	Water Weight X **kg** of Substrate	Moisture fraction
0-10 cm	Soluble	0.855	0.599	0.256	1.00	0.855	0.599	0.256	
	Cell/Hemic	2.414	1.692	0.723		2.414	1.692	0.723	
	Lignin	0.713	0.500	0.214		0.713	0.500	0.214	
	Ash/Inorga	0.062	0.044	0.019		0.062	0.044	0.019	
						4.045	2.834	1.211	0.299
10-20 cm	Soluble	0.880	0.595	0.285	1.00	0.880	0.595	0.285	
	Cell/Hemic	2.466	1.668	0.798		2.466	1.668	0.798	
	Lignin	0.784	0.529	0.255		0.784	0.529	0.255	
	Ash/Inorga	0.062	0.042	0.020		0.062	0.042	0.020	
						4.191	2.834	1.357	0.324
20-30 cm	Soluble	0.904	0.591	0.314	1.00	0.904	0.591	0.314	
	Cell/Hemic	2.517	1.645	0.872		2.517	1.645	0.872	
	Lignin	0.855	0.559	0.296		0.855	0.559	0.296	
	Ash/Inorga	0.061	0.040	0.021		0.061	0.040	0.021	
						4.338	2.834	1.504	0.347
30-40 cm	Soluble	0.915	0.599	0.316	1.00	0.915	0.599	0.316	
	Cell/Hemic	2.509	1.643	0.866		2.509	1.643	0.866	
	Lignin	0.842	0.551	0.290		0.842	0.551	0.290	
	Ash/Inorga	0.062	0.040	0.021		0.062	0.040	0.021	
						4.327	2.834	1.493	0.345
40-50 cm	Soluble	0.925	0.607	0.318	1.00	0.925	0.607	0.318	
	Cell/Hemic	2.501	1.642	0.859		2.501	1.642	0.859	
	Lignin	0.828	0.544	0.285		0.828	0.544	0.285	
	Ash/Inorga	0.063	0.041	0.022		0.063	0.041	0.022	
						4.317	2.834	1.483	0.344
50-60 cm	Soluble	0.936	0.607	0.328	1.00	0.936	0.607	0.328	
	Cell/Hemic	2.535	1.645	0.890		2.535	1.645	0.890	
	Lignin	0.833	0.540	0.292		0.833	0.540	0.292	
	Ash/Inorga	0.064	0.041	0.022		0.064	0.041	0.022	
						4.367	2.834	1.533	0.351
60-70 cm	Soluble	0.946	0.607	0.339	1.00	0.946	0.607	0.339	
	Cell/Hemic	2.570	1.649	0.921		2.570	1.649	0.921	
	Lignin	0.837	0.537	0.300		0.837	0.537	0.300	
	Ash/Inorga	0.065	0.042	0.023		0.065	0.042	0.023	
						4.417	2.834	1.583	0.358
70-80 cm	Soluble	0.946	0.607	0.339	0.84	0.795	0.510	0.285	
	Cell/Hemic	2.570	1.649	0.921		2.159	1.385	0.774	
	Lignin	0.837	0.537	0.300		0.703	0.451	0.252	
	Ash/Inorga	0.065	0.042	0.023		0.054	0.035	0.019	
						3.710	2.381	1.330	0.358
Total Weight		34.419	22.672	11.747	7.84	33.713	22.219	11.494	0.341
						4.300	2.834	1.466	

Total Weight kg	Dry kg	Water kg
4.300	2.834	1.466

Moisture (fraction) 0.341

Soluble

Layer	wet	dry	water
0-10 cm	0.855	0.599	0.256
10-20 cm	0.880	0.595	0.285
20-30 cm	0.904	0.591	0.314
30-40 cm	0.915	0.599	0.316
40-50 cm	0.925	0.607	0.318
50-60 cm	0.936	0.607	0.328
60-70 cm	0.946	0.607	0.339
70-80 cm	0.795	0.510	0.285
subtotal	7.155	4.715	2.440
Ave	0.913	0.601	0.311

Cellulose / Hemicellulose

	wet	dry	water
0-10 cm	2.414	1.692	0.723
10-20 cm	2.466	1.668	0.798
20-30 cm	2.517	1.645	0.872
30-40 cm	2.509	1.643	0.866
40-50 cm	2.501	1.642	0.859
50-60 cm	2.535	1.645	0.890
60-70 cm	2.570	1.649	0.921
70-80 cm	2.159	1.385	0.774
subtotal	19.670	12.968	6.703
Average	2.509	1.654	0.855

Lignin

	wet	dry	water
0-10 cm	0.713	0.500	0.214
10-20 cm	0.784	0.529	0.255
20-30 cm	0.855	0.559	0.296
30-40 cm	0.842	0.551	0.290
40-50 cm	0.828	0.544	0.285
50-60 cm	0.833	0.540	0.292
60-70 cm	0.837	0.537	0.300
70-80 cm	0.703	0.451	0.252
subtotal	6.394	4.211	2.184
Aveage	0.816	0.537	0.279

Ash / Inorganic

	wet	dry	water
0-10 cm	0.062	0.044	0.019
10-20 cm	0.062	0.042	0.020
20-30 cm	0.061	0.040	0.021
30-40 cm	0.062	0.040	0.021
40-50 cm	0.063	0.041	0.022
50-60 cm	0.064	0.041	0.022
60-70 cm	0.065	0.042	0.023
70-80 cm	0.054	0.035	0.019
subtotal	0.492	0.325	0.168
Aveage	0.063	0.041	0.021

ckeck on total	33.713	22.219	11.494
TOTAL	4.300	2.834	1.466

Resistant-to-Biodegradation
Lab Results, 15 May 08
B4 Reactor 11 p. 3 of 3
Mixture 2
Run time: 165.5 hr

	Total Wt	Water	Dry Matter	Soluble	Cell / Hemi	Lignin	Ash / Inorganic
				Dry Basis			
Initial		32.4%	67.6%	22.2%	58.8%	17.6%	1.4%
Final		34.1%	65.9%	21.2%	58.4%	19.0%	1.5%
Initial weight (kg)	4.14	1.34	2.80	0.62	1.65	0.493	0.039
Final weight (kg)	4.30	1.47	2.83	0.60	1.65	0.537	0.041
Difference (kg)	-0.16	-0.13	-0.03	0.02	-0.01	-0.044	-0.002
Percent Change	-3.9%	-9.3%	-1.2%	3.1%	-0.4%	-9.0%	-6.3%

Total Weight adjusted to 1.0

	Total Wt	Water	Dry Matter	Soluble	Cell / Hemi	Lignin	Ash / Inorganic
					Dry Basis		
Initial weight (kg)	1.00	0.32	0.68	0.15	0.40	0.119	0.009
Final weight (kg)	1.04	0.35	0.68	0.15	0.40	0.130	0.010
Difference (kg)	-0.04	-0.03	-0.01	0.00	0.00	-0.011	-0.001
Percent Change	-3.9%	-9.3%	-1.2%	3.1%	-0.4%	-9.0%	-6.3%

Readily-Biodegradable **Analysis: By Layer**
Lab Results, 15 May 08
C2 Reactor 6 p. 1 of 3
Mixture 3
Run Time: 974.5 hr

	Dry Basis Soluble	Cell / Hemi	Lignin	Ash / Inorganic	Wet Basis Water	Soluble	Cell / Hemi	Lignin	Ash / Inorganic
# 6 0-10 cm	62.7%	19.2%	9.1%	9.1%	71.72	17.73	5.42	2.56	2.57
# 6 10-20 cm	60.7%	20.1%	10.0%	9.3%	78.60	12.98	4.29	2.14	1.99
# 6 20-30 cm	61.1%	14.6%	11.1%	13.2%	81.08	11.57	2.75	2.10	2.50
# 6 40-50 cm	55.6%	28.8%	7.9%	7.6%	80.63	10.78	5.58	1.53	1.47
Mixture 3	69.5%	23.6%	2.7%	4.2%	65.76	23.80	8.07	0.92	1.45

Layer		conversion factor dry to wet	percent composition	wet weight per unit of dry	% of water	water present per unit		Wet Weght per X **kg** of dry	Dry Weight per X kg	Water Weight per X **kg** of Substrate
0-10 cm	SOLUBLE	3.536	0.627	2.2169	0.717	1.590	0-10 cm	**2.217**	**0.627**	**1.590**
	CELL/HEMI	3.536	0.192	0.6773	0.717	0.486		**0.677**	**0.192**	**0.486**
	LIGNIN	3.536	0.091	0.3207	0.717	0.230		**0.321**	**0.091**	**0.230**
	ASH/INORG	3.536	0.091	0.3215	0.717	0.231		**0.321**	**0.091**	**0.231**
10-20 cm	SOLUBLE	4.672	0.607	2.8346	0.786	2.228	10-20 cm	**2.835**	**0.607**	**2.228**
	CELL/HEMI	4.672	0.201	0.9369	0.786	0.736		**0.937**	**0.201**	**0.736**
	LIGNIN	4.672	0.100	0.4669	0.786	0.367		**0.467**	**0.100**	**0.367**
	ASH/INORG	4.672	0.093	0.4341	0.786	0.341		**0.434**	**0.093**	**0.341**
20-30 cm	SOLUBLE	5.285	0.611	3.2314	0.811	2.620	20-30 cm	**3.231**	**0.611**	**2.620**
	CELL/HEMI	5.285	0.146	0.7694	0.811	0.624		**0.769**	**0.146**	**0.624**
	LIGNIN	5.285	0.111	0.5867	0.811	0.476		**0.587**	**0.111**	**0.476**
	ASH/INORG	5.285	0.132	0.6973	0.811	0.565		**0.697**	**0.132**	**0.565**
40-50 cm	SOLUBLE	5.163	0.556	2.8725	0.806	2.316	40-50 cm	**2.872**	**0.556**	**2.316**
	CELL/HEMI	5.163	0.288	1.4886	0.806	1.200		**1.489**	**0.288**	**1.200**
	LIGNIN	5.163	0.079	0.4091	0.806	0.330		**0.409**	**0.079**	**0.330**
	ASH/INORG	5.163	0.076	0.3929	0.806	0.317		**0.393**	**0.076**	**0.317**

Readily-Biodegradable
Lab Results, 15 May 08
C2 Reactor 6 p. 2 of 3
Mixture 3
Run Time: 974.5 hr

Multiplication Factor
2.6587 No. of times unit values are
12.060 Final Weight

Actual / Projected Values

Layer		Wet Weght per X **kg** of d	Dry Weight per X kg	Water Weight X **kg** of Substrate	weighted value cm in layer / 10
0-10 cm	Soluble	5.894	1.667	4.227	1.00
	Cell/Hemic	1.801	0.509	1.291	
	Lignin	0.853	0.241	0.611	
	Ash/Inorga	0.855	0.242	0.613	
10-20 cm	Soluble	6.715	1.640	5.075	1.00
	Cell/Hemic	2.146	0.521	1.625	
	Lignin	1.047	0.253	0.794	
	Ash/Inorga	1.004	0.244	0.760	
20-30 cm	Soluble	7.536	1.613	5.923	1.00
	Cell/Hemic	2.491	0.533	1.958	
	Lignin	1.241	0.266	0.976	
	Ash/Inorga	1.154	0.247	0.907	
30-40 cm	Soluble	8.064	1.619	6.445	1.00
	Cell/Hemic	2.268	0.460	1.808	
	Lignin	1.401	0.280	1.120	
	Ash/Inorga	1.504	0.299	1.205	
40-50 cm	Soluble	8.591	1.626	6.966	1.00
	Cell/Hemic	2.046	0.387	1.658	
	Lignin	1.560	0.295	1.265	
	Ash/Inorga	1.854	0.351	1.503	
50-60 cm	Soluble	8.114	1.552	6.562	0.15
	Cell/Hemic	3.002	0.577	2.425	
	Lignin	1.324	0.253	1.071	
	Ash/Inorga	1.449	0.277	1.173	
60-70 cm	Soluble	7.637	1.479	6.158	0.00
	Cell/Hemic	3.958	0.767	3.191	
	Lignin	1.088	0.211	0.877	
	Ash/Inorga	1.044	0.202	0.842	
70-80 cm	Soluble	7.637	1.479	6.158	0.00
	Cell/Hemic	3.958	0.767	3.191	
	Lignin	1.088	0.211	0.877	
	Ash/Inorga	1.044	0.202	0.842	
Total Weight		101.367	21.270	80.097	5.15

Weighted Values
Times Number of cm present

Wet Weght per X **kg** of dr	Dry Weight per X kg	Water Weight X **kg** of Substrate	Moisture fraction
5.894	1.667	4.227	
1.801	0.509	1.291	
0.853	0.241	0.611	
0.855	0.242	0.613	
9.402	2.659	6.743	0.717
6.715	1.640	5.075	
2.146	0.521	1.625	
1.047	0.253	0.794	
1.004	0.244	0.760	
10.912	2.659	8.254	0.756
7.536	1.613	5.923	
2.491	0.533	1.958	
1.241	0.266	0.976	
1.154	0.247	0.907	
12.423	2.659	9.764	0.786
8.064	1.619	6.445	
2.268	0.460	1.808	
1.401	0.280	1.120	
1.504	0.299	1.205	
13.237	2.659	10.578	0.799
8.591	1.626	6.966	
2.046	0.387	1.658	
1.560	0.295	1.265	
1.854	0.351	1.503	
14.051	2.659	11.392	0.811
1.217	0.233	0.984	
0.450	0.087	0.364	
0.199	0.038	0.161	
0.217	0.041	0.176	
2.083	0.399	1.685	0.809
0.000	0.000	0.000	
0.000	0.000	0.000	
0.000	0.000	0.000	
0.000	0.000	0.000	
0.000	0.000	0.000	#DIV/0!
0.000	0.000	0.000	
0.000	0.000	0.000	
0.000	0.000	0.000	
0.000	0.000	0.000	#DIV/0!
62.108	13.692	48.415	0.780
12.060	2.659	9.401	

Total Weight kg 12.060 Dry kg 2.659 Water kg 9.401

Moisture (fraction) 0.780

Soluble

Layer	wet	dry	water
0-10 cm	5.894	1.667	4.227
10-20 cm	6.715	1.640	5.075
20-30 cm	7.536	1.613	5.923
30-40 cm	8.064	1.619	6.445
40-50 cm	8.591	1.626	6.966
50-60 cm	1.217	0.233	0.984
60-70 cm	0.000	0.000	0.000
70-80 cm	0.000	0.000	0.000
subtotal	38.018	8.397	29.620
Ave	7.382	1.631	5.752

Cellulose / Hemicellulose

	wet	dry	water
0-10 cm	1.801	0.509	1.291
10-20 cm	2.146	0.521	1.625
20-30 cm	2.491	0.533	1.958
30-40 cm	2.268	0.460	1.808
40-50 cm	2.046	0.387	1.658
50-60 cm	0.450	0.087	0.364
60-70 cm	0.000	0.000	0.000
70-80 cm	0.000	0.000	0.000
subtotal	11.201	2.497	8.704
Average	2.175	0.485	1.690

Lignin

	wet	dry	water
0-10 cm	0.853	0.241	0.611
10-20 cm	1.047	0.253	0.794
20-30 cm	1.241	0.266	0.976
30-40 cm	1.401	0.280	1.120
40-50 cm	1.560	0.295	1.265
50-60 cm	0.199	0.038	0.161
60-70 cm	0.000	0.000	0.000
70-80 cm	0.000	0.000	0.000
subtotal	6.300	1.374	4.926
Aveage	1.223	0.267	0.957

Ash / Inorganic

	wet	dry	water
0-10 cm	0.855	0.242	0.613
10-20 cm	1.004	0.244	0.760
20-30 cm	1.154	0.247	0.907
30-40 cm	1.504	0.299	1.205
40-50 cm	1.854	0.351	1.503
50-60 cm	0.217	0.041	0.176
60-70 cm	0.000	0.000	0.000
70-80 cm	0.000	0.000	0.000
subtotal	6.589	1.424	5.164
Aveage	1.279	0.277	1.003

ckeck on total	62.108	13.692	48.415
TOTAL	12.060	2.659	9.401

Readily-Biodegradable
Lab Results, 15 May 08
C2 Reactor 6 p. 3 of 3
Mixture 3
Run Time: 974.5 hr

	Total Wt	Water	Dry Matter	Soluble	Cell / Hemi	Lignin	Ash / Inorganic
		Dry Basis					
Initial		65.8%	34.2%	69.5%	23.6%	2.7%	4.2%
Final		78.0%	22.0%	61.3%	18.2%	10.0%	10.4%
Initial weight (kg)	15.53	10.21	5.32	3.70	1.25	0.142	0.225
Final weight (kg)	12.06	9.40	2.66	1.63	0.48	0.267	0.277
Difference (kg)	3.47	0.81	2.66	2.07	0.77	-0.124	-0.051
Percent Change	22.3%	7.9%	50.0%	55.9%	61.3%	-87.2%	-22.8%

Total Weight adjusted to 1.0

	Total Wt	Water	Dry Matter	Soluble	Cell / Hemi	Lignin	Ash / Inorganic
					Dry Basis		
Initial weight (kg)	1.00	0.66	0.34	0.24	0.08	0.009	0.014
Final weight (kg)	0.78	0.61	0.17	0.10	0.03	0.017	0.018
Difference (kg)	0.22	0.05	0.17	0.13	0.05	-0.008	-0.003
Percent Change	22.3%	7.9%	50.0%	55.9%	61.3%	-87.2%	-22.8%

Readily-Biodegradable **Analysis: By Layer**
Lab Results, 15 May 08
C1 Reactor 3 p. 1 of 3
Mixture 3
Run Time:552 hr

		Dry Basis Soluble	Cell / Hemi	Lignin	Ash / Inorganic		Wet Basis Water	Soluble	Cell / Hemi	Lignin	Ash / Inorganic
C1 0-10 cm		61.6%	23.8%	7.7%	6.9%		64.09	22.12	8.55	2.75	2.49
C1 10-20 cm		58.2%	24.6%	9.0%	8.2%		80.69	11.24	4.74	1.74	1.58
C1 30-40 cm		48.8%	31.6%	9.7%	9.8%		82.31	8.64	5.59	1.72	1.74
C1 50-60 cm		54.4%	31.7%	6.2%	7.7%		80.71	10.49	6.11	1.20	1.48
Mixture 3	Initial	69.5%	23.6%	2.7%	4.2%		65.76	23.80	8.07	0.92	1.45

Layer		conversion factor dry to wet	percent composition	wet weight per unit of dry	% of water	water present per unit		Wet Weght per X **kg** of dry	Dry Weight per X kg	Water Weight per X **kg** of Substrate
0-10 cm	SOLUBLE	2.785	0.616	1.7154	0.641	1.099	0-10 cm	**1.715**	**0.616**	**1.099**
	CELL/HEMI	2.785	0.238	0.6630	0.641	0.425		**0.663**	**0.238**	**0.425**
	LIGNIN	2.785	0.077	0.2131	0.641	0.137		**0.213**	**0.077**	**0.137**
	ASH/INORG	2.785	0.069	0.1931	0.641	0.124		**0.193**	**0.069**	**0.124**
10-20 cm	SOLUBLE	5.179	0.582	3.0149	0.807	2.433	10-20 cm	**3.015**	**0.582**	**2.433**
	CELL/HEMI	5.179	0.246	1.2722	0.807	1.027		**1.272**	**0.246**	**1.027**
	LIGNIN	5.179	0.090	0.4667	0.807	0.377		**0.467**	**0.090**	**0.377**
	ASH/INORG	5.179	0.082	0.4251	0.807	0.343		**0.425**	**0.082**	**0.343**
30-40 cm	SOLUBLE	5.652	0.488	2.7605	0.823	2.272	30-40 cm	**2.761**	**0.488**	**2.272**
	CELL/HEMI	5.652	0.316	1.7869	0.823	1.471		**1.787**	**0.316**	**1.471**
	LIGNIN	5.652	0.097	0.5490	0.823	0.452		**0.549**	**0.097**	**0.452**
	ASH/INORG	5.652	0.098	0.5554	0.823	0.457		**0.555**	**0.098**	**0.457**
50-60 cm	SOLUBLE	5.185	0.544	2.8209	0.807	2.277	50-60 cm	**2.821**	**0.544**	**2.277**
	CELL/HEMI	5.185	0.317	1.6438	0.807	1.327		**1.644**	**0.317**	**1.327**
	LIGNIN	5.185	0.062	0.3234	0.807	0.261		**0.323**	**0.062**	**0.261**
	ASH/INORG	5.185	0.077	0.3969	0.807	0.320		**0.397**	**0.077**	**0.320**

Readily-Biodegradable
Lab Results, 15 May 08
C1 Reactor 3 p. 2 of 3
Mixture 3
Run Time:552 hr

Multiplication Factor
2.8638 No. of times unit values are multiplied
13.51 Final Weight

		Actual / Projected Values				**Weighted Values** Times Number of cm present					
Layer		Wet Weght per X **kg** of d	Dry Weight per X kg	Water Weight X **kg** of Substrate	weighted value cm in layer / 10	Wet Weght per X **kg** of dr	Dry Weight per X kg	Water Weight X **kg** of Substrate	Moisture fraction	Layer	
0-10 cm	Soluble	4.912	1.764	3.148	1.00	4.912	1.764	3.148			
	Cell/Hemic	1.899	0.682	1.217		1.899	0.682	1.217			
	Lignin	0.610	0.219	0.391		0.610	0.219	0.391			
	Ash/Inorga	0.553	0.199	0.354		0.553	0.199	0.354			
						7.975	2.864	5.111	0.641		
10-20 cm	Soluble	6.773	1.716	5.058	1.00	6.773	1.716	5.058			
	Cell/Hemic	2.771	0.693	2.078		2.771	0.693	2.078			
	Lignin	0.974	0.239	0.735		0.974	0.239	0.735			
	Ash/Inorga	0.885	0.217	0.668		0.885	0.217	0.668			
						11.403	2.864	8.539	0.749	Ave	
20-30 cm	Soluble	8.634	1.667	6.967	1.00	8.634	1.667	6.967			
	Cell/Hemic	3.643	0.703	2.940		3.643	0.703	2.940			
	Lignin	1.337	0.258	1.079		1.337	0.258	1.079			
	Ash/Inorga	1.217	0.235	0.982		1.217	0.235	0.982			
						14.831	2.864	11.968	0.807		
30-40 cm	Soluble	8.270	1.533	6.737	1.00	8.270	1.533	6.737			
	Cell/Hemic	4.380	0.804	3.576		4.380	0.804	3.576			
	Lignin	1.454	0.268	1.186		1.454	0.268	1.186			
	Ash/Inorga	1.404	0.258	1.146		1.404	0.258	1.146			
						15.509	2.864	12.645	0.815		
40-50 cm	Soluble	7.906	1.399	6.507	1.00	7.906	1.399	6.507			
	Cell/Hemic	5.117	0.905	4.212		5.117	0.905	4.212			
	Lignin	1.572	0.278	1.294		1.572	0.278	1.294			
	Ash/Inorga	1.591	0.281	1.309		1.591	0.281	1.309			
						16.186	2.864	13.322	0.823		
50-60 cm	Soluble	7.992	1.478	6.514	0.82	6.553	1.212	5.341			
	Cell/Hemic	4.912	0.907	4.006		4.028	0.743	3.285			
	Lignin	1.249	0.228	1.021		1.024	0.187	0.837			
	Ash/Inorga	1.364	0.250	1.113		1.118	0.205	0.913			
						12.724	2.348	10.376	0.815		
60-70 cm	Soluble	8.078	1.558	6.520	0.00	0.000	0.000	0.000			
	Cell/Hemic	4.708	0.908	3.800		0.000	0.000	0.000			
	Lignin	0.926	0.179	0.748		0.000	0.000	0.000			
	Ash/Inorga	1.137	0.219	0.917		0.000	0.000	0.000			
						0.000	0.000	0.000	#DIV/0!	Aveage	
70-80 cm	Soluble	8.078	1.558	6.520	0.00	0.000	0.000	0.000			
	Cell/Hemic	4.708	0.908	3.800		0.000	0.000	0.000			
	Lignin	0.926	0.179	0.748		0.000	0.000	0.000			
	Ash/Inorga	1.137	0.219	0.917		0.000	0.000	0.000			
						0.000	0.000	0.000	#DIV/0!		
Total Weight		111.118	22.910	88.208	5.82	78.628	16.667	61.960	0.788		
						13.510	2.864	10.646			

Total Weight kg	Dry kg	Water kg
13.510	2.864	10.646

Moisture (fraction) 0.788

Soluble

Layer	wet	dry	water
0-10 cm	4.912	1.764	3.148
10-20 cm	6.773	1.716	5.058
20-30 cm	8.634	1.667	6.967
30-40 cm	8.270	1.533	6.737
40-50 cm	7.906	1.399	6.507
50-60 cm	6.553	1.212	5.341
60-70 cm	0.000	0.000	0.000
70-80 cm	0.000	0.000	0.000
subtotal	43.049	9.291	33.758
Ave	7.397	1.596	5.800

Cellulose / Hemicellulose

	wet	dry	water
0-10 cm	1.899	0.682	1.217
10-20 cm	2.771	0.693	2.078
20-30 cm	3.643	0.703	2.940
30-40 cm	4.380	0.804	3.576
40-50 cm	5.117	0.905	4.212
50-60 cm	4.028	0.743	3.285
60-70 cm	0.000	0.000	0.000
70-80 cm	0.000	0.000	0.000
subtotal	21.839	4.531	17.308
Average	3.752	0.779	2.974

Lignin

	wet	dry	water
0-10 cm	0.610	0.219	0.391
10-20 cm	0.974	0.239	0.735
20-30 cm	1.337	0.258	1.079
30-40 cm	1.454	0.268	1.186
40-50 cm	1.572	0.278	1.294
50-60 cm	1.024	0.187	0.837
60-70 cm	0.000	0.000	0.000
70-80 cm	0.000	0.000	0.000
subtotal	6.972	1.450	5.522
Aveage	1.198	0.249	0.949

Ash / Inorganic

	wet	dry	water
0-10 cm	0.553	0.199	0.354
10-20 cm	0.885	0.217	0.668
20-30 cm	1.217	0.235	0.982
30-40 cm	1.404	0.258	1.146
40-50 cm	1.591	0.281	1.309
50-60 cm	1.118	0.205	0.913
60-70 cm	0.000	0.000	0.000
70-80 cm	0.000	0.000	0.000
subtotal	6.768	1.395	5.373
Aveage	1.163	0.240	0.923

ckeck on total	78.628	16.667	61.960
TOTAL	13.510	2.864	10.646

Readily-Biodegradable
Lab Results, 15 May 08
C1 Reactor 3 p. 3 of 3
Mixture 3
Run Time:552 hr

	Total Wt	Water	Dry Matter	Soluble	Cell / Hemi	Lignin	Ash / Inorganic
		Dry Basis					
Initial		65.8%	34.2%	69.5%	23.6%	2.7%	4.2%
Final		78.8%	21.2%	55.7%	27.2%	8.7%	8.4%
Initial weight (kg)	15.92	10.47	5.45	3.79	1.28	0.146	0.231
Final weight (kg)	13.51	10.65	2.86	1.60	0.78	0.249	0.240
Difference (kg)	2.41	-0.18	2.59	2.19	0.51	-0.103	-0.009
Percent Change	15.1%	-1.7%	47.5%	57.9%	39.4%	-70.5%	-3.9%

Total Weight adjusted to 1.0

	Total Wt	Water	Dry Matter	Soluble	Cell / Hemi	Lignin	Ash / Inorganic
					Dry Basis		
Initial weight (kg)	1.00	0.66	0.34	0.24	0.08	0.009	0.014
Final weight (kg)	0.85	0.67	0.18	0.10	0.05	0.016	0.015
Difference (kg)	0.15	-0.01	0.16	0.14	0.03	-0.006	-0.001
Percent Change	15.1%	-1.7%	47.5%	57.9%	39.4%	-70.5%	-3.9%

Readily-Biodegradable **Analysis: By Layer**
Lab Results, 15 May 08
C3 Reactor 9 **p. 1 of 3**
Mixture 3
Run Time:327.5 hr

		Dry Basis Soluble	Cell / Hemi	Lignin	Ash / Inorganic	Wet Basis Water	Soluble	Cell / Hemi	Lignin	Ash / Inorganic
# 9 0-10 cm		59.6%	26.8%	5.7%	7.9%	65.60	20.51	9.22	1.95	2.72
# 9 20-30 cm		61.4%	27.4%	4.3%	6.9%	70.26	18.25	8.16	1.29	2.04
# 9 40-50 cm		50.1%	31.0%	6.9%	12.0%	76.84	11.60	7.19	1.59	2.78
# 9 60-70 cm		57.9%	30.0%	5.6%	6.5%	77.33	13.12	6.81	1.28	1.47
Mixture 3	initial	69.5%	23.6%	2.7%	4.2%	65.76	23.80	8.07	0.92	1.45

Layer		conversion factor dry to wet	percent composition	wet weight per unit of dry	% of water	water present per unit		Wet Weght per X **kg** of dry	Dry Weight per X kg	Water Weight per X **kg** of Substrate
0-10 cm	SOLUBLE	2.907	0.596	1.7330	0.656	1.137	0-10 cm	**1.733**	**0.596**	**1.137**
	CELL/HEMI	2.907	0.268	0.7793	0.656	0.511		**0.779**	**0.268**	**0.511**
	LIGNIN	2.907	0.057	0.1649	0.656	0.108		**0.165**	**0.057**	**0.108**
	ASH/INORG	2.907	0.079	0.2297	0.656	0.151		**0.230**	**0.079**	**0.151**
20-30 cm	SOLUBLE	3.363	0.614	2.0637	0.703	1.450	20-30 cm	**2.064**	**0.614**	**1.450**
	CELL/HEMI	3.363	0.274	0.9228	0.703	0.648		**0.923**	**0.274**	**0.648**
	LIGNIN	3.363	0.043	0.1460	0.703	0.103		**0.146**	**0.043**	**0.103**
	ASH/INORG	3.363	0.069	0.2305	0.703	0.162		**0.230**	**0.069**	**0.162**
40-50 cm	SOLUBLE	4.318	0.501	2.1626	0.768	1.662	40-50 cm	**2.163**	**0.501**	**1.662**
	CELL/HEMI	4.318	0.310	1.3400	0.768	1.030		**1.340**	**0.310**	**1.030**
	LIGNIN	4.318	0.069	0.2968	0.768	0.228		**0.297**	**0.069**	**0.228**
	ASH/INORG	4.318	0.120	0.5189	0.768	0.399		**0.519**	**0.120**	**0.399**
60-70 cm	SOLUBLE	4.412	0.579	2.5525	0.773	1.974	60-70 cm	**2.553**	**0.579**	**1.974**
	CELL/HEMI	4.412	0.300	1.3245	0.773	1.024		**1.324**	**0.300**	**1.024**
	LIGNIN	4.412	0.056	0.2484	0.773	0.192		**0.248**	**0.056**	**0.192**
	ASH/INORG	4.412	0.065	0.2863	0.773	0.221		**0.286**	**0.065**	**0.221**

Readily-Biodegradable
Lab Results, 15 May 08
C3 Reactor 9
Mixture 3
Run Time:327.5 hr

Multiplication Factor
3.671 No. of times unit values are multiplied
13.570 Final Weight

		Actual / Projected Values				**Weighted Values** Times Number of cm present				
Layer		Wet Weght per X **kg** of d	Dry Weight per X kg	Water Weight X **kg** of Substrate	weighted value cm in layer / 10	Wet Weght per X **kg** of dr	Dry Weight per X kg	Water Weight X **kg** of Substrate	Moisture fraction
0-10 cm	Soluble	6.362	2.189	4.173	1.00	6.362	2.189	4.173	
	Cell/Hemic	2.861	0.984	1.877		2.861	0.984	1.877	
	Lignin	0.605	0.208	0.397		0.605	0.208	0.397	
	Ash/Inorga	0.843	0.290	0.553		0.843	0.290	0.553	
						10.671	3.671	7.000	0.656
10-20 cm	Soluble	6.969	2.221	4.748	1.00	6.969	2.221	4.748	
	Cell/Hemic	3.124	0.996	2.129		3.124	0.996	2.129	
	Lignin	0.571	0.184	0.387		0.571	0.184	0.387	
	Ash/Inorga	0.845	0.271	0.574		0.845	0.271	0.574	
						11.509	3.671	7.838	0.681
20-30 cm	Soluble	7.576	2.253	5.323	1.00	7.576	2.253	5.323	
	Cell/Hemic	3.388	1.007	2.380		3.388	1.007	2.380	
	Lignin	0.536	0.159	0.377		0.536	0.159	0.377	
	Ash/Inorga	0.846	0.252	0.595		0.846	0.252	0.595	
						12.346	3.671	8.675	0.703
30-40 cm	Soluble	7.757	2.046	5.712	1.00	7.757	2.046	5.712	
	Cell/Hemic	4.153	1.073	3.080		4.153	1.073	3.080	
	Lignin	0.813	0.206	0.607		0.813	0.206	0.607	
	Ash/Inorga	1.375	0.346	1.029		1.375	0.346	1.029	
						14.099	3.671	10.428	0.740
40-50 cm	Soluble	7.939	1.838	6.100	1.00	7.939	1.838	6.100	
	Cell/Hemic	4.919	1.139	3.780		4.919	1.139	3.780	
	Lignin	1.090	0.252	0.837		1.090	0.252	0.837	
	Ash/Inorga	1.905	0.441	1.464		1.905	0.441	1.464	
						15.852	3.671	12.181	0.768
50-60 cm	Soluble	8.655	1.981	6.673	1.00	8.655	1.981	6.673	
	Cell/Hemic	4.891	1.121	3.770		4.891	1.121	3.770	
	Lignin	1.001	0.230	0.771		1.001	0.230	0.771	
	Ash/Inorga	1.478	0.340	1.138		1.478	0.340	1.138	
						16.024	3.671	12.353	0.771
60-70 cm	Soluble	9.370	2.124	7.246	0.35	3.280	0.743	2.536	
	Cell/Hemic	4.862	1.102	3.760		1.702	0.386	1.316	
	Lignin	0.912	0.207	0.705		0.319	0.072	0.247	
	Ash/Inorga	1.051	0.238	0.813		0.368	0.083	0.284	
						5.668	1.285	4.383	0.773
70-80 cm	Soluble	9.370	2.124	7.246	0.00	0.000	0.000	0.000	
	Cell/Hemic	4.862	1.102	3.760		0.000	0.000	0.000	
	Lignin	0.912	0.207	0.705		0.000	0.000	0.000	
	Ash/Inorga	1.051	0.238	0.813		0.000	0.000	0.000	
						0.000	0.000	0.000	#DIV/0!
Total Weight		112.891	29.368	83.523	6.35	86.169	23.311	62.858	0.729
						13.570	3.671	9.899	

Total Weight kg	Dry kg	Water kg
13.570	3.671	9.899

Moisture (fraction) 0.729

Soluble

Layer	wet	dry	water
0-10 cm	6.362	2.189	4.173
10-20 cm	6.969	2.221	4.748
20-30 cm	7.576	2.253	5.323
30-40 cm	7.757	2.046	5.712
40-50 cm	7.939	1.838	6.100
50-60 cm	8.655	1.981	6.673
60-70 cm	3.280	0.743	2.536
70-80 cm	0.000	0.000	0.000
subtotal	48.537	13.270	35.266
Ave	7.644	2.090	5.554

Cellulose / Hemicellulose

Layer	wet	dry	water
0-10 cm	2.861	0.984	1.877
10-20 cm	3.124	0.996	2.129
20-30 cm	3.388	1.007	2.380
30-40 cm	4.153	1.073	3.080
40-50 cm	4.919	1.139	3.780
50-60 cm	4.891	1.121	3.770
60-70 cm	1.702	0.386	1.316
70-80 cm	0.000	0.000	0.000
subtotal	25.038	6.706	18.332
Average	3.943	1.056	2.887

Lignin

Layer	wet	dry	water
0-10 cm	0.605	0.208	0.397
10-20 cm	0.571	0.184	0.387
20-30 cm	0.536	0.159	0.377
30-40 cm	0.813	0.206	0.607
40-50 cm	1.090	0.252	0.837
50-60 cm	1.001	0.230	0.771
60-70 cm	0.319	0.072	0.247
70-80 cm	0.000	0.000	0.000
subtotal	4.934	1.311	3.623
Aveage	0.777	0.207	0.571

Ash / Inorganic

Layer	wet	dry	water
0-10 cm	0.843	0.290	0.553
10-20 cm	0.845	0.271	0.574
20-30 cm	0.846	0.252	0.595
30-40 cm	1.375	0.346	1.029
40-50 cm	1.905	0.441	1.464
50-60 cm	1.478	0.340	1.138
60-70 cm	0.368	0.083	0.284
70-80 cm	0.000	0.000	0.000
subtotal	7.660	2.023	5.637
Aveage	1.206	0.319	0.888

ckeck on total	86.169	23.311	62.858
TOTAL	13.570	3.671	9.899

Readily-Biodegradable
Lab Results, 15 May 08
C3 Reactor 9 p. 3 of 3
Mixture 3
Run Time:327.5 hr

	Total Wt	Water	Dry Matter	Dry Basis Soluble	Cell / Hemi	Lignin	Ash / Inorganic
Initial		65.8%	34.2%	69.5%	23.6%	2.7%	4.2%
Final		72.9%	27.1%	56.9%	28.8%	5.6%	8.7%
Initial weight (kg)	15.75	10.36	5.39	3.75	1.27	0.144	0.23
Final weight (kg)	13.57	9.90	3.67	2.09	1.06	0.207	0.32
Difference (kg)	2.18	0.46	1.72	1.66	0.22	-0.062	-0.09
Percent Change	13.8%	4.4%	31.9%	44.3%	16.9%	-42.9%	-39.5%

Total Weight adjusted to 1.0

	Total Wt	Water	Dry Matter	Dry Basis Soluble	Cell / Hemi	Lignin	Ash / Inorganic
Initial weight (kg)	1.00	0.66	0.34	0.24	0.08	0.009	0.014
Final weight (kg)	0.86	0.63	0.23	0.13	0.07	0.013	0.020
Difference (kg)	0.14	0.03	0.11	0.11	0.01	-0.004	-0.006
Percent Change	13.8%	4.4%	31.9%	44.3%	16.9%	-42.9%	-39.5%

Readily-Biodegradable **Analysis: By Layer**
Lab Results, 15 May 08
C4 Reactor 12 p. 1 of 3
Mixture 3
Run Time: 163.5 hr

		Dry Basis Soluble	Cell / Hemi	Lignin	Ash / Inorganic		Wet Basis Water	Soluble	Cell / Hemi	Lignin	Ash / Inorganic
Tube 12 0-10 cm		62.4%	29.0%	3.4%	5.3%		65.28	21.66	10.06	1.16	1.84
Tube 12 20-30 cm		67.0%	26.3%	2.7%	4.0%		68.31	21.23	8.34	0.86	1.27
Tube 12 40-50 cm		63.9%	27.4%	2.7%	6.0%		66.62	21.33	9.13	0.91	2.01
Tube 12 60-70 cm		66.0%	27.3%	2.7%	3.9%		67.33	21.58	8.92	0.89	1.28
Mixture 3	initial	69.5%	23.6%	2.7%	4.2%		65.76	23.80	8.07	0.92	1.45

Layer		conversion factor dry to wet	percent composition	wet weight per unit of dry	% of water	water present per unit		Wet Weght per X **kg** of dry	Dry Weight per X kg	Water Weight per X **kg** of Substrate
0-10 cm	SOLUBLE	2.880	0.624	1.7963	0.653	1.173	0-10 cm	**1.796**	**0.624**	**1.173**
	CELL/HEMI	2.880	0.290	0.8342	0.653	0.545		**0.834**	**0.290**	**0.545**
	LIGNIN	2.880	0.034	0.0966	0.653	0.063		**0.097**	**0.034**	**0.063**
	ASH/INORG	2.880	0.053	0.1530	0.653	0.100		**0.153**	**0.053**	**0.100**
20-30 cm	SOLUBLE	3.155	0.670	2.1134	0.683	1.444	20-30 cm	**2.113**	**0.670**	**1.444**
	CELL/HEMI	3.155	0.263	0.8302	0.683	0.567		**0.830**	**0.263**	**0.567**
	LIGNIN	3.155	0.027	0.0858	0.683	0.059		**0.086**	**0.027**	**0.059**
	ASH/INORG	3.155	0.040	0.1261	0.683	0.086		**0.126**	**0.040**	**0.086**
40-50 cm	SOLUBLE	2.996	0.639	1.9146	0.666	1.275	40-50 cm	**1.915**	**0.639**	**1.275**
	CELL/HEMI	2.996	0.274	0.8196	0.666	0.546		**0.820**	**0.274**	**0.546**
	LIGNIN	2.996	0.027	0.0814	0.666	0.054		**0.081**	**0.027**	**0.054**
	ASH/INORG	2.996	0.060	0.1801	0.666	0.120		**0.180**	**0.060**	**0.120**
60-70 cm	SOLUBLE	3.061	0.660	2.0212	0.673	1.361	60-70 cm	**2.021**	**0.660**	**1.361**
	CELL/HEMI	3.061	0.273	0.8359	0.673	0.563		**0.836**	**0.273**	**0.563**
	LIGNIN	3.061	0.027	0.0837	0.673	0.056		**0.084**	**0.027**	**0.056**
	ASH/INORG	3.061	0.039	0.1198	0.673	0.081		**0.120**	**0.039**	**0.081**

Readily-Biodegradable
Lab Resul 163.5 Hours
C4 Reactor 12 p. 2 of 3
Mixture 3
Run Time: 163.5 hr

Multiplication Factor
5.232 No. of times unit values are multiplied
15.86 Final Weight

		Actual / Projected Values				**Weighted Values** Times Number of cm present				
Layer		Wet Weight per X **kg** of d	Dry Weight per X kg	Water Weight X **kg** of Substrate	weighted value cm in layer / 10	Wet Weight per X **kg** of dr	Dry Weight per X kg	Water Weight X **kg** of Substrate	Moisture fraction	
0-10 cm	Soluble	9.398	3.263	6.135	1.00	9.398	3.263	6.135		
	Cell/Hemic	4.365	1.515	2.849		4.365	1.515	2.849		
	Lignin	0.505	0.175	0.330		0.505	0.175	0.330		
	Ash/Inorga	0.800	0.278	0.523		0.800	0.278	0.523		
						15.069	5.232	9.837	0.653	
10-20 cm	Soluble	10.228	3.384	6.844	1.00	10.228	3.384	6.844		
	Cell/Hemic	4.354	1.446	2.908		4.354	1.446	2.908		
	Lignin	0.477	0.159	0.318		0.477	0.159	0.318		
	Ash/Inorga	0.730	0.243	0.487		0.730	0.243	0.487		
						15.789	5.232	10.557	0.669	
20-30 cm	Soluble	11.057	3.504	7.553	1.00	11.057	3.504	7.553		
	Cell/Hemic	4.343	1.376	2.967		4.343	1.376	2.967		
	Lignin	0.449	0.142	0.307		0.449	0.142	0.307		
	Ash/Inorga	0.660	0.209	0.451		0.660	0.209	0.451		
						16.509	5.232	11.277	0.683	
30-40 cm	Soluble	10.537	3.424	7.113	1.00	10.537	3.424	7.113		
	Cell/Hemic	4.316	1.404	2.912		4.316	1.404	2.912		
	Lignin	0.437	0.142	0.295		0.437	0.142	0.295		
	Ash/Inorga	0.801	0.262	0.539		0.801	0.262	0.539		
						16.091	5.232	10.859	0.675	
40-50 cm	Soluble	10.017	3.344	6.673	1.00	10.017	3.344	6.673		
	Cell/Hemic	4.288	1.431	2.857		4.288	1.431	2.857		
	Lignin	0.426	0.142	0.284		0.426	0.142	0.284		
	Ash/Inorga	0.942	0.314	0.628		0.942	0.314	0.628		
						15.674	5.232	10.442	0.666	
50-60 cm	Soluble	10.296	3.400	6.897	1.00	10.296	3.400	6.897		
	Cell/Hemic	4.331	1.430	2.901		4.331	1.430	2.901		
	Lignin	0.432	0.143	0.289		0.432	0.143	0.289		
	Ash/Inorga	0.785	0.260	0.525		0.785	0.260	0.525		
						15.844	5.232	10.612	0.670	
60-70 cm	Soluble	10.575	3.455	7.120	1.00	10.575	3.455	7.120		
	Cell/Hemic	4.373	1.429	2.944		4.373	1.429	2.944		
	Lignin	0.438	0.143	0.295		0.438	0.143	0.295		
	Ash/Inorga	0.627	0.205	0.422		0.627	0.205	0.422		
						16.013	5.232	10.781	0.673	
70-80 cm	Soluble	10.575	3.455	7.120	0.20	2.115	0.691	1.424		
	Cell/Hemic	4.373	1.429	2.944		0.875	0.286	0.589		
	Lignin	0.438	0.143	0.295		0.088	0.029	0.059		
	Ash/Inorga	0.627	0.205	0.422		0.125	0.041	0.084		
						3.203	1.046	2.156	0.673	
Total Weight		127.002	41.856	85.146	7.20	114.192	37.670	76.521	0.670	
						15.860	5.232	10.628		

Total Weight kg	Dry kg	Water kg
15.860	5.232	10.628

Moisture (fraction) 0.670

Soluble

Layer	wet	dry	water
0-10 cm	9.398	3.263	6.135
10-20 cm	10.228	3.384	6.844
20-30 cm	11.057	3.504	7.553
30-40 cm	10.537	3.424	7.113
40-50 cm	10.017	3.344	6.673
50-60 cm	10.296	3.400	6.897
60-70 cm	10.575	3.455	7.120
70-80 cm	2.115	0.691	1.424
subtotal	74.225	24.465	49.760
Ave	10.309	3.398	6.911

Cellulose / Hemicellulose

	wet	dry	water
0-10 cm	4.365	1.515	2.849
10-20 cm	4.354	1.446	2.908
20-30 cm	4.343	1.376	2.967
30-40 cm	4.316	1.404	2.912
40-50 cm	4.288	1.431	2.857
50-60 cm	4.331	1.430	2.901
60-70 cm	4.373	1.429	2.944
70-80 cm	0.875	0.286	0.589
subtotal	31.245	10.318	20.927
Average	4.340	1.433	2.906

Lignin

	wet	dry	water
0-10 cm	0.505	0.175	0.330
10-20 cm	0.477	0.159	0.318
20-30 cm	0.449	0.142	0.307
30-40 cm	0.437	0.142	0.295
40-50 cm	0.426	0.142	0.284
50-60 cm	0.432	0.143	0.289
60-70 cm	0.438	0.143	0.295
70-80 cm	0.088	0.029	0.059
subtotal	3.253	1.075	2.177
Aveage	0.452	0.149	0.302

Ash / Inorganic

	wet	dry	water
0-10 cm	0.800	0.278	0.523
10-20 cm	0.730	0.243	0.487
20-30 cm	0.660	0.209	0.451
30-40 cm	0.801	0.262	0.539
40-50 cm	0.942	0.314	0.628
50-60 cm	0.785	0.260	0.525
60-70 cm	0.627	0.205	0.422
70-80 cm	0.125	0.041	0.084
subtotal	5.470	1.812	3.658
Aveage	0.760	0.252	0.508

ckeck on total	114.192	37.670	76.521
TOTAL	15.860	5.232	10.628

Readily-Biodegradable
Lab Results, 15 May 08
C4 Reactor 12 p. 3 of 3
Mixture 3
Run Time: 163.5 hr

	Total Wt	Water	Dry Matter	Dry Basis Soluble	Cell / Hemi	Lignin	Ash / Inorganic
Initial		65.8%	34.2%	69.5%	23.6%	2.7%	4.2%
Final		67.0%	33.0%	64.9%	27.4%	2.9%	4.8%
Initial weight (kg)	16.25	10.69	5.56	3.87	1.31	0.149	0.24
Final weight (kg)	15.86	10.63	5.23	3.40	1.43	0.149	0.25
Difference (kg)	0.39	0.06	0.33	0.47	-0.12	0.000	-0.02
Percent Change	2.4%	0.5%	6.0%	12.1%	-9.3%	-0.2%	-6.8%

Total Weight adjusted to 1.0

	Total Wt	Water	Dry Matter	Dry Basis Soluble	Cell / Hemi	Lignin	Ash / Inorganic
Initial weight (kg)	1.00	0.66	0.34	0.24	0.081	0.009	0.014
Final weight (kg)	0.98	0.65	0.32	0.21	0.088	0.009	0.015
Difference (kg)	0.02	0.00	0.02	0.03	-0.007	0.000	-0.001
Percent Change	2.4%	0.5%	6.0%	12.1%	-9.3%	-0.2%	-6.8%

Appendix E - Mathematical Composting Model Program Coding

In MATLAB®

```
clear;
format short;
%*************************************************************************
%*************************************************************************
%
%                  IN-VESSEL COMPOSTING MODEL
%          WITH MULTIPLE SUBSTRATE AND MICROORGANISM TYPES
%
%*************************************************************************
%*************************************************************************
%***    SYMBOLS: GENERAL RULES

%***    PRIME SYMBOLS
%   CC          = Concentration compost mass
%   CH          = Specific heat
%   CX          = Concentration of microbes
%   d           = Rate of change
%   H           = Humidity
%   h           = Enthalpy
%   k           = factor
%   kd          = Death of organisms
%   M           = Moisture
%   m           = mass
%   P           = Pressure
%   S           = Mass of substrate
%   T           = temperature
%   t           = Time
```

```
%  v            = Velocity
%  W            = Water
%  Y            = Yield coefficient


%***    PRIME AND 1ST SUBSCRIPT
%  o            = Oxygen
%  ss           = Soluble substrate (sugars)
%  sc           = Cellulose/hemicellulose substrate
%  si           = Inert (ash/inorganic) substrate
%  sl           = Lignin substrate
%  w            = Water


%***    SUBSTRIPTS ONLY
%  a            = Actinomycetes
%  b            = Bacteria
%  da           = Dry air
%  db           = Dry bulb (ambiant)temperature
%  dm           = Dry matter
%  dp           = Dew point
%  f            = Fungi
%  m            = Mesophilic
%  t            = Thermophlic
%  wb           = Wet bulb temperature


%*************************************************************************
%                       SYMBOLS
%*************************************************************************
%  Awall        = Area of compost vessel wall  (m^2)

%  CHsc         = Specific heat of cellulose/hemicellulose substrate(kJ kg-sc^-1 K^-1)
%  CHsi         = Specific heat of inert substrate (kJ kg-si^-1 K^-1)
```

```
%   CHsl          = Specific heat of lignin substrate (kJ kg-sl^-1 K^-1)
%   CHss          = Specific heat of soluble substrate (kJ kg-ss^-1 K^-1)
%   CHw           = Specific heat of water (kJ kg-w^-1 K^-1)
%   C_O2          = Concentration of oxygen (kg-O2 m^-3)
%   C_CO2         = concentration of carbon dioxide produced (kg-CO2 m^-3)
%   CSsc          = Concentration of cellulose/hemicellulose substrate per increment volume (kg-sc m^-3)
%   CSsl          = Concentration of lignin substrate per increment volume (kg-sl m^-3)
%   CSsi          = Concentration of inert substrate per increment volume (kg-si m^-3)
%   CSss          = Concentration of soluble substrate per increment volume (kg-ss m^-3)
%   CW            = Concentration of water in substrate per increment volume (kg-w m^-3)
%   CXma & CXma1  = Concentration of mesophilic actinomycetes (kg-xma m^-3)
%   CXmb & CXmb1  = Concentration of mesophilic bacteria (kg-xmb m^-3)
%   CXmf & CXmf1  = Concentration of mesophilic fungi (kg-xmf m^-3)
%   CXta & CXta1  = Concentration of thermophilic actinomycetes (kg-xta m^-3)
%   CXtb & Cxtb1  = Concentration of thermophilic bacteria (kg-xtb m^-3)
%   CXtf & CXtf1  = Concentration of thermophilic fungi (kg-xtf m^-3)

%   d             = Number of increments or layers the compost bed is divided (no units)
%   dCSsc         = Rate of change in the concentration of cellulose/hemicellulose substrate (kg-sc m^-3 h^-1)
%   dCSsCXkd  = Rate of change in the concentration of soluble substrate generated due to microbial population that died during time
Delta_t (kg-s m^-3 h^-1)
%   dCSsl         = Rate of change in the concentration of lignin substrate (kg-sl m^-3 h^-1)
%   dCSss         = Rate of change in the concentration of soluble substrate (kg-ss m^-3 h^-1)
%   dCW           = Rate of change in the concentration of water (kg-w m^-3 h^-1)
%   dCWa          = Rate of change in the concentration of water due to aeration (kg-w m^-1 h^-1)
%   dCWp          = Rate of change in the concentration of water produced due to consumption of substrate (kg-w m^-3 h^-1)
%   dCXgma        = Rate of change in the concentration of mesophilic actinomycetes population due to growth (kg-xma m^-3 h^-1)
%   dCXgmb        = Rate of change in the concentration of mesophilic bacterial population due to growth (kg-xmb m^-3 h^-1)
%   dCXgmf        = Rate of change in the concentration of mesophilic fungal population due to growth  (kg-xmf m^-3 h^-1)
%   dCXgta        = Rate of change in the concentration of thermophlic actinomycetes population due to growth (kg-xta m^-3 h^-1)
%   dCXgtb        = Rate of change in the concentration of thermophlic bacterial population due to growth (kg-xtb m^-3 h^-1)
%   dCXgtf        = Rate of change in the concentration of thermophlic fungal population due to growth (kg-xtf m^-3 h^-1)
%   dCXkdma   = Rate of change in the concentration of mesophilic actinomycetes population due to that portion of the population which
are dying (kg-xma m^-3 h^-1)
```

```
%   dCXkdmb   = Rate of change in the concentration of mesophilic bacterial population due to that portion of the population which are
dying (kg-xmb m^-3 h^-1)
%   dCXkdmf    = Rate of change in the concentration of mesophilic fungal population due to that portion of the population which are
dying (kg-xmf m^-3 h^-1)
%   dCXkdta     = Rate of change in the concentration of thermophilic actinomycetes population due to that portion of the population
which are dying (kg-xta m^-3 h^-1)
%   dCXkdtb     = Rate of change in the concentration of thermophilic bacterial population due to that portion of the population which are
dying (kg-xtb m^-3 h^-1)
%   dCXkdtf     = Rate of change in the concentration of thermophilic fungal population due to that portion of the population which are
dying (kg-xtf m^-3 h^-1)
%   dCXma       = Rate of change in the concentration of mesophilic actinomycetes (kg-xma m^-3 h^-1)
%   dCXmb       = Rate of change in the concentration of mesophilic bacteria (kg-xmb m^-3 h^-1)
%   dCXmf       = Rate of change in the concentration of mesophilic fungi (kg-xmf m^-3 h^-1)
%   dCXta       = Rate of change in the concentration of thermophilic actinomycetes (kg-xta m^-3 h^-1)
%   dCXtb       = Rate of change in the concentration of thermophilic bacteria (kg-xtb m^-3 h^-1)
%   dCXtf       = Rate of change in the concentration of thermophilic fungi (kg-xtf m^-3 h^-1)
%   dC_CO2      = Rate of change in the concentration of carbon dioxide produced due to consumption of substrate (kg-CO2 m^-3 h^-1)
%   dC_O2       = Rate of change in the concentration of oxygen (kg-O2 m^-3 h^-1)
%   dC_O2a      = Rate of change in the concentration of oxygen consumed due to consumption of substrate (kg-O2 m^-3 h^-1)
%   dC_O2c      = Rate of change in the concentration of oxygen increase due to seration (kg-O2 m^-3 h^-1)
%   Delta_t     = Time increment between each step (h)
%   DepthCB     = Depth of compost bed (m)
%   DepthCL     = Depth of each increment in the compost bed (m)
%   Dia         = Inside diameter of compost vessel (m)
%   dT          = Rate of change in temperature (K h^-1)
%   dTa         = Rate of change in temperature due to aeration (K h^-1)
%   dTp         = Rate of change in temperature due to substrate consumption (K h^-1)
%   dTq         = Rate of change in temperature due to heat loss through compost vessel wall (K h^-1)

%   Fair        = Volume of air flowing into reactor (L h^-1)

%   H           = Humidity ratio (kg-w kg-da^-1)
%   h           = Enthalpy of mixture (kJ kg-da^-1)
%   HCsc        = Heat of combustion of cellulose/hemicellulose substrate (kJ kg-sc^-1)
```

```
%   HCsl        = Heat of combustion of lignin substrate (kJ kg-sl^-1)
%   HCss        = Heat of combustion of soluble substrate (kJ kg-ss^-1)
%   hprimefg    = Latent heat of vaporization (h'fg) at Twb (kJ kg^-1)
%   h2primefg   = Latent heat of vaporization (h"fg) at Tdp (kJ kg^-1)

%   ip          = Indexing notation representing all nodes from 1 to p [ip=(1,p)].
%                 Is part of the cell reference number (k,ip) identifying the cell's location:
%                 k equals the time step whose length is defined by Delta T
%                  ip equals the difference levels within the composter reactor.

%   k           = Indexing notation representing the time step.
%                  Is part of the cell reference number (k,ip)identifying the cell's location:
%                  k equals the time step whose length is defined by Delta T
%                  ip equals the difference levels within the composter reactor.
%   kdm         = Fraction of mesophilic microbial population which die each hour (kg-x h^-1)
%   kdt         = Fraction of thermophilic microbial population which die each hour (kg-x h^-1)
%   KS          = 'Half-Velocity' coefficient for substrate (kg-s m^-3)
%   KO2         = 'Half-Velocity' coefficient for oxygen (kg-O2 m^-3)
%   k_H20       = Moisture coefficient: factor that weights the effect of moisture present on microbial growth (no units)
%   k_O2        = Oxygen availability coefficient: amount of oxygen available for decomposition of substrate based on stoichiometric
balance (no units)

%   Mfda        = Mass flow of dry air (kg-da h^-1)
%   muma        = Specific growth rate for mesophilic actinomycetes (kg-sc kg-xma^-1 h^-1)
%   mumaxma     = Maximum specific growth rate for mesophilic actinomycetes (kg-sc kg-xma^-1 h^-1)
%   mumaxmb     = Maximum specific growth rate for mesophilic bacteria (kg-ss kg-xmb^-1 h^-1)
%   mumaxmf     = Maximum specific growth rate for mesophilic fungi (kg-sl kg-xmf^-1 h^-1)
%   mumaxta     = Maximum specific growth rate for thermophilic actinomycetes (kg-sc kg-xta^-1 h^-1)
%   mumaxtb     = Maximum specific growth rate for thermophilic bacteria (kg-ss kg-xtb^-1 h^-1)
%   mumaxtf     = Maximum specific growth rate for thermophilic fungi (kg-sl kg-xtf^-1 h^-1)
%   mumb        = Specific growth rate for mesophilic bacteria (kg-ss kg-xmb^-1 h^-1)
%   mumf        = Specific growth rate for mesophilic fungi (kg-sl kg-xmf^-1 h^-1)
%   muta        = Specific growth rate for thermophilic actinomycetes (kg-sc kg-xta^-1 h^-1)
%   mutb        = Specific growth rate for thermophilic bacteria (kg-ss kg-xtb^-1 h^-1)
```

```
%  mutf       = Specific growth rate for thermophilic fungi (kg-sl kg-xtf^-1 h^-1)

%  numa       = Microbial maintenence coefficient for mesophilic actinomycetes (kg-sc kg-xma^-1 hr^1)
%  numaxm     = Maximum mesophilic microbial maintenence coefficient (kg-s kg-x^-1 hr^1)
%  numaxt     = Maximum thermophilic microbial maintenence coefficient (kg-s kg-x^-1 hr^1)
%  numb       = Microbial maintenence coefficient for mesophilic bacteria (kg-ss kg-xmb^-1 hr^1)
%  numf       = Microbial maintenence coefficient for mesophilic fungi (kg-sl kg-xmf^-1 hr^1)
%  nuta       = Microbial maintenence coefficient for thermophilic actinomycetes (kg-sc kg-xta^-1 hr^1)
%  nutb       = Microbial maintenence coefficient for thermophilic bacteria (kg-ss kg-xtb^-1 hr^1)
%  nutf       = Microbial maintenence coefficient for thermophilic fungi (kg-sl kg-xtf^-1 hr^1)

%  p          = Number of nodes: number of increments the compost bed is divided into (d) plus 1 for increment below container (no
                units)
%  Patm       = Atmospheric pressure at sea level (Pa) (kg m^-1 s^-2)
%  Psa        = Saturation vapor pressure at atmospheric pressure (Pa) (kg m^-1 s^-2)
%  Pswb       = Saturation vapor pressure at wet bulb temperature (Pa) (kg m^-1 s^-2)
%  Pv         = Partial vapor pressure    (Pa) (kg m^-1 s^-2)

%  qm         = Sensible heat stored in compost material (kJ .C^-1 m^-3)

%  RT         = Thermal resistance of vessel wall in which the compost placed (K m^2 h J^-1)

%  Sc         = Mass of cellulose substrate (kg-sc)
%  Si         = Mass of inert substrate (kg-si)
%  Sl         = Mass of lignin substrate (kg-sl)
%  Ss         = Mass of soluble substrate (kg-ss)
%  Ssc        = Mass of cellulose/hemicellulose substrate per layer (kg-sc)
%  Ssi        = Mass of inert substrate per layer (kg-si)
%  Ssl        = Mass of lignin substrate per layer (kg-sl)
%  Sss        = Mass of soluble substrate per layer (kg-ss)
%  Sst        = Mass of all substrate per layer (kg-s)
%  St         = Mass of all substrate (kg-s)

%  T & T1     = Temperature in degrees Kelvin (.C+273.16=K)
```

```
%  t            = Time (h)
%               Time is required to be in hours. If less than one hour, use fraction (45/60)or decimal (0.75)
%  Tc           = Initial (ambient) temperature reading in degrees Celsius (.C)
%  Tcmmax       = Maximum temperature for mesophilic organisms in degrees Celsius (.C)
%  Tcmmin       = Minumin temperature for mesophilic organisms in degrees Celsius (.C)
%  Tctmax       = Maximum temperature for thermophilic organisms in degrees Celsius (.C)
%  Tctmin       = Minimum temperature for thermophilic organisms in degrees Celsius (.C)
%  Tcwb         = Initial wet bulb temperature in degrees Celsius (.C)
%  Tdp          = Dew point temperature in degrees Kelvin (K)
%  Time_Stop    = Time at which the run will terminate
%  Tmmax        = Maximum temperature for mesophilic organisms in degrees Kelvin (K)
%  Tmmin        = Minumin temperature for mesophilic organisms in degrees Kelvin (K)
%  Ttmax        = Maximum temperature for thermophilic organisms in degrees Kelvin (K)
%  Ttmin        = Minimum temperature for thermophilic organisms in degrees Kelvin (K)
%  Twb          = Wet bulb temperature in degrees Kelvin (K)
%  t_step       = Time step parameter to set program (h)

%  Vair         = Volume flow of air (m^3 h^-1)
%  Vcsa         = Cross sectional area of volume of compost bed: for a cylinder vessel (pi*radius^2) (m^2)
%  VolCB        = Total volume of compost bed (pi*radius^2*height) (m^3)
%  VolCL        = Volume of compost in each layer (m^3)
%  Vsa          = Specific volume of dry air (ideal gas equation) (m^3 kg-da^-1)

%  Wadd         = Mass of water added to the substrate (kg-w)
%  Wmc          = Moisture content (wet bases): the fraction of mass of water comparied to the mass of all ingredients, both water and
                  substrate (kg-w kg-w&s^-1)
%  Ws           = Total mass of water persent in the substrate initially (kg-w)
%  Wst          = Mass of total water present per layer  (kg-w)
%  Wt           = Mass of total water present (Ws + Wadd)(kg-w)

%  YCO2Ssc      = Yield coefficient: amount of carbon dioxide produced per unit mass of cellulose/hemicellulose substrate utilized
                  (decomposed) (kg-CO2 kg-sc^-1)
 %  YCO2Ssl     = Yield coefficient: amount of carbon dioxide produced per unit mass of lignin substrate utilized (decomposed) (kg-CO2
                  kg-sl^-1)
```

```
%   YCO2Sss     = Yield coefficient: amount of carbon dioxide produced per unit mass of soluble substrate utilized (decomposed) (kg-CO2
                  kg-ss^-1)
%   YO2Ssc      = Yield coefficient: amount of oxygen consumed per mass of cellulose/hemicellulose substrate utilized (kg-O2 kg-sc^-1)
%   YO2Ssl      = Yield coefficient: amount of oxygen consumed per mass of lignin substrate utilized (kg-O2 kg-sl^-1)
%   YO2Sss      = Yield coefficient: amount of oxygen consumed per mass of soluble substrate utilized (kg-O2 kg-ss^-1)
%   YWSsc       = Yield coefficient: amount of water generated per unit mass of cellulose/hemicellulose substrate utilized (decomposed)
                  (kg-w kg-sc^-1)
%   YWSsl       = Yield coefficient: amount of water generated per unit mass of lignin substrate utilized (decomposed) (kg-w kg-sl^-1)
%   YWSss       = Yield coefficient: amount of water generated per unit mass of soluble substrate utilized (decomposed) (kg-w kg-ss^-1)
%   YXaSsc      = Yield coefficient: amount of actinomyces-biomass produced per unit mass of cellulose/hemicellulose substrate utilized
                  (decomposed) (kg-xa kg-sc^-1)
%   YXbSss      = Yield coefficient: amount of bacteria-biomass produced per unit mass of soluble substrate utilized (decomposed) (kg-xb
                  kg-ss^-1)
%   YXfSsl      = Yield coefficient: amount of fungi-biomass produced per unit mass of lignin substrate utilized (decomposed) (kg-xf kg-
                  sl^-1)

%*************************************************************************
%*************************************************************************
%
%                       PARAMETERS
%
%*************************************************************************
%*************************************************************************

%   TIME PARAMETERS
t_step=1/60;
t_stop=600.0;
t=0:t_step:t_stop;

%   COMPOSTING VESSEL PARAMETERS
DepthCB=0.80;                   % Depth of compost bed in compost vessel
d=8;                            % Number of increments of compost bed
DepthCL=DepthCB/d;               % Depth of each increment
p=d+1;                           % Array size
```

```
Dia=0.203;                          % Diameter of compost bed

%   Calculate cross-sectional area of bed (Vcsa), volume of compost bed layer (VolCL)
%   Volume of compost bed (total volume) (VolCB), and area of compost bed - side walls only
Vcsa=pi*((Dia/2)^2);
VolCL=Vcsa*DepthCL;
VolCB=Vcsa*DepthCB;
Awall=2*pi*(Dia/2)*DepthCB;

RT=0.4500;                          %Thermal resistance wall surrounding the compost

%   SUBSTRATE PARAMETERS:
%   Weight of dry substrate
Ss=3.79;
Sc=1.28;
Sl=0.146;
Si=0.231;
%   Weight of water in substrate
Ws=10.47;
%   Water added
Wadd=0.0;
%   Air flow rate
Fair=104.0;

%   Total weight of dry substrate
St=Ss+Sc+Sl+Si;

%   Total weight of water in substrate mixture
Wt=Ws+Wadd;

%   TEMPERATURE PARAMETERS
%   Temperature:  average ambiant air source
Tc= 23.74;
%   Temperature: wet bulb reading
```

```
Tcwb=15.0;

%   Temperature range in which microorganisms will survive
%   Mesophilic range
Tcmmin=15;
Tcmmax=53;
Tmmin=Tcmmin+273.16;
Tmmax=Tcmmax+273.16;

%   Thermophilic range
Tctmin=40;
Tctmax=75;
Ttmin=Tctmin+273.16;
Ttmax=Tctmax+273.16;

%   ATMOSPHERIC PRESSURE
Patm=101325;

%   HEAT OF COMBUSTION
HCss=19100;
HCsc=19100;
HCsl=19100;

%   SPECIFIC HEAT
CHss=1.48;
CHsc=1.48;
CHsl=1.48;
CHsi=0.84;
CHw=4.18;

%   COEFFICIENTS
KS=62.0;
KO2=0.07;
```

```
%   Carbon Dioxide generated per unit of substrate utilized
YCO2Sss=0.4478;
YCO2Ssc=1.0535;
YCO2Ssl=0.7695;

%   Oxygen consumption per unit of substrate utilized
YO2Sss=0.3570;
YO2Ssc=0.7156;
YO2Ssl=0.8374;

%   Water generated per unit of substrate utilized
YWSss=0.4312;
YWSsc=0.3898;
YWSsl=0.2520;

%   Biomass generated per unit of substrate utilized
YXbSss=0.5782;
YXaSsc=0.3281;
YXfSsl=0.9160;

%**************************************************************************
%                          SET ARRAYS
%**************************************************************************
CSsc=zeros(length(t),p);
CSsi=zeros(length(t),p);
CSsl=zeros(length(t),p);
CSss=zeros(length(t),p);
CW=zeros(length(t),p);
CXma=zeros(length(t),p);
CXma1=zeros(length(t),p);
CXmb=zeros(length(t),p);
CXmb1=zeros(length(t),p);
CXmf=zeros(length(t),p);
CXmf1=zeros(length(t),p);
```

```
CXta=zeros(length(t),p);
CXta1=zeros(length(t),p);
CXtb=zeros(length(t),p);
CXtb1=zeros(length(t),p);
CXtf=zeros(length(t),p);
CXtf1=zeros(length(t),p);
C_CO2=zeros(length(t),p);
C_O2=zeros(length(t),p);
dCSsc=zeros(length(t),p);
dCSsCXkd=zeros(length(t),p);
dCSsl=zeros(length(t),p);
dCSss=zeros(length(t),p);
dCW=zeros(length(t),p);
dCWa=zeros(length(t),p);
dCWp=zeros(length(t),p);
dCXgma=zeros(length(t),p);
dCXgmb=zeros(length(t),p);
dCXgmf=zeros(length(t),p);
dCXgta=zeros(length(t),p);
dCXgtb=zeros(length(t),p);
dCXgtf=zeros(length(t),p);
dCXkdma=zeros(length(t),p);
dCXkdmb=zeros(length(t),p);
dCXkdmf=zeros(length(t),p);
dCXkdta=zeros(length(t),p);
dCXkdtb=zeros(length(t),p);
dCXkdtf=zeros(length(t),p);
dCXma=zeros(length(t),p);
dCXmb=zeros(length(t),p);
dCXmf=zeros(length(t),p);
dCXta=zeros(length(t),p);
dCXtb=zeros(length(t),p);
dCXtf=zeros(length(t),p);
dC_CO2=zeros(length(t),p);
```

```
dC_O2=zeros(length(t),p);
dC_O2a=zeros(length(t),p);
dC_O2c=zeros(length(t),p);
dT=zeros(length(t),p);
dTa=zeros(length(t),p);
dTp=zeros(length(t),p);
dTq=zeros(length(t),p);
hprimefg=zeros(length(t),p);
h2primefg=zeros(length(t),p);
H=zeros(length(t),p);
h=zeros(length(t),p);
kdm=zeros(length(t),p);
kdt=zeros(length(t),p);
k_H2O=zeros(length(t),p);
Mfda=zeros(length(t),p);
muma=zeros(length(t),p);
mumaxma=zeros(length(t),p);
mumaxmb=zeros(length(t),p);
mumaxmf=zeros(length(t),p);
mumaxta=zeros(length(t),p);
mumaxtb=zeros(length(t),p);
mumaxtf=zeros(length(t),p);
mumb=zeros(length(t),p);
mumf=zeros(length(t),p);
muta=zeros(length(t),p);
mutb=zeros(length(t),p);
mutf=zeros(length(t),p);
numa=zeros(length(t),p);
numaxm=zeros(length(t),p);
numaxt=zeros(length(t),p);
numb=zeros(length(t),p);
numf=zeros(length(t),p);
nuta=zeros(length(t),p);
nutb=zeros(length(t),p);
```

```
nutf=zeros(length(t),p);
Psa=zeros(length(t),p);
Pswb=zeros(length(t),p);
Pv=zeros(length(t),p);
qm=zeros(length(t),p);
Ssc=zeros(length(t),p);
Ssi=zeros(length(t),p);
Ssl=zeros(length(t),p);
Sss=zeros(length(t),p);
Sst=zeros(length(t),p);
T=zeros(length(t),p);
Tdp=zeros(length(t),p);
Twb=zeros(length(t),p);
T1=zeros(length(t),p);
Vair=zeros(length(t),p);
Vsa=zeros(length(t),p);
Wmc=zeros(length(t),p);
Wst=zeros(length(t),p);

%**************************************************************************
%**************************************************************************
%                       SET PARAMATERS
%                          for
%             ENVIRONMENTAL CONDITIONS EXTERIOR TO VESSEL
%                BOUNDARY CONDITIONS WITHIN VESSEL
%**************************************************************************
%**************************************************************************
for ip=1:p
   T(1,ip)= Tc + 273.16;
   Twb(1,ip) = Tcwb + 273.16;
   Vair(1,ip)= 0.001*Fair;
   C_O2(1,ip) = 0.2992;
```

```
   Psa(1,ip)=22105649.25*exp(((-27405.526)+(97.5413.*T(1,ip))+(-0.146244.*(T(1,ip).^2))+((0.12558*10.^-3).*(T(1,ip).^3))+((-
      0.48502*10.^-7).*(T(1,ip).^4)))./(4.34903*T(1,ip)-((0.39381*10.^-2).*(T(1,ip).^2))));
   Pswb(1,ip)=22105649.25*exp(((- 27405.526)+(97.5413*Twb(1,ip))+(-0.146244*(Twb(1,ip).^2))+((0.12558*10.^-
      3).*(Twb(1,ip).^3))+((-0.48502*10.^-7).*(Twb(1,ip).^4)))./(4.34903*Twb(1,ip)-((0.39381*10.^-2).*(Twb(1,ip).^2))));
   hprimefg(1,ip)=2502535.259-(2385.76424*(Twb(1,ip)-273.16));
   Pv(1,ip)=((0.62194.*hprimefg(1,ip).*Pswb(1,ip))-(1.0069254.*(Pswb(1,ip)-Patm).*(Twb(1,ip)-
      T(1,ip)))./(0.62194.*hprimefg(1,ip)+((0.15684877.*(Pswb(1,ip)-Patm).*(Twb(1,ip)-T(1,ip)))./Patm));

   Tdp(1,ip)=real(255.38+19.5322*((log(0.00145*Pv(1,ip))).^0)+13.6626*((log(0.00145*Pv(1,ip))).^1)+1.17678*((log(0.00145*Pv(1,ip))
      ).^2)+(-0.189693*((log(0.00145*Pv(1,ip))).^3))+0.087453*((log(0.00145*Pv(1,ip))).^4)+(-
      0.0174053*((log(0.00145*Pv(1,ip))).^5))+0.00214768*((log(0.00145*Pv(1,ip))).^6)+(-
      0.000138343*((log(0.00145*Pv(1,ip))).^7))+0.0000038*((log(0.00145*Pv(1,ip))).^8));
   h2primefg(1,ip)=2502.535259-2.38576424*(Tdp(1,ip)-273.16);
   H(1,ip)=(0.6219*Pv(1,ip))./(Patm-Pv(1,ip));
   h(1,ip)=(1.00692540*(T(1,ip)-273.16))+(4.1868*(H(1,ip).*(Tdp(1,ip)-
      273.16)))+(h2primefg(1,ip).*H(1,ip))+(1.8756864*(H(1,ip).*(T(1,ip)-Tdp(1,ip))));
end

for ip=2:p;
   %   Mass of substrate per increment
   Sss(1,ip)=Ss/d;
   Ssc(1,ip)=Sc/d;
   Ssl(1,ip)=Sl/d;
   Ssi(1,ip)=Si/d;
   Sst(1,ip)=Sss(1,ip)+Ssc(1,ip)+Ssl(1,ip)+Ssi(1,ip);

   %   Mass of water per increment
   Wst(1,ip)=Wt/d;

   %   Concentration of substrate per increment volume
   CSss(1,ip)=Sss(1,ip)./VolCL;
   CSsc(1,ip)=Ssc(1,ip)./VolCL;
   CSsl(1,ip)=Ssl(1,ip)./VolCL;
   CSsi(1,ip)=Ssi(1,ip)./VolCL;
```

```
    %   Concentration of water
    CW(1,ip)=Wst(1,ip)./VolCL;

    %   Microbial seed population
    CXmb(1,ip)=0.008;
    CXma(1,ip)=0.008;
    CXmf(1,ip)=0.008;
    CXtb(1,ip)=0.008;
    CXta(1,ip)=0.008;
    CXtf(1,ip)=0.008;

    %   Moisture content
    Wmc(1,ip)=Wst(1,ip)./(Wst(1,ip)+Sst(1,ip));

    %   Moisture coefficient
    %   Weighted factor accounts for the reduction in microbial growth when insufficient or too much moisture is present
    if Wmc(1,ip )>=0.00 && Wmc(1,ip)<0.10;
       k_H2O(1,ip)=0.00;
    elseif Wmc(1,ip)>=0.10 && Wmc(1,ip)<0.20;
       k_H2O(1,ip)=-0.0759+0.9011.*Wmc(1,ip);
    elseif Wmc(1,ip)>=0.20 && Wmc(1,ip)<0.60;
       k_H2O(1,ip)=-0.3482+2.2597.*Wmc(1,ip);
    elseif Wmc(1,ip)>0.60 && Wmc(1,ip)<=1.0;
       k_H2O(1,ip)=7.5844-20.5315.*Wmc(1,ip)+19.8468.*(Wmc(1,ip).^2)-6.5147.*(Wmc(1,ip).^3);
    else Wmc(1,ip)=0.60;
       k_H2O(1,ip)=1.00;
    end
end
```

```
%*************************************************************************
%*************************************************************************
%                       BEGIN TIME LOOP
%                CALCULATE PARAMETERS WITHING VESSEL
%*************************************************************************
%*************************************************************************
for k = 2:length(t);
   t(k);
   Delta_t=t(k)-t(k-1);
   for ip=1:p

      if ip==1
         % Incoming parameters
         T(k,ip)=T(k-1,ip);
         C_O2(k,ip)=C_O2(k-1,ip);
         Twb(k,ip)=Twb(k-1,ip);
         Psa(k,ip)=Psa(k-1,ip);
         Pswb(k,ip)=Pswb(k-1,ip);
         hprimefg(k,ip)=hprimefg(k-1,ip);
         Pv(k,ip)=Pv(k-1,ip);
         Tdp(k,ip)=Tdp(k-1,ip);
         h2primefg(k,ip)=h2primefg(k-1,ip);
         H(k,ip)=H(k-1,ip);
         h(k,ip)=h(k-1,ip);

         %   Mass flow of air
         %   Change in oxygen concentration if air is turned off
         %   if k >= 114/Delta_t  &&  k <=  140/Delta_t;
         %       Vair(k,ip)=0.0;
         %    else
         Vair(k,ip)=Vair(1,ip);
         %    end
```

```
    %   Mass flow of dry air
    Vsa(k,ip)=(287*T(k-1,ip))./(Patm-Pv(k,ip));
    Mfda(k,ip)=Vair(k,ip)./Vsa(k,ip);

  else  % for ip=(2,p)
    %   Moisture balance: determine humidity ratio
    Twb(k,ip)=Twb(k-1,ip);
    Psa(k,ip)=22105649.25*exp(((-27405.526)+(97.5413.*T(k-1,ip))+(-0.146244.*(T(k-1,ip).^2))+((0.12558*10.^-3).*(T(k-
        1,ip).^3))+((-0.48502*10.^-7).*(T(k-1,ip).^4))./(4.34903*T(k-1,ip)-((0.39381*10.^-2).*(T(k-1,ip).^2))));
    Pv(k,ip)=(0.0007.*((T(k-1,ip)-273.16)^4))-(0.001.*((T(k-1,ip)-273.16)^3))+(2.1126.*((T(k-1,ip)-273.16)^2))+(38.161.*(T(k-1,ip)-
        273.16))+623.37;

    Tdp(k,ip)=real(255.38+19.5322*((log(0.00145*Pv(k,ip))).^0)+13.6626*((log(0.00145*Pv(k,ip))).^1)+1.17678*((log(0.00145*Pv(
        k,ip))).^2)+(-0.189693*((log(0.00145*Pv(k,ip))).^3))+0.087453*((log(0.00145*Pv(k,ip))).^4)+(-
        0.0174053*((log(0.00145*Pv(k,ip))).^5))+0.00214768*((log(0.00145*Pv(k,ip))).^6)+(-
        0.000138343*((log(0.00145*Pv(k,ip))).^7))+0.0000038*((log(0.00145*Pv(k,ip))).^8));

    if Tdp(k,ip) <= 338.72
       h2primefg(k,ip)=2502.535259-2.38576424*(Tdp(k,ip)-273.16);
    else
       h2primefg(k,ip)=(7329155978.000-15995.96408.*(Tdp(k,ip)-273.16)).^0.5;
    end

    H(k,ip)=(0.6219*Pv(k,ip))./(Patm-Pv(k,ip));
    h(k,ip)=(1.00692540*(T(k-1,ip)-273.16))+(4.1868*(H(k,ip).*(Tdp(k,ip)-
        273.16)))+(h2primefg(k,ip).*H(k,ip))+(1.8756864*(H(k,ip).*(T(k-1,ip)-Tdp(k,ip))));

    %   Mass flow of air
    Vair(k,ip)=Vair(k,ip-1);

    %   Mass flow of dry air
    Vsa(k,ip)=(287*T(k-1,ip))./(Patm-Pv(k,ip));
    Mfda(k,ip)=Vair(k,ip)./Vsa(k,ip);
```

```
        %   Cell maintenence requirement
        numaxm(k,ip)=0.48;
        numaxt(k,ip)=0.48;

        %   Death rate during normal growth
        kdm(k,ip)=0.025;
        kdt(k,ip)=0.025;

%*************************************************************************
        %   MESOPHILIC / THERMOPHILIC MICROORGANISMS GROWTH-DEATH
        %   MESOPHILIC RANGE
        if (T(k-1,ip)>=Tmmin) && (T(k-1,ip)<Tmmax);
          %   for soluble
          mumaxmb(k,ip)=0.22;
          %   for cellulose/hemicellulose
          mumaxma(k,ip)=0.06;
          %   for lignin
          mumaxmf(k,ip)=0.02;

          %   Microbial growth - mesophilic
          mumb(k,ip)=(mumaxmb(k,ip).*(CSss(k-1,ip)./(KS+CSss(k-1,ip))).*(C_O2(k-1,ip)./(KO2+C_O2(k-1,ip)))).*k_H2O(k-1,ip);
          muma(k,ip)=(mumaxma(k,ip).*(CSsc(k-1,ip)./(KS+CSsc(k-1,ip))).*(C_O2(k-1,ip)./(KO2+C_O2(k-1,ip)))).*k_H2O(k-1,ip);
          mumf(k,ip)=(mumaxmf(k,ip).*(CSsl(k-1,ip)./(KS+CSsl(k-1,ip))).*(C_O2(k-1,ip)./(KO2+C_O2(k-1,ip)))).*k_H2O(k-1,ip);
          %  Spore/seed condition if microbial population had expired
          if CXmb(k-1,ip)==0.00;
            CXmb1(k,ip)=CXmb(1,ip);
          else CXmb1(k,ip)=CXmb(k-1,ip);
          end

          if CXma(k-1,ip)==0.00;
            CXma1(k,ip)=CXma(1,ip);
          else CXma1(k,ip)=CXma(k-1,ip);
          end
```

```
   if CXmf(k-1,ip)==0.00;
      CXmf1(k,ip)=CXmf(1,ip);
   else CXmf1(k,ip)=CXmf(k-1,ip);
   end
end

%   THERMOPHILIC RANGE
if (T(k-1,ip)>=Ttmin) && (T(k-1,ip)<=Ttmax);
   %   for soluble
   mumaxtb(k,ip)=0.22;
   %   for cellulose/hemicellulose
   mumaxta(k,ip)=0.06;
   %   for lignin
   mumaxtf(k,ip)=0.02;

   %   Thermophilic - microbial growth
   mutb(k,ip)=(mumaxtb(k,ip).*(CSss(k-1,ip)./(KS+CSss(k-1,ip))).*(C_O2(k-1,ip)./(KO2+C_O2(k-1,ip)))).*k_H2O(k-1,ip);
   muta(k,ip)=(mumaxta(k,ip).*(CSsc(k-1,ip)./(KS+CSsc(k-1,ip))).*(C_O2(k-1,ip)./(KO2+C_O2(k-1,ip)))).*k_H2O(k-1,ip);
   mutf(k,ip)=(mumaxtf(k,ip).*(CSsl(k-1,ip)./(KS+CSsl(k-1,ip))).*(C_O2(k-1,ip)./(KO2+C_O2(k-1,ip)))).*k_H2O(k-1,ip);

   %  Spore/seed condition if microbial population had expired
   if CXtb(k-1,ip)==0.00;
      CXtb1(k,ip)=CXtb(1,ip);
   else CXtb1(k,ip)=CXtb(k-1,ip);
   end

   if CXta(k-1,ip)==0.00;
      CXta1(k,ip)=CXta(1,ip);
   else CXta1(k,ip)=CXta(k-1,ip);
   end

   if CXtf(k-1,ip)==0.00;
      CXtf1(k,ip)=CXtf(1,ip);
   else CXtf1(k,ip)=CXtf(k-1,ip);
```

```
    end
  end


%**************************************************************************
    %      Death of cells outside of their temperature range
    if (T(k-1,ip)>Tmmin) && (T(k-1,ip)<Ttmin);
      kdt(k,ip)=0.40;
    end
    if (T(k-1,ip)>Tmmax) && (T(k-1,ip)<Ttmax)
      kdm(k,ip)=0.40;
    end
%**************************************************************************
    %   Microbial growth and maintenance - Mesophilic
    numb(k,ip)=(numaxm(k,ip).*(CSss(k-1,ip)./(KS+CSss(k-1,ip))).*(C_O2(k-1,ip)./(KO2+C_O2(k-1,ip)))).*k_H2O(k-1,ip);
    numa(k,ip)=(numaxm(k,ip).*(CSsc(k-1,ip)./(KS+CSsc(k-1,ip))).*(C_O2(k-1,ip)./(KO2+C_O2(k-1,ip)))).*k_H2O(k-1,ip);
    numf(k,ip)=(numaxm(k,ip).*(CSsl(k-1,ip)./(KS+CSsl(k-1,ip))).*(C_O2(k-1,ip)./(KO2+C_O2(k-1,ip)))).*k_H2O(k-1,ip);

    %   Mesophilic - bacteria
    dCXgmb(k,ip)=mumb(k,ip).*CXmb1(k,ip);
    dCXkdmb(k,ip)=kdm(k,ip).*CXmb1(k,ip);
    dCXmb(k,ip)=dCXgmb(k,ip)-dCXkdmb(k,ip);
    CXmb(k,ip)=CXmb(k-1,ip)+dCXmb(k,ip).*Delta_t;
    if CXmb(k,ip)<0.00;
      CXmb(k,ip)=0.00;
    end

    %   Mesophilic - actinomycetes
    dCXgma(k,ip)=muma(k,ip).*CXma1(k,ip);
    dCXkdma(k,ip)=kdm(k,ip).*CXma1(k,ip);
    dCXma(k,ip)=dCXgma(k,ip)-dCXkdma(k,ip);
    CXma(k,ip)=CXma(k-1,ip)+dCXma(k,ip).*Delta_t;
    if CXma(k,ip)<0.00;
      CXma(k,ip)=0.00;
```

```
end

%   Mesophilic - fungii
dCXgmf(k,ip)=mumf(k,ip).*CXmf1(k,ip);
dCXkdmf(k,ip)=kdm(k,ip).*CXmf1(k,ip);
dCXmf(k,ip)=dCXgmf(k,ip)-dCXkdmf(k,ip);
CXmf(k,ip)=CXmf(k-1,ip)+dCXmf(k,ip).*Delta_t;
if CXmf(k,ip)<0.00;
   CXmf(k,ip)=0.00;
end

%   Microbial growth and maintenance - Thermophilic
nutb(k,ip)=(numaxt(k,ip).*(CSss(k-1,ip)./(KS+CSss(k-1,ip))).*(C_O2(k-1,ip)./(KO2+C_O2(k-1,ip)))).*k_H2O(k-1,ip);
nuta(k,ip)=(numaxt(k,ip).*(CSsc(k-1,ip)./(KS+CSsc(k-1,ip))).*(C_O2(k-1,ip)./(KO2+C_O2(k-1,ip)))).*k_H2O(k-1,ip);
nutf(k,ip)=(numaxt(k,ip).*(CSsl(k-1,ip)./(KS+CSsl(k-1,ip))).*(C_O2(k-1,ip)./(KO2+C_O2(k-1,ip)))).*k_H2O(k-1,ip);

%   Thermophilic - bacteria
dCXgtb(k,ip)=mutb(k,ip).*CXtb1(k,ip);
dCXkdtb(k,ip)=kdt(k,ip).*CXtb1(k,ip);
dCXtb(k,ip)=dCXgtb(k,ip)-dCXkdtb(k,ip);
CXtb(k,ip)=CXtb(k-1,ip)+dCXtb(k,ip).*Delta_t;
if CXtb(k,ip)<0.00;
   CXtb(k,ip)=0.00;
end

%   Thermophilic - actinomycetes
dCXgta(k,ip)=muta(k,ip).*CXta1(k,ip);
dCXkdta(k,ip)=kdt(k,ip).*CXta1(k,ip);
dCXta(k,ip)=dCXgta(k,ip)-dCXkdta(k,ip);
CXta(k,ip)=CXta(k-1,ip)+dCXta(k,ip).*Delta_t;
if CXta(k,ip)<0.00;
   CXta(k,ip)=0.00;
end
```

```
%   Thermophilic - fungii
dCXgtf(k,ip)=mutf(k,ip).*CXtf1(k,ip);
dCXkdtf(k,ip)=kdt(k,ip).*CXtf1(k,ip);
dCXtf(k,ip)=dCXgtf(k,ip)-dCXkdtf(k,ip);
CXtf(k,ip)=CXtf(k-1,ip)+dCXtf(k,ip).*Delta_t;
if CXtf(k,ip)<0.00;
   CXtf(k,ip)=0.00;
end



%**************************************************************************
%   SUBSTRATE
%   Substrate generated as a result of death
dCSsCXkd(k,ip)=dCXkdmb(k,ip)+dCXkdma(k,ip)+dCXkdmf(k,ip)+dCXkdtb(k,ip)+dCXkdta(k,ip)+dCXkdtf(k,ip);

%   Change in substrate consumption
dCSss(k,ip)=(dCXgmb(k,ip)./YXbSss)+(numb(k,ip).*CXmb(k,ip))+(dCXgtb(k,ip)./YXbSss)+(nutb(k,ip).*CXtb(k,ip));
dCSsc(k,ip)=(dCXgma(k,ip)./YXaSsc)+(numa(k,ip).*CXma(k,ip))+(dCXgta(k,ip)./YXaSsc)+(nuta(k,ip).*CXta(k,ip));
dCSsl(k,ip)=(dCXgmf(k,ip)./YXfSsl)+(numf(k,ip).*CXmf(k,ip))+(dCXgtf(k,ip)./YXfSsl)+(nutf(k,ip).*CXtf(k,ip));

%   Concentration of substrate
CSss(k,ip)=CSss(k-1,ip)-(dCSss(k,ip).*Delta_t)+(0.95*dCSsCXkd(k,ip).*Delta_t);
CSsc(k,ip)=CSsc(k-1,ip)-(dCSsc(k,ip).*Delta_t);
CSsl(k,ip)=CSsl(k-1,ip)-(dCSsl(k,ip).*Delta_t)+(0.05*dCSsCXkd(k,ip).*Delta_t);
CSsi(k,ip)=CSsi(k-1,ip);

%   OXYGEN CONCENTRATION
%   Oxygen consumption per unit mass of substrate consumed
dC_O2c(k,ip)=((YO2Sss.*dCSss(k,ip))+(YO2Ssc.*dCSsc(k,ip))+(YO2Ssl.*dCSsl(k,ip))).*Delta_t;
%   Change in oxygen concentration due to air flow
dC_O2a(k,ip)=((Vair(k,ip)./VolCL).*(C_O2(k-1,ip-1)-C_O2(k-1,ip))).*Delta_t;

dC_O2(k,ip)=-dC_O2c(k,ip)+dC_O2a(k,ip);
```

```
C_O2(k,ip)=C_O2(k-1,ip)+dC_O2(k,ip);

if C_O2(k,ip)>0.2992;
   C_O2(k,ip)=0.2992;
elseif C_O2(k,ip)<0.00;
   C_O2(k,ip)=0.00;
else C_O2(k,ip)=C_O2(k,ip);
end

%   CARBON DIOXIDE PRODUCED
dC_CO2(k,ip)=(YCO2Sss.*dCSss(k,ip))+(YCO2Ssc.*dCSsc(k,ip))+(YCO2Ssl.*dCSsl(k,ip));
C_CO2(k,ip)=C_CO2(k-1,ip)+(dC_CO2(k,ip).*Delta_t);

%  SUBSTRATE VOLUME
%  Change in substrate
Sss(k,ip)=CSss(k,ip).*VolCL;
if Sss(k,ip)<0;
   Sss(k,ip)=0;
end

Ssc(k,ip)=CSsc(k,ip).*VolCL;
if Ssc(k,ip)<0;
   Ssc(k,ip)=0;
end

Ssl(k,ip)=CSsl(k,ip).*VolCL;
if Ssl(k,ip)<0;
   Ssl(k,ip)=0;
end

Ssi(k,ip)=CSsi(k,ip).*VolCL;
Sst(k,ip)=Sss(k,ip)+Ssc(k,ip)+Ssl(k,ip)+Ssi(k,ip);
```

```
%   WATER CONTENT
%   Water produced per unit mass of substrate consumed
dCWp(k,ip)=((YWSss.*dCSss(k,ip))+(YWSsc.*dCSsc(k,ip))+(YWSsl.*dCSsl(k,ip))).*Delta_t;
%   Change in water consentration due to air flow
dCWa(k,ip)=(Mfda(k,ip)./VolCB).*(H(k,ip-1)-H(k,ip)).*Delta_t;
%   Water concentration
dCW(k,ip)=dCWp(k,ip)+dCWa(k,ip);
CW(k,ip)=CW(k-1,ip)+dCW(k,ip);
Wst(k,ip)=CW(k,ip).*VolCL;

%   Change in moisture content factor k_H2O
Wmc(k,ip)=Wst(k,ip)./(Wst(k,ip)+Sst(k,ip));

%   Weighted moisture coefficient
if Wmc(k,ip) >= 0.00  &&  Wmc(k,ip) < 0.10;
   k_H2O(k,ip) = 0.00;
elseif Wmc(k,ip) >= 0.10  &&  Wmc(k,ip) < 0.20;
   k_H2O(k,ip)=-0.0759+0.9011.*Wmc(k,ip);
elseif Wmc(k,ip) >= 0.20  &&  Wmc(k,ip) < 0.60;
   k_H2O(k,ip)=-0.3482+2.2597.*Wmc(k,ip);
elseif Wmc(k,ip) > 0.60  &&  Wmc(k,ip) <= 1.0;
   k_H2O(k,ip)=7.5844-20.5315.*Wmc(k,ip)+19.8468.*(Wmc(k,ip).^2)-6.5147.*(Wmc(k,ip).^3);
else Wmc(k,ip)=0.60;
   k_H2O(k,ip)=1.00;
end;

%   ENERGY BALANCE
qm(k,ip)=((CHw.*CW(k,ip))+(CHss.*CSss(k,ip))+(CHsc.*CSsc(k,ip))+(CHsl.*CSsl(k,ip))+(CHsi.*CSsi(k,ip)));

dTa(k,ip)=(HCss*dCSss(k,ip))+(HCsc*dCSsc(k,ip))+(HCsl*dCSsl(k,ip));
dTp(k,ip)=(Mfda(k,ip)./VolCL).*(h(k,ip)-h(k-1,ip-1));
dTq(k,ip)=(((Awall.*(T(k-1,ip)-T(1,1))./RT)./VolCL);
dT(k,ip)=(dTa(k,ip)-dTp(k,ip)-dTq(k,ip))./qm(k,ip);
T1(k,ip)=T(k-1,ip)+real(dT(k,ip).*Delta_t);
```

```
        if T1(k,ip)< T(1,ip)
           T(k,ip)=T(1,ip);
        else T(k,ip)=T1(k,ip);
        end
      end
   end
end

%**************************************************************************
%                    PLOT AND PRINT RESULTS
%**************************************************************************
%   Temperature
T1=T(:,8);
T2=T(:,7);
T3=T(:,6);
T4=T(:,5);
T5=T(:,4);
T6=T(:,3);
T7=T(:,2);
T8=T(:,1);
figure;
plot(t,T1,'k',t,T2,'y',t,T3,'m',t,T4,'c',t,T5,'r',t,T6,'g',t,T7,'b',t,T8,'k');
legend('70 cm','60 cm','50 cm','40 cm','30 cm','20 cm','10 cm','0 cm');
grid on
title('Temperature over Time')
xlabel('Time (h)')
ylabel('Temperature (K)')
% print

%   Substrate
Sss1=Sss;
Ssc2=Ssc;
Ssl3=Ssl;
```

```
Ssi4=Ssi;
figure
plot(t,Sss1,'b',t,Ssc2,'g', t,Ssl3,'c',t,Ssi4,'r');
grid on
title('Change in Substrate over Time')
xlabel('Time (h)')
ylabel('Substrate (kg)')
% print

%   Soluble Substrate Concentration
CSss2=CSss(:,8);
CSss3=CSss(:,7);
CSss4=CSss(:,6);
CSss5=CSss(:,5);
CSss6=CSss(:,4);
CSss7=CSss(:,3);
CSss8=CSss(:,2);
figure
plot(t,CSss2,'k',t,CSss3,'y',t,CSss4,'m',t,CSss5,'c',t,CSss6,'r',t,CSss7,'g',t,CSss8,'b');
legend('70 cm','60 cm','50 cm','40 cm','30 cm','20 cm','10 cm');
grid on
title('Change in Soluble Substrate Concentration over Time')
xlabel('Time (h)')
ylabel('Soluble Substrate (kg m^-3)')
% print



%   Cellulose/Hemicellulose Substrate Concentration
CSsc2=CSsc(:,8);
CSsc3=CSsc(:,7);
CSsc4=CSsc(:,6);
CSsc5=CSsc(:,5);
CSsc6=CSsc(:,4);
```

```
CSsc7=CSsc(:,3);
CSsc8=CSsc(:,2);
figure
plot(t,CSsc2,'k',t,CSsc3,'y',t,CSsc4,'m',t,CSsc5,'c',t,CSsc6,'r',t,CSsc7,'g',t,CSsc8,'b');
legend('70 cm','60 cm','50 cm','40 cm','30 cm','20 cm','10 cm');
grid on
title('Change in Cellulose/Hemicellulose Substrate Concentration over Time')
xlabel('Time (h)')
ylabel('Cellulose/Hemicellulose Substrate (kg m^-3)')
% print

%   Lignin Substrate
CSsl2=CSsl(:,2);
CSsl3=CSsl(:,3);
CSsl4=CSsl(:,4);
CSsl5=CSsl(:,5);
CSsl6=CSsl(:,6);
CSsl7=CSsl(:,7);
CSsl8=CSsl(:,8);
figure
plot(t,CSsl2,'k',t,CSsl3,'y',t,CSsl4,'m',t,CSsl5,'c',t,CSsl6,'r',t,CSsl7,'g',t,CSsl8,'b');
legend('70 cm','60 cm','50 cm','40 cm','30 cm','20 cm','10 cm');
grid on
title('Change in Lignin Substrate Concentration over Time')
xlabel('Time (h)')
ylabel('Lignin Concentration (kg m^-3)')
% print

%   Oxygen
CO_21=C_O2(:,8);
CO_22=C_O2(:,7);
CO_23=C_O2(:,6);
CO_24=C_O2(:,5);
CO_25=C_O2(:,4);
```

```
CO_26=C_O2(:,3);
CO_27=C_O2(:,2);
CO_28=C_O2(:,1);
figure;
plot(t,CO_21,'k',t,CO_22,'y',t,CO_23,'m',t,CO_24,'c',t,CO_25,'r',t,CO_26,'g',t,CO_27,'b',t,CO_28,'k');
legend('70 cm','60 cm','50 cm','40 cm','30 cm','20 cm','10 cm','0 cm');
grid on
title('Oxygen Concentration over Time')
xlabel('Time (h)')
ylabel('Oxygen Concentration (kg m^-3)')
% print

%   Carbon Dioxide Production
CCO_21=C_CO2(:,8);
CCO_22=C_CO2(:,7);
CCO_23=C_CO2(:,6);
CCO_24=C_CO2(:,5);
CCO_25=C_CO2(:,4);
CCO_26=C_CO2(:,3);
CCO_27=C_CO2(:,2);
CCO_28=C_CO2(:,1);
figure;
plot(t,CCO_21,'k',t,CCO_22,'y',t,CCO_23,'m',t,CCO_24,'c',t,CCO_25,'r',t,CCO_26,'g',t,CCO_27,'b',t,CCO_28,'k');
legend('70 cm','60 cm','50 cm','40 cm','30 cm','20 cm','10 cm','0 cm');
grid on
title('Carbon Dioxide Concentration over Time')
xlabel('Time (h)')
ylabel('Carbon Dioxode Concentration (kg m^-3)')
% print

%   Water Concentration
CW1=CW(:,8);
CW2=CW(:,7);
CW3=CW(:,6);
```

```
CW4=CW(:,5);
CW5=CW(:,4);
CW6=CW(:,3);
CW7=CW(:,2);
CW8=CW(:,1);
figure;
plot(t,CW1,'k',t,CW2,'y',t,CW3,'m',t,CW4,'c',t,CW5,'r',t,CW6,'g',t,CW7,'b',t,CW8,'k');
legend('70 cm','60 cm','50 cm','40 cm','30 cm','20 cm','10 cm','0 cm');
grid on
title('Water Concentration over Time')
xlabel('Time (h)')
ylabel('Water Concentration (kg m^-3)')
% print
```

Appendix F - Experimental Temperature Data (Electronic Dissertation Only)

The corrected temperature data of each reactor tube, as recorded by the data logger, are presented in this appendix only in the electronic copy. The corrections made involved the removal of erroneous data points, where the thermocouple reading was out of bounds. The corrections made are: 1) the reading was below or exceed the data points before and after in the same profile and the reading was below or exceed the data points in the temperature profile above and below; 2) the reading registered no reading; and 3) the reading exceeded the value possible for microbial activity (> 85 °C).